CONF-8804100

Proceedings of the
2nd DOE/ornl

Heat Pump Conference

Research and Development on Heat Pumps for Space Conditioning Applications

Crystal Gateway Marriott
Washington, D.C.
April 17–20, 1988

Sponsor:
U.S. Department of Energy
Office of Buildings
and Community Systems

Conference Committee

T. G. Statt
U.S. Department of Energy

P. D. Fairchild
Oak Ridge National Laboratory

P. J. Lewis
Oak Ridge National Laboratory

Conference Staff

Secretary
Terri Simmons

Coordinator
Norma Cardwell

Publications Coordinator
Raleigh Powell

ORNL Editor
Eleanor Rogers

CONF-8804100

Proceedings of the 2nd DOE/ORNL Heat Pump Conference: Research and Development on Heat Pumps for Space Conditioning Applications

Crystal Gateway Marriott
Washington, D.C.
April 17–20, 1988

Published: August 1988

Prepared by the
Oak Ridge National Laboratory
Oak Ridge, Tennessee 37831
operated by
Martin Marietta Energy Systems, Inc.
for the
U.S. DEPARTMENT OF ENERGY

Contents

Foreword v

Session 1. Electric Heat Pump Technology: Current Activities

Advanced Refrigeration Systems Program Overview
T. G. Statt 3
Laboratory Capacity Modulation Experiments, Analyses, and Validation
W. A. Miller 7
Capacity Modulation Component Characterization and Design Tool Development
C. K. Rice 23
Evaluation of Vapor Compression Cycles Using Nonazeotropic Refrigerant Mixtures
R. L. Merriam 35
Evaluation of Nonazeotropic Refrigerant Mixtures for Capacity Modulation
E. A. Vineyard and *J. R. Sand* 47
Experimental Evaluation of Two Refrigerant Mixtures in a Breadboard Air Conditioner
W. Mulroy, M. Kauffeld, M. McLinden, and *D. A. Didion* 55

Session 2. Electric Heat Pump Technology: Related Research

Heat Pump Research at the Electric Power Research Institute
A. Lannus 65
Overview of Ground-Coupled Heat Pump Research and Technology Transfer Activities
V. D. Baxter and *V. C. Mei* 75

Session 3. What Should Influence the Future Direction of the DOE/ORNL R&D Program?

Assessment of Japanese Variable-Speed Heat Pump Technology
Kenji Ushimaru 85
CFC Restrictions: Energy Impacts and Technological Alternatives
F. A. Creswick and *S. K. Fischer* 93
International Cooperation in Heat Pump and Refrigeration Research Through the International Energy Agency
J. D. Ryan 101

Session 4. Thermally Activated Heat Pumps: Absorption Systems

DOE Absorption Program Overview
R. C. DeVault 105
Development of an Advanced-Cycle Absorption Heat Pump for Residential Applications
B. A. Phillips 111
Evaluation of a Commercial Advanced Absorption Heat Pump Breadboard
R. J. Modahl and *F. C. Hayes* 117
Development and Proof-Testing of Advanced Absorption Refrigeration-Cycle Concepts — Phase II
R. C. Reimann and *Gorken Melikian* 127

Absorption Enhancement Research and Related Diagnostics
H. Perez-Blanco, M. R. Patterson, D. T. Bostick, and *L. N. Klatt* 133
Worldwide Survey of Absorption Fluids Data
R. A. Macriss and *T. S. Zawacki* 145

Session 5. Heat-Actuated Heat Pumps: Engine-Driven Heat Pumps

GRI Heat Pump R&D Program Overview
A. R. Maret 153
Engine-Driven Heat Pump Program Overview
G. T. Privon and *A. T. Braun* 155
Status of the Braun Engine-Driven Heat Pump Development
A. T. Braun, R. J. Prekker, and *A. P. Schneeberger* 161
An Analytical Study of Hybrid Ejector/Internal Combustion Engine-Driven Heat Pumps
R. W. Murphy 163
Entrainment Enhancement of a Supersonic Jet for Advanced Ejectors
W-H. Jou, G. S. Knoke, and *C-M. Ho* 169

Session 6. Thermally Activated Heat Pumps: Stirling Engine-Driven Heat Pumps

An Overview of the Stirling Engine Heat Pump Program
F. C. Chen 177
Development of a Residential Free-Piston Stirling Engine Heat Pump
R. A. Ackermann 189
Preliminary Assessment of a Magnetically Coupled Free-Piston Stirling Engine Heat Pump Compressor
W. T. Beale and *G. Chen* 197
Integration of Analysis and Experiment for Stirling Cycle Processes. Part 1: Gas Spring Hysteresis Loss
A. A. Kornhauser and *J. L. Smith, Jr.* 203
Comparative Assessment of Free-Piston and Kinematic Stirling Engine Technologies
W. P. Teagan 209
Author Index 211
Conference Attendees 213
Appendix A 221

Foreword

This conference was planned to provide information on current R&D activities on residential and commercial heat pumps in the U.S. Department of Energy (DOE) and Oak Ridge National Laboratory (ORNL) Building Equipment Research (BER) Program. It was primarily for the benefit of HVAC equipment manufacturers who could use the technology in future products, but was also of value to a wider audience, including utilities, independent R&D organizations, universities, other government groups, and research funding and management organizations.

Because this conference was intended to be a significant part of our technology transfer efforts, the presentations emphasized energy performance objectives, technical results, development status, and potential HVAC equipment applications. In addition, the conference was organized to facilitate information exchange among attendees, speakers, and the DOE and ORNL Program staff, and to create an opportunity to receive constructive input from the private sector.

The technical presentations were grouped into two principal subject areas: electric heat pump technology and thermally activated heat pump systems. Electric heat pump topics included capacity modulation experiments and system design analysis development, nonazeotropic refrigerant mixtures, and ground-coupled systems. In the area of thermally activated heat pumps, presentations centered on the development of absorption systems, engine-driven heat pumps, and Stirling engine-driven heat pumps.

Because of the strong ties between the BER Program and the Electric Power Research Institute (EPRI) and Gas Research Institute (GRI) heat pump research and development programs, overview presentations on the EPRI and GRI programs were included. To stimulate industry feedback on future directions for the BER Program, there was also a special session that addressed two major issues facing the HVAC industry: CFC restrictions and international competition. Response to the conference has been valuable to ORNL in planning both program content and future industry interaction activities.

On behalf of DOE and ORNL, the undersigned wish to take this opportunity to again express our appreciation to all participants.

Conference Committee

P. D. Fairchild, ORNL
T. G. Statt, DOE
P. J. Lewis, ORNL

Session 1

Electric Heat Pump Technology: Current Activities

Organizer and Chairman:
V. D. Baxter
Oak Ridge National Laboratory

Advanced Refrigeration Systems Program Overview

T. G. Statt
U.S. Department of Energy
Washington, DC 20585

Introduction

The U.S. Department of Energy (DOE) has been managing research activities for advanced refrigeration systems since 1977. The overall program objective is to advance the scientific knowledge in the reduction of energy losses in refrigeration systems, primarily for electrically driven heat pumps. The advancements in scientific understanding are then applied in developing promising technical concepts into new, emerging technologies that are substantially more energy efficient than existing technologies. The Building Equipment Division in the Office of Buildings and Community Systems (OBCS) is the DOE office responsible for the overall management of the refrigeration program.

The Oak Ridge National Laboratory (ORNL) is the lead national laboratory and provides technical and project management for the Advanced Refrigeration Systems Program. The Building Equipment Research program in the ORNL Efficiency and Renewables Research section leads the research effort for the laboratory. ORNL also performs in-house research in support of the overall program.

Program Justification

In 1985, the residential sector accounted for about 15.0 quads of primary energy (Fig 1).[1] Approximately 9.0 quads or 60 percent of the residential energy use was for space heating (40%), refrigerators (9%), air conditioning (8%), and freezers (3%). Technologies developed by the Advanced Refrigeration Systems program can be applied to these four end uses. Preliminary assessments of new concepts typically estimate energy savings potentials ranging from 30-50 percent.[2,3] As the residential sector uses a lot of energy and substantial energy savings potentially exist, there is support for a strong role for DOE in conducting research in this area.

One program objective for OBCS is to save 10 quads of primary energy annually by the year 2010.[1] To show how the Advanced Refrigeration Systems program contributes to this overall program goal, estimates of the potential energy savings for three technologies were made. The three technologies are continuously variable-speed heat pumps (CVSHP), nonazeotropic refrigerant mixtures (NARM), and ground coupled heat pumps (GCHP).

The methodology used to estimate the potential energy savings was based on several assumptions. The number of households in the year 2010 was estimated to be 99.1 million. One-half of these households were assumed to have heat pumps. About half of all households today are heated electrically, whether by heat pumps or strip heaters. The product mix of heat pumps in operation in the year 2010 was assumed to be CVSHP (50%), NARM (25%), single-speed heat pumps (15%), and GCHP (10%). Results from this preliminary assessment of energy savings in the year 2010 were estimated to range from 1.26-1.99 quads, as reported in Table 1. The savings for CVSHP were estimated to range from 0.62-1.03 quads. The savings were estimated to be from 0.32-0.57 quads for NARM. For GCHP, the energy savings were estimated to range from 0.32-0.39 quads. In summary, technologies developed by the Advanced Refrigeration Systems program were projected to contribute from about 12-20 percent of the overall OBCS program goal (10 quads) of primary energy saved yearly by 2010.

Completed Research Efforts

Through the years, DOE has successfully completed many research projects that resulted in the introduction of energy efficient equipment into the market place. Three projects typical of previous DOE research efforts are the supermarket refrigeration system, the high efficiency refrigerator compressor, and GCHP's. These three projects are discussed below.

Supermarket Refrigeration Systems -- Supermarkets consume about 4 percent of the nation's electricity with refrigeration of display cases as the dominant energy use by accounting for 40 to 60 percent of the electricity used by supermarkets.[4] In an effort to reduce the energy consumption in this sector, DOE and a leading manufacturer of supermarket refrigeration equipment pioneered the development of a novel concept for supermarket refrigeration. The innovative design, which featured multiple unequal parallel compressors and advanced microprocessor controls, reduced the energy required for refrigeration by over 40 percent.[5] As a result of the DOE research effort, all leading manufacturers now offer these advanced features on their equipment. A second result is that supermarket refrigeration systems, with multiple unequal parallel compressors, captured 25 percent of the market in 1987.[6] Advanced supermarket refrigeration systems are estimated to save from about 0.25 to 0.37 quads of primary energy in the year 2010.

High Efficiency Refrigerator Compressor -- Household refrigerators and freezers consume approximately 12 percent of the primary

energy used in the residential sector. In an effort to reduce the energy consumption of refrigerators, DOE supported the research efforts by one major appliance manufacturer in developing a more efficient refrigerator compressor.[7] By implementing several innovative design changes in the motor, suction muffler, intake and exhaust valves, and oil management system, the Kelvinator Company achieved a 44 percent improvement in compressor efficiency over existing refrigerator compressors. Kelvinator then manufactured over 30,000 refrigerators with this new high efficiency compressor. Based on the success of this compressor design, Kelvinator recently introduced a more advanced compressor that is the industry's first compressor rated over 5 Btu per watt-hour. Full market penetration of high efficiency compressors in household refrigerators and freezers would produce energy savings estimated from approximately 0.42 to 0.62 quads by the year 2010.

Ground Coupled Heat Pumps -- Presently, about one-third of all new homes constructed are heated and cooled by air source heat pumps. As GCHP's could possibly save over half of the energy used by air source heat pumps, DOE managed a multi-faceted research and development program to develop an advanced GCHP. Analytical design tools were developed, tested, and validated. These design tools were distributed to the private sector to assist system manufacturers in designing more cost-effective ground coil heat exchangers and more efficient mechanical packages for the heat pump. These design tools were then applied in the development of an advanced GCHP system in which DOE, a utility company, and a leading manufacturer collaborated in the design, fabrication, and field evaluation of two experimental systems. The advanced systems improved the cost effectiveness of GCHP's compared with that of air source heat pumps by reducing the payback period of about 6-10 years to about 3-5 years.[8,9] The utility company estimates that this savings realization should increase sales of GCHP's by about 60 percent. Based on this advanced design, ground coupled heat pumps are estimated to save approximately 0.32-0.39 quads in the year 2010.

Present Research Efforts

Currently, the Advanced Refrigeration Systems program is conducting research in four project areas. These are capacity modulation, nonazeotropic refrigerant mixtures, chlorofluorocarbons (CFC), and novel cycles. One program goal for this research is the development of a new generation of heat pumps by 1995 that can achieve heating COPs of 4.0 at 47°F and 2.9 at 17°F and a cooling COP of 6.0.[10] These goals are 40 percent better than heat pumps available today. Specifically, the objectives are to advance the scientific understanding of the dynamic losses associated in operating heat pumps; to develop capacity modulation concepts for reducing these dynamic losses; and to develop and validate the requisite design tools necessary to assist manufacturers in designing more advanced heat pumps.

Capacity Modulation -- In 1983, ORNL conducted a preliminary assessment of CVSHP.[2] The assessment predicted potential energy savings of over 25 percent against single-speed heat pumps, as shown in Fig. 2. Due to this promising outcome, a two-prong experimental and analytical approach was initiated to investigate more accurately the potential benefits of variable-speed heat pump technology.

In 1987, a workshop was held to present initial results of the research on variable-speed heat pumps to the industry. Recent research efforts on capacity modulation include several cooperative ventures with system and component manufacturers. The first public domain variable-speed heat pump computer code is being released at this conference. The code is a first generation steady-state model for an inverter-driven reciprocating compressor. Over the next year, ORNL intends to add an operational charge inventory submodel, second generation frost/defrost algorithms, and a permanent magnet/electronically commutated motor (PM/ECM) compressor option to the computer code. An annual performance factor (APF) model will be developed. Analyses of optimizing the system performance for an ECM-driven reciprocating compressor and an ECM-driven scroll compressor are planned.

Nonazeotropic Refrigerant Mixtures -- In 1978 at the Univeristy of Illinois, DOE initiated research on NARM in which a thermodynamic analysis concluded that using a mixture of two refrigerants in a household refrigerator could result in energy savings of about 12 percent.[11]

In 1987, ORNL tested refrigerant mixtures on an experimental heat pump water heater loop. ORNL has recently completed a systematic approach for identifying those novel refrigerant mixtures that have the greatest potential for improving heat pump performance.[12] The primary purpose of the research was to comprehensively screen refrigerant mixtures that, through a shift in composition, could improve the performance of heat pump systems by modulating the system capacity to better follow the building load. This investigation identified several promising refrigerant mixtures that have not been previously identified by other researchers. During 1988, ORNL plans to test these new refrigerant mixtures on an experimental heat pump apparatus.

The National Bureau of Standards (NBS) measured a 32 percent improvement in COP for one refrigerant mixture over pure R-22 on their experimental heat pump apparatus. During 1988, NBS plans to test advanced vapor compression cycles which theoretically could

result in efficiency improvements of 40-50 percent.[3] Arthur D. Little, Inc., is developing and validating a computer code for heat pumps using nonazeotropic refrigerant mixtures. This code will be used to quickly screen refrigerant mixtures and refrigerant cycle configurations.

Chlorofluorocarbons -- In 1985, the US manufactured 1.54 billion lbs of CFC, halons, carbon tetrachloride, and methyl chloroform, all substances that potentially deplete stratospheric ozone.[13] Roughly 40 percent or 580 million lbs were used in energy-related applications, namely, as the working fluid in refrigeration equipment or as the blowing agent in foam insulations. To gain greater insight on the energy-related impacts of CFC, ORNL investigated the energy impacts of CFC restrictions and prepared a R&D program plan. With appropriate funding, DOE intends to implement the plan by conducting cooperative research projects with industry.

Novel Cycles -- Novel refrigeration cycles possibly could result in substantial energy savings for heat pumps over the technologies currently being developed by DOE. As a normal part of the overall research effort, preliminary technical evaluations of innovative concepts are made. Those promising concepts that pass this initial screening are to be included as individual research projects, whenever funding permits.

In 1983, ORNL conducted a preliminary assessment in which a reverse Stirling cycle heat pumps was compared with a midline air-source heat pump. The projected energy savings for the reverse Stirling cycle heat pump were estimated to range from 10-28 percent, depending on climate. In 1987, ORNL experimentally measured the performance of a commercial reverse Stirling machine under controlled laboratory conditions.[14] These tests confirmed the potential performance advantages, as the measured performance ranged from 8-18 percent of the ideal COP (Carnot cycle).

In 1987, ORNL evaluated a novel heat pump concept. A ground coupled heat pump was coupled to a thermoelectric cooling (GCHP/TE) system.[15] The evaluation found the performance of the combined GCHP/TE system superior to a conventional GCHP in cooling, as the cooling COP was estimated to be about 6.4 (EER = 22). However, due to the increased temperature lift experienced in heating, the COP was estimated as about 1.75 for the GCHP/TE system, while the conventional system had a heating COP of 3.2.

In another area, one firm reported a 30-40 percent savings for magnetic refrigeration over conventional refrigeration technologies.[16] Magnetic refrigeration is thought to be appropriate for large unitary equipment, when the large size could justify the use of superconducting magnets. This technology is a good example of the type of advanced concepts that DOE would like to explore in the novel cycles area, as this technology exhibits large potential energy savings.

Technical Challenges

As can be seen from this paper, DOE has made considerable progress in improving heat pump technologies. DOE also has identified promising newer concepts to continue making advancements in heat pump technologies in which several technical challenges still exist. For capacity modulation, the technical challenges include refrigerant charge management, controlling refrigerant migration during off-cycles, improved defrost strategies, intelligent and adaptive controls, and increased performance of heat exchangers. For NARM, the technical challenges are development of a methodology for accurately predicting thermodynamic and transport properties of novel refrigerant mixtures, investigation of innovative cycle concepts to better utilize the unique attributes of refrigerant mixtures, research on heat transfer phenomena with innovative heat exchanger concepts to reduce the heat transfer losses experienced by most refrigerant mixtures, and development of dynamic composition control techniques. Research on CFC potentially addresses a wide variety of fundamental technical barriers associated with novel refrigeration processes, new refrigerants and blowing agents. The research on CFC could also include novel refrigeration processes, including reverse Stirling, magnetic refrigeration, and thermoelectric cooling.

Bringing these promising novel refrigeration concepts to fruition requires a sizeable research effort and a continued close cooperation with industry. Hopefully, the potential benefits offered by these innovative concepts can be successfully used to substantially reduce the energy consumption in the residential and commercial sectors.

References

1. "Energy Conservation: Multi-Year Plan FY 1989-93," U.S. Department of Energy, Washington, DC, September 1987.

2. C. K. Rice and S. K. Fischer, "A Comparative Analysis of Single- and Continuously Variable-Capacity Heat Pump Concepts," CONF-841231, Proceedings of the DOE/ORNL Heat Pump Conference: Research and Development on Heat Pumps for Space Conditioning Applications, Washington, DC, December 1984.

3. R. Radermacher, "Advanced Versions of Heat Pumps with Zeotropic Refrigerant Mixtures," ASHRAE Trans. 92(2B), June 1986.

4. W. Toscano, et al, "Research and Development of Highly Energy-Efficient Supermarket Refrigeration Systems: Volume 1 - Executive Summary and Task Reports," ORNL/Sub/80-61601/1, Foster-Miller Associates, Inc., October 1981.

5. Friedrich Air Conditioning & Refrigeration Co., Product Literature.

6. D. Hiches, "Trends to Continue to Shift in Supermarket Refrigeration," Air Conditioning, Heating & Refrigeration News," June 1987.

7. M. Middleton and R. Sauber, "Research and Development of Energy-Efficient High Back-Pressure Compressors," ORNL/Sub/78-7229/5, Kelvinator Compressor Company, September 1983.

8. P. Hughes and R. Hackner, "Field Performance Validation of an Advanced Design Earth-Coupled Heat Pump System," ORNL/Sub/85-22035/1, W. S. Fleming and Associates, Inc., January 1988.

9. T. Statt, "A Regional Economic Comparison of Ground-Source Heat Pump Systems," HPC-WR-2, Proceedings of the Workshop on Ground-Source Heat Pumps, IEA Heat Pump Center, September 1987.

10. "Present and Projected Efficiency Improvements in Central Air Conditioners and Heat Pumps, 1985-1992," DHR C5133-23, DHR Incorporated, December 1985.

11. W. Stoecker, "Improving the Energy Effectiveness of Domestic Refrigerators by the Application of Refrigerant Mixtures," ORNL/Sub-78/55463/1, University of Illinois at Urbana-Champaign, September 1978.

12. E. Vineyard and J. Sand, "Selection of Ozone-Safe, Nonazeotropic Refrigerant Mixtures for Capacity Modulation in Residential Heat Pumps," Task Report (draft), Oak Ridge National Laboratory, March 1988.

13. T. Statt, "The Use of Chlorofluorocarbons in Refrigeration, Insulation and Mobile Air Conditioning in the United States," EPA Conference on Substitutes and Alternatives to CFCs and Halons, Washington, DC, January 1988.

14. E. Keshock and R. Murphy, "Performance Testing of a Commercially Produced Cryogenic Refrigerator," draft report, Oak Ridge National Laboratory.

15. V. Mei, et al., "Comparison of a Ground Water Coupled Thermoelectric Cooling System and a Ground Water Heat Pump," ASME Winter Annual Meeting, Boston, MA, December 1987.

16. "Refrigerating with Magnets," High Technology, November, 1986.

TABLE 1.
PROJECTED ENERGY SAVINGS IN THE YEAR 2010
(QUADS OF PRIMARY ENERGY)

Technology	Range
1. Continuously variable-speed heat pumps	0.62 - 1.03
2. Nonazeotropic refrigerant mixtures	0.32 - 0.57
3. Ground coupled heat pumps	0.32 - 0.39
Total	1.26 - 1.99

Laboratory Capacity Modulation Experiments, Analyses, and Validation*

W. A. Miller
Oak Ridge National Laboratory
Oak Ridge, TN 37831

Abstract

A combined experimental and analytical project was conducted on a breadboarded continuously variable speed air-to-air heat pump (CVSHP). The split-system residential unit of nominal 2 3/4-ton (9.7-kW) cooling capacity was instrumented and tested in environmental chambers. The steady-state, frosting/demand defrosting, and cycling efficiency characteristics of the CVSHP with first generation components (e.g., heat exchangers, compressor, and indoor blower, both having variable speed induction motors) were measured in the laboratory for compressor drive frequencies ranging from 15 through 90 Hz. Steady-state efficiency data were used to validate an initial version of the Oak Ridge National Laboratory steady-state modulating heat pump design program. Algorithms were developed from reduced dynamic loss data from which calculations were made of the seasonal losses for the test CVSHP.

Introduction

A planned series of experiments were conducted to characterize the efficiency and efficiency trends of a continuously variable speed heat pump (CVSHP). The primary objectives of this study were to determine the efficiency of a CVSHP at different speeds and ambients, to identify the effect of dynamic losses, to develop control strategies to reduce the dynamic losses, and to perform seasonal analyses to assess the benefits of the CVSHP technology as applied to the particular system tested. Steady-state test data were also used to validate the Oak Ridge National Laboratory (ORNL) modulating heat pump computer code.

Calorimeter testing of advanced variable speed compressors and testing of state-of-the-art CVSHPs is planned.

Summary of Work

A continuously variable speed, air-to-air split-system residential heat pump of nominal 2 3/4-ton (9.7-kW) cooling capacity was instrumented with temperature and pressure sensors, with locations displayed in Fig. 1. Testing was conducted in environmental chambers, which were capable of controlling indoor and outdoor ambient dry bulb and dew point temperatures. A host computer and data acquisition system were used to monitor all temperatures, pressures, powers, and flows. Salient features of both the breadboard CVSHP and the test stand are discussed in previous work by Miller.[1]

A series of tests were conducted on the test CVSHP in the laboratory to demonstrate optimal refrigerant flow and airflow control for best coefficient of performance (COP) as constrained by comfort. The capillary tubes originally supplied with the test unit were replaced with variable area, hand-controlled valves (Fig. 1) to improve control of refrigerant flow during testing. As seen in Fig. 1, the compressor was driven by a motor-generator (M-G) set (i.e., ideal induction motor drive), and the indoor blower was driven by a first generation inverter drive, which was originally supplied with the test unit.

The optimal flow control experiments were conducted in the heating mode at outdoor ambient temperatures of 40 and 10°F (4.4 and -12.2°C) and in the cooling mode at outdoor ambient temperatures of 95 and 82°F (35 and 27.2°C). Test parameters were compressor speed, indoor blower speed, and refrigerant subcooling at the condenser exit. A range of condenser exit subcoolings (controlled by the variable area throttling valve) and indoor airflows for compressor drive frequencies ranging from 15 to 90 Hz were tested to observe their effect on

*Research sponsored by the Office of Buildings and Community Systems, U.S. Department of Energy, under Contract DE-AC05-84OR21400 with Martin Marietta Energy Systems, Inc.

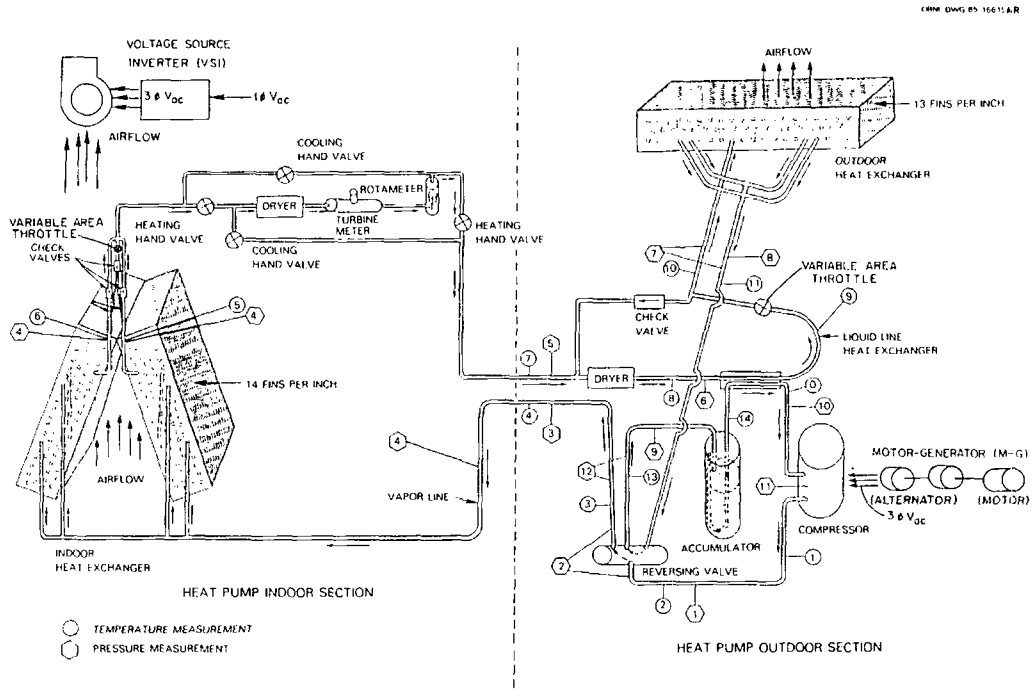

Fig. 1. Schematic and sensor locations for the tested continuously variable speed heat pump (CVSHP).

COP, capacity, and component efficiencies. From these tests, an optimal ratio of compressor motor speed to indoor blower speed and the optimal level of subcooling at condenser exit as a function of compressor speed were identified in the laboratory.

The data from the optimal flow control study and the calorimetry data, obtained from a compressor manufacturer on an identical reciprocating compressor as tested in the laboratory CVSHP, were both used to validate the initial version of the ORNL steady state modulating heat pump design model (MHPDM).[2]

The operating efficiencies of the first generation variable speed hermetic reciprocating compressor and indoor centrifugal blower, both having induction motors, were characterized while operating under optimal flow control conditions as determined from the experiments discussed above. The indoor blower was tested using a six-step voltage source inverter (VSI) designed in the late 1970s and also using an M-G set (ideal induction motor drive) for a motor drive frequency range of 20 to 60 Hz. The reciprocating compressor was driven in separate tests by a VSI,[a] a pulse-width modulated inverter (PWMI),[b] and the M-G set to observe the effect of each adjustable-speed drive on the efficiency of the compressor for drive frequencies ranging from 15 to 90 Hz.

Follow-up laboratory work was conducted on the optimally controlled system to measure the COP and system capacity during frosting/demand defrosting tests and during both heating and cooling mode cycling tests. Frosting/demand defrosting tests were conducted for a range of compressor speeds, outdoor air temperatures, and relative humidities. Cycling tests were conducted for a range of compressor speeds and outdoor temperatures. Cycling rate was set at 12 min on and 48 min off as suggested by some heat pump manufacturers.[3] The dynamic loss testing was

a Commercially available in 1979 and supplied with the test unit.

b International product commercially available in 1983 and designed to have diminished harmonics and torque pulsation effects as compared with earlier design PWMI drives.

conducted while the CVSHP operated under previously determined optimal refrigerant flow and airflow control settings. Previous studies by Tanaka et al.[4] and by Miller,[5] dealing with cycling dynamics, and by Kuwahara et al.,[6] dealing with defrosting efficiency, and by Glamm,[7] dealing with dynamic control, were gleaned for techniques to minimize the dynamic losses of the test CVSHP. A best dynamic control strategy for the test system was developed in the laboratory and dynamic loss algorithms were developed from the data. Seasonal analysis simulations were then made using a binned seasonal performance computer code developed by Rice et al.[8] to estimate the energy savings directly attributable to (1) the reduction of dynamic losses for single-speed heat pumps (SSHPs), and (2) the efficiency improvement due to compressor and indoor blower speed modulation.

Technical Accomplishments

CVSHP Optimal Flow Control - Laboratory Demonstration

Optimal levels of refrigerant subcooling at the condenser exit were identified at discrete compressor speeds during heating and cooling mode laboratory tests. Refrigerant-side COP measurements observed in the heating mode at 40°F (4.4°C) outdoor temperature and in the cooling mode at 82°F (27.7°C) outdoor temperature are plotted in Figs. 2 and 3, respectively. Various families of refrigerant subcooling (at the condenser exit) per compressor speed tested are displayed as functions of indoor blower speed. The dashed curves in Figs. 2 and 3 are simulation results of the initial version of the ORNL steady state MHPDM. These curves are included for indication of model absolute and trend accuracy in predicting optimal COP and capacity performance of the test CVSHP.

Heating mode. Refrigerant subcooling of 5-10 F° (3-6 C°) was observed to yield optimal or near optimal COP for compressor speeds of 30 to 90 Hz operating in 40 and 10°F (4.4 and -12°C) outdoor air ambients. For these heating mode test results, the indoor blower (inverter driven) could actually be set at a constant 45-Hz speed with less than a 2% drop in COP measured at the optimum blower speed (Fig. 2).

Best COP measurements (Fig. 2) indicate approximately an 8% increase in COP when the compressor speed is lowered from 60 to 30 Hz. However, when the speed is lowered from 30 to 15 Hz, the measured COP dropped by 20%. This drop in COP at 15 Hz can be attributed to (1) a loss in heat exchanger efficiency and (2) a drop in

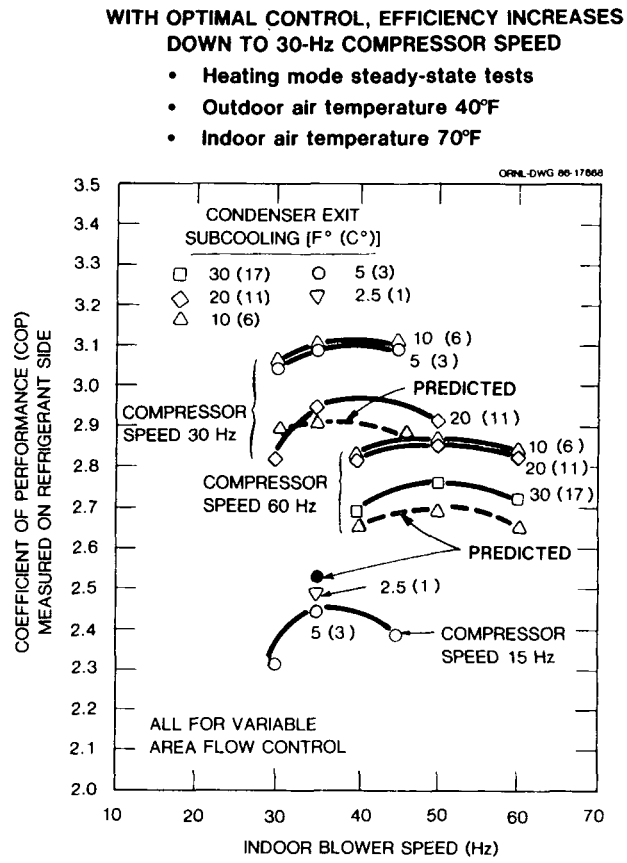

Fig. 2. Measured and predicted heating mode COP for the variable speed heat pump operating at 40°F (4.4°C) outdoor air temperature.

the isentropic efficiency[c] of the compressor, as explained in previous work by Miller.[9] It should be noted that testing at 55°F (12.7°C) outdoor temperature (not shown in Fig. 2) did not show a drop in COP, as compressor speed was reduced from 30- to 15-Hz compressor drive frequency. The refrigerant mass flow rate was greater at 55°F (12.7°C) outdoor temperature than at 40°F (4.4°C), and the pressure ratio across the compressor was reduced. Therefore both compressor and heat exchanger efficiencies were improved, resulting in improvement of COP trends as speed decreased at the 55°F (12.7°C) outdoor ambient.

c Compressor isentropic efficiency is defined here as the ratio of isentropic compressor work (computed across the shell) to the measured power input.

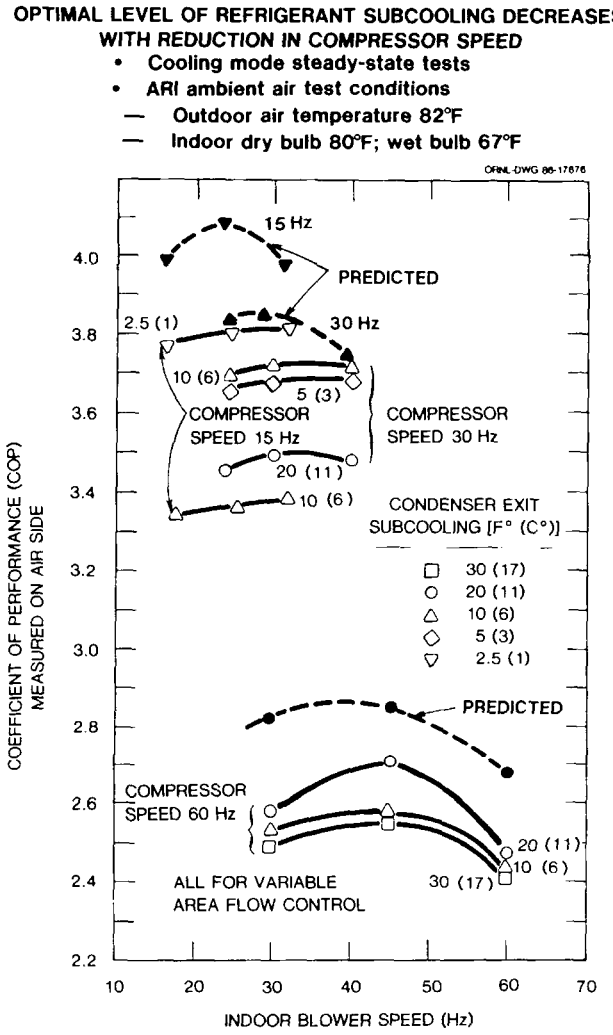

Fig. 3. Cooling mode COP measurements and predictions made at 82°F (27.7°C) outdoor air temperature.

Cooling mode. Best COPs in cooling mode required a greater change in blower speed and refrigerant subcooling with change in compressor speed. The indoor blower speed varied from 45 Hz at a compressor drive frequency of 60 to 16.7 Hz at compressor drive frequency of 15 Hz, as indicated in Fig. 3. Refrigerant subcooling for optimal COP at 60-Hz compressor speed and 82 and 95°F (27.7 and 35°C) outdoor air temperature was 20 F° (11 C°), while at 45- through 15-Hz compressor speed, optimal subcooling varied from 20 to 2.5 F° (11 to 1.4 C°).

Reducing the compressor drive frequency from 60 to 30 to 15 Hz at the 82°F (27.7°C) outdoor ambient[d] resulted in an improvement in COP (Fig. 3), a trend not previously observed in heating mode testing at 40°F (4.4°C).[e] At 15-Hz compressor drive frequency, the cooling mode refrigerant mass flowrate, measured at 82°F (27.7°C), was double the heating mode mass flowrate, measured at 40°F (4.4°C), because of the higher operating evaporator temperature. Thus, apparently there was no reduction in refrigerant-side heat flux in cooling mode as compared to heating mode, when operating at 15-Hz compressor drive frequency.

CVSHP Optimal Flow Control - Model Validation

The initial version of the MHPDM, based on the single-speed model developed by Rice and Fischer,[10] was validated against optimal flow control test data of the CVSHP. The model matched the measured trends of COP and capacity very well, slightly underpredicting heating COP and capacity and overpredicting cooling COP and capacity (COP predictions illustrated in Figs. 2 and 3). Prediction agreement was best at low-speed conditions for both heating and cooling. The poorest agreement occurred at the 95°F (35°C) nominal speed (60 Hz) rating condition where predictions were 10% greater than measured data. The overprediction in cooling at higher speeds was due to the inaccuracy of the simplified heat exchanger submodels when simulating complex circuitry under high levels of refrigerant subcooling at condenser exit. The validation results indicated that the model was well suited for use in evaluating design and operating options, provided that the heat exchangers were efficiently circuited and operated with low to moderate [<20 F° (11 C°)] condenser subcooling and low evaporator superheat. Outside these situations, the use of tube-by-tube heat exchanger models may be required.

Demonstrated Refrigerant Charge Variation for CVSHP

Testing was conducted to determine the optimal refrigerant charge required for both low superheat at the inlet to the compressor and optimal level of refrigerant subcooling at condenser exit. Results displayed in Fig. 4 indicated optimal refrigerant charges varied by roughly 1.5 lbs (0.6 kg) over the range of compressor speeds tested in cooling and heating modes, except for heating mode operation at 15-Hz compressor speed. Here 11.5 lb (5.2 kg) of refrigerant was required to duplicate optimal system efficiency, 2.5 lb (1.1 kg) more refrigerant than required in cooling mode operation.

d Near the expected minimum speed balance point in cooling mode.

e Near the expected minimum speed balance point in the hating mode.

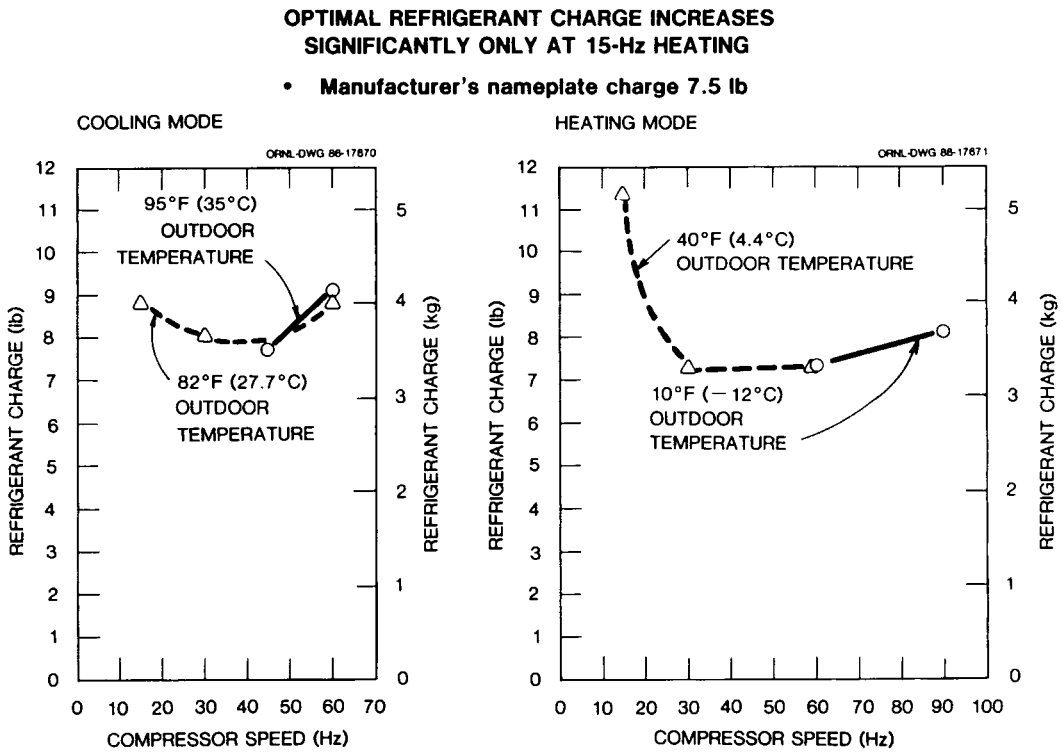

Fig. 4. Optimal refrigerant charge required for both low superheat at the inlet of the compressor and optimal level of refrigerant subcooling at the condenser exit.

This difference occurred because of the low refrigerant velocity in heating versus cooling mode (implied from mass flowrate comparison), which resulted in a less efficient condenser heat transfer in heating mode, as discussed by Miller.[9]

Proved CVSHP Would Maintain Comfort

Laboratory work demonstrated that the CVSHP would maintain comfort at least as well as a single-speed heat pump under most conditions. Comparison of the CVSHP performance, having optimal airflow and refrigerant flow control settings, to a manufacturer's data for a single-speed heat pump (SSHP) indicated that the CVSHP satisfied both heating and cooling comfort requirements, while better following house load through capacity modulation.

Heating comfort. Capacity and delivery air temperature for an SSHP are listed in Table 1, with similar data for the optimal COP operating points of the CVSHP. Comfort is maintained with the CVSHP operating at 30-Hz compressor speed, and the part-load capacity would better match house load as compared with a single-speed unit. At the lower temperature of 10°F (-12°C) and 90-Hz compressor speed, the CVSHP had a measured capacity of 22.6 kBtu/h (6.6 kW), while the SSHP had a capacity of 16.1 kBtu/h (4.7 kW). Delivery temperature for the CVSHP is 93°F (34°C), while for the single-speed unit (operating without supplemental heaters), the delivery temperature is only 82.4°F (28°C). By overspeeding the compressor, comfort is maintained below the balance point of the single-speed unit

TABLE 1
Capacity and supply air temperature for a single-speed heat pump and the continuously variable speed heat pump

Outdoor temperature (°F)	Heat pump type	Capacity (kBtu/h)	Supply air (°F)	Compressor speed (Hz)
40	Single speed[a]	32.1	94.8	60
	Variable speed	31.2	98.5	60
		17.0	92.4	30
		11.5	85.7	20
		8.5	81.6	15
10	Single speed	16.1	82.4	60
	Variable speed	22.6	92.8	90
		17.3	86.7	60

[a]Manufacturer's data for a single-speed heat pump operating with a capillary tube flow control.

with less added energy due to supplemental heat. These results indicate that the test unit, operating as a CVSHP with optimal blower speed and refrigerant subcooling satisfies comfort requirements as well as the single-speed unit does and better follows house load.

Cooling mode. Sensible heat ratios (SHRs) for the optimal test operating points of the CVSHP are plotted in Fig. 5, with manufacturer single-speed data. Also a SHR boundary line is displayed that represents the required latent load simulated for an 1800-ft^2 (167-m^2) house in Knoxville, Tennessee. Optimal operating points tabulated and plotted in Fig. 5 indicate, in terms of SHR, the test heat pump to have adequate latent capacity for humidity control within a residence. The optimum operating points for the CVSHP unit have an SHR comparable to or lower than the single-speed unit for outdoor temperatures of 95 and 82°F (35 and 27.7°C).

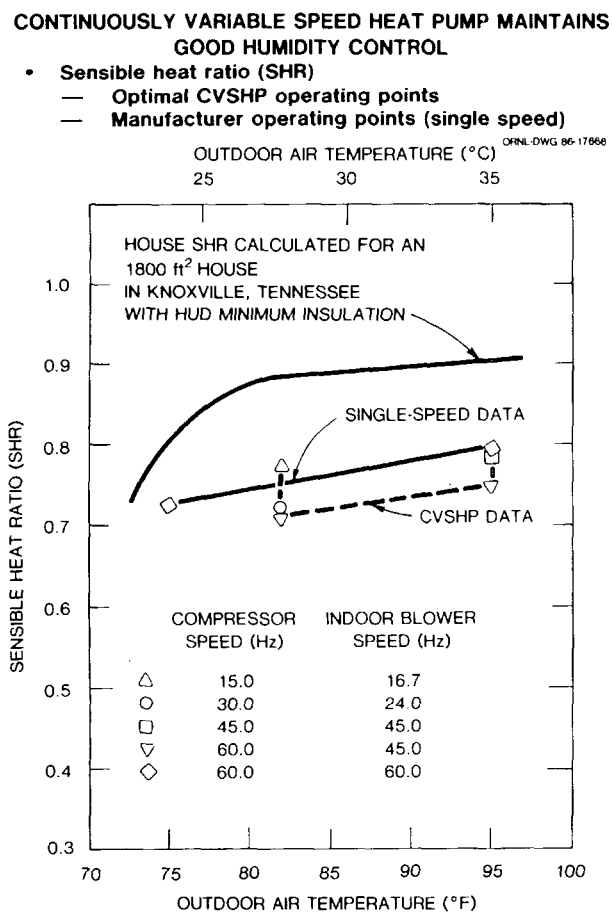

Fig. 5. The SHRs from manufacturer data for a single-speed heat pump (SSHP) compared to measured values for the optimal operating points of the continuously variable speed heat pump (CVSHP).

These results indicate that the CVSHP, having near equal total capacity at 60 Hz to the SSHP, has greater latent capacity and, thus, should provide a greater degree of comfort.

Characterized Efficiency Limits of First Generation Variable Speed Reciprocating Compressor

Laboratory data were used to characterize the effect of various adjustable speed drives on the overall isentropic efficiency of the test compressor. The compressor isentropic efficiency was measured during both heating and cooling mode optimal flow control tests and is plotted as a function of compressor drive frequency in Fig. 6. The lower curves in Fig. 6 represent the efficiency losses of the PWMI and the efficiency losses of the compressor and induction motor due to harmonics of the PWMI. The sum of the lower two curves in each cooling and heating mode plot therefore represents the combined compressor, motor, and drive efficiency losses.

Compressor and M-G drive. The compressor isentropic efficiency remained fairly constant from 60 to about 20 Hz (i.e., one-third nominal speed), with the compressor driven by the M-G set. At 15-Hz speed, the efficiency decreased 20% from the efficiency measured at 60 Hz. The rapid drop in efficiency for constant torque application below 20% speed was similar to results observed by Skogsholm,[11] and was partly due to an increase in the relative slip.

Compressor and PWMI drive. Efficiency trends with the PWMI drive were similar to those observed with the M-G drive; however, the losses in compressor isentropic efficiency due to the PWMI drive increased as speed decreased. In Fig. 6, results of testing at 60-Hz drive frequency and 40°F (21°C) outdoor temperature indicated that compressor efficiency, with the PWMI drive efficiency included, dropped 12% from that with the M-G drive. Roughly half of the efficiency degradation was due to efficiency losses in the PWMI (i.e., 5% loss), and the remainder was due to the effect of inverter harmonics on the compressor and motor as depicted by the efficiency loss curves in Fig. 6. Similar results were also observed in the cooling mode for tests conducted at 82°F (28°C) outdoor temperature and 60-Hz drive frequency.

At 15-Hz drive frequency, the compressor efficiency losses due to the PWMI drive increased to 25% in the heating mode and to 30% in the cooling mode. The efficiency losses from only the inverter ranged from 5% at 60 Hz, near full-rated load, to 7.5% at 15 Hz, and therefore did not nearly account for the total losses as speed was reduced (Fig. 6). The observed increase in efficiency losses was a result of the effect of current harmonics on the induction

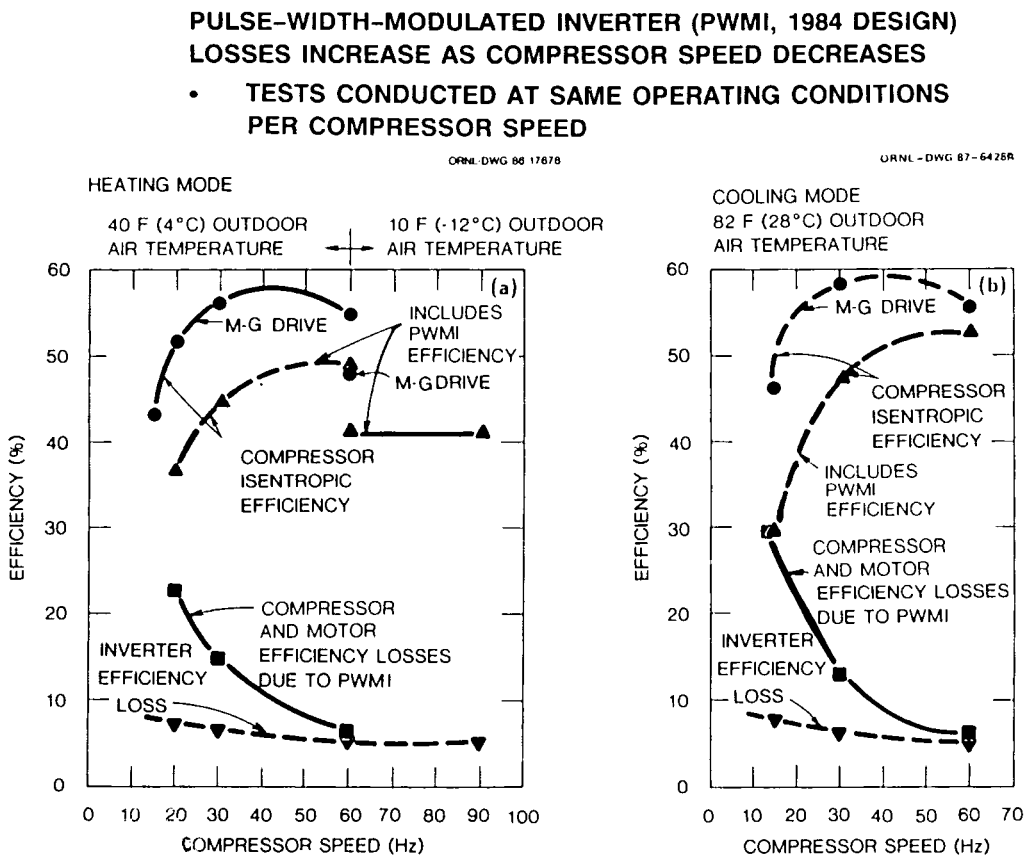

Fig. 6. Compressor isentropic efficiency and efficiency losses measured during steady state optimal flow control testing of the CVSHP.

motor of the compressor. Mohan[12] attributed the increase in induction motor losses due to inverter harmonics to be principally a result of increased stator and rotor winding losses and stray load losses.

These high-frequency harmonics of the PWMI can lead to excessive losses by imposing a series of high-voltage impulses on the motor windings. Andreas[13] stated that these high-frequency currents tend to be concentrated in areas of high flux density and to result in heat generation that increases motor winding temperature, which will in turn lead to additional suction gas superheating prior to compression. Jacobs[14] determined experimentally that as the amount of superheating increases, the effective compressor efficiency decreases [i.e., observed a 2% loss in compressor performance for every 10 F° (5.5 C°) rise in suction temperature]. Therefore, the harmonic content of the PWMI drive (a direct loss in motor efficiency) and the resultant additional suction gas superheating combine to result in the drop in compressor isentropic efficiency shown in Fig. 6.

Compressor and VSI drive. Testing with the VSI drive caused a noticeable drop in compressor isentropic efficiency similar to that of the PWMI drive as compressor speed was reduced. At 60 Hz for both heating and cooling mode tests, the isentropic efficiency was 10% below that measured with the M-G drive. At 50% speed (i.e., 30-Hz speed) the compressor efficiency losses due to the VSI increased to 30% in heating mode and to 20% in cooling mode. Further lowering of the compressor speed to 15 Hz resulted in even larger efficiency losses of roughly 35%. The increase in compressor efficiency losses as speed is reduced is due to the effect of harmonics produced by the VSI drive. The VSI produced fairly high third, fifth, seventh, eleventh, and thirteenth harmonic currents for all modulation frequencies. These harmonics do not contribute to the output torque and result in increased motor losses and motor temperature, both of which decrease the compressor isentropic efficiency.

Characterized the Magnitude of Compressor Efficiency Losses Resulting from First Generation Inverter Drives

Compressor efficiency losses measured with specific models of both PWMI and VSI style inverters operating at nearly identical conditions are plotted in Fig. 7. It must be noted that this comparison should not be generalized due to the continuing advancement of both VSI and PWMI designs and the specific technologies of the components utilized. Also, the effect of harmonic currents would be different with a different motor design. Mohan[12] indicated that induction motors with high values of leakage reactance (i.e., leakage flux through airgap that leads magnetizing current by 90°) will have less harmonic currents and lower harmonic losses. With due regard for the above caveats, results in Fig. 7 show that in the cooling mode at near full load, the compressor efficiency losses due to the PWMI were similar to losses due to the VSI. In the heating mode, the PWMI caused roughly 30% less compressor efficiency losses for drive frequencies of 20 and 30 Hz. Compared with the results shown by Skogsholm[11] and Lloyd,[15] both of which compared PWMI with VSI, the micro-processor control of the PWMI voltage pulse rate reduced current harmonics and improved PWMI efficiency to levels comparable to, if not better than, VSI designs of the late 1970s. The results shown here indicate the magnitude of losses to expect with these first generation drives. Rice[16] has shown that an advanced prototype variable speed motor and inverter drive (i.e., permanent magnet electronically commutated motor) would have a combined efficiency even higher than that of an induction motor with ideal induction motor drive (M-G set).

Characterized Efficiency Limits of First Generation Variable Speed Indoor Blower

Measured efficiency of the combined blower and blower motor when driven by the M-G drive with optimal voltage control was compared with measured efficiencies when the blower was driven by the VSI. The blower and drive system (motor and inverter) efficiency trends for the VSI drive and for an assumed 100% efficient VSI drive were calculated using measured single-phase input and and three-phase output power, respectively (Fig. 8). The combined blower and blower motor efficiency for the 100% efficient VSI was only 5% less than that measured with the blower driven by the M-G set with optimal voltage control. This small difference indicates

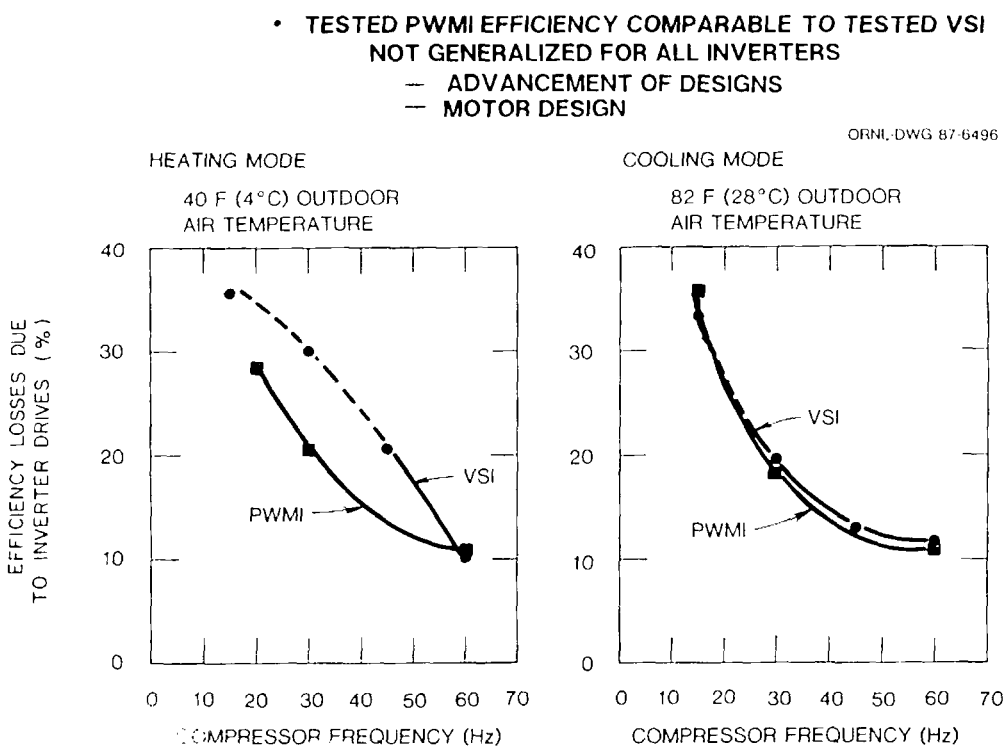

Fig. 7. Combined compressor, compressor motor and inverter efficiency losses for first generation inverter drives.

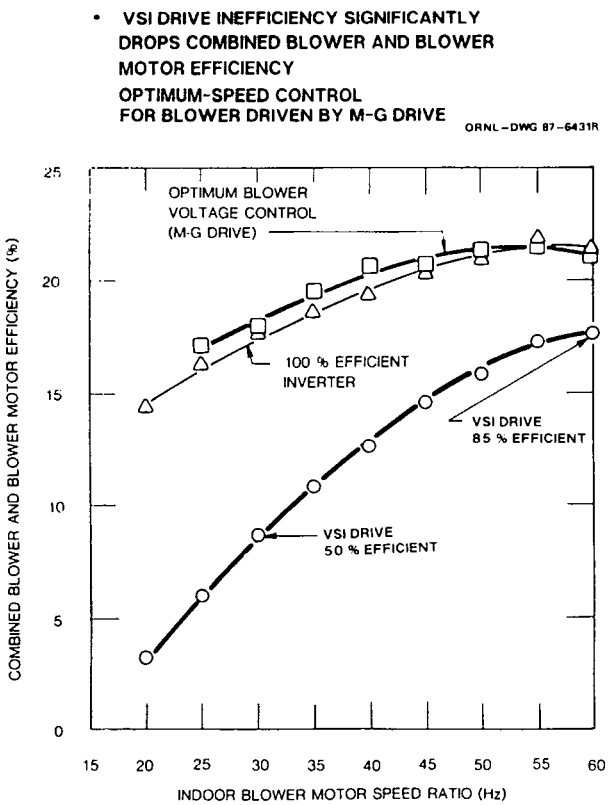

Fig. 8. Combined blower and blower motor efficiencies observed for VSI drive and M-G drive, both having optimal voltage control.

that the choppy waveform of the VSI had little effect on blower motor efficiency because the power measurement included inverter harmonics.

Similar trends for another VSI-inverter-driven and sine-wave-driven induction motor were observed by a motor/control manufacturer as reported by Rice.[16] In the data shown by Rice,[16] the efficiency of a three-phase, 1/3-hp (0.25-kW) induction motor (driven by M-G) dropped from 75% at full speed (1075 rpm) to 40% at one-third of full speed (400 rpm). The drop in motor efficiency was caused by the fixed losses of the stator core becoming a larger percentage of the total losses at reduced power output (i.e., power reduces roughly by the cube of the speed). Motor slip has little effect on efficiency as speed drops, because the torque drops as the speed squared and therefore the relative slip does not increase as in a constant torque application.

The combined blower and VSI drive system efficiency dropped sharply compared with efficiency observed for the M-G driven motor with optimal voltage control. At 60-Hz drive frequency, the VSI was measured to be 85% efficient. The VSI inefficiency and VSI harmonics caused the efficiency at 60 Hz to be 16% less than that measured with the blower driven by the optimally controlled M-G set. Decreasing the blower speed to 20 Hz caused these losses to increase (Fig. 8) resulting in roughly a 77% drop in combined blower and blower motor efficiency compared with that of the M-G set.

Characterized the Frosting Dynamics of the CVSHP

Tests conducted at 35, 25, and 17°F (1.7, -3.9, and -8.3°C) outdoor temperature and 80% relative humidity revealed slight degradation in COP and heating capacity due to frosting of the outdoor coil. The density of refrigerant entering the compressor remained fairly constant over time for each test; as a result the evaporator capacity did not drop appreciably. The near constant refrigerant density caused the refrigerant mass flowrate and compressor power to be only slightly affected by frosting of the outdoor coil. Therefore, only marginal drops in COP and capacity were observed despite the accumulation of frost on the slanted outdoor heat exchanger, which had 13 wavy fins per inch. The defrost interval, defined as the time between defrosts, is carpet plotted in Fig. 9 as a function of both compressor drive frequency and outdoor temperature for a relative humidity of 70%. An operating line for simulated CVSHP operation in Nashville, Tennessee, is also shown in Fig. 9.

The operating line in Fig. 9 shows that a minimum defrost interval occurs at 60-Hz drive frequency and 21°F (-6.1°C) outdoor air temperature. Reducing the compressor speed along the operating line increases the defrost interval due to the increase in evaporator temperature as speed decreases. Overspeeding above 60 Hz operation in Nashville would occur at outdoor temperatures less than 21°F (-6.1°C). Therefore defrost intervals increase because the ambient air holds very little moisture.

Each frosting test was followed by an automatically initiated demand defrost based on outdoor coil air pressure drop. Visual observations indicated that the outdoor coil was heavily frosted at the start of each defrost. As seen in Fig. 9, reducing the outdoor temperature and/or the compressor drive frequency caused significant increases in the time to defrost initiation. Figure 9 indicates that no frosting of the outdoor coil would occur at 15°F (-9.4°C) or less with the compressor driven at modulation frequencies less than 60 Hz.

Characterized CVSHP Demand Defrosting Dynamics and Improved Defrosting Efficiency

Tests were conducted where the compressor drive frequency was increased to 90 Hz and/or the indoor variable area throttle was controlled

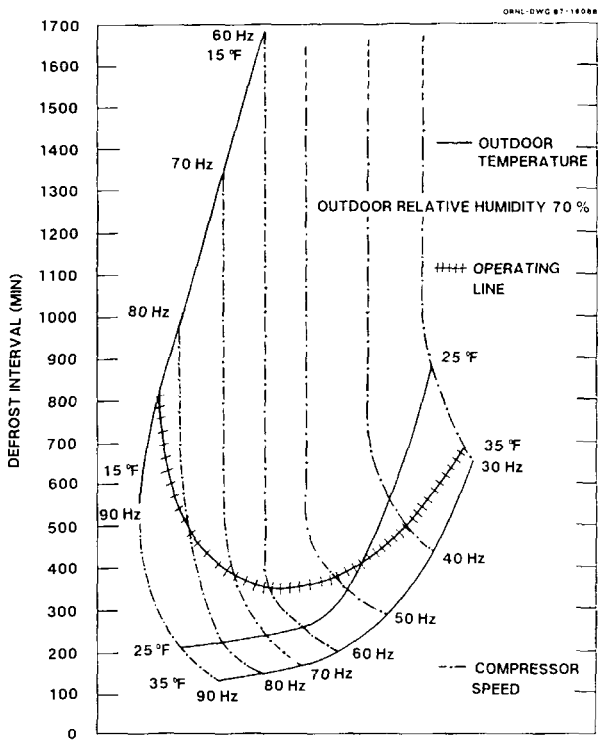

Fig. 9. Defrost intervals as a function of compressor drive frequency and outdoor air temperature with relative humidity held constant at 70%. Operating line is for simulated CVSHP operation in Nashville, Tennessee.

to determine any improvement in defrost efficiency due to these actions. Defrost data and test results are listed in Table 2. Data in Table 2 are from defrost tests that immediately followed frosting tests conducted at 60-Hz compressor speed and 35°F (1.7°C) temperature.

TABLE 2
Defrost efficiency as affected by flow area of the indoor throttle and compressor overspeeding

Laboratory data	Compressor frost/defrost speed (Hz) 60/60		60/90	
Effective throttle area (in.^{2})	0.06	0.10	0.06	0.10
Defrost interval (min)	105.50	104.80	99.10	102.40
Defrost time (min)	5.70	4.80	5.30	4.50
Defrost power (W-H)[a]	210.30	190.00	280.60	244.20
Frost/Defrost COP[b]	2.22	2.27	2.18	2.20

[a] Measured power consumption of compressor and indoor blower.

[b] Integrated average COP inculdes 5 kW of auxiliary heat during defrost period.

Previous work by Miller[17] indicated that increasing the effective flow area through the indoor throttle, active in defrost mode, would improve defrost efficiency by increasing refrigerant flow during the first few minutes of defrost. The defrost intervals for tests listed in Table 2 are similar, indicating similar frost loads. Roughly doubling the flow area through the indoor throttle caused the defrosting time to decrease 15% and the defrost power to decrease roughly 10% compared to tests with fixed throttle opening. This control resulted in a 2% increase in COP (including 5 kW of auxiliary heat), integrated over the frosting and defrosting cycles. Doubling the throttle flow area and overspeeding the compressor to 90 Hz during defrost caused a 1% drop in integrated average frost/demand defrost COP as compared to defrosting at 60 Hz.

The works of Kuwahara et al.[6] and Itoh[18] indicated improvement in defrosting and system efficiency through compressor overspeeding and control of the throttle flow area during defrosting. Glamm[7] indicated only slight improvement in average frost/demand defrost COP resulting from control of the throttle flow area. The results in Table 2 indicate, for the given configured system, that the best average frost/defrost COP results by increasing the flow area of the indoor throttle and by operating the compressor at 60-Hz drive frequency during defrosting. Further testing also revealed that regardless of compressor drive frequency prior to the defrost cycle, the best average frost/demand defrost COP was observed with the compressor driven at 60 Hz during defrosting.

Characterized CVSHP Cycling Dynamics and Improved Cycling Efficiency

The slow response of the test unit at speeds less than 60 Hz caused an increase in the degradation coefficient (C_D) for normal mode cycling (i.e., compressor and fans cycle on and off simultaneously), as seen in Table 3. Attempts were made to improve cycling efficiency by initially increasing the area of the throttle at start-up. Heating mode results indicated that the larger flow area only increased the level of refrigerant in the accumulator after start-up (visually observed through sight glasses on the accumulator) and caused a decrease in cycling efficiency. In cooling mode the refrigerant charge was more evenly distributed between the heat exchangers prior to start-up. At start-up the larger flow area through the indoor throttle caused less restriction to the flow and allowed the compressor to more rapidly establish charge distribution. Therefore, by controlling the indoor throttle, the C_Ds measured during low compressor speed operation were improved for normal cooling mode cycling.

TABLE 3
Degradation coefficients (C_D) observed for various compressor speeds and cycling strategies

Mode of operation	Compressor speed (Hz)	C_Ds for various cycling control strategies				
		Normal		Overspeed 20S[a]	Refrigerant control, blower delay (off-cycle)	
Expansion valve setting		Fixed	Variable	Fixed	Fixed	Variable
Heating	60	0.225			0.113	
	30	0.329	0.391	0.295	0.215	0.133
	15	0.405				
Cooling	60	0.169			0.060	
	30	0.365	0.237			
	15	0.362	0.217	0.209	0.162	0.102

[a]At start-up the compressor is driven at 60 Hz for 20 S.

Cycling control strategies. Heating and cooling mode tests were conducted with the refrigerant isolated in the system high-side during the off-cycle and with the indoor blower continuing to operate for 2 min into the off-cycle. At start-up the throttle was controlled for best cycling efficiency. The results of both heating and cooling mode tests with refrigerant migration and throttle control are displayed in Fig. 10 and are compared to normal mode cycling test results.

Heating mode cycling test results in Fig. 10 reveal significant improvement in efficiency. The tests, conducted at 30-Hz compressor drive frequency, show the CVSHP to achieve near steady state performance in roughly 10 min by controlling the off-cycle refrigerant migration. The C_D decreased from 0.329 for normal mode cycling to 0.133 with combined control of off-cycle migration, 2 min of indoor blower delay, and throttle control (Table 3).

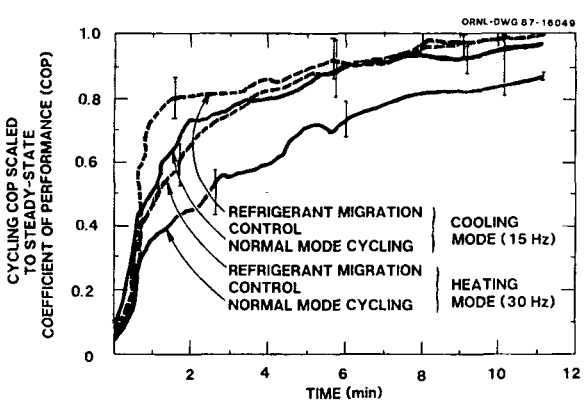

Fig. 10. Improvement in heating and cooling mode cycling COP. Cycling rate 12 min on, 48 min off.

Cooling mode cycling test results with refrigerant migration and throttle control observed at 15-Hz compressor drive frequency were not as dramatic as results observed in the heating mode. However, off-cycle control of refrigerant migration did improve the cycling COP of the CVSHP (Fig. 10). The C_D decreased from 0.362, for normal mode cycling at 15-Hz speed, to 0.102, for cycling with off-cycle migration control, 2-min delay in indoor blower operation, and throttle control (Table 3).

Seasonal Performance Analyses for SSHP and CVSHP

Comparisons of seasonal performance simulations were made for the different heat pump configurations listed in Table 4. Steady state COPs of each system were based on the compressor and indoor blower both powered by ideal induction motor drives (i.e., sine-wave driven). A conventional SSHP,[f] having capillary tube flow control and a 90-min time/temperature defrost control, was compared with the optimally controlled CVSHP operating only at 60 Hz drive frequency (i.e., single-speed unit with optimal flow control and reduced dynamic losses).[17] The optimally controlled breadboard CVSHP, having reduced dynamic losses, was then compared with the CVSHP operating only at 60-Hz drive frequency (i.e., optimal control single-speed) to quantify the benefit of modulation on a seasonal

f Actually the original unmodified CVSHP operated with the compressor driven by 60-Hz sine wave.

TABLE 4
Heat Pump Systems used in APF Comparisons, Compresor and Fans Sine-Wave Driven

Heat Pump System	Refrigerant Flow Control	Indoor Airflow	Cycling C_D Heat	Cycling C_D Cool	Defrost Control	COP[a] Heat	EER[b] Cool
Conventional Single-Speed	Capillary	Constant	0.25	0.18	90-min Time & Temperature	3.0	8.70
Optimal Control Single-Speed	Variable Area	Constant	0.11	0.06	Demand	3.1	9.66
CVSHP	Variable Area	Variable	0.13	0.10	Demand	3.1	9.66

[a]Heating COP measured at 47 F (8.3°C) outdoor air temperature (60-Hz compressor drive frequency).

[b]Cooling EER measured at ARI rating point of 80 F (27°C) DB/67 F (19°C) WB indoor and 82 F (28°C) outdoor temperature (60-Hz compressor drive frequency).

basis for the particular system tested. For the seasonal simulations the CVSHP modulation ratio was 3:1 (90- to 30-Hz compressor speed) in heating mode and 4:1 (60- to 15-Hz compressor speed) in cooling mode.

Total annual energy use due to frosting/defrosting, cycling, and supplemental heat was calculated for the heat pump systems (Table 4), operating in Fort Worth, Knoxville, and Syracuse. Energy use for each of the loss categories along with steady state and total annual operating energy use are listed in Table 5.

SSHP reduced dynamic losses. Only 1% of annual energy consumption was attributable to frosting. Demand defrost control as compared to a 90-min time-temperature defrost control reduced the number of seasonal defrosts by roughly a factor of 3 for all three locations. Both demand defrost control and improvement in defrost efficiency[g] caused the frosting/defrosting energy consumptions for an optimally controlled SSHP to be roughly half that observed for an SSHP, having fixed throttle and time-temperature defrost control.

The combined control of off-cycle refrigerant migration and delay in shutdown of the indoor blower substantially reduced cycling losses for the optimally controlled SSHP by roughly 50% for simulated operation in Fort Worth, Knoxville, and Syracuse (Table 5).

CVSHP modulation effect. The added feature of continuous modulation of the compressor and indoor blower motors further improved system efficiency significantly as seen by the reduction of energy consumption (Table 5). This improvement in system efficiency can be attributed to (1) reduced supplemental heat, (2) reduced cycling losses, (3) heat exchanger unloading, and (4) reduced frosting/defrosting losses as explained in the following paragraphs.

Reduced supplemental heat. Overspeeding the compressor reduced the balance point of the CVSHP as compared with the optimally controlled SSHP and reduced the amount of supplemental heat required to match load (i.e., balance points listed in Table 5). In the more severe winter climate of Syracuse the CVSHP reduced supplemental heat usage by 43%. The compressor overspeeding capability would also reduce the peak power demand for the public utility company.

Reduced cycling losses. For operation at ambient temperatures greater than the balance point, the better load following capability of the CVSHP reduced cycling losses simply by reducing the number of cycles. Assuming both configured heat pumps to have reduced dynamic losses, compressor and indoor blower speed modulation decreased cycling energy consumption roughly by 40% of cycling energy for the optimally controlled SSHP.

g Throttle fully open during defrost to increase refrigerant circulation for improved defrost efficiency.

TABLE 5
Simulated annual energy use breakdown for single-speed heat pump and continuously variable speed heat pumps

City and state	Heat pump configuration	Heating balance point [F (°C)]	Annual back-up heat[a] (kWh)	Dynamic loss energy		Steady-state energy (kWh)	Total annual energy[d] (kWh)	Yearly defrosts	Annual performance factor (APF)
				Fr/Def[b] (kWh)	Cycling[c] (kWh)				
Ft. Worth, Tex.	Conventional single-speed	21.0 (-6.1)	94.5	437.3	1257.7	9032.4	10822.0	519	2.13
	Optimal control single-speed	21.0 (-6.1)	91.6	140.7	549.0	8332.6	9114.0	139	2.52
	CVSHP	17.5 (-8.1)	30.3	97.2	293.0	6742.3	7162.8	105	3.21
Knoxville, Tenn.	Conventional single-speed	22.0 (-5.6)	234.7	784.1	1278.5	7502.2	9799.4	911	2.03
	Optimal control single-speed	22.0 (-5.6)	244.9	338.0	594.7	6815.0	7992.6	304	2.49
	CVSHP	18.0 (-7.8)	94.1	225.7	345.0	5618.3	6283.2	236	3.16
Syracuse, N.Y.	Conventional single-speed	27.0 (-2.8)	3073.2	1994.7	1156.3	10232.3	16456.5	2008	1.73
	Optimal control single-speed	27.0 (-2.8)	3178.1	1192.8	545.4	9555.2	14471.6	855	1.97
	CVSHP	21.0 (-6.1)	1806.3	950.8	321.0	9344.0	12422.2	847	2.30

[a] Auxiliary heat required to satisfy house heating load when heat pump operates below balance point. Does not include auxiliary heat (5 kW) attributed to defrost.

[b] Frosting/defrosting includes recovery energy following defrost and 5 kW of auxiliary heat during reverse-cycle defrost.

[c] Cycling includes off-cycle parasitics.

[d] Heat pump yearly energy consumption including back-up heat.

Heat exchanger unloading. Modulating the CVSHP at low loads reduced the condensing and raised the evaporating pressure (heat exchanger unloading) and thereby improved steady state COP as previously observed by Miller.[9] This heat exchanger unloading yielded the largest reduction in heat pump energy usage for Fort Worth and Knoxville. The steady state energy consumption of the CVSHP was reduced by 19% compared with the optimally controlled SSHP in Fort Worth. In Knoxville, the steady state usage was reduced by 17.5%, and in Syracuse, by only 2%. The small reduction in Syracuse probably occurred because the majority of load hours occurred at nominal compressor speed (i.e., 60-Hz drive frequency) in this predominantly heating load climate.

Reduced frosting/demand defrosting losses. The frosting/demand defrosting efficiency of the CVSHP improved slightly over that of the optimally controlled SSHP. A maximum decrease in frost/demand defrost energy consumption of 30% was observed for the CVSHP in Knoxville as compared with the optimally controlled SSHP. The number of simulated defrosts in Knoxville for the CVSHP was 236 as compared with 304 defrosts for the SSHP. During low-speed modulation the evaporator temperature increased and therefore the defrost interval increased resulting in the reduced number of seasonal defrosts. In Syracuse the number of defrosts were nearly equal, again probably because the majority of heating load hours occurred at nominal compressor speed (i.e., 60-Hz drive frequency).

Benefits of the CVSHP

The seasonal analysis results for simulated operation in Syracuse showed that a CVSHP improved annual performance factor (APF) 16% compared to an optimally controlled SSHP. The test CVSHP operating in Knoxville or Fort Worth would improve APF roughly 27%. The major improvement in seasonal efficiency in the moderate climates resulted from the ability to unload the heat exchangers during low load operation. In the predominantly heating load climate of Syracuse, the major improvement resulted from the reduction of supplemental heat usage. The CVSHP reduces dynamic losses roughly 50 to 70% of dynamic losses observed for the optimally controlled SSHP.

CVSHPs offer other benefits that are not easily quantifiable. In the heating season the CVSHP can reduce utility peak demand by overspeeding the compressor. In the cooling mode the CVSHP's near constant operation would help improve humidity control as compared to an SSHP. Also the fewer number of on/off and defrost cycles would improve compressor reliability. Finally, the CVSHP could be used for zone control by adjusting capacity appropriately for the zoned load.

Future Activities

A compressor calorimeter, having a capacity range of 6 to 50 kBtus, is currently being installed for the testing of variable speed compressors. The test facility will provide the capability to generate a more complete data base for state-of-the-art variable speed compressors as described further by Rice,[2] and will allow improvement of present modulating compressor submodels for the ORNL modulating heat pump analytical design tool package. Modulating scroll and rotary compressors are planned to be tested during the upcoming year. Compressor testing may also be conducted with alternative refrigerants that could substitute for fully halogenated CFC refrigerants.

A request for proposal is being issued for experimental evaluation of the performance of state-of-the-art variable speed Japanese heat pumps. Tests will be conducted to characterize the system performance under steady state, cycling, and frosting/defrosting conditions.

References

1. W. A. Miller, *Laboratory Study of the Dynamic Losses of a Single-Speed, Split System Air-to-Air Heat Pump Having Tube and Plate Fin Heat Exchangers*, ORNL/CON-253, Oak Ridge National Laboratory, Oak Ridge, Tenn. (to be published).

2. C.K. Rice, "Capacity Modulation Component Characterization and Design Tool Development," *Proc. of the ORNL/DOE Heat Pump Conference*, April 17-20, 1988.

3. D.G. Erbs, C.E. Bullock, and R.J. Voorhis, "New Testing and Rating Procedures for Seasonal Performance of Heat Pumps with Variable Speed Compressors," *ASHRAE Trans.*, 92 (Pt. 2), 1986.

4. N. Tanaka and G. Yamanaka, "Experimental Study on the Dynamic Characteristics of a Heat Pump," *ASHRAE Trans.*, 88 (Pt. 2) (1982).

5. W. A. Miller, "The Laboratory Evaluation of the Heating Mode Part-Load Operation of an Air-to-Air Heat Pump," *ASHRAE Trans.*, 91 (Pt. 2B) (1985).

6. E. Kuwahara, T. Kawamura, and M. Yamazaki, "Shortening the Defrost Time on a Heat-Pump

Air Conditioner," *ASHRAE Trans.*, **92** (Pt. 2A) (1986).

7. P. Glamm, *Dynamic Control of Heat Pumps*, EPRI EM-5082, Electric Power Research Institute, Palo Alto, Calif., Project 2033-11.

8. C. K. Rice, S. K. Fischer, and C. J. Emerson, *The Oak Ridge Heat Pump Models: II. An annual performance factor/loads model for residential air-source heat pumps*, ORNL/CON-160, Oak Ridge National Laboratory, Oak Ridge, Tenn., to be published.

9. W. A. Miller, "Steady State Refrigerant Flow and Airflow Control Experiments Conducted on a Continuously Variable Speed Air-to-Air Heat Pumps," *ASHRAE Trans*, **93** (Pt. 2) (1987).

10. S. K. Fischer and C. K. Rice, *The Oak Ridge Heat Pump Models: I. A Steady-State Computer Design Model for Air-to-Air Heat Pumps*, ORNL/CON-80/R1, Oak Ridge National Laboratory, Oak Ridge, Tenn., August, 1983.

11. E. A. Skogsholm, "Efficiency and Power Factor for a Square Wave Inverter Drive," *IEE-IAS*, October 1978.

12. N. Mohan, *Techniques for Energy Conservation in AC Motor-Driven Systems*, EPRI EM-2037, Electric Power Research Institute, Palo Alto, Calif., 1981.

13. J. C. Andreas, *Energy-Efficient Electric Motors*, Marcel Dekker, Inc., New York, 1982.

14. J. J. Jacobs, "Analytical and Experimental Techniques for Evaluating Compressor Performance Losses," *Proceedings of the 1976 Purdue Compressor Technology Conference*, West Lafayette, Indiana, July 1976.

15. J. D. Lloyd, "Variable-Speed Compressor Motors Operating on Inverters," *ASHRAE Trans.*, **88** (Pt. 1) (1982).

16. C. K. Rice, "Efficiency Characteristics of Speed Modulated Drives at Predicted Torque Conditions for Air-to-Air Heat Pumps," *ASHRAE Trans.*, **84** (Pt. 1) (1988).

17. W. A. Miller, "Laboratory Examination and Seasonal Analysis of Frosting and Defrosting for an Air-to-Air Heat Pump," *ASHRAE Trans.*, **93** (Pt. 1) (1987).

18. H. Itoh, "Improvement of a Heat Pump Room Air-Conditioner by Use of Pulse-Motor-Driven Expansion Valve," *ASHRAE Trans.*, **92** (Pt. 92) (1986).

Capacity Modulation Component Characterization and Design Tool Development*

C. K. Rice
Oak Ridge National Laboratory
Oak Ridge, TN 37831

Objective

This effort has been focused on obtaining and evaluating modulating component and drive performance data for electric-driven, air-to-air residential heat pumps. The modulation means considered here are continuously variable-speed drives. The modulating performance data were obtained for purposes of:

- establishing a technology base for modulating components,
- providing a foundation for modulating model development, and
- screening compressor and drive types to be used in modulating system design assessments.

For the screening analyses, the relative performance of various compressors and drives was evaluated under appropriate modulating conditions. With the modulating components sufficiently characterized and the modulating models developed, the potential of advanced modulating heat pump systems for residential application can be assessed accurately.

Background

Preliminary capacity modulation assessment work was reported at the previous DOE/ORNL Heat Pump Conference.[1] In that work, annual performance gains of 36% (26.5% energy savings) compared to that of conventional single-speed heat pumps (with rather large cycling losses[a]) were predicted for a moderate climate. These predictions were based on early estimates of possible compressor and blower modulating-drive efficiencies, and they contained significant uncertainties with regard not only to drive efficiencies but also to basic hermetic reciprocating compressor performance over the assumed speed ranges. The dynamic losses for such modulating systems were likewise roughly estimated.

The need to better define modulating component performance led to the development, since the last conference,[1] of cooperative working arrangements between ORNL and manufacturers of modulating drives and compressors. From this industry cooperation, we have obtained performance data on:

- prototype permanent-magnet electrically commutated motor (PM-ECM) drives for compressor and blower applications,
- state-of-the-art inverter-driven induction motor (SOA IDIM) drives for compressor and blower application,
- reference sine-wave-driven induction motor (SWDIM) drives for first-generation and SOA modulating compressors,
- modulating reciprocating and scroll compressors driven by reference variable-frequency sine-wave power, and
- a modulating rotary compressor driven by a PM-ECM.

These data were augmented with modulating compressor and blower data taken by Miller[2] using first-generation IDIM and reference SWDIM drives in a continuously variable-speed heat pump (CVSHP).

Current Status

Modulating Drive Data

The preliminary ORNL modulating model[1] was modified to allow prediction of the compressor speed/torque requirements for heating and cooling mode operation.[3] With these speed/torque requirements established, operating efficiencies were evaluated for prototype PM-ECM, SOA IDIM, and reference SWDIM drives. These results were used in conjunction with the data taken by Miller[2] to obtain modulating drive (combined motor and inverter) efficiency comparisons over a range of technology levels.[3]

The resultant range of compressor drive efficiencies is shown in Fig. 1 for heating and cooling mode operation. Similar comparisons are shown in Fig. 2 for blower drives. Also shown in Figs. 1 and 2 are the initial assumed drive efficiencies of the preliminary ORNL analytical study[1] that were to have approximated advanced PM-ECM drive performance.

---

*Research sponsored by the Office of Buildings and Community Systems, U.S. Department of Energy, under Contract DE-AC05-84OR21400 with Martin Marietta Energy Systems, Inc.

[a]Equivalent cyclic degradation coefficients between 0.25 and 0.35 (including crankcase heater effect).

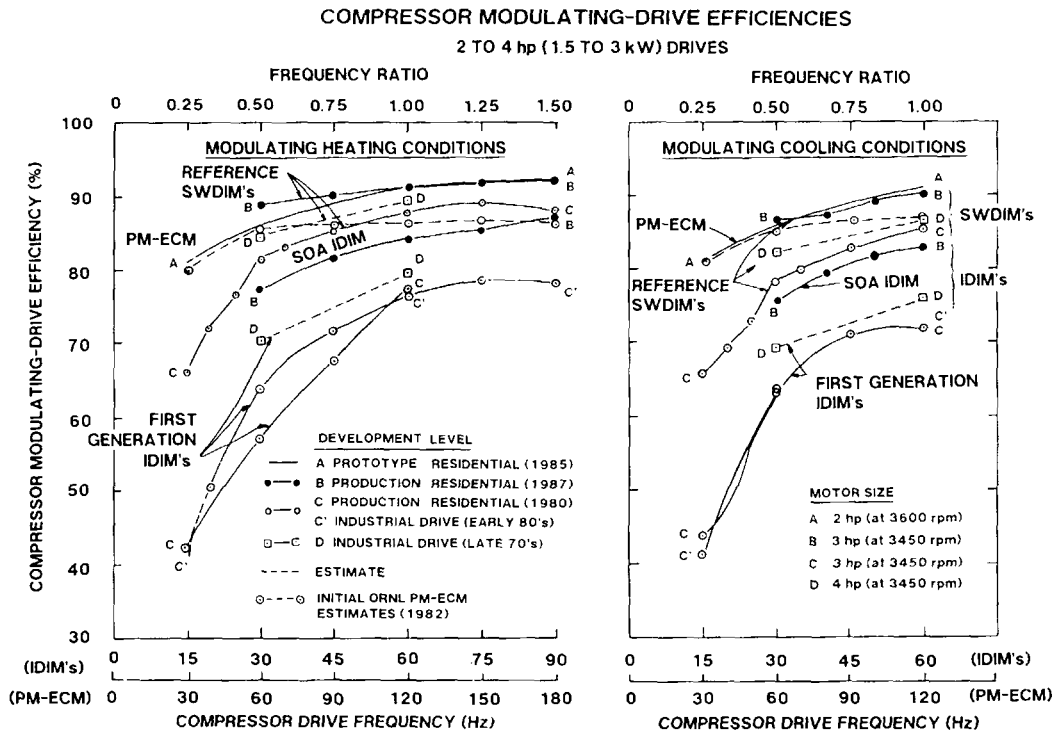

Fig. 1. Comparison of compressor modulating-drive system efficiencies vs frequency ratio / drive frequency for predicted modulating compressor load conditions.

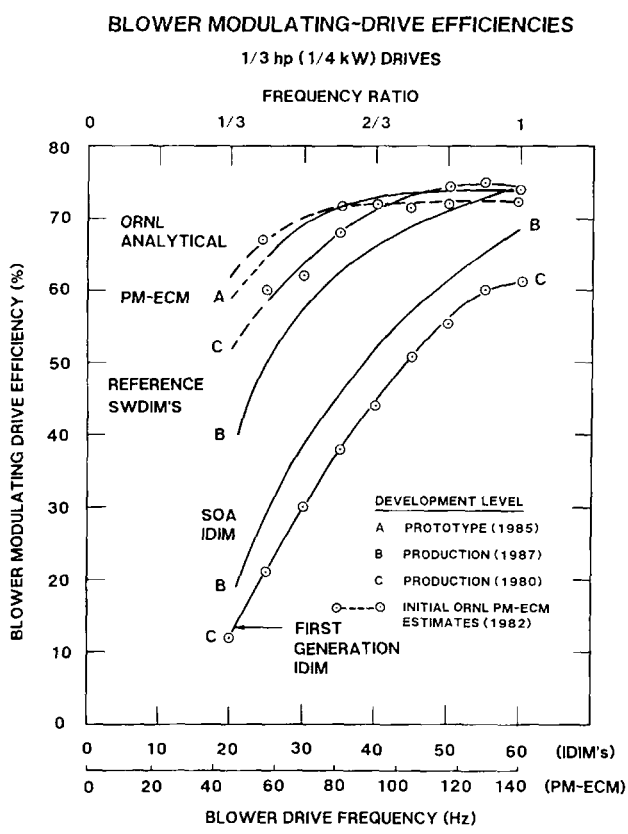

Fig. 2. Comparison of blower modulating-drive system efficiencies vs frequency ratio / drive frequency for typical modulating blower load conditions.

Modulating Compressor Data

Calorimeter data on hermetic reciprocating, rotary, and scroll compressors obtained from industry sources were reduced at ORNL to yield isentropic and volumetric efficiency values at discrete speeds as a function of saturation temperature and pressure ratio. From the preliminary modulating analysis,[1] predicted refrigerant conditions along the heating and cooling operating lines[3] were applied to the compressor efficiency data to obtain operating performance for speed ranges appropriate for each compressor.

These modulating results are shown in Figs. 3 and 4 where the isentropic and volumetric efficiencies, respectively, have been normalized to that of an SOA reciprocating compressor (compressor

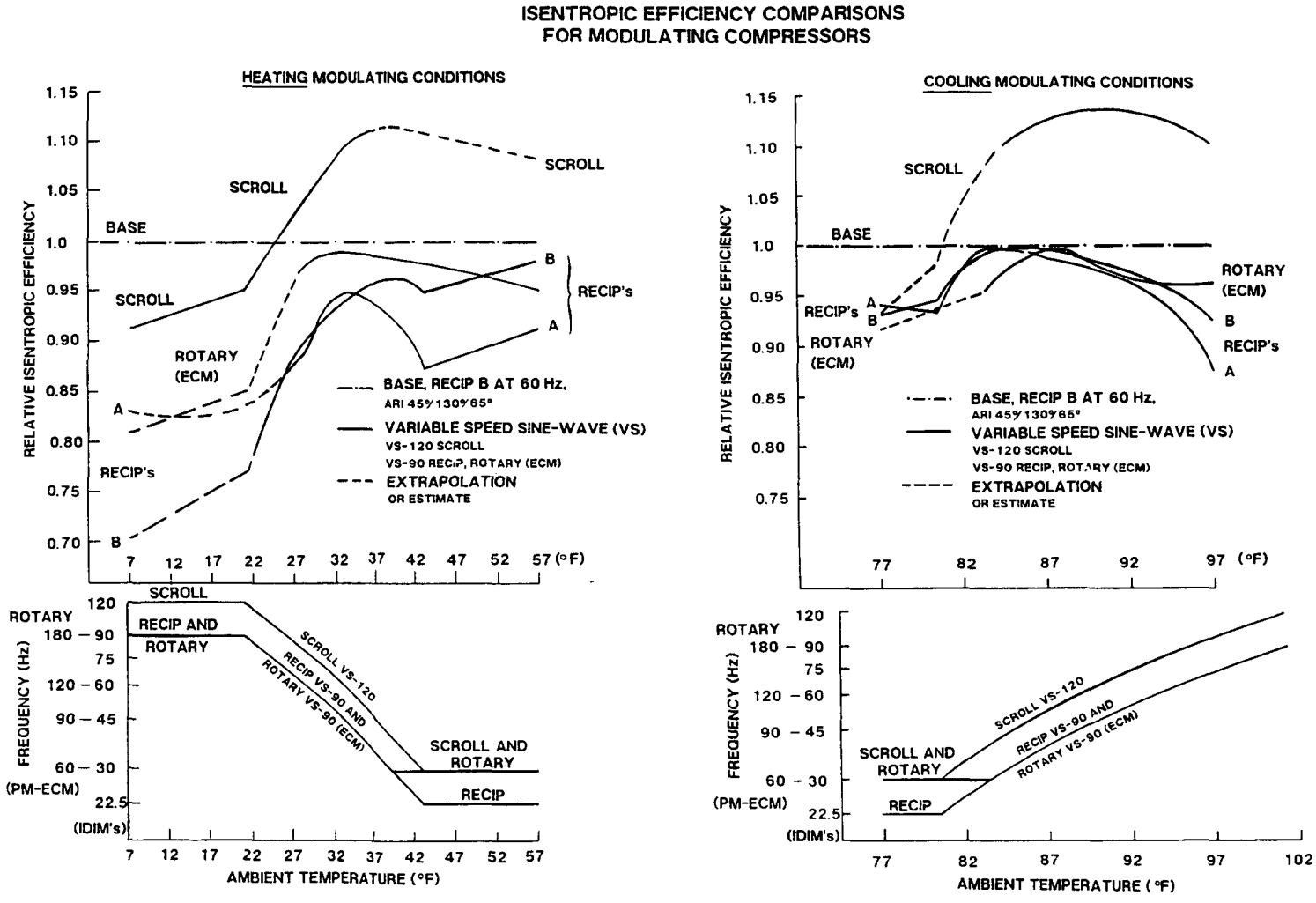

Fig. 3. Modulating compressor shell isentropic efficiency comparisons between sine-wave, frequency-modulated, scroll and reciprocating types (4 to 1 turndown ratios) and a PM-ECM modulated, rotary type (3 to 1 turndown ratio).

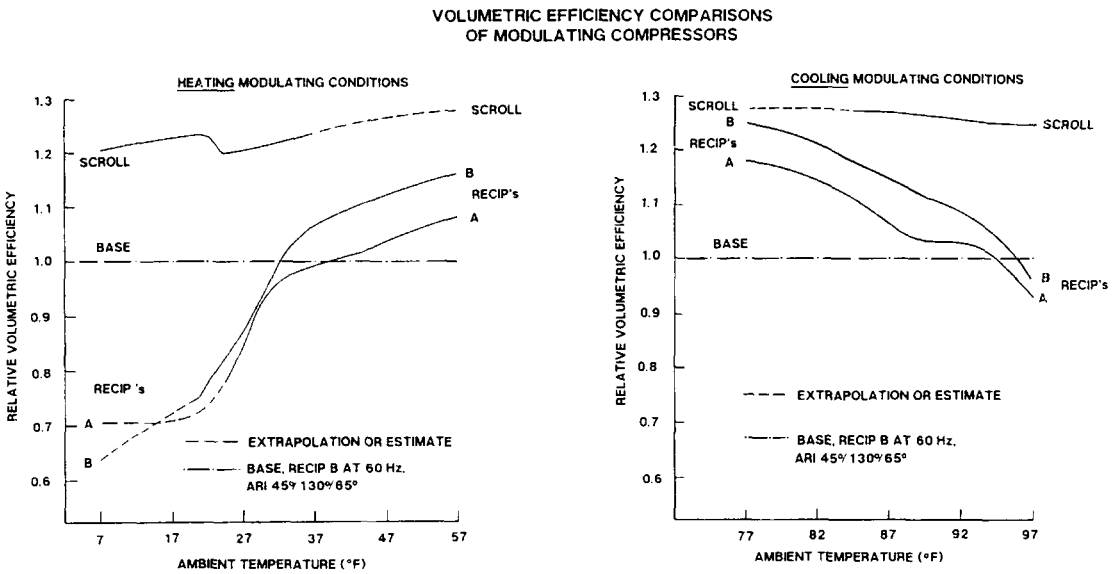

Fig. 4. Volumetric efficiency comparisons of modulating scroll and reciprocating compressors.

B operating at 60 Hz at the ARI cooling condition rating point[4]). In all cases, the compressors were driven by variable-frequency *sine-wave* power except for the rotary modulating case which was *PM-ECM* driven. Because all the compressors had approximately equivalent drive types, the differences in efficiency are mainly due to the specific compressor characteristics. Also shown in Fig. 3 are the frequency ranges used in the comparisons between compressor types.

In Fig. 5, comparable *single-speed* isentropic efficiency curves for the three types of compressors (at single-speed conditions but with three-phase motors) are added to those of Fig. 3. Also shown in Fig. 5, below the comparative efficiency curves, are the load-hour (load times hours) distributions for the assumed moderate climate (60% heating load) that were used to establish the heating and cooling operating lines.[1] These distributions can be used to determine the significance of the efficiency differences between compressors by noting the correspondence to the ambients where most heat pump output (load-hours) is required.

The results given in Figs. 3 and 4 were obtained from data sets that were each limited in some way (as noted by the dotted lines) as to the range of saturation temperatures and/or speed ranges over which the compressors were tested.[b] We are presently working to obtain more complete data sets -- both by further industry testing, where possible, and by complementary testing in our recently acquired modulating compressor calorimeter facility. Plans are to test additional selected modulating rotary, scroll, and possibly more reciprocating compressors, as they are available, over *appropriate speed ranges and operating* conditions. These tests will initially be with R-22 but will likely be expanded to alternative refrigerants or refrigerant mixtures as these become better identified.

[b]Also, the scroll and reciprocating compressors shown in Figs. 3 and 4 have approximately 4 tons of cooling capacity at maximum speed compared to 2 tons for the rotary. The effects of downsizing the reciprocating and especially the scroll compressors by a factor of 1/2 on the relative compressor performances remain to be evaluated.

Modulating Model Development

Curve fits to available calorimeter and application[2] data for reciprocating compressor A in Figs. 3-5 were used (as described by Miller[5]) in initial model validations against system laboratory data taken at ORNL[6] on a first-generation modulating heat pump. However, a more recent inspection of the triquadratic curve fits to the compressor data used there[5] indicated that some significant efficiency trends with speed were not being represented adequately. Through experience gained from different curve fitting attempts to more recently obtained reciprocating and scroll data, improved representations were achieved and implemented for, what we will call, the first level *modulating heat pump design model (MHPDM)*. These representations generally will improve the absolute validation comparisons given by Miller[5] (especially in the heating mode, where initial underpredictions were mainly due to compressor data curve fitting errors).

This first level MHPDM requires the user to input compressor map-based coefficients for power and mass flow rate (or alternatively, for derived isentropic and volumetric efficiency) at each speed for which sufficient data are available.

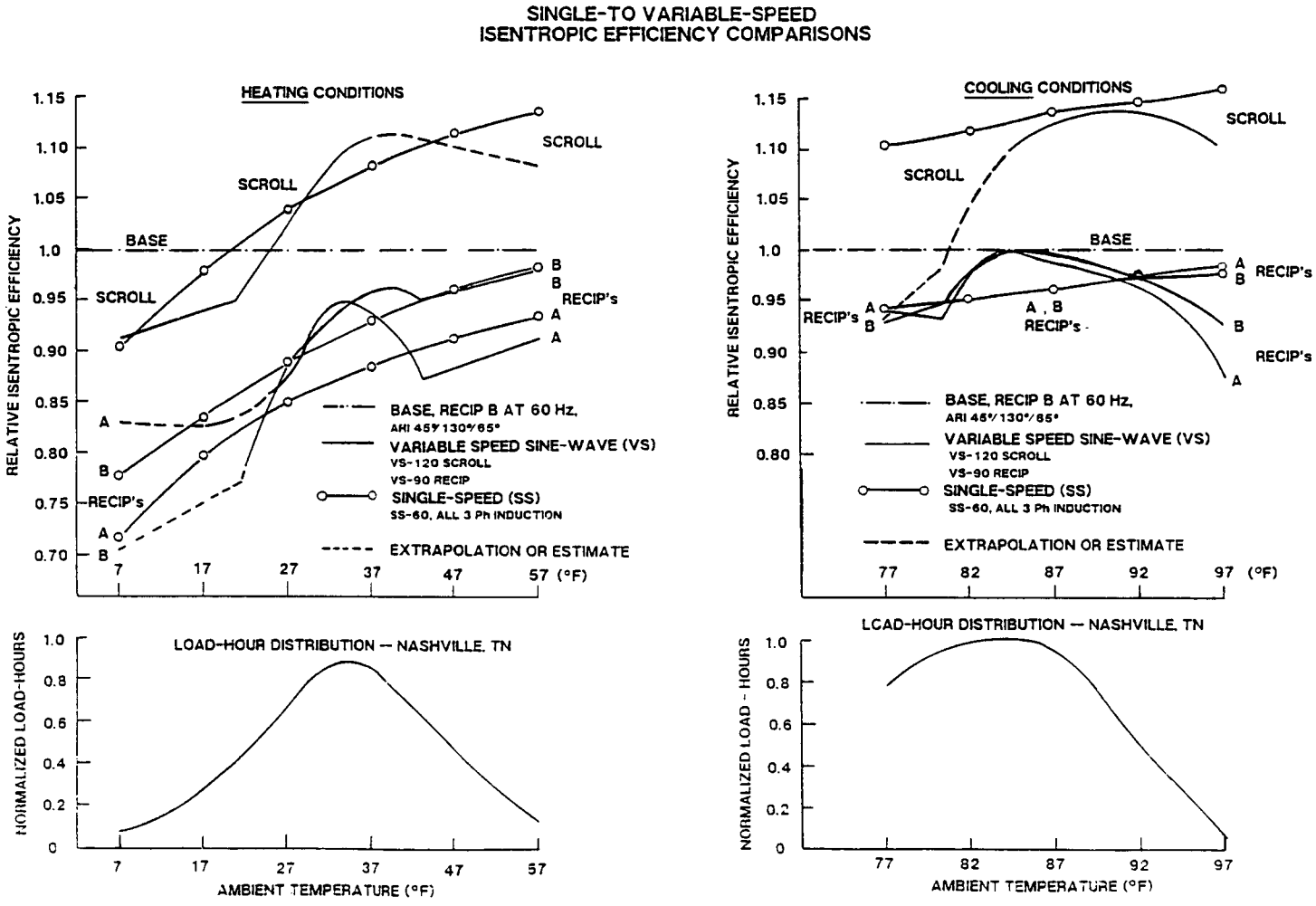

Fig. 5. Single(60 Hz)-to-variable speed compressor isentropic efficiency comparisons and corresponding load hour distributions for Nashville, Tenn.

In cases where minimal data are available, curve fits to the derived efficiency values have been found to give more reliable interpolations and extrapolations than similar representations based on basic power and mass flow data.

The supplied compressor data can be for an inverter-driven system, in which case the compressor map data are used directly, or for a reference SWDIM compressor. In the latter case, the user can have the program apply either first-generation or SOA inverter losses to the ideally driven (reference SWDIM) compressor. Alternatively, the user can use the SWDIM data directly to approximate performance with a PM-ECM compressor drive (as can be inferred from Fig. 1).

For the indoor blower and/or the outdoor fan, the user can select first-generation or SOA IDIMs or reference SWDIMs (again to approximate PM-ECMs as shown in Fig. 2).

In the second level modulating model (presently under development), the user will be able to replace the SWDIM compressor drive with a PM-ECM drive or another SWDIM drive (e.g., a more state-of-the-art modulating induction motor). This replacement option will allow the same basic modulating compressor characteristics to be applied with a different drive characteristic. In this way, calorimeter data on a given compressor can be generalized for significantly different drive combinations. We plan to use this version to more firmly establish the potential annual performance gains for ECM-driven reciprocating and scroll or rotary compressor combinations.

Modulating Design Tools

A key to the effective use of single-speed or modulating design models is a convenient yet flexible means to parametrically evaluate the effect of design, control, and operating variables. Such a "front-end" program is being made operational with the MHPDM for steady-state analysis with parametric evaluation of seasonal and annual performance to follow. The front-end program will allow use of the MHPDM and APF programs to parametrically generate sets of steady- state or seasonal performance data suitable for tabulation or for contour plotting with generally available PC contouring packages. Once these programs are sufficiently documented, they will be made available to the HVAC industry along with the second level modulating model.

A second generation Annual Performance Factor (APF)/Loads Model[7] to conduct seasonal performance analyses is presently operational but not yet fully documented. The second generation model includes the single-speed and variable-speed frosting and defrosting loss factors obtained by Miller[8,9] for a wavy fin outdoor heat exchanger with demand or timed[c] defrost operation. This version was used by Miller[5,9] to predict annual energy savings for modulating heat pumps based on laboratory measured steady-state and cycling performance improvements demonstrated at ORNL.[6,9]

[c]Single-speed case only.

Technical Accomplishments

The characterization and modeling work done since the last DOE/ORNL Heat Pump Conference[1] represents a logical complement to and progression from Miller's[5] laboratory and seasonal analysis of a first generation CVSHP with an ideally driven reciprocating compressor. In this project, data have been obtained and evaluated on advanced modulating drives capable of approaching (with SOA IDIMs) or exceeding (with PM-ECMs) the reference first-generation SWDIM performance obtained by Miller.[2] State-of-the-art and advanced compressors of three types have been characterized as to their relative modulating performance potential. Finally, a means of incorporating this data base into a modulating system model has been developed.

Summarized in this section are the more general results as well as some specific observations made in the course of the work on modulating component characterizations. The major features of the resultant first level MHPDM and related design tools are also described as are related applications to other projects. These data and programs provide the capability to look broadly yet accurately at important modulating system design issues.

Modulating Drives

Determined drive-efficiency characteristics for residential-sized compressors and blowers. These characteristics were shown in Figs. 1 and 2 for a range of technology levels (first-generation to SOA) at conditions representative of modulating system operation. The results indicate that advanced PM-ECM drives perform significantly better than first-generation and SOA IDIM drives.

Determined that PM-ECMs were the appropriate choice for advanced modulating system evaluation. Average reductions in seasonal component energy use with PM-ECMs in a moderate climate are summarized in Table 1. The energy savings are calculated for estimated average frequency ratios of operation for compressors and blowers. From this table and Figs. 1 and 2 the following conclusions can be made. *For a moderate climate*:

- PM-ECM compressor and blower drives offer average energy savings of more than 30 and 50%, respectively, over first-generation IDIM drives,[3]
- SOA IDIM drives can possibly provide up to two-thirds of the PM-ECM compressor energy savings but less than one-fourth of the ECM blower savings,[3]
- With first-generation modulating heat pumps, the drive inefficiencies take back essentially all of the 26.5% energy savings from heat exchanger unloading and from reductions in back-up heat and dynamic losses found in the preliminary ORNL modulation assessment.[1]
- PM-ECM drives perform at approximately the same level to better than ideally driven

Table 1. Estimated average reductions in component energy use with PM-ECMs (moderate climate)

Component	Estimated average frequency ratio	PM-ECM energy use reductions from base IDIMs	
		1st Generation	SOA
Compressor			
Heating	1/2	30%	10%
Cooling	1/3	25%	12%
Blower	1/2	57%	45%

(reference SWDIM), high-efficiency, three-phase induction motors and better than single-speed, single-phase induction motors (<85% efficient). On the basis of drive efficiency alone, PM-ECM-driven modulating systems would have an advantage in lowering peak cooling demand compared to single-speed (single-phase) systems.

Furthermore, from discussions of reliability and cost issues of PM-ECMs with manufacturers of both PM-ECM and IDIM drives, we concluded that ECM-driven compressors were an appropriate choice for use in the evaluation of advanced modulating systems.[3]

Identified modulating motor/drive design requirements. Through an analysis of compressor and blower torque loadings (as a function of speed) weighted by operating hours, we found[3] that:

- compressor drives should be designed for peak efficiency at or just below full load compressor torque and
- blower drives need performance maximized near 25% of full load compressor torque.

From this work, we also determined that compressor motors required to run 50% above nominal speed in cooling will require a motor twice as strong as if the motor is only required to be oversped at low ambients in the heating mode.

Modulating Compressors

Developed a set of representative operating conditions for modulating compressors. Starting from an optimized variable speed design,[1] we obtained contour plots of heat exchanger saturation temperatures and pressure ratio as functions of compressor frequency ratio and ambient temperature.[3] These plots were generated for both heating and cooling mode operation over reasonably wide speed ranges. As such, the contour plots serve as generalized mappings of approximate modulating compressor conditions ranging from fully loaded (high flow) to unloaded (low flow) heat exchanger operation.

Using these condition maps, we found that modulating compressors would experience the most operating hours at pressure ratios (P_r) near 2.0 in cooling mode and 3.0 in heating as compared to 2.6 and 4.0, respectively, for a comparable single-speed compressor. These results indicate that compressors for modulating heat pumps should be designed for best isentropic efficiency at pressure ratios around 2.5 (the average of the ratios over both modes) as compared to an average pressure ratio of 3.3 for the conventional single-speed application.

Conducted initial modulating compressor screening and quantified potential modulation advantages of scroll vs reciprocating compressors. From the compressor screening analysis, comparative modulating performance of three compressor types was obtained, as shown earlier in Figs. 3 and 4. In Fig. 3, the scroll compressor (overall) isentropic efficiencies are seen generally to exceed those of the reciprocating and ECM-rotary compressors by 10 to 15%. An exception to this occurs at the lowest speed, mild ambient cooling conditions, where the relative efficiencies are nearly equivalent.

With regard to volumetric efficiency comparisons, in Fig. 4 the reciprocating compressor trends (of increasing volumetric efficiencies at milder ambients) are seen to be opposite to modulating needs in both heating and cooling modes. In contrast, the volumetric trends for the scroll compressor were close to neutral. This volumetric advantage for scroll compressors (and to a similar extent for rotaries) will allow either a wider modulation capability over a given frequency range or will require less of a drive frequency range for the same modulation capability (e.g., approximately a 3:1 frequency ratio for a scroll compared to 4:1 for reciprocating).

Determined that modulating compressors have isentropic efficiencies approximately equivalent to those of single-speed compressors under their respective application conditions. This result is observed in Fig. 5 where isentropic efficiencies are compared for single and variable speed compressors (both with the same three-phase motors).

In general, the variable-speed compressors have efficiency advantages up to 5% (over the single-speed) for the ambient temperatures about which the required heat pump heating and cooling outputs (load-hour distributions in Fig. 5) are a maximum. At the milder and more severe ambients, the situation is reversed with the single-speed compressors having a slight advantage.

The major exception to this rough equivalence is for the scroll-to-scroll comparisons at low speed, mild ambient cooling conditions. Here the variable-speed scroll performance is 10 to 15% below that for a single- speed scroll. However, as will be shown in the next section, the heat exchanger unloading advantage of the modulating system at these conditions will more than offset the compressor efficiency loss. Even so, improved scroll compressor design for these mild ambient, low pressure ratio conditions (P_r less than 2.0) would further boost the modulating compressor isentropic efficiency at the low-speed cooling rating conditions (of 67 and 82°F). The use of by-pass ports to improve low-pressure ratio performance has been recently reported by the Japanese.[10]

Determined that the peak cooling demand of modulating systems can be equivalent to or lower than that of single-speed systems. At the maximum cooling design conditions (95°F for Nashville, Tenn.), the variable-speed compressors show about a 5% isentropic efficiency penalty compared to single-speed (Fig. 5). This efficiency penalty occurs because the variable speed design has fewer heat exchanger circuits (and thus a greater coil pressure drop at these conditions) in order to boost the per circuit flow rates at low speed operation. The 5% efficiency penalty is for the same drive type between the single- and variable-speed compressors.

A modulating compressor *with an advanced ECM drive* (having a 4 to 5% efficiency advantage over a single-speed motor) would therefore yield an overall peak cooling demand *equivalent* to that of a single-speed compressor. The use of ECM *blower* drives would result in a *lower* overall system demand compared to that of a single-speed system. Futhermore, the circuiting on the variable-speed system could be made more equivalent to the single-speed system if reducing peak demand were a higher priority than maximizing low speed performance.

From the above observations on modulating drive and compressor performance compared to single-speed components, the following can be concluded. For modulating applications, *heat exchanger unloading changes* from different compressor speed / frequency range capabilities, different compressor volumetrics, and various flow control options *will be as or more important than differences in compressor isentropic efficiency*. Therefore, issues in both these areas need to be considered in advanced modulating system assessment.

Modulating Component Models

Completed first level speed-modulated compressor models. These models can be used to predict compressor performance with first-generation or SOA IDIM systems or for reference SWDIM cases (approximating PM-ECMs). The modulating compressor models are based on:

- inverter losses derived from ORNL tests of a first generation CVSHP,[3,2] and SOA IDIM loss data obtained from industry bench tests,[3] and
- modulating sine-wave-driven compressor data from manufacturers.[3]

The user also has the option to directly provide curve fits for inverter-driven compressor data.

Completed first level modulating indoor blower and outdoor fan models. Models can be used to similarly predict modulating blower or fan efficiency with first-generation or SOA IDIM drives or for a reference SWDIM case (approximating a PM-ECM). The blower models are based on:

- first-generation IDIM and SWDIM blower drive efficiency data obtained from ORNL tests of a CVSHP,[3] and
- SOA IDIM and SWDIM efficiency data obtained from a manufacturer.[3]

Completed first level charge inventory model to allow prediction of charge effects in modulating systems and to accommodate advanced modulating flow control devices (by fixing refrigerant charge and determining required condenser subcooling or evaporator superheat levels). The charge inventory model includes:

- user choice of inventory methods ranging from simplified to SOA,[11] (We determined that a simplified analytical formulation was sufficient for early design work and much faster than more accurate methods requiring numerical integration.[11])
- tabulations of steady-state on- and off-cycle charge distributions, and
- a j-tube accumulator model adapted from NBS mixed-refrigerant heat pump simulation.[12]

Completed major update of air-side heat transfer and pressure drop calculations for improved prediction *for modulating air flows* based on work by Gray and Webb.[13] Other heat exchanger modeling improvements included improved augmentation factors dependent on Reynolds number and fin pattern specifics. These were:

- much improved wavy fin correlations obtained from DOE/ORNL supported work at the Westinghouse R & D Center[14] and
- expanded louvered (strip) fin correlations.[15]

Modulating Applications, Validations, and Design Tools

Assisted in the application of ORNL Heat Pump Design Model to variable-speed engine-driven heat pump simulations. Through a Work-for-Others

contract, ORNL adapted the Mark III ORNL Heat Pump Design Model (single-speed) to a variable-speed (1000 to 3000 rpm) Stirling-engine-driven heat pump application.[16] This adaptation was accomplished using proprietary Borg-Warner / Stirling Power Systems (SPS) engine, compressor, and radiator representations for a 10-ton commercial system. The modified model was transferred to Borg Warner for their use in system design and control analysis for the Gas Research Institute (GRI).[17]

We also provided the Mark III ORNL Heat Pump Design Model[6] and Mark I APF/Loads Model on an advance basis to Battelle Columbus Laboratory. These programs were selected[18] and modified by Battelle to model residential internal-combustion, engine-driven gas-fired heat pumps[19] for another GRI development project. The Battelle project was also a variable-speed application (again 1000 to 3000 rpm).

Completed first level electric-driven ORNL MHPDM including charge inventory capability. This involved integrating the developed modulating component models into the existing ORNL single-speed design model.[6] Program input requirements were modified with an emphasis on minimizing changes required to existing heat pump model data sets to convert to the newer model.

Conducted validation of initial ORNL MHPDM using ORNL breadboard variable-speed system data.[5,6] Results indicated that best model agreement was obtained at the lower speeds, while some performance overpredictions occurred at higher speeds because of limitations of the simplified circuiting models with higher subcooled (or superheated), more heavily loaded heat exchanger conditions.

Additional validations of the original single-speed version in nonmodulating and modulating applications have been reported as satisfactory to excellent by Fischer,[20] Westinghouse (dual stroke application),[21] Battelle Columbus,[18] and Borg-Warner.[17]

Developed framework for integrating the ORNL Steady-State and APF Design Models into a design package for generating parametric performance data (suitable for contour plotting). Performance data parametric options include:

- choice of at least 25 design, control, and operating variables,
- steady-state performance results for fixed ambients or range of ambients, and
- seasonal or annual results for various operating or sizing strategies.

Potential Benefits from Capacity Modulation

Estimates of Steady-State Benefits

The net compressor efficiency changes and heat exchanger unloading benefits from modulation can be related directly to system EER gains. Provided the fan power is roughly a constant fraction of the compressor power, the modulating (vs) system EER gains (steady-state) compared to a single-speed (ss) system are given approximately, at each ambient temperature, by

$$\frac{\text{System EER}_{vs}}{\text{System EER}_{ss}} = \frac{\eta_{is,vs}}{\eta_{is,ss}} \bullet \frac{EER_{hx,vs}}{EER_{hx,ss}} \quad (1)$$

$$= \text{compressor efficiency effect} \bullet \text{heat exchanger, unloading effect}$$

where η_{is} represents compressor shell overall isentropic efficiency (including inverter drive losses) and EER_{hx} is the ideal compressor EER based on heat exchanger saturation conditions.

In Eq. (1), the compressor efficiency effect can be obtained from comparisons given in Fig. 5 between single- and variable-speed compressors (assuming the same motor type). Adjustments for modulating drive differences from reference SWDIM values can be obtained from Fig. 1.

The second factor in Eq. (1), *the heat exchanger unloading effect, is the dominant steady-state modulation benefit. This effect is determined by the compressor effective modulating range* (from both speed range and volumetric efficiency factors) *and by the refrigerant flow control design.* The resultant reduction in modulating system pressure ratio from these factors determines the heat exchanger unloading gain.[d] In first-generation designs, the primary question was whether losses in the modulating drive and compressor combination at the lower speeds would offset the obtained heat exchanger unloading benefits.

Examples of heat exchanger unloading effects are given in Fig. 6 for heating and cooling mode operation. The examples are based on the same compressor operating conditions[3] used in the compressor screening shown in Figs. 3-5. Refrigerant control strategies approximately optimal for single- and variable-speed cases were assumed to calculate the ideal heat exchanger (compressor) EER ratios. The reference for each ambient was the computed $EER_{hx,ss}$ based on heat exchanger conditions under single-speed operation.

In Fig. 6, *the heat exchanger unloading benefits* are seen to *give large system EER gains* at the *lower speed, milder ambient conditions* in either mode. For example, with a 4:1 modulation ratio, *a steady-state gain of 55% is indicated at an 82°F ambient in cooling mode, with a 46% gain*

---

[d]Eq. (1) can also be applied to modulating-to-modulating system comparisons. In this case, the single-speed terms in Eq. (1) would be replaced by the base modulating system. Here the heat exchanger unloading effect will cancel out if both systems have the same effective modulation ratios.

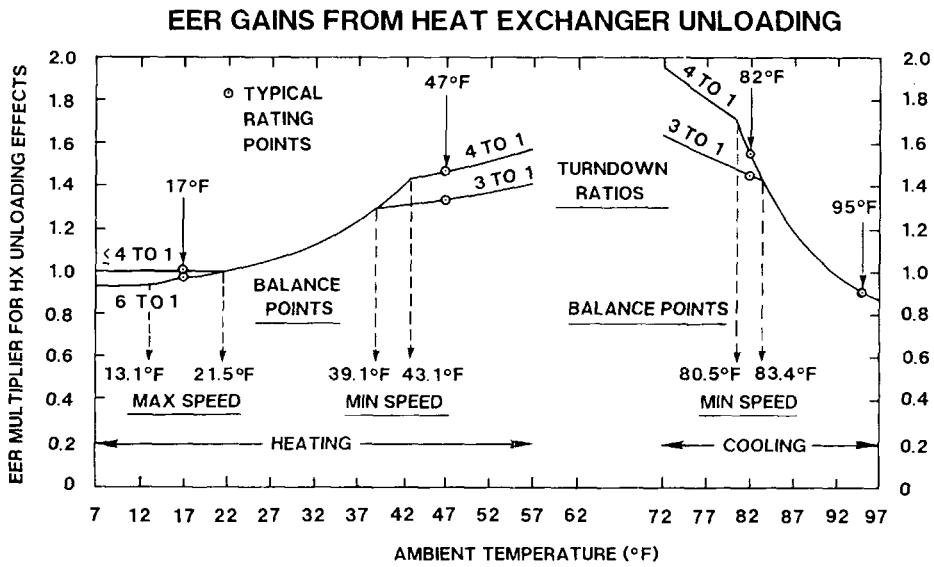

Fig. 6. Examples of steady-state EER multipliers for heat exchanger unloading effects for various turndown ratios in heating and cooling modes.

seen at 47°F heating. The reduction in heat exchanger unloading benefit from a smaller modulation range can also be seen from Fig. 6. In conjunction with Figs.1 and 5, Fig. 6 can be used to predict approximately the system EER (steady-state) gain from modulation at any selected ambient for the available compressors and speed ranges.

From this discussion, it can be seen that, to evaluate the steady-state benefits of modulating systems,[e] the unloading effects and the resultant compressor isentropic efficiencies must be considered together. Heat exchanger unloading is a rather involved interplay of compressor and blower speed ranges, compressor volumetrics, and system control strategies. The simplified relational analysis presented in Eq. (1) illustrates the need for optimal modulating system design and control to fully realize the performance potential of such systems. The design tools currently being developed and demonstrated are intended to assist the HVAC industry with this task.

Estimates of Annual Benefits

To evaluate the benefits of advanced modulating systems in terms of annual performance gains, we must add to the above considerations the effects of cycling, frosting/defrosting, and back-up heat reductions. At present, our best basis for overall savings estimates are the results of our initial analytically[1] and experimentally[6] optimized designs as evaluated on an annual basis with the ORNL APF/Loads Model.[1,5] Because the efficiency of the first-generation SWDIM drive (SWDIM curve C in Fig. 1) tested by Miller[6] is lower than that of the prototype ECM drive performance (also in Fig. 1), we would estimate higher possible annual performance gains than those given by Miller.[5]

For a PM-ECM-driven, reciprocating compressor system, we now estimate annual performance gains for Nashville, Tenn. (with 60% heating load) *of 30 to 35%* (23 to 26% energy savings) as compared to those of an optimally designed, single-speed system with comparatively reduced cycling loss factors.[5] *For a PM-ECM-driven scroll system*, the compressor efficiency comparisons shown in Figs. 3 and 4 suggest that the *annual performance gains, compared to an optimally designed single-speed reciprocating system, could be 45 to 50%* (31 to 33% energy savings). A major part of our analysis work in the near future will be to firmly establish benchmark efficiency improvement levels that can be expected on a nationwide basis for these two PM-ECM-driven systems.

Future Work

Ongoing and planned work is directed toward areas intended to assist industry in developing modulating systems capable of approaching these performance potentials.[f] Benefits from work to be accomplished in the near future include:

* establishment of a broader technical performance base of drive and compressor efficiencies for use in modeling modulating components and in providing perspective on progress made in modulating component performance,

[e]Compared to either single-speed systems or to other modulating systems.

[f]Within the constraints of general energy economics and specific economic criteria established by each company.

* transfer of design programs to the HVAC industry for development and improvement of future generation modulating heat pumps, and

* evaluation of near- and longer-term benchmarks of potential modulating heat pump performance (i.e.,

  - near-term, PM-ECM / reciprocating compressor-based and

  - longer-term, PM-ECM / scroll or rotary compressor-based)

through the identification of general sizing, component configuration, and control characteristics for best modulating system efficiency in different climates.

References

1. C. K. Rice and S. K. Fischer, "A Comparative Analysis of Single- and Continuously Variable-Capacity Heat Pump Concepts," Proc. DOE/ORNL Heat Pump Conference: Research and Development on Heat Pumps for Space Conditioning Applications, CONF-841231, Washington, D.C., 1985.

2. W. A. Miller, "Laboratory Efficiency Comparisons of Modulating Heat Pump Components Using Adjustable Speed Drives," ASHRAE Trans., 94, Pt. 1, 1988.

3. C. K. Rice, "Efficiency Characteristics of Speed-Modulated Drives at Predicted Torque Conditions for Air-to-Air Heat Pumps," ASHRAE Trans., 84, Pt. 1, 1988.

4. ARI. Standard for Positive Displacement Refrigerant Compressors, Compressor Units and Condensing Units, Standard 520-78, Arlington, Virginia: Air-Conditioning and Refrigeration Institute, 1978.

5. W. A. Miller, "Laboratory Capacity Modulation Experiments, Analyses and Validation," Proc. DOE/ORNL Heat Pump Conference: Research and Development on Heat Pumps for Space Conditioning Applications, Washington, D.C., April 17-20, 1988.

6. W. A. Miller, "Steady-State Refrigerant Flow and Airflow Control Experiments Conducted on a Continuously Variable Speed Air-to-Air Heat Pumps," ASHRAE Trans., 93, Pt. 2, 1987.

7. C. K. Rice, S. K. Fischer, and C. J. Emerson, The Oak Ridge Heat Pump Models: II. An Annual Performance Factor/Loads Model for Residential Air-Source Heat Pumps, ORNL/CON-160, Oak Ridge National Laboratory (to be published).

8. W. A. Miller, "Laboratory Examination and Seasonal Analysis of Frosting and Defrosting for an Air-to-Air Heat Pump," ASHRAE Trans., 93, Pt. 1, 1987.

9. W. A. Miller, "Laboratory Examination and Seasonal Analyses of the Dynamic Losses for a Continuously Variable Speed Heat Pump," ASHRAE Trans., 94, Pt. 2, 1988 (to be published).

10. T. Senshu and H. Terada, "Research and Development on Packaged Heat Pump Air-Conditioners in Japan," March 1988, presented at JAR International Seminar.

11. C. K. Rice, "The Effect of Void Fraction Correlation and Heat Flux Assumption on Refrigerant Charge Inventory Predictions," ASHRAE Trans., 93, Pt. 1, 1987.

12. P. Domanski, personal communication, National Bureau of Standards, Building Equipment Division, Gaithersburg, Maryland, August 1985.

13. D. L. Gray and R. L. Webb, "Heat Transfer and Friction Correlations for Plate Finned-Tube Heat Exchangers Having Plain Fins," Proc. Eighth International Heat Transfer Conference, San Francisco, Heat Transfer 1986, Vol. 6, pp. 2745-2750, Hemisphere: New York, 1986.

14. D. T. Beecher and T. J. Fagan, "The Effects of Fin Pattern on the Air-Side Heat Transfer Coefficient in Plate Finned-Tube Heat Exchangers," ASHRAE Trans., 93, Pt. 2, 1987.

15. W. Makayama and L. P. Xu, "Enhanced Fins for Air-Cooled Heat Exchangers -Heat Transfer and Friction Factor Correlations," Proc. ASME-JSME Thermal Engineering Joint Conference, Hawaii, March 1983, eds. Yasuo Mori and Wen-Jei Yang, New York, 1983.

16. S. K. Fischer, C. K. Rice, and W. L. Jackson, The Oak Ridge Heat Pump Models: Mark III Version Program Documentation, ORNL/TM-10192, Oak Ridge National Laboratory, March 1988.

17. R. E. Monahan, Phase I-B Development of Kinematic Stirling/Rankine Commercial Gas-Fired Heat Pump System, Final Report (September 1983-December 1985), GRI-86/0192, July 1986.

18. R. D. Fischer, State-of-the-Art Review of Vapor-Compression Heat Pump System Models, Task 2.1-Technical Report, GRI, February 1986.

19. R. D. Fischer, Gas Engine Heat Pump Cycle Analysis, Volume I. Model Description and Generic Analysis, GRI-86/0235, October 1986.

20. S. K. Fischer and C. K. Rice, "System Design Optimization and Validation for Single-Speed Heat Pumps," ASHRAE Trans., 91, Pt. 2, 1985.

21. T. J. Fagan, R. A. Lucheta, and D. T. Beecher, Oak Ridge National Laboratory Heat Pump Performance Prediction Computer Code: Additions and Verification, Westinghouse Research Report 87-9J8-MATHP-R1, November 1987.

Evaluation of Vapor Compression Cycles Using Nonazeotropic Refrigerant Mixtures

R. L. Merriam
Arthur D. Little, Inc.
Cambridge, MA 02140

OBJECTIVES

A comprehensive investigation is carried out, on a systematic and consistent basis, to explore a range of advanced heat pump cycle concepts using nonazeotropic refrigerants for COP enhancement and capacity modulation along with the trade-offs associated with refrigerant mixture selection.

The objectives of the study were to: identify candidate nonazeotropic mixtures and advanced heat pump cycle concepts with emphasis on their potential for single-speed capacity modulation with mixture composition control; assess the effect of compressor-enhanced capacity modulation in conjunction with nonazeotropic mixture cycles; evaluate the cycles analytically and recommend the most promising cycles and mixtures for further development; and provide recommendations relating to the needs for additional refrigerant property data, experimental studies of basic heat transfer phenomena with mixed refrigerants, development of system components, and/or more detailed modeling of specific components.

BACKGROUND

The use of nonazeotropic refrigerant mixtures has been long considered as a means for improving the coefficient of performance of refrigeration systems[1, 2, 3] and of providing a means for capacity control in heat pumps[4, 5, 6, 7]. Since the phase change in a nonazeotropic fluid occurs over a temperature range, appropriate design of the evaporator and condenser provides a means for lowering the thermodynamic irreversibilities occurring in these heat exchangers. In addition, if some practical means can be provided for partially separating the fluids within the cycle, the capacity of a heat pump may be varied to meet the load.

Drawbacks to the use of such fluids in heat pumps include the necessity for redesigned (and perhaps larger) heat exchangers and the additional complexity associated with the means for separating and recombining the fluids. A number of other practical considerations must also be addressed in a complete evaluation of the benefits of mixed refrigerants. Among these are: the ability to provide counter-flow heat exchange in the evaporator and condenser; refrigerant feed control; the influence of mixture composition on the condensing and evaporation heat exchange processes; possible effects of refrigerant composition on isentropic compressor efficiency; the cost and complexity of cycle hardware used for capacity control; preferential leakage of mixture components; and refrigerant selection considerations involving physical properties of the components. Important refrigerant parameters that need to be considered are oil miscibility, flammability, toxicity, stability, and dielectric strength.

The emphasis in the present study is on the thermodynamic performance of candidate cycles and mixtures. More practical considerations are left to hardware design activities. Most of the previous analytical investigations have relied upon the use of simplified equations of state employing ideal gas assumptions and assumptions concerning the relationship between source and sink temperatures and the refrigerant temperatures in the heat exchangers[8]. It appears as if few prior analyses have been performed employing realistic heat exchanger models for an air-to-air heat pump application.

APPROACH

The work was carried out in three stages: 1) a description of potential concepts for advanced cycles was developed; 2) initial performance evaluations of the candidate cycles were carried out; and 3) detailed analyses of the most promising air-to-air heat pump cycles were made.

DESCRIPTION OF CONEPTS FOR ADVANCED CYCLES

Review of basic cycles proposed by various investigators raised fundamental issues that needed to be addressed:

- Is liquid subcooling important, and if so, what is the most effective means of accomplishing it?
- Are there certain combinations of methods for liquid subcooling and capacity modulation that are particularly favorable?
- What are the requirements for heat exchanger design?
- Must the design be refrigerant-mixture sensitive, or are there preferred designs that are relatively independent of the particular mixture?
- Which cycle concepts are applicable to both the heating and cooling functions and which are best suited to the cooling function only?

To focus on answering the above questions, twelve candidate cycle concepts were generalized into four capacity-modulation concepts (Figure 1) and three liquid-subcooling concepts (Figure 2). An understanding of the advantages and disadvantages of the basic concepts shown in Figures 1 and 2 provides a basis for deriving more complex cycles to fully exploit the attributes of nonazeotropic cycles.

Refrigerant selection began with a compilation of refrigerants and a screening according to thermodynamic properties, toxicity, flammability and potential commercial availability at a reasonable cost. Thirteen refrigerants passed the screening process (Table 1). A more comprehensive screening process is described in another paper in this proceeding[9].

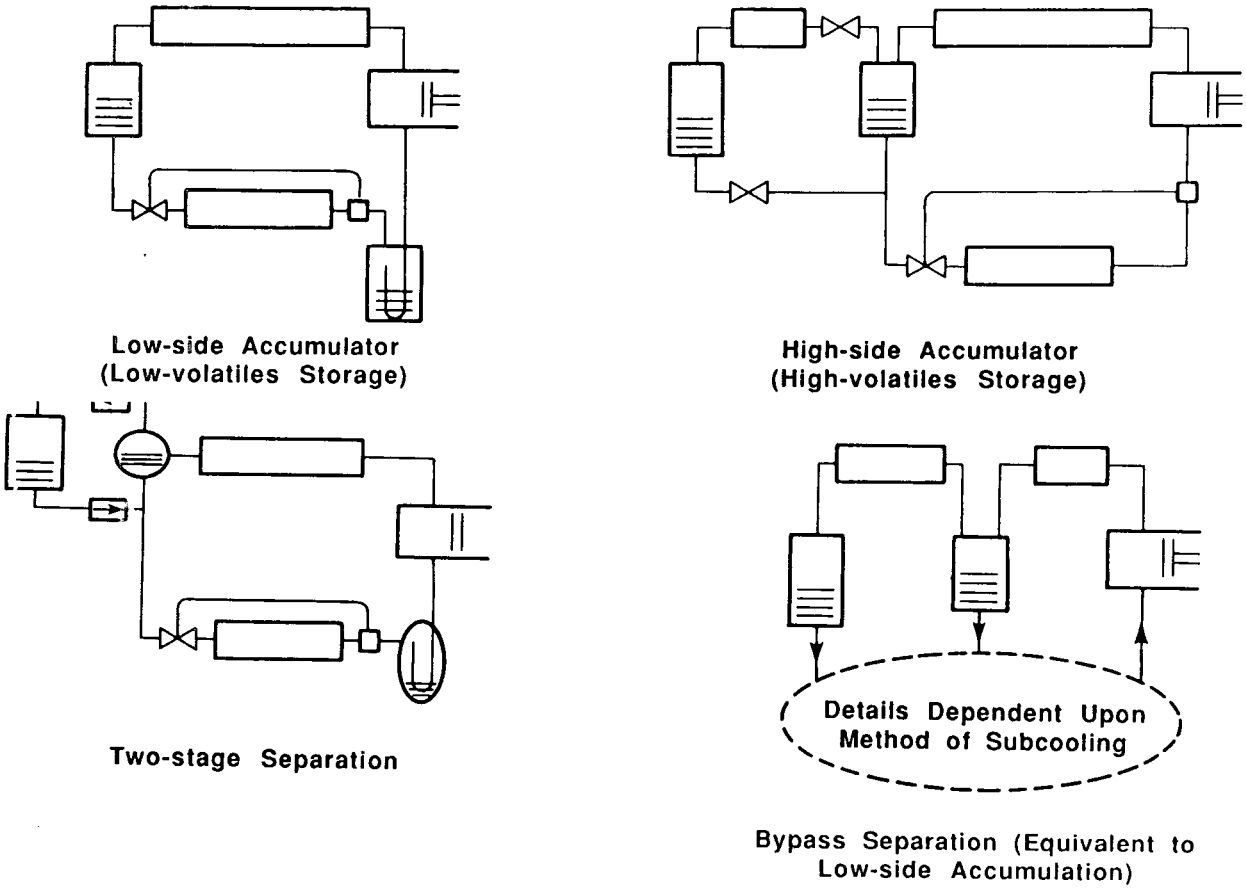

Figure 1. Capacity Modulation Concepts

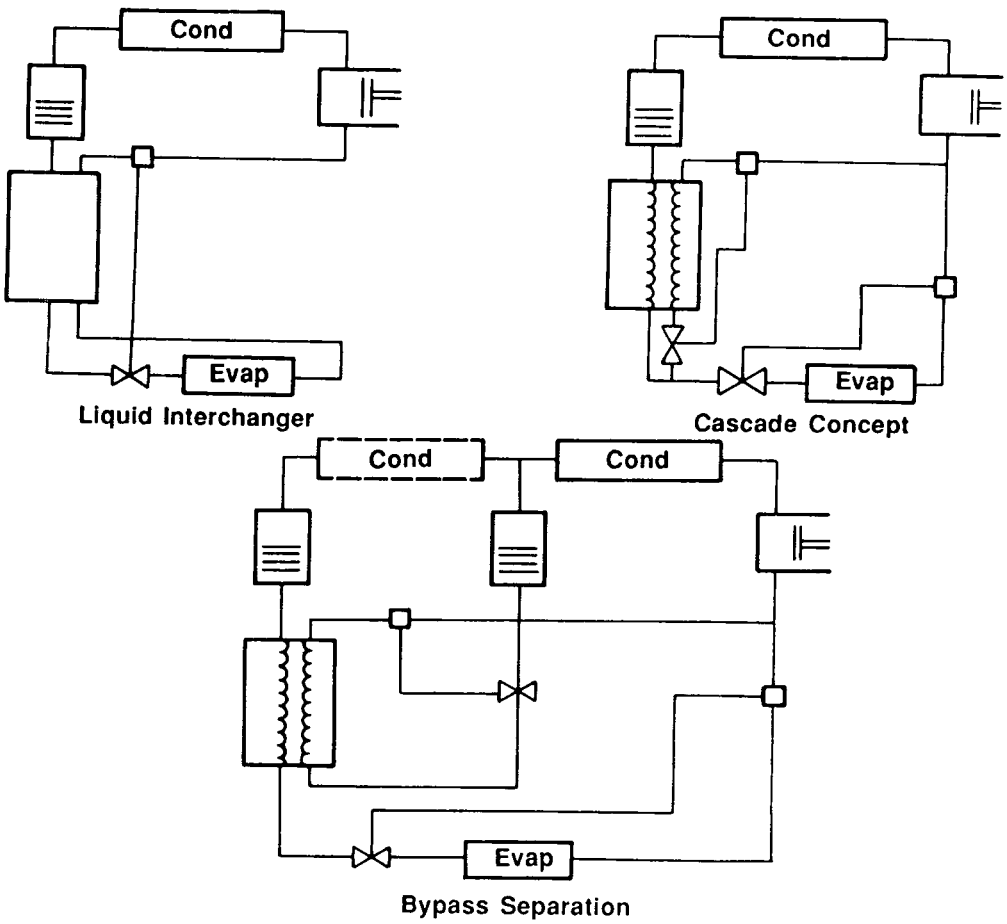

Figure 2. Liquid Subcooling Concepts

Table 1

REFRIGERANTS SELECTED FOR ANALYSIS

	Refrigerant Name	Normal Boiling Point (°F)	Critical Pressure (psig)	Flammable
Low Boiler	23	-116	701	
	13	-115	561	
	CO_2	-110	1070	
	SF_6	- 83	548	
	13B1	- 72	575	
Intermediate Boiler	502	- 50	591	
	22	- 41	726	
	12	- 22	597	
	152a	- 13	652	Yes
High Boiler	142b	14	598	Yes
	114	39	473	
	11	75	640	
	113	118	499	

The refrigerants were divided into three classifications: low boilers, intermediate boilers and high boilers. The rationale for this classification is that promising mixtures tend to be comprised of refrigerants that are in dissimilar classifications.

EVALUATION OF BASIC CONCEPTS

The primary objectives of the initial evaluation of mixed refrigerant cycle performance were to establish the relative merits of the basic generalized cycles and the attributes of various refrigerant combinations. This initial evaluation was, in effect, an additional screening exercise to permit a greater depth of analysis of the most interesting cycles and mixtures.

The analysis methodology was based upon the adaptation and use of an existing simplified heat pump model designed specifically for mixed refrigerant applications. The program, CYCLE, was developed by the DuPont Company[10, 11, 12]. Thermodynamic calculations were carried out using the Redlich-Kwong-Soave (RKS) equation of state.

The CYCLE model does not contain heat exchanger algorithms; all calculations were made on the refrigerant side at this stage of the work; the relationships between the refrigerant temperatures and air temperatures were estimated on the basis of approach temperature differences for the R22 cycle. Alterations made to the model to enable these preliminary evluations included: installation of a simple physically based compressor model; addition of capability to handle ternary mixtures; incorporation of liquid subcooling modules (see Figure 2); and representation of two-stage distillation (high-side and low-side).

From analyses carried out with the program the following general findings emerged:

- Low-side (less-volatile) accumulation appears to be more effective and easier to implement than high-side accumulation for composition shifting;
- Two-stage separation (Figure 1) probably represents a practical upper limit to the complexity allowable with residential- and light-commercial-sized heat pumps;
- The liquid interchanger (with incomplete phase change in the evaporator) design is more effective and probably easier to control than the bypass-separation system or cascade-type interchanger (Figure 2); and
- Effective heat transfer (counter-flow) is essential with mixed refrigerants to achieve higher performance than an R22 cycle.

Because of a need to focus the analysis, the efforts were concentrated on four particular refrigerant mixtures:

- R13B1-R152a, selected because of its good potential for component separation and operation at moderate condenser pressures;
- R22-R114, selected because of its operation at low condenser pressures and enhanced COP afforded by nonisothermal phase change;

- SF_6 - R12, selected because very little information has appeared to date on SF_6 as a refrigerant and because of the good refrigerant properties of R12; and
- R23-R22-R114, selected to examine the attributes of a ternary mixture containing a low boiler (R23).

DETAILED ANALYSIS OF PROMISING CYCLES

Heat Pump System Models

Two generalized heat pump system models chosen for further study are shown in Figures 3 and 4.*

System 2 incorporates a single-stage (low-side) accumulator for capacity modulation and employs a cascade-type interchanger. The system is somewhat more complex than System 1 because of the presence of an additional expansion device and because an optimum bypass of refrigerant through the interchanger must occur to maximize the performance. In one mode of operation, fluid flow through the interchanger will be counter-flow; in the other mode, the direction will be parallel flow with a somewhat reduced degree of subcooling. The particular flow direction can be optimized according to the application.

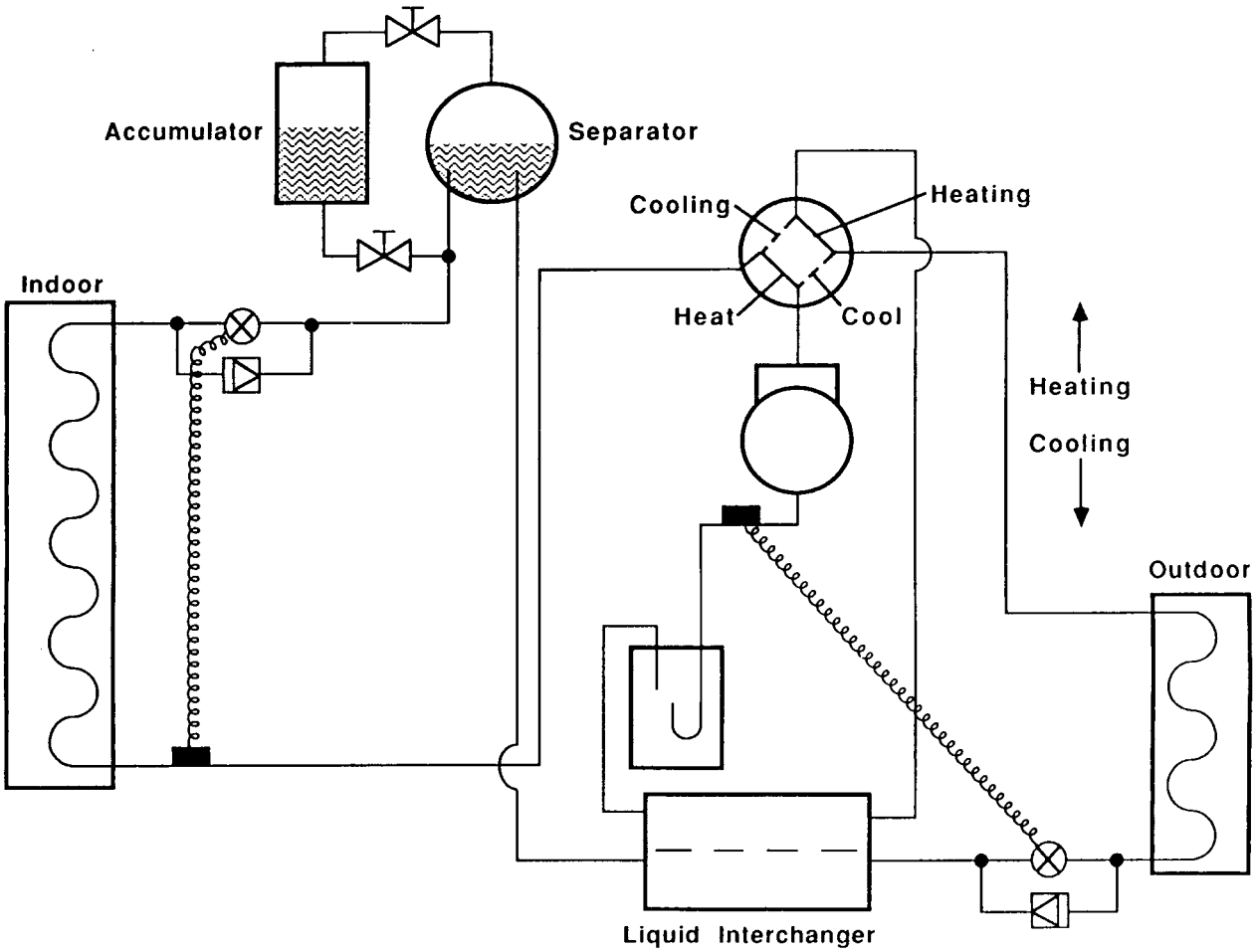

Figure 3. System Model No. 1: Two-Stage Distillation with Liquid Interchanger

System 1 utilizes a liquid interchanger for subcooling and contains two accumulators and a separator for capacity modulation (two-stage separation). A four-way valve allows operation in both the heating and cooling modes. Fluid flow from the low-side accumulator to the compressor is unidirectional; the flow direction throughout the remainder of the cycle depends upon the space-conditioning mode. This bidirectional nature may cause complications for the evaporator and condenser designs. Since the flow direction will change in the cooling mode, some arrangement must be made to ensure counter-flow heat transfer is maintained across the indoor coil.

Analysis Methodology

Steady-state performance predictions of the candidate cycles and refrigerants were made using a detailed computer model developed using the existing Oak Ridge Steady State Heat pump Model[13], which embodied the following major attributes:

- Evaporator and condenser heat exchange was explicitly modeled, including the effects of moisture removal on the capacity and COP;

* Selection of these system models was not intended to imply that the cycles are considered ideal. The system models have the capability of being able to represent subsystems that may be more ideal. For example, with system No. 1 both accumulators could be deleted and the system could be used for cooling only.

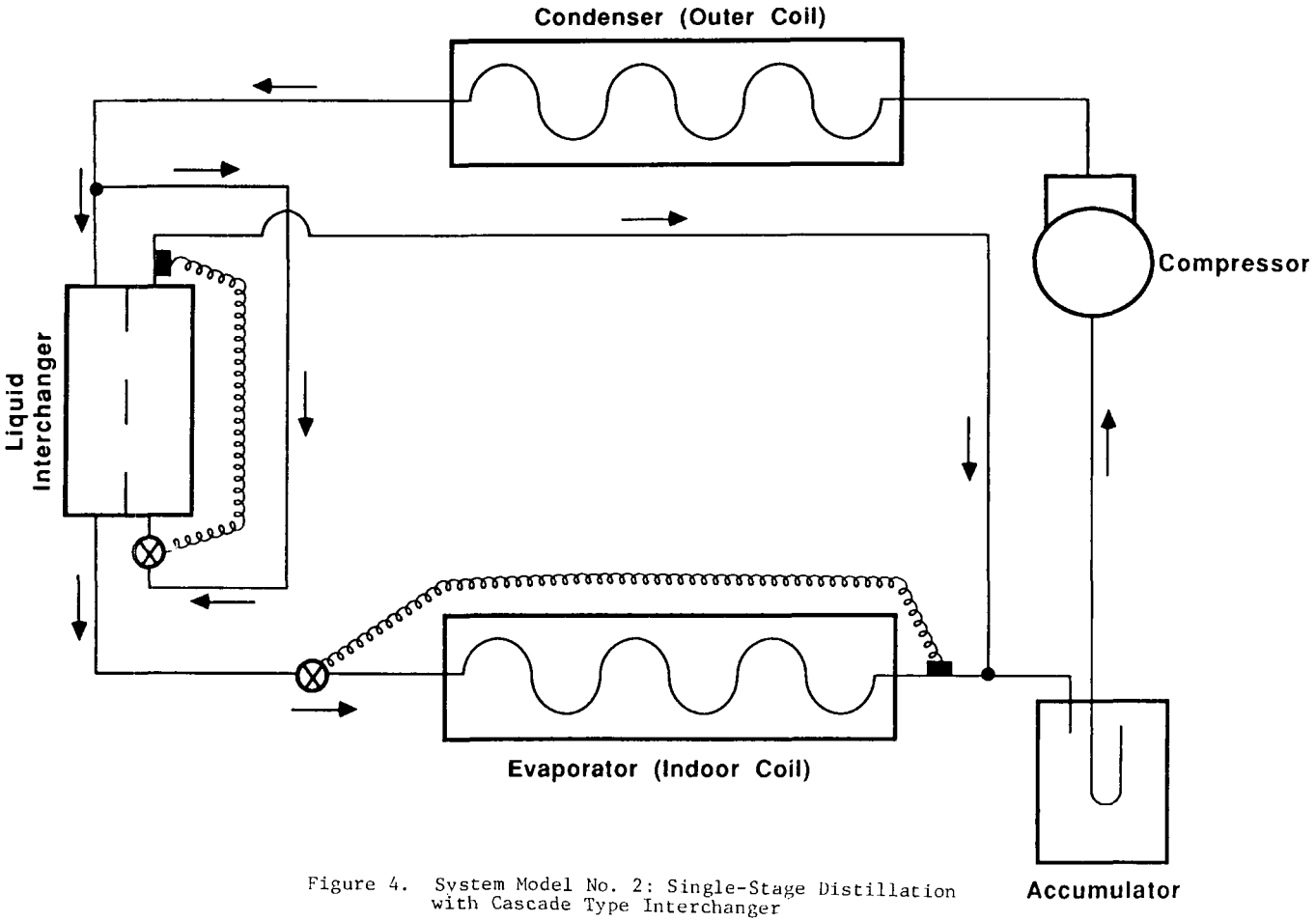

Figure 4. System Model No. 2: Single-Stage Distillation with Cascade Type Interchanger

- A physical model for the compressor (single-speed) was utilized, which included calculation of the effects of internal heat transfer on the suction gas density; and
- Generalized thermophysical relationships and the RKS equation of state were used to provide a consistent method of treating the full range of refrigerants of interest (see Table 1).

The analyses were based upon a sample heat pump and heat exchanger configuration provided in Reference 13. Parameter adjustments to some of the design details were carried out to establish which parameters control the predicted performance.

No attempt was made to optimize the hardware configuration for each refrigerant pair (except that counterflow air-refrigerant heat exchanger was assumed). The analyses were designed to compare the relative performance of candidate mixtures to R22 in a single heat pump configuration. As such, the results are somewhat specific to the hardware modeled.

Alterations were made to the ORNL model in the following areas[14]:

- thermodynamic properties--the RKS equation of state algorithms used in the CYCLE program were adapted;
- thermophysical properties--generalized correlations based upon pseudo-critical properties of a mixture were developed;
- heat exchanger models--algorithms for counter-flow and (dry-coil) parallel-flow heat transfer were added;
- mixture composition--liquid-vapor equilibrium models, combined with mass balances between the circulating and accumulated refrigerant, were used; and
- subcooling--submodels for liquid-type and cascade-type interchangers were incorporated.

For simplicity, analyses were carried out assuming a fixed subcooling of 20°F for all conditions, 10°F superheat for the evaporator outlet or for refrigerant flow control through the interchanger.

Model Validation

Validation of the mixed refrigerant computer model consisted of the four following steps:

- Compare model predictions for pure components with predictions from the original ORNL heat pump model[13];
- Compare thermodynamic and thermophysical property predictions with those of the NBS computer model for mixed refrigerants[15];
- Compare model predictions in heating and cooling modes for pure R22 with NBS test data[16]; and
- Compare model predictions in heating and cooling modes for mixed refrigerant (35% R152a/65% R13B1) with NBS test data[16].

Agreement between the original ORNL model and the revised model was within 1%, even though completely different methods were used to establish thermodynamic and thermophysical property data. Similarly, agreement between the mixed refrigerant model and the NBS model for thermodynamic properties of an R13B1-R152a mixture was within 2%. However, agreement between the two models for thermophysical properties was only within 20%, with the largest differences found for the liquid thermal conductivity and liquid viscosity. Given the uncertain accuracy of the mixture property correlations used by the NBS model, the agreement was considered adequate[17].

Comparison of test data[16] with model predictions revealed the compressor volumetric efficiency to be the most sensitive uncertain parameter. The chosen compressor submodel uses an empirical relationship with two parameters that are related to the type of compressor. Adjustments to the parameters, with the parameter ratio arbitrarily held constant, were made to fit the data for heating at 47°F. Comparisons made for other conditions, with the parameters held constant, provided reasonable agreement with test data for both pure R22 and an R13B1-R152a mixture. Although other uncertain parameters from the test data (e.g., superheat and subcooling during heating mode) had to be guessed, the agreement between the model predictions and test data was considered adequate to carry out the cycle analyses (Tables 2 and 3).

Table 2

COMPARISON OF TEST DATA AND MIXED REFRIGERANT MODEL PREDICTIONS FOR R22 REFRIGERANT

	Cooling at 95°F		Cooling at 82°F		Heating at 47°F		Heating at 17°F	
	Test	Model	Test	Model	Test	Model	Test	Model
Outdoor Temp (°F)	95	95	82	82	47	47	17	17
Superheat (°F)	13.5[a]	13.5[a]	21.0[a]	21.0[a]	?	5	?	1
Subcooling (°F)	13.9[a]	13.9[a]	16.9[a]	16.9[a]	?	10	5.8% quality	2[b]
Mass Flow (lbm/hr)	483	484	449	491	383	375	222	215
Capacity (Btuh)	32,270	31,500	33,060	34,801	36,200	36,069	20,500	20,742
EER or COP	7.42	7.30	8.30	8.60	2.79	2.83	1.92	2.09
Suction Press (psia)	84.8	99	76.6	95	64.7	69.8	40.4	44.8
Discharge Press (psia)	280	287	236	250	208	223	177	181
Indoor Fan (W)	483	483	484	484	473	473	484	484
Outdoor Fan (W)	303	303	309	309	320	320	340	340
Compressor Pwr (W)	3,564	3,530	3,189	3,253	3,007	2,940	2,302	2,084
Percent Latent (%)	22.4	20.1	22.3	24.5	-	-	-	-

a. Superheat and subcooling levels were set equal to test conditions.

b. Specified subcooling was set at 2°F rather than at 5.8% vapor quality because of model stability considerations.

Table 3

COMPARISON OF PREDICTED AND MEASURED HEATING PERFORMANCE DATA FOR NBS TEST HEAT PUMP WITH R13B1-R152a MIXTURE

	Heating at 17°F		Heating at 47°F	
PARAMETER	TEST	MODEL	TEST	MODEL
Operating Composition* (% R13B1/% R152a)	6.9/30.2	69.8/30.2	65.0/35.0	65.0/35.0
Subcooling (°F)	unknown	5	unknown	5
Superheat (°F)	-	5	unknown	5
Capacity (Btuh)	20,980	19,535	33,345	33,037
COP (Total System)	1.92	1.99	2.64	2.72
Mass Flow (Lb/hr)	299	248	416	430
Compressor Suction (psia)	46.5	42.1	63.5	63.8
Compressor Discharge (psia)	204	191	233	206

*Composition was set equal to test conditions.

Factors Affecting Cycle Performance

Heating system performance studies were carried out for the four selected refrigerant mixtures: R13B1-R152a, SF_6-R12, R22-R114, and R23-R22-R114. A number of important issues were addressed in the studies:

- Are there significant differences between various mixtures that would recommend specific refrigerant combinations in particular situations? Is there a "winner"?
- Is a ternary mixture any "better" than a binary mixture in terms of optimizing the heat pump operating parameters?
- Can the results be generalized to provide rules of thumb to explain the factors most affecting performance and to assist in a design selection?
- How sensitive is the performance to the presence or absence of various types of interchangers or to the design of the indoor or outdoor coil? and
- What are the trade-offs between design simplification and performance?

Figure 5 illustrates the result of exploiting the evaporator temperature rise by incorporating an interchanger and counter-flow heat exchangers into the design. Both the capacity and COP are increased signficantly. At the concentration where the capacity matches that of an R22 cycle (60% R13B1), the COP, obtained for counter-flow heat exchanger with an interchanger used for subcooling, is close to (slightly above) that obtained with R22. Note that the increase in COP resulting from use of counter-flow heat exchangers is greatest in the range of concentration where the evaporator temperature rise is maximum. Figure 5 also illustrates the effect of the liquid interchanger on the quality of the vapor entering the evaporator. The subcooling brings the entering refrigerant closer to the bubble point. As a consequence of the heat exchange process, the evaporator will achieve a higher pressure level and, therefore, a higher vapor pressure at the evaporator exit.

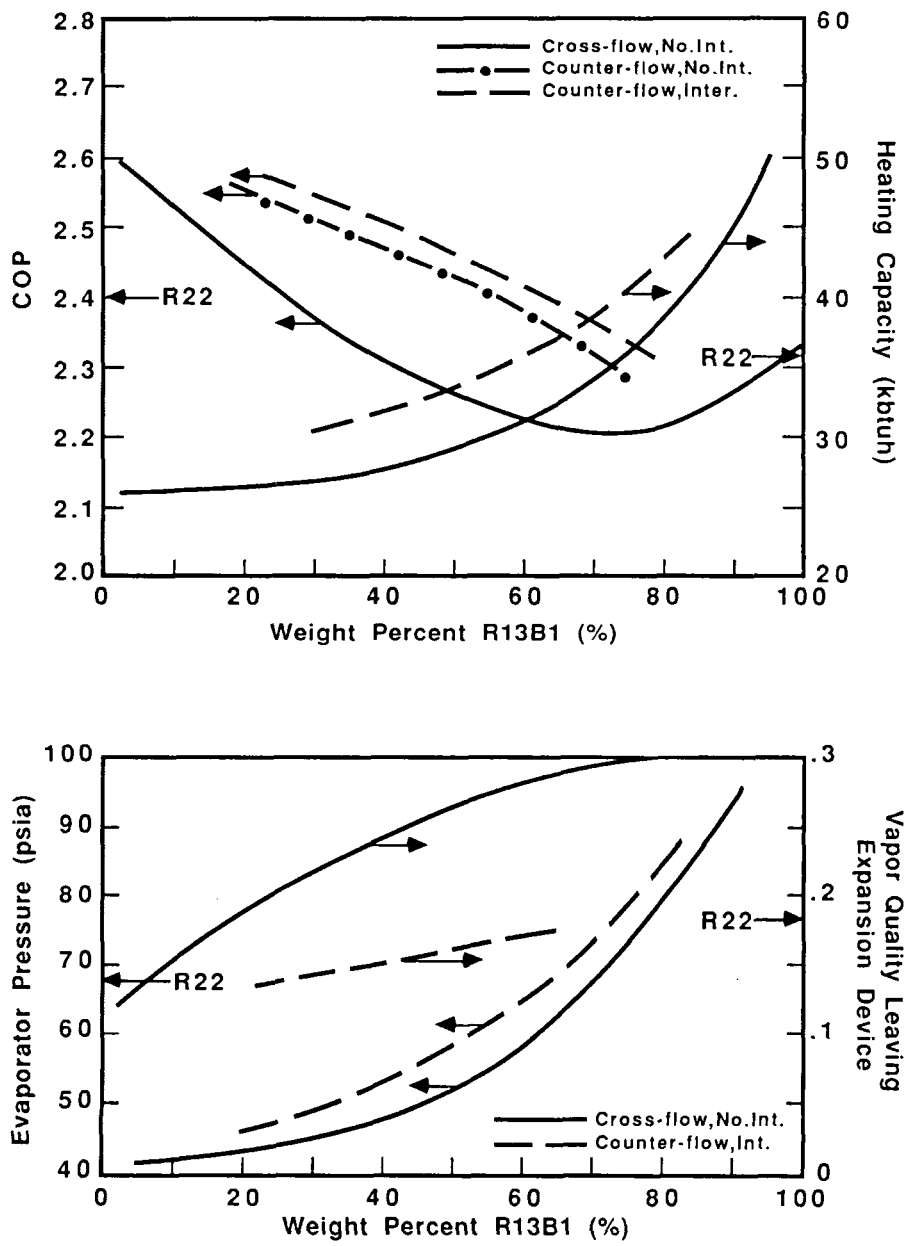

Figure 5. Influence of Heat Exchanger Design and Interchanger on Performance: R13B1-R152a Mixture, 47°F Ambient

Figure 6 shows the relationship between evaporator pressure and heating capacity for six mixtures over a full range of concentrations, for designs with and without an interchanger, and for cross-flow and counter-flow heat exchangers. The correlation is very tight given the range of conditions covered. It emphasizes that the net effect of incorporating a liquid subcooler and of using counter-flow heat exchangers is to increase the evaporator pressure.

- None of the mixtures achieve a significantly higher COP than R22 at its evaporator pressure;
- At pressure (capacity) near the R22 level, the R22-R114 mixtures have the highest COP;
- Although the ternary mixture, R23-R22-R114, allows operation at higher pressures and hence higher capacities, it yields the lowest COP at any given pressure level;

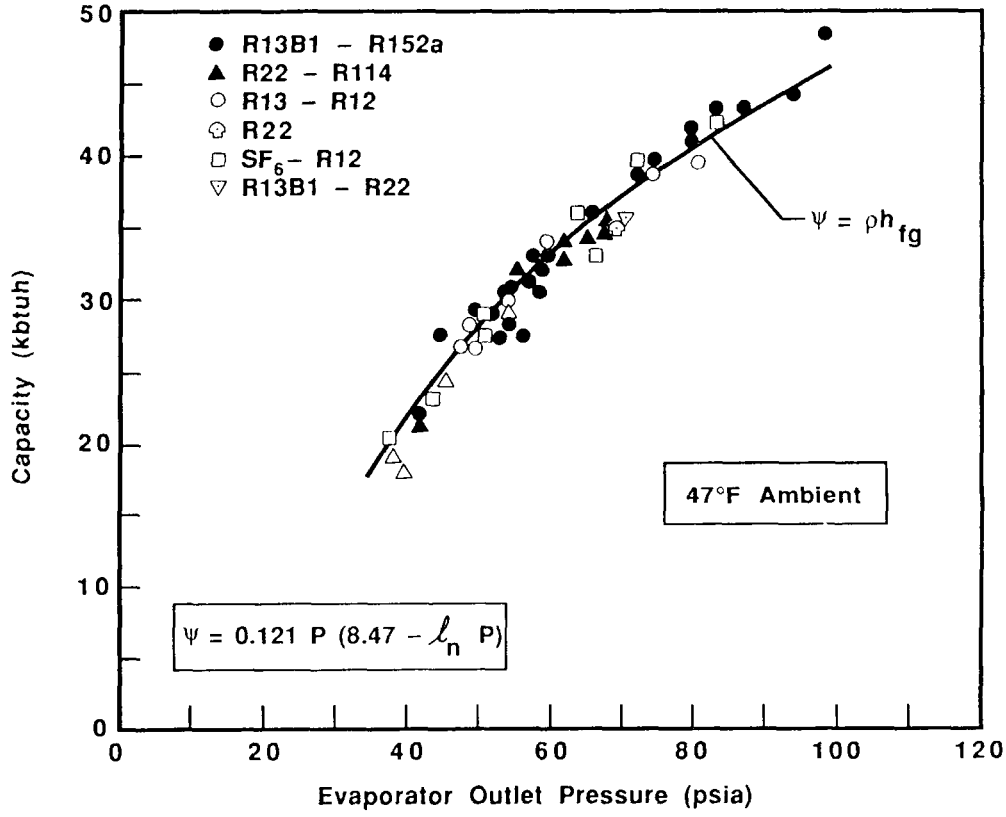

Figure 6. Variation of Heating Capacity with Evaporator Pressure at 47°F: 6 Refrigerant Mixtures, With and Without Interchangers, Counter- and Cross-Flow Heat Exchangers, Various Compositions

The relationship between the COP and the various refrigerant mixtures is shown in Figure 7 for cycles using counter-flow heat exchangers and a 50% effective liquid interchanger. To enable comparisons between the different mixtures, the data are plotted against the evaporator pressure. At low ambient temperature, the COP increases with evaporator pressure (capacity), whereas at higher ambient temperatures (above 32°F) the COP decreases with evaporator pressure. At least two factors combine to result in this consistent relationship: the fan power is the same at all ambient temperatures and is a larger fraction of the total power draw at lower temperatures; and the approach temperature of the air over the coils is near the coil-outlet refrigerant temperature at low ambient temperatures, whereas at higher ambient temperatures, departure from ideal heat transfer conditions increases as the capacity is increased. Some slight differences between the various mixtures appear:

- At the higher pressure level, the R13B1-R152a mixture has slightly higher COP's; and
- Although the condenser pressure levels correlate well with evaporator pressure, somewhat higher pressure levels are sustained with SF_6-R12 and with the ternary mixtures containing R23.

Figure 8 shows a similar set of relationships between COP and evaporator pressure for the cooling mode. In this instance, several of the mixtures appear to offer opportunity for higher COP's than does the R22 cycle. R13B1-R152a mixtures have the highest COP's at a given evaporator pressure whereas SF_6-R12 mixtures have the lowest. The ternary mixture also has high COP's at a given evaporator pressure. However, the ternary cannot have a very high concentration of R23 without the condenser pressure becoming excessive. Hence, although the highly-volatile component provides a means of achieving higher capacities than possible with R22-R114, only small amounts may be present in the mixture during cooling.

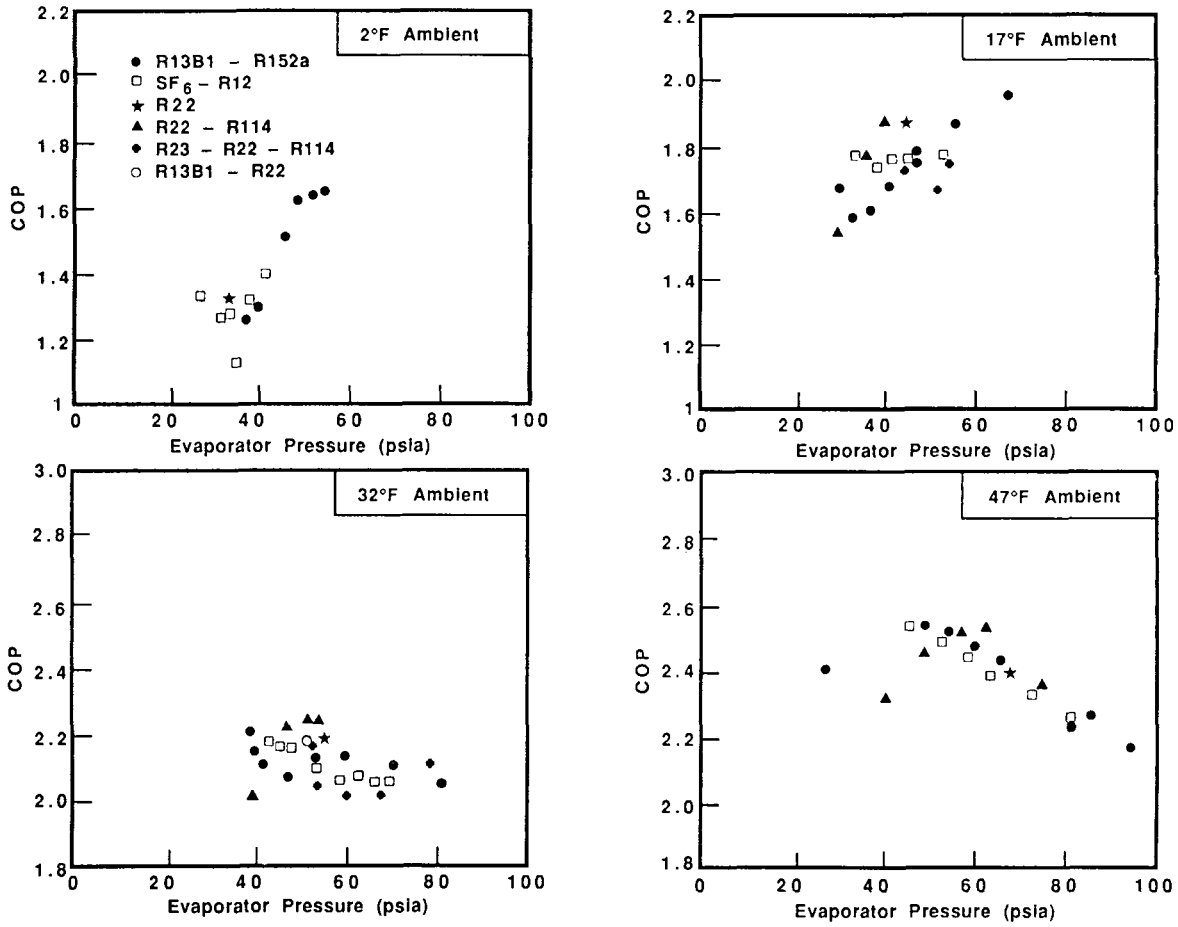

Figure 7. Heating COP Correlated with Evaporator Pressure

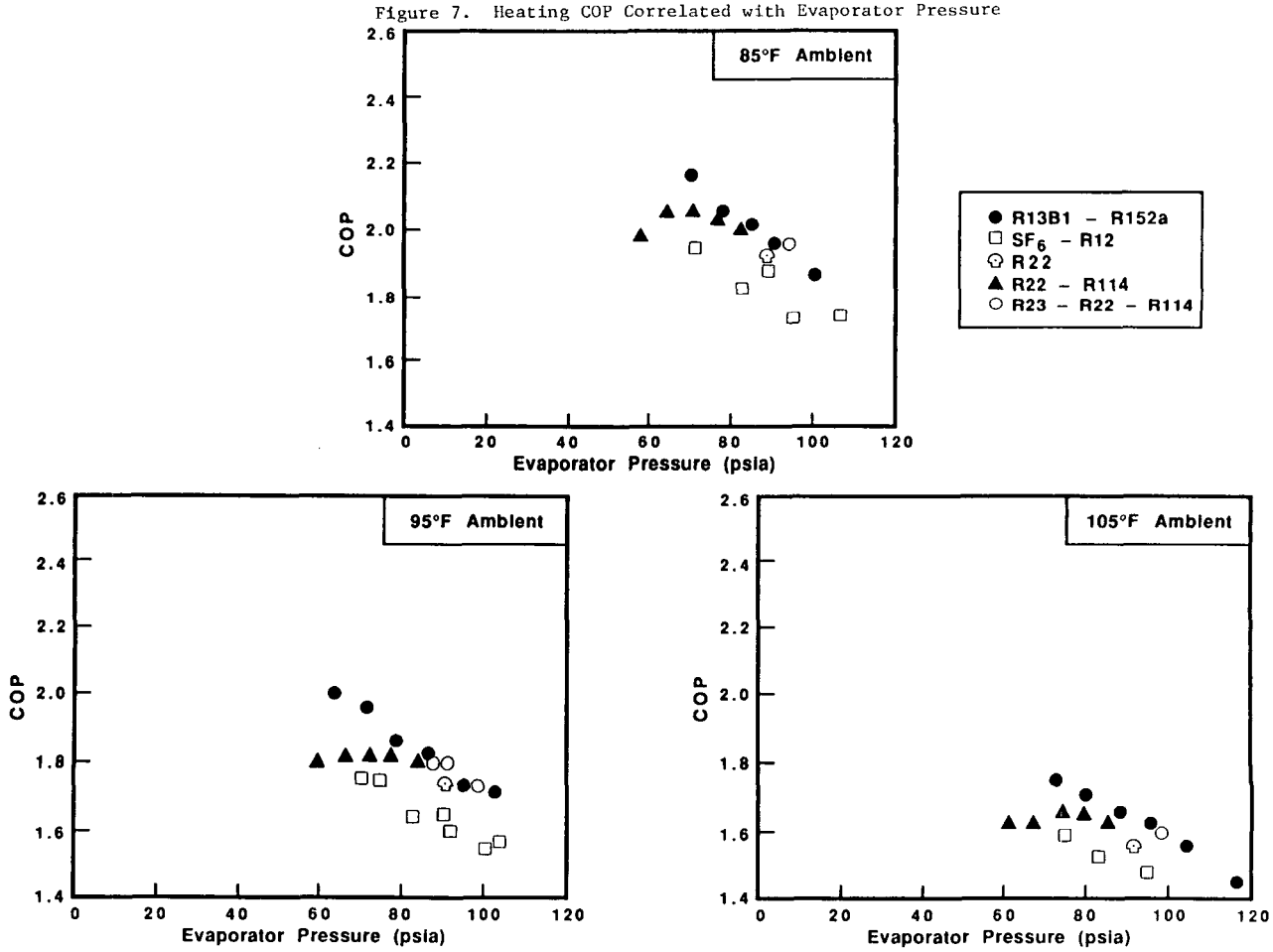

Figure 8. Cooling COP Correlated with Evaporator Pressure

CONCLUSIONS

Mixture Composition

No specific mixtures emerged as "winners". A binary or ternary mixture composed of refrigerants with boiling points lower and higher than R22 can provide capacities similar to those obtained with R22 using a similar comparison. No clear advantage offered by a ternary mixture was uncovered; only a very small amount of a low boiler, such as R23 or R13, can be added to a mixture without exceeding normal condenser pressure limits.

Generalization Results

Both heating and cooling capacities were found to be very tightly correlated with evaporator pressure level. The correlation was found to hold for all source and sink temperatures and for the various liquid-subcooler and evaporator and condenser heat-exchanger designs. At given evaporator pressure levels, the highest COP's were generally obtained with the R13B1-R152a and R22-R114 mixtures.

Interchanger and Heat Exchanger

Both an effective means to obtaining liquid subcooling and an approximation to counter-flow heat exchange in the indoor coil are required to achieve capacities and COP's comparable to those of the R22 cycle.

Design Trade-offs

Some means of achieving counter-flow heat transfer, at least in the indoor coil, is necessary to realize the potential performance improvements of refrigerant mixtures. Control of liquid subcooling, while reducing the superheat of the gas going to the compressor, is necessary. The interchanger design must accommodate both two-phase evaporation and gas super heating. Special control requirements are also associated with managing the shifting of refrigerant mixtures between accumulator and storage vessels to accomplish composition shifting. A minimum ratio of 4:1 total charge to working fluid seems reasonable.

RECOMMENDATIONS

We recommend the following actions relative to data needs:

- obtain experimental data for thermophysical properties of mixtures (thermal conductivity, viscosity, density, specific heat). Use the data to calibrate procedures for estimating these properties; and
- Continue the investigation, by experimental and theoretical means, of the relationship between mixture composition and two-phase heat transfer. Establish through breadboard experiments the significance of related heat transfer resistance on system heating and cooling performance.

We recommend the following actions relative to hardware needs:

- Experimentally investigate methods to achieve counter-flow heat transfer in air-to-refrigerant heat exchangers with a minimum of added complexity. Such experiments should establish the relative importance of the design of the indoor and outdoor coils, and verify the impact of alternative heat exchange designs on system performance. Use of water-to-refrigerant heat exchangers to achieve improved heat transfer should be explored;
- Develop and test high-efficiency liquid-subcooling interchangers. Both the cascade-type and liquid-interchanger concepts could be developed, although we recommend initial focus on the liquid interchanger method;
- Experimentally investigate the sensitivity in interchanger effectiveness and flow stability to the methods for fluid flow control; and
- Focus initial development efforts on air conditioner systems which attempt to exploit the potential for enhanced COP's through use of an effective interchanger and a well-designed counter-flow evaporator. This appears to be the most cost effective application in the near term.

We recommend the following actions relative to model needs:

- Improve the present model algorithms for the heat exchanger by adding more detail to the treatment of these components;
- Improve the model algorithms for compressor volumetric efficiency and shell loss or develop a means of obtaining compressor performance maps for nonazeotropic refrigerants; and
- Document and make available the present model to researchers or designers of mixed-refrigerant heat pumps.

FUTURE ACTIVITIES

Evaluations of water-to-air heat pumps are planned using the mixed refrigerant model. Alterations will be made to the computer model to utilize nonazeotropic mixtures, compressor models developed elsewhere, and to handle simple water-to-refrigerant heat exchangers used in an ORNL test rig. Breadboard test data obtained at ORNL[18] and NBS will be used to validate the upgraded model.

REFERENCES

1. W. F. Stoecker, "Improving the Energy Effectiveness of Domestic Refrigerators by the Application of Refrigerant Mixtures," Report No. ORNL/Sub-78/55463/1, Oak Ridge National Laboratory, September 1978.

2. P. F. Launay, "Improving the Efficiency of Refrigerators and Heat Pumps by Using a Nonazeotropic Mixture of Refrigerants," Report No. ORNL/Sub 81/7762/1, Oak Ridge National Laboratory, October 1981.

3. W. F. Stoecker and C. I. McCarthy, "The Simulation and Performance of a System Using an R-12/R-114 Refrigerant Mixture," Report No. ORNL/Sub 81-7762/3, Oak Ridge National Laboratory, May 1984.

4. R. Jakobs and H. Kruse, "The Use of Non-Azeotropic Refrigerant Mixtures in Heat Pumps for Energy Saving", Proc. of Meeting of Commission B2, Int. Institute of Refrigeration, Delft, 1987. pp. 207-218

5. W. D. Cooper and H. J. Borchardt, "The Use of Refrigerant Mixtures in Air-to-Air Heat Pumps, "Institute of Refrigeration Proceedings, 1979.

6. W. D. Cooper, "The Use of Mixed Refrigerants in Air-to-Air Heat Pumps," ASHRAE Transactions, 1982, Vol. 88, Pt. 1. pp. 1159-1169.

7. H. Vakil, "New Concepts in Capacity Modulation Using Nonazeotropic Mixtures," Proc. XVI International Congress of Refrigeration 5 (1983).

8. "High Temperature Working Fluids and Nonazeotropic Mixtures in Compressor Driven Heat Pumps," A State of the Art Report of Annex VI of the International Energy Agency Working Group Advanced Heat Pumps, 1985.

9. E. A. Vineyard and J. R. Sand. "Experimental Evaluation of Nonazeotropic Refrigerant Mixtures for Capacity Modulation," DOE/ORNL Heat Pump Conference Proceedings, April 1988.

10. "Computer Programs for Refrigerant Mixtures," Freon Products Laboratory, E. I. duPont de Nemours & Company, Programs: SATTABLE, SUPERTABLE, VPFIT, FITPALL.

11. H.A. Connon, "A Generalized Computer Program for Analysis of Mixture Refrigeration Cycles," ASHRAE Transactions, Vol. 89, Pt. 1. pp. 628-639.

12. "Computer Programs for Refrigerant Mixtures," Freon Products Laboratory, E. I. duPont de Nemours & Company, Program: CYCLE.

13. S. K. Fischer and C. K. Rice, "The Oak Ridge Heat Pump Models: I. A Steady-State Computer Design Model for Air-to-Air Heat Pumps," ORNL/CON-80/R1, August 1983.

14. R. L. Merriam and S. Mathias. "Evaluation of Advanced Vapor Compression Cycles for Use With Nonazeotropic Refrigerant Mixtures," Draft final report to Oak Ridge National Laboratory, January 1988.

15. P.A. Domanski, "Modeling of a Heat Pump Charged with a Non-Azeotropic Refrigerant Mixture," NBS Technical Note 121B.

16. W. Mulroy and D. Didion, "The Performance of a Conventional Residential Sized Heat Pump Operating with a Nonazeotropic Binary Refrigerant Mixture," NBSIR 860-3422, October 1986.

17. Discussions with P.A. Domanski, NBS, June 1987.

18. W. Mulroy, et al., "Experimental Evaluation of Two Refrigerant Mixtures in a Breadboard Air Conditioner," DOE/ORNL Heat Pump Conference, Proceedings, April, 1988.

Evaluation of Nonazeotropic Refrigerant Mixtures for Capacity Modulation*

E. A. Vineyard and *J. R. Sand*
Oak Ridge National Laboratory
Oak Ridge, TN 37831

Abstract

A test program is under way at the Oak Ridge National Laboratory (ORNL) to evaluate the potential performance improvements from the use of nonazeotropic refrigerant mixtures in residential heat pumps. The goals of the research effort are to achieve (1) capacity control by adjusting the composition, (2) increased capacity, relative to R22, at low ambient temperatures, and (3) matching of the refrigerant temperature differentials to the source and sink fluid temperature differentials. Performance improvements are expected to result from decreasing the cycling losses and the amount of resistance heat required at low ambient temperatures while reducing the irreversibilities in the heat exchangers. Initial results for a mixture of R13B1/R152a show a potential capacity modulation from 12431 Btu/h (3643 W) at 17°F (-8.3°C) to 8550 Btu/h (2506 W) at 47°F (8.3°C) in heating and from 7451 Btu/h (2184 W) at 82°F (27.8°C) to 9188 Btu/h (2693 W) at 95°F (35°C) in cooling. Other refrigerant pairs that are safer from an ozone depletion standpoint are under consideration for later testing.

Introduction

Nonazeotropic refrigerant mixtures (NARMs) have been investigated as a means of improving the efficiency of vapor compression refrigeration systems by taking advantage of a NARM's gliding temperature characteristics to reduce the irreversibilities associated with heat transfer in the heat exchangers. Research has shown, however, that degradations in the heat transfer coefficient for mixtures have produced results that yield approximately the same efficiencies as those for pure refrigerants.[1] The reduced heat transfer coefficients lead to increased log mean temperature differences (ΔT_M) in both heat exchangers, thus negating any potential gains from the temperature glide effect. More recent results[2] indicate that the use of enhanced surfaces and counterflow heat exchangers can negate the reduced heat transfer coefficients and yield a significantly higher coefficient of performance (COP) for the mixture R22/R114 over that of R22.

Most recently, interest has focused on the ability to achieve single-speed capacity modulation in heat pump applications. In principle, the concentrations of the different refrigerants can be controlled to optimize the system operation for cooling and heating by means of high and low side storage of each of the components. While several concepts for accomplishing composition shifting have been proposed, it is beyond the scope of this investigation to determine the relative merits of each. As shown in Fig. 1, changing the composition could result in a higher heating capacity than that of R22 at low ambient temperatures, resulting in a reduction in the amount of resistance heat required. At higher ambient temperatures, a reduction in cycling would occur in heating and cooling as a result of changing the composition to give a lower capacity than that of R22.

Following are descriptions of two ORNL projects. One project was an initial laboratory assessment of capacity modulation potential, using an R13B1/R152a mixture.

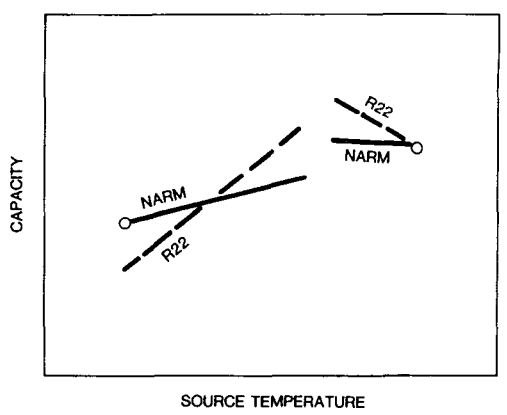

Fig. 1. Capacity versus source temperature for pure and mixed refrigerants.

The second is an analytical screening of available refrigerants to select promising fluids for future testing.

Initial Tests with the Mixture of R13B1/R152a

Tests were performed with a mixture of R13B1/R152a to quantify the potential for capacity modulation in a residential heat pump. The mixture R13B1/R152a was selected for the initial analysis because of its difference in boiling points for the pure components, which allowed for a moderate degree of capacity modulation without exceeding a temperature glide of 30°F (16.7°C). For applications in residential heat pumps, the temperature glide should not exceed this value.[3] In addition, sufficient data on this mixture were known to permit a determination of property data, using subroutines developed by Morrison and McLinden.[4] We recognize that the mixture is composed of two components that pose potential problems. R13B1 has been mentioned as potentially damaging to the ozone layer, while R152a could present safety problems because it is a flammable material. However, this mixture had the characteristics for matching most of our objectives, and we felt it could be utilized to quantify the potential gains in efficiency.

The test apparatus used in the initial tests (Fig. 2) is a heat pump water heater modified by replacing the air-to-refrigerant evaporator with a counterflow water-to-refrigerant heat exchanger. Temperatures, pressures, and flow rates were measured on the refrigerant circuit and the water circuit as indicated in Fig. 2. In addition, compressor wattage was measured using a watt transducer.

It was desirable to test at conditions similar to those found in a conventional air-source system because the research focused on a residential heat pump application. However, it was not practical to test at Department of Energy standard rating conditions for an air-source system because the test rig was equipped with water-to-refrigerant heat exchangers. The decision was made to adjust the entering water temperatures to yield equivalent saturation pressures as those determined appropriate for an air-source system previously tested by Miller.[5] Test

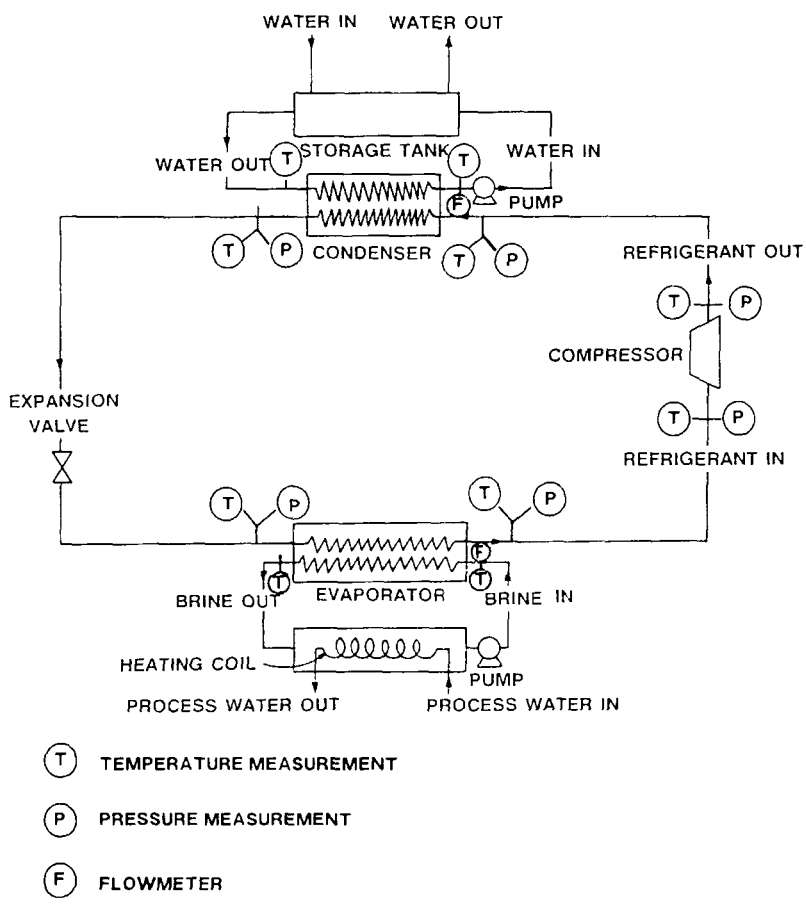

Fig. 2. Test rig schematic.

Table 1

Operating Conditions for NARM Testing

Variable	Cooling mode	Heating mode
Evaporator inlet water temperature, F (°C)	80 (26.7)	42 (5.6), [17 (-8.3)] 60 (15.6), [47 (8.3)]
Condenser inlet water temperature, F (°C)	85 (29.4), [82 (27.8)] 102 F (38.9), [95 (35)]	60 (15.6)
Water Δ T, (evaporator), F° (C°)	20 (11.1)	10 (5.6)
Water Δ T, (condenser), F° (C°)	20 (11.1)	20 (11.1)

conditions are listed in Table 1. Initial testing was with R22 to determine a baseline for comparison. The mixture R13B1/R152a was then tested by varying the composition in increments of 25% by weight, starting with pure R13B1 and concluding with pure R152a.

Results of COP and capacity are presented for both heating and cooling operation in terms of the simulated air-source temperatures. This type of presentation allows an assumed building load line to be superimposed on the graphs to show what the expected savings in cycling and resistance heat could be for a system that changes the composition to follow the building load. The results shown are summarized from a study by Vineyard.[6]

Heating

Heating capacity versus outdoor temperature is plotted in Fig. 3. The slopes of the lines for heating capacity versus outdoor temperature for pure R13B1 and R152a were estimated based on the same slope as that of R22, because the limitations of the test rig made it impractical to obtain a second data point. From Fig. 3, one can see that if it were possible to shift the composition to pure R13B1 at low outdoor temperatures, the capacity would be increased to 12431 Btu/h (3643 W), which is an increase of 2332 Btu/h (683 W) or 23% over that for R22 at 17°F (-8.3°C). This amount of increase would result in shifting the balance point from 30°F (-1.1°C) to 25°F (-3.9°C), yielding a savings in resistance heat. At higher outdoor temperatures, a shift in the composition to pure R152a would enable a decrease in the capacity to 8550 Btu/h (2506 W) at 47°F (8.3°C). This is 33% lower than the capacity for R22 at the same temperature and would permit the unit to cycle less, thus saving energy normally lost due to start-up transients and off-cycle parasitics.

Figure 3 also shows the measured COP versus outdoor temperature. The graph indicates that as the concentration of R13B1 decreases, the COP increases. In addition, the pure refrigerants R152a and R22 have higher COPs than the mixtures, while the COP for R13B1 is lower.

In an attempt to explain the values for the COP, the log mean temperature difference (ΔT_M) was calculated for the two-phase region in the condenser and evaporator. Also calculated was the difference in the fluid temperature differences at each end of the evaporator and of the condenser (ΔT_{STREAM}), which is an indication of how well the glide of the refrigerant matches the glide of the source or sink. The quantity ΔT_{STREAM} is defined by the following equation.

$$\Delta T_{STREAM} = | (T_{R_I} - T_{W_O}) - (T_{R_O} - T_{W_I}) | ,$$

where

T_{R_I} = inlet refrigerant temperature, °F (°C),
T_{W_O} = exit water temperature, °F (°C),
T_{R_O} = exit refrigerant temperature, °F (°C),
T_{W_I} = inlet water temperature, °F (°C).

Mixtures theoretically have the ability to match the glide of the source and sink fluid; the COP therefore, will be higher for the mixtures because of a decrease in the heat exchanger irreversibilities. However, all the mixtures had lower COPs than those of the pure refrigerants, with the exception of R13B1.

As Table 2 shows, the ΔT_M is higher in both the condenser and evaporator for all the mixtures as compared with that of the pure refrigerants. The increased ΔT_M causes the pressure ratio to be increased, thus contributing to a smaller COP for the mixtures. R152a had the lowest ΔT_M, thus explaining its high COP. An analysis of the results at 17°F (-8.3°C), while not shown, reveals that R13B1 has a much

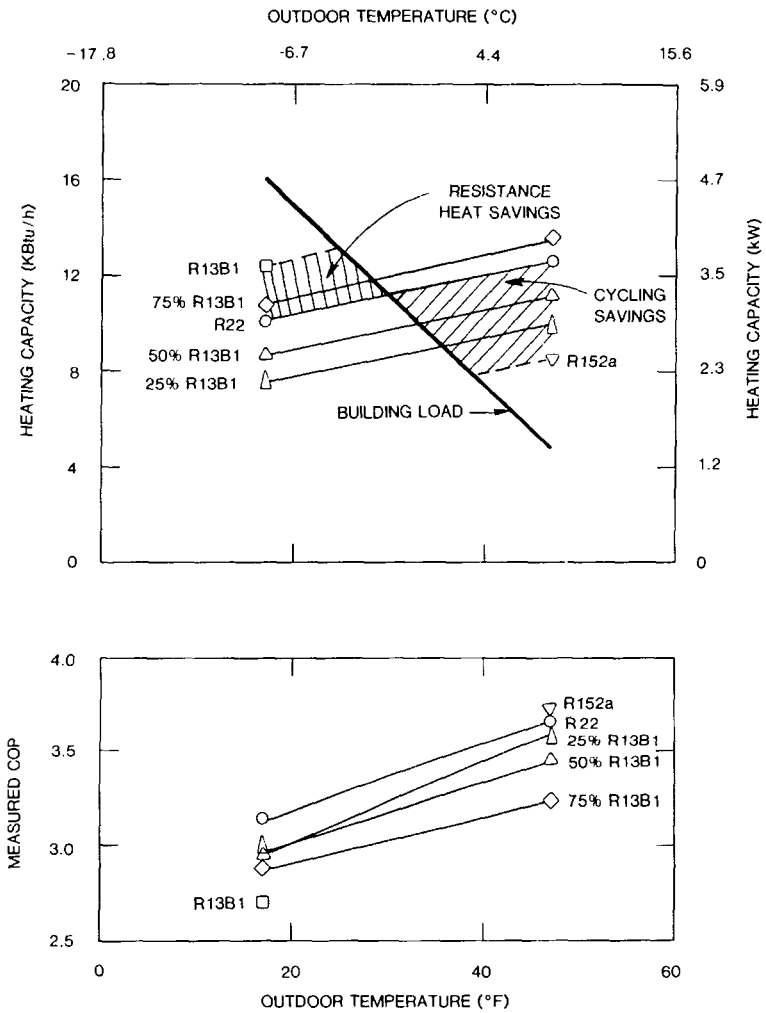

Fig. 3. Heating capacity and measured COP as functions of outdoor temperature.

Table 2

Log Mean Temperature Differences for
Pure and Mixed Refrigerants at the 47 F (8.3°C) Rating Condition

	Refrigerant				
Variable	R22	75% R13B1 25% R152a	50% R152a 50% R152a	25% R13B1 75% R152a	R152a
$\Delta T_{M_{COND}}$, F° (C°)	25.1 (13.9)	34.0 (18.9)	28.1 (15.6)	27.5 (15.3)	21.4 (11.9)
$\Delta T_{M_{EVAP}}$, F° (C°)	12.6 (7.0)	16.0 (8.9)	17.2 (9.6)	14.2 (7.9)	9.0 (5.0)

Table 3

Fluid Temperature Differences for
the Evaporator and Condenser at the 47 F (8.3°C) Rating Condition

	Refrigerant				
Variable	R22	75% R13B1 25% R152a	50% R13B1 50% R152a	25% R13B1 75% R152a	R152a
$\Delta T_{STREAM_{COND}}$, F° (C°)	16.1 (9.0)	5.3 (3.0)	3.9 (2.2)	0.0 (0.0)	15.9 (8.9)
$\Delta T_{STREAM_{EVAP}}$, F° (C°)	14.4 (8.0)	0.3 (0.2)	6.0 (3.3)	4.4 (2.4)	11.9 (6.6)

higher ΔT_M than the rest of the refrigerants, resulting in a lower COP.

Looking next at the ΔT_{STREAM}, Table 3 shows that it is much lower for the mixtures, thus tending to increase the COP. For the mixtures, this effect was obviously not enough to overcome the decrease in the COP, which was caused by the increased ΔT_M.

Cooling

Cooling capacity and measured COP versus outdoor temperatures ranging from 82°F (27.8°C) to 95°F (35°C) are plotted in Fig. 4 for mixtures of 50% R13B1/50% R152a and 25% R13B1/75% R152a along with those for the pure refrigerants R22 and R152a. The results show that the possibility exists for a reduction in the cycling

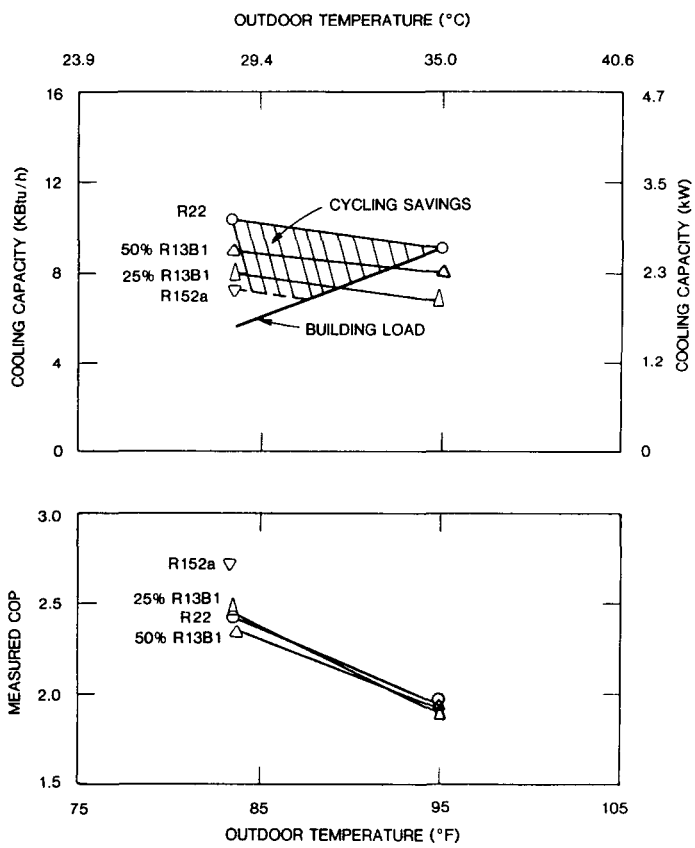

Fig. 4. Cooling capacity and measured COP as functions of outdoor temperature.

losses by gradually reducing the amount of R13B1 in the mixture. At 82°F (27.8°C), assuming a shift to pure R152a could be accomplished, the capacity would decrease by 28% from 10419 Btu/h (3053 W) for R22 to 7452 Btu/h (2184 W).

The measured COPs were approximately the same for all tested refrigerants except for R152a. A comparison of each mixture with R22 showed that the measured COPs were approximately equal because the reduced heat exchanger irreversibility was offset by an increase in the ΔT_M. R152a had a higher COP than the other refrigerants as the result of a much lower ΔT_M.

Candidate Mixture Selection Process

The primary purpose of this research effort is to perform a comprehensive analysis of refrigerant pairs for further testing. Previously, several combinations of refrigerants have been tested in efforts to improve the efficiency of heat pumps. Among the most widely reported of these mixtures are R22/R114, R12/R114, R22/R11, R12/R11, and R13B1/R152a. No systematic approach has been employed to determine which pairs of fluids have the greatest potential for improving heat pump performance. Several criteria are being considered in the selection of pure compounds for components of a NARM. These criteria can be broken down into two groups: "hard" criteria, which relate to issues that cannot be compromised and would eliminate a refrigerant from consideration, and "soft" criteria, which are items that may be used as a basis for elimination but can be changed or relaxed to allow for including refrigerants that are needed to fill in a gap for a capacity or boiling point of interest. Examples of hard criteria are: (1) toxicity, (2) instability, and (3) ozone depletion potential. Soft criteria include: (1) flammability, (2) boiling point temperature, and (3) commercial availability.

Once a compound is determined to be suitable for further analysis on the basis of the hard and soft criteria, its performance is being evaluated using computer models to determine the capacity and COP at the DOE standard rating conditions for an air-source heat pump. These performance estimates will then be used in conjunction with estimates for the temperature glide of the mixtures to determine which refrigerant pairs exhibit the greatest potential for accomplishing the goals of our project.

Potential components are being compiled from several sources that included vendors, researchers, and trade organizations such as the American Society of Heating, Refrigeration, and Air-conditioning Engineers.[7-10] Most of the combinations and structural isomers obtained from substituting chlorine and fluorine on methane, ethane, and propane are included. Property values are being obtained from chemical handbooks, ASHRAE tables, and vendor contacts. The list of components is comprehensive in that it contains relatively new chemical compounds as well as ones in various stages of development.

Future Work

Following the selection process, the most promising refrigerant pairs will be tested in the experimental apparatus shown in Fig. 5. This rig, which is different from the one used in the previous testing, is equipped with a variable speed compressor to allow for testing at different capacities to determine optimum compressor performance for each mixture. The inlet conditions at the evaporator and condenser will be automatically controlled to maintain the temperature and flow rate at the required set points. A gas chromatograph will be used to monitor the real-time composition of the circulating charge.

Fig. 5. Nonazeotropic refrigerant mixtures test rig.

References

1. W. F. Stoecker, "*Improving the Energy Effectiveness of Domestic Refrigerators by Refrigerators by the Application of Refrigerant Mmixtures*," ORNL/Sub-78/55-463/1 Oak Ridge, Tennessee: Oak Ridge National Laboratory, 1978.

2. W. Mulroy, M. Kauffeld, M. O. McLinden, and D. A. Didion, "An Evaluation of Two Refrigerant Mixtures in a Breadboard Air-Conditioner," Transactions of the 1988 International Institute of Refrigeration Meeting, Purdue University (to be published), 1988.

3. R. Radermacher, "Advanced Versions of Heat Pumps with Zeotropic Refrigerant Mixtures," *ASHRAE Trans.*, 92, (2), 52-59 (1986).

4. G. Morrison, and M. O. McLinden, "*Application of a Hard Sphere Equation of State to Refrigerants and Refrigerant Mixtures*", NBS Technical Note 1226 Gaithersburg, Maryland; National Bureau of Standards, 1986.

5. W. A. Miller, "*Laboratory Evaluation of the Heating Capacity and Efficiency of a High-Efficiency, Air-to-Air Heat Pump with Emphasis on Frosting / Defrosting Operation*", ORNL/CON-69, Oak Ridge National Laboratory, Oak Ridge, Tennessee, 1982.

6. E. A. Vineyard, "Laboratory Testing of a Heat Pump System using an R13B1/R152a Refrigerant Mixture," ASHRAE Trans., 94, (1), 1988.

7. ASHRAE Handbook - 1985 Fundamentals, Chapter 16 - Refrigerants, ASHRAE, Inc., 1985.

8. D. E. Bivens, E. I. du Pont de Nemours and Company, Inc. (personal communication), 1988.

9. W. Braker, and A. L. Mossman, 5th Ed., Matheson Gas Book, Matheson Gas Products, 1971.

10. R. C. Reid, J. M. Prausnitz, and T. K. Sherwood, The Properties of Liquids and Gases, 3rd Ed., McGraw-Hill, New York, New York, 1977.

Table 4

Mixture Components and Related Temperature Glides

32	3	3	4	4	8	8	23	23	23	28	44
	125	3	3	4	6	6	19	19	19	23	40
		143a	3	4	5	5	17	17	17	23	38
			22	3	4	4	11	11	11	15	29
				218	3	3	7	7	7	10	23
					134a	3	3	3	3	5	11
						152a	3	3	3	4	8
							124	3	3	3	4
								124a	3	3	4
									142b	3	4
										C318	3
											143

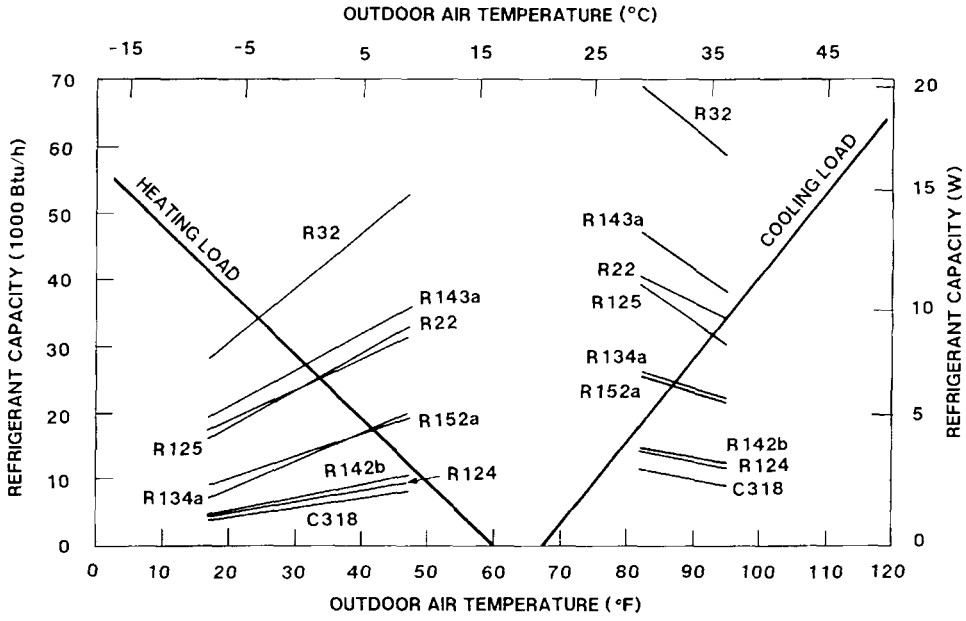

Refrigerant capacity versus outdoor temperature.

Experimental Evaluation of Two Refrigerant Mixtures in a Breadboard Air Conditioner

W. Mulroy, M. Kauffeld, M. McLinden,
and *D. A. Didion*
National Bureau of Standards
Gaithersburg, MD 20899

Abstract

An experimental, water-to-water, breadboard heat pump (that is one designed to be easily reconfigured) was constructed for comparison of pure R22 to the refrigerant mixtures R22/R114 and R13/R12. Three evaporator configurations were extensively studied. In all cases the best mixture outperformed R22. The best efficiency with R22/R114 was 32% higher and with R13/R12 was 16% higher than the best efficiency measured with R22. Other observations were, first, that mixtures can take advantage of heat exchanger efficiency that, in a gliding temperature application, a pure refrigerant is incapable of utilizing. Secondly, that heat exchange between the condensed and evaporating refrigerant is beneficial to some mixed refrigerants. Finally, mixtures exhibit nonlinearity of enthalpy versus temperature in the two phase region which has significant impact on both heat exchanger and cycle design.

Introduction

The National Bureau of Standards has evaluated two nonazeotropic refrigerant mixtures, R22/R114 and R13/R12, in a water-to-water breadboard heat pumping apparatus at temperatures typical of air conditioning applications. As is shown in figure 1, the best performing test series with the mixture R22/R114 resulted in a coefficient of performance of 6.9 (EER = 23.6), 32% higher than the best efficiency obtained with pure R22. In figure 2, the best efficiency with the mixture R13/R12 was 16% better than R22.

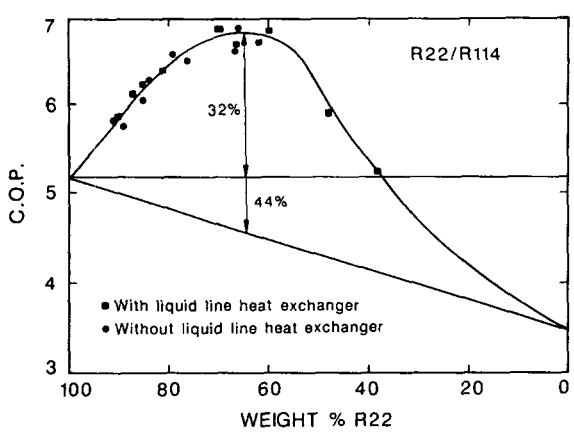

Figure 1: Performance of the mixture R22/R114 for evaporator configuration No. 4.

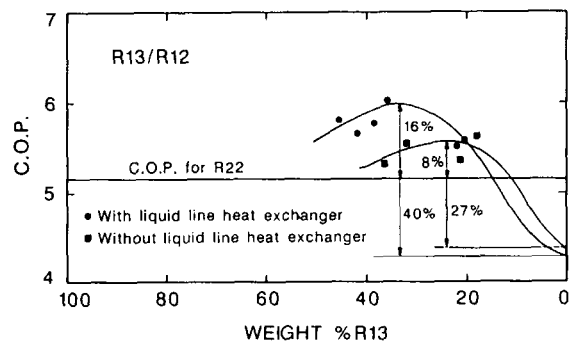

Figure 2: Performance of the mixture R13/R12 for evaporator configuration No. 4.

Test Conditions

The two primary criteria used to define comparable conditions for evaluating the tested refrigerants were fixed water temperatures and constant capacity. The fixed water temperatures chosen as typical of air conditioning were 80°F (26.7°C) inlet and 55°F (12.8°C) outlet for the evaporator, and 82°F (27.8°C) inlet and 117°F (47.2°C) outlet for the condenser. Because water temperatures were fixed, refrigerant temperatures and pressures were dependent on refrigerant properties. Since the evaporator area was to be kept constant for each test series, the constant heat flux criteria required constant capacity. For this reason, as refrigerant properties changed it was necessary to change compressor speed.

The test variables other than refrigerant compositions were the evaporator overall heat transfer coefficient times area (UA) and the use of intracycle heat exchange. The evaporator heat exchanger had three passages as shown in figure 3. By routing water or evaporating refrigerant through passages of different cross section or surface area, different pressure drops and water-to-refrigerant heat exchange coefficients were obtained. Three configurations were examined for a full range of refrigerant mixture compositions. The third evaporator passage was available for heat exchange between the condensed liquid refrigerant and the evaporating refrigerant in counter flow throughout the length of the evaporator. The tested evaporator configurations are summarized in table 1.

	Configuration			
	1	2	3	4
Evaporating Refrigerant	C	B	A	A
Liquid Refrigerant	B	C	B	C
Water	A	A	C	B

Table 1: Tested evaporator configurations (letters refer to Figure 3).

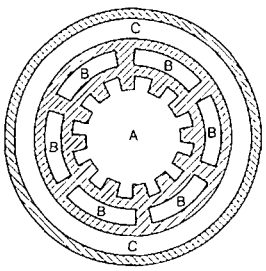

	Cross Sectional Area	Perimeter
A	227 mm^2	100 mm
B	122 mm^2	120 mm
C	310 mm^2	80 mm

Figure 3: Evaporator cross section (not to scale).

Apparatus

A schematic diagram of the breadboard heat pump is shown in figure 4. The open compressor is belt driven by a variable speed motor. A shaft dynamometer (strain gage torquemeter plus magnetic pickup tachometer) mounted between the compressor pulley and flywheel was used as the primary cycle power input measurement. From the compressor the refrigerant passes through an oil separator and then enters the condenser which rejects its heat to a counterflow water loop. Condenser capacity was measured by a water side measurement and by comparison of the water temperature rise to that over the metered electric trimming heater. The manual expansion valve was adjusted to maintain slight subcooling as observed at the condenser exit sightglass.

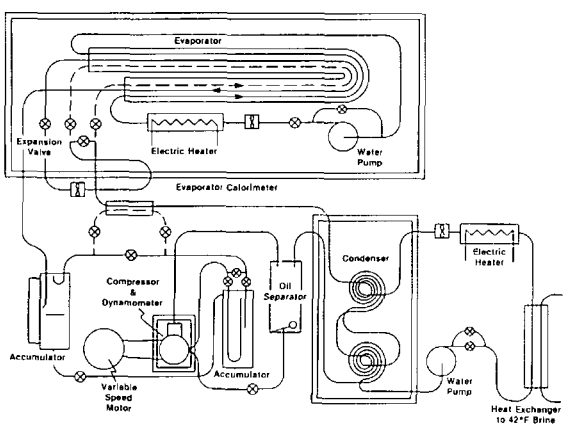

Figure 4: Schematic of breadboard heat pump.

The primary measure of evaporator capacity which was used to calculate cycle efficiency was provided by measuring the total heat input (electric heaters, water circulating pump, calorimeter through-the-wall heat gain) to the calorimeter box which surrounded the evaporator and its water loop. Secondary measures of evaporator capacity were a water side calculation and comparison of the water temperature drop through the evaporator to the water temperature rise through the metered heaters used to match the evaporator capacity.

A special accumulator which lacked an oil return hole was used at the evaporator outlet to allow flooded coil operation with only saturated vapor returning to the compressor so that the evaporator area in two-phase refrigerant-side heat transfer would stay constant and the system be charge insensitive. Mixed refrigerant composition was determined by analysis of compressor discharge gas samples using a gas chromatograph.

Figure 5 shows variation of system efficiency with compressor speed for pure R22 while holding suction and discharge pressures constant. Efficiency was felt to be sufficiently constant to allow mixture testing without correction for this variable. Because of vibrations in the compressor mounting and drive systems (resulting in a marked decrease in measured system efficiency) tests were not run near the speed of 750 rpm.

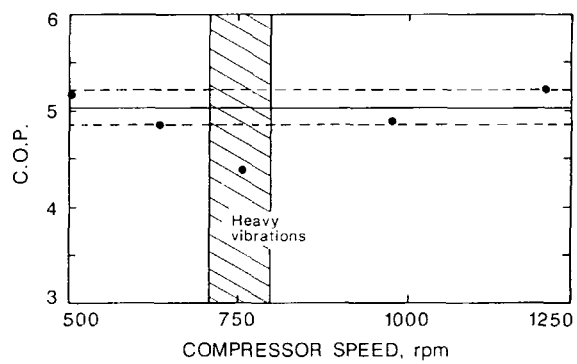

Figure 5: System efficiency as a function of compressor speed for pure R22.

Discussion and Results

Water and refrigerant temperature profiles through the evaporators for pure R22 are shown in figure 6. The four parts of this figure are for four different evaporator configurations (i.e. flow routed through different passages) which resulted in different overall heat transfer coefficient times area (UA) values. In the best configuration (figure 6d-configuration 4) the water temperature has reached that of the refrigerant in a quarter of the length of the evaporator. The remainder of the evaporator is

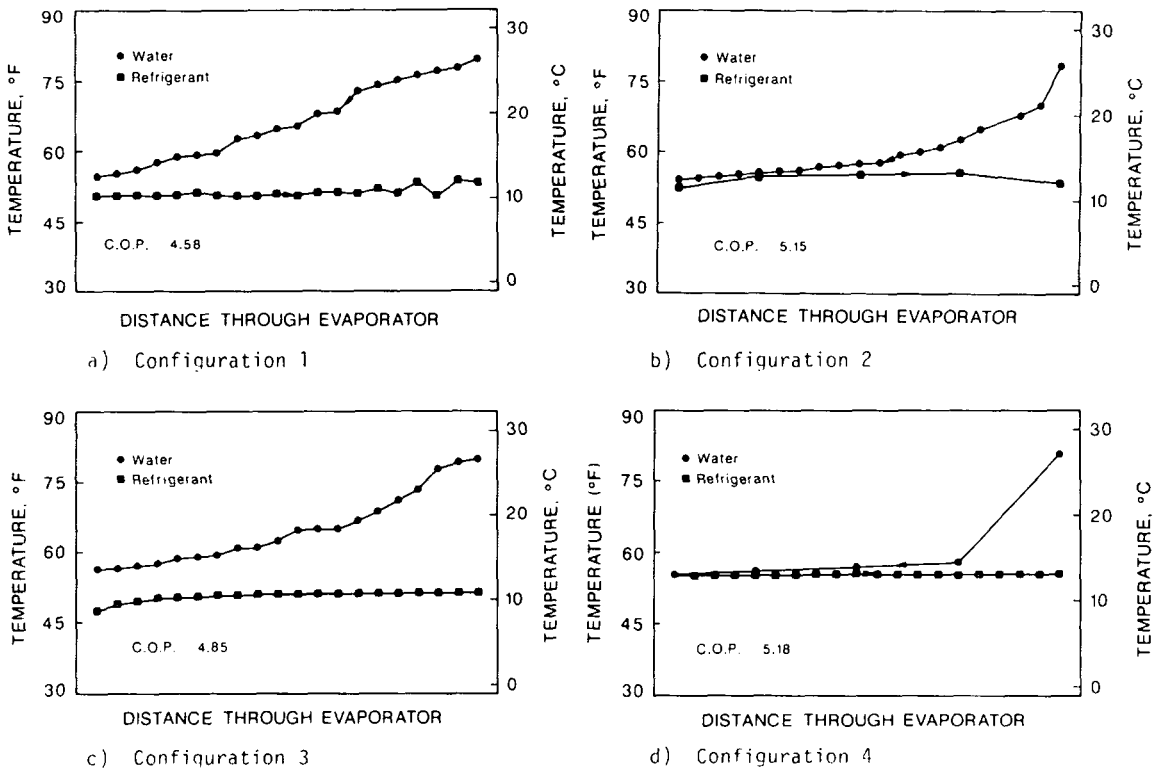

Figure 6: Water and refrigerant evaporator temperature profiles using pure R22.

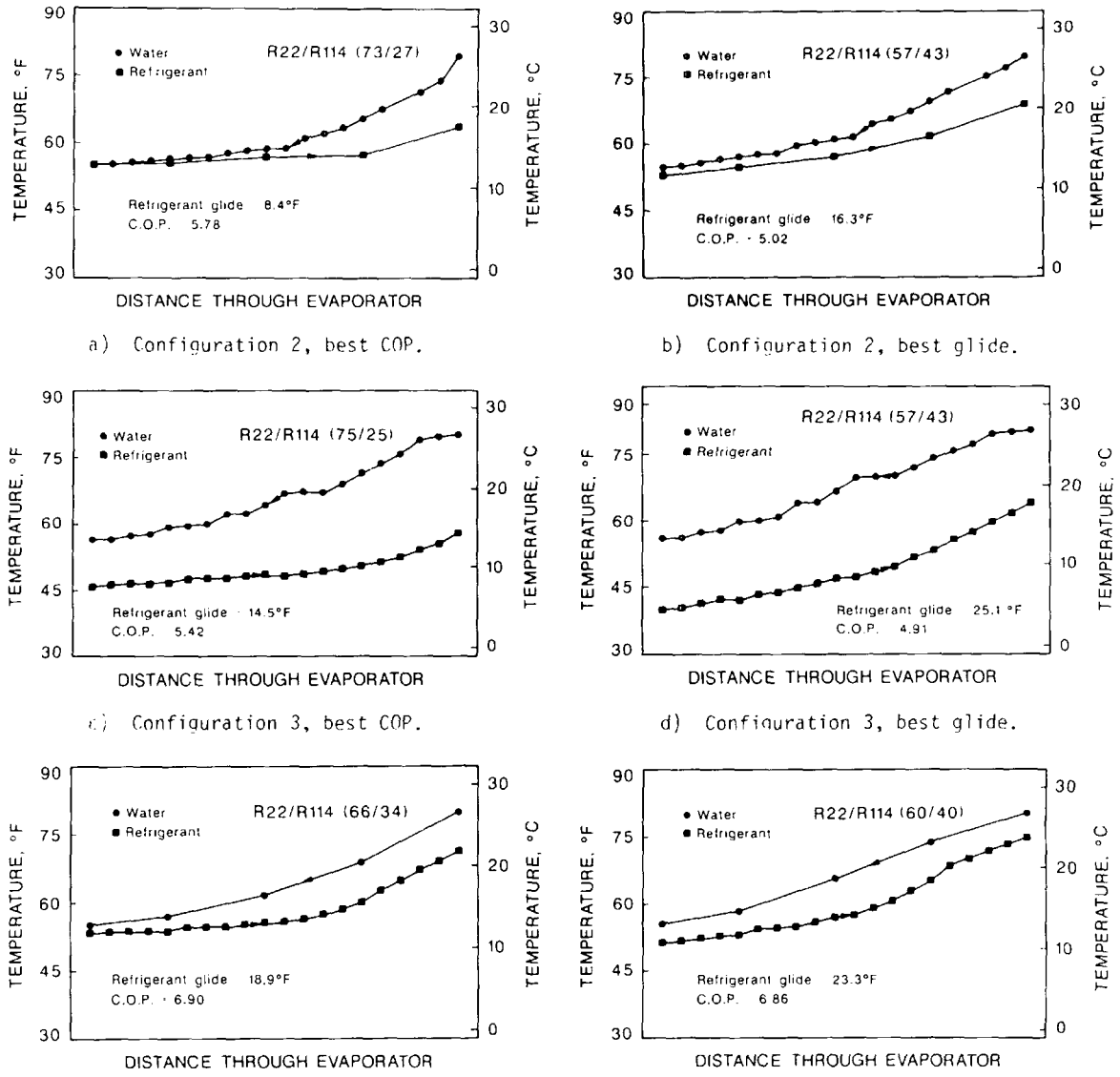

a) Configuration 2, best COP.

b) Configuration 2, best glide.

c) Configuration 3, best COP.

d) Configuration 3, best glide.

e) Configuration 4, best COP.

f) Configuration 4, best glide.

Figure 7: Evaporator temperature profiles for mixtures of R22/R114 which resulted in the highest COP and in a refrigerant glide most nearly matching that of the water (25°F, 3.9°C).

ineffective. This "pinch point" resulting from a mismatch of the refrigerant and water temperature glides limits the efficiency attainable with a pure refrigerant to that resulting from its thermodynamic properties and the LMTD (log mean temperature difference) when pinching first occurs.

As can be seen in figure 7 (for the mixture R22/R114) properly chosen mixtures do not have a pinch point. Unlike a pure refrigerant, their LMTD continuously decreases and cycle efficiency continuously increases with increasing heat exchanger size. It should be noted that mixtures always have a thermodynamic advantage over pure refrigerants because of Carnot versus Lorenz cycle considerations and this advantage is greatest when temperature lifts are low and pinch points approached. Whether this theoretical advantage results in better efficiency relative to a given pure refrigerant depends on the respective performance of the refrigerants in question.

Figures 7c and d are temperature profiles for a heat exchanger configuration (configuration 3 is shown, configuration 1 would be similar) in which pure R22 has not reached a pinch point. The best efficiency (Figure 7c) occurs with a mixture containing considerably more R22 (75% R22) than that resulting in the temperature glide most nearly matching the water temperature (Figure 7d, 57% R22). In figure 1 it could be seen that pure R22 resulted in a much higher cycle efficiency in the test apparatus than did pure R114. Hence, in this case where the mixture and the pure refrigerant can operate at comparable LMTD's, best performance occurs in a mixture rich in the better performing component. However, as can be seen in figure 8, the mixture still results in improved cycle efficiency compared to pure R22.

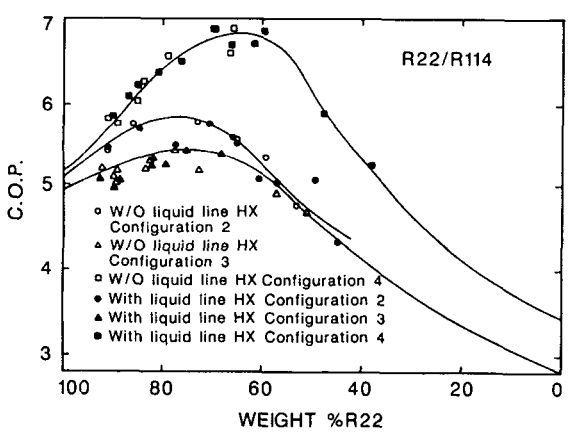

Figure 8: Performance of the mixture R22/R114 for evaporator configurations 2, 3 and 4.

Figure 7a and b are for a case in which there is a high evaporator UA and a high refrigerant pressure drop (configuration 2). Because of the tendency for saturation temperature to drop with pressure, much of the glide is lost. Both figure 7b and 7d are for a 57% R22 mixure, but the high pressure drop case has only a 16°F glide where the low pressure drop case has a 25°F glide. A second liability for mixtures in the high pressure drop configuration results from the constant heat flux test criterion. Refrigerant capacity is reduced with increased R114 concentrations which was compensated for by increased compressor speed resulting in higher gas velocities and, consequently, increased pressure drop. For this case in which pressure drop was high enough to have a significant effect on system performance, this resulted in best efficiency with a higher than expected concentration of R22.

Figure 7e and 7f are for configuration 4 which had low pressure drop and the best overall UA. In this case best efficiency occurs at an R22 concentration which results in a refrigerant temperature glide closer to the water temperature glide than in the other configurations and in the best cycle efficiency measured in this study. Referring to figure 1, a 32% improvement over pure R22 is shown. Simple cycle simulations predict equal efficiency for cycles using pure R22 and pure R114. Greatly reduced efficiency, believed to be caused by the compressor design being unsuited to the operating pressures, was observed with pure R114. If compressor designs were available to suit the various mixture requirements it is then estimated, as shown in figure 1, that a 44% improvement over pure R22 may be possible.

It should again be noted that this configuration which resulted in the greatest improvement over pure R22 employed four times the heat heat exchanger area that would be reasonable for a pure R22 system (see figure 6d). The pure R22 experiences a "pinch point" which limits its ability to effectively utilize large heat exchangers - a limitation that mixtures with appropriate temperature glides do not experience. If the heat exchanger were still larger, the system, when operating with the mixture, would be expected to have a still better efficiency which would not occur with pure R22.

Figure 9 summarizes the test results for evaporator configuration two; three, and four for the mixture R13/R12. Tests were not run at high compositions of R13 because of high discharge pressures.

An outstanding difference between the system performance for the mixture R13/R12, as shown in figure 9, and that with R22/R114, as shown in figure 8, is the effect of heat exchange between the evaporating refrigerant and subcooled liquid refrigerant leaving the condenser. This heat exchange dramatically improved efficiency for the mixture R13/R12 but has little effect for the mixture R22/R114.

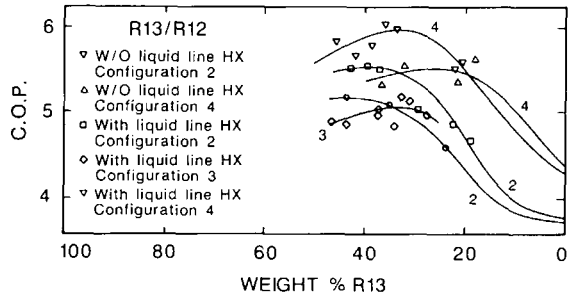

Figure 9: Performance of the mixture R13/R12 for evaporator configuration 2, 3 and 4.

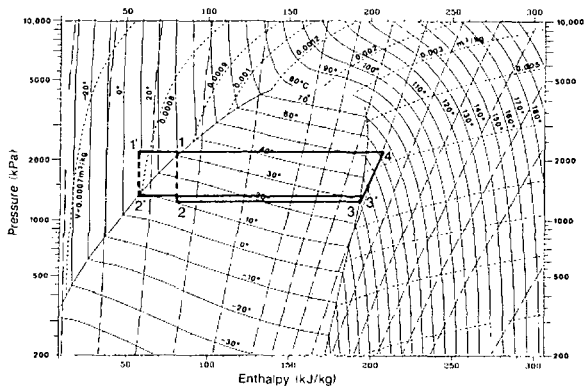

Figure 10: Effect of heat exchange between subcooled liquid and evaporating refrigerant a 40%/60% mixture of R13/R12.

The benefits to be expected from this heat exchange can be seen in figure 10, a pressure enthalpy plot of the cycle with and without this heat exchange for the mixture R13/R12. The intracycle heat exchange results in expansion from point 1' to point 2' instead of flashing from 1 to 2. Because of the slope of the isotherms in the two phase region evaporation from point 2' to point 3' results in the same average temperature as from point 2 to 3 but at a higher pressure resulting in less compressor work. Note that to achieve the requisite subcooling, heat exchange must take place in counterflow throughout the length of the evaporator because of the nearly vertical isotherms in the subcooled region.

Similar cycle plots for the mixture R22/R114 are shown in figure 11. It can be seen that the isotherms in the low quality portion of the two phase region are nearly flat resulting in no significant difference in evaporator pressure for the cycles with and without heat exchange as is also the case with pure refrigerants.

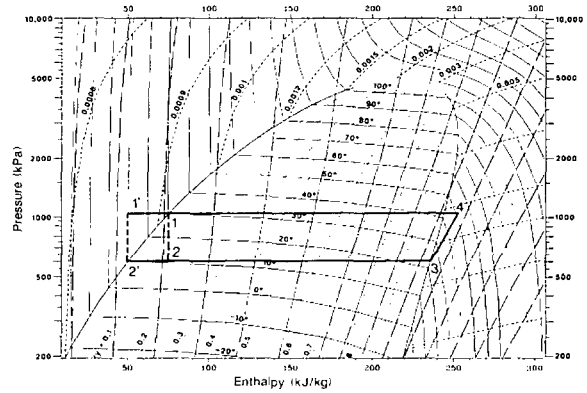

Figure 11: Effect of heat exchange between subcooled liquid and evaporating refrigerant a 60%/40% of R22/R11.

The reason that intracycle heat exchange can benefit one mixture and not the other is that enthalpy is not necessarily a linear function of temperature as is generally supposed. A further demonstration of the importance of this nonlinearity is shown in figure 12, comparing plots of refrigerant and water temperatures through the evaporator. In these figures a

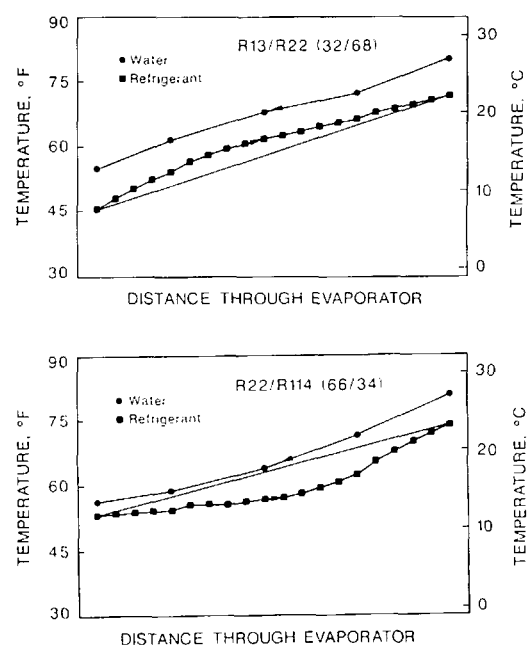

Figure 12: Comparison of typical evaporator temperature profiles for the mixtures R22/R114 and R13/R12.

straight line has been drawn between the entering and leaving refrigerant temperatures to emphasize that one refrigeant has a concave and the other a convex temperature profile. This manifestation of nonlinearity would interfere with cycle performance prediction using simple computer programs in which only inlet and outlet temperatures are specified and linearity is assumed within the heat exchangers. Additionally, the pinch points which result from this nonlinearity reduce cycle efficiency.

Conclusion

A mixture of R22/R114 was found to be 32% better, and a mixture of R13/R12 16% better, in efficiency than R22 in an air conditioning application. Some system design characteristics that make it likely that mixtures will substantially outperform pure refrigerants are counterflow heat exchangers, large heat exchangers, high temperature glide in the heat source/sink fluid, matching of refrigerant and heat source/sink temperature glides and a low temperature lift.

Nonlinearity of enthalpy as a function of temperature in the two phase region was observed to have an effect on system design with respect to intracycle heat exchange and cycle simulation using models.

Session 2

Electric Heat Pump Technology: Related Research

Organizer : V. D. Baxter
Oak Ridge National Laboratory
Chairman: T. G. Statt
U. S. Department of Energy

Heat Pump Research at the Electric Power Research Institute

A. Lannus
Electric Power Research Institute
Palo Alto, CA 94303

EPRI's research program on heat pumps is aimed at developing equipment and systems with improved efficiency and cost effectiveness to customers, improved power demand characteristics to utilities and broader applications in existing and new buildings. This paper outlines the reason for electric utilities' interest in heat pumps and describes the key projects in EPRI's heat pump R&D program.

Electric Utility Perspective

Electric energy consumption in this country has been growing steadily (Figure 1), while overall energy use has had its ups and downs. Moreover, increased electricity consumption correlates very well with economic growth, whereas consumption of other forms of energy does not (Figure 2). Eighty-four per cent of the 2.6 trillion kilowatthours of electricity generated in this country comes from relatively abundant primary energy sources such as coal, nuclear and hydrostatic energy (Figure 3). Only 15% of generation is based on critical, albeit currently cheap, energy resources such as oil and natural gas.

About two-thirds of the utilities in the U.S. are summer-peaking, due largely to the growth in residential and commercial air conditioning (Figure 4). The balance of the utility industry is either winter-peaking or has leap-frogging summer and winter peaks. Winter peaks are growing slightly faster than summer peaks, 2.1% vs. 2.0% per year. Although one would think that summer-peaking utilities are in the South and winter-peaking utilities in the North, this is not always the case. For example, commercial and residential air conditioning demand makes Northern States Power Co., serving the Minneapolis area, summer peaking, whereas Florida Power and Light Co., serving Miami and the southern and eastern parts of the state, is winter-peaking, due to high saturation of electric heat, used only a few days per year.

Air Conditioning and Heating Demand

Air conditioning demand in this country has been growing steadily since World War II. In 1986, about 70% of new single-family homes were equipped with central air conditioning and about 90% of new multifamily dwelling units were fitted with air conditioning in some form. Because there are few alternatives to electric cooling, the central issue for electric utilities is to reverse the decline in system annual load factors (i.e. the ratio of the average annual demand to the peak demand) by aggressively competing for the heating load. Moreover, north of the latitude of north Texas or so, many more hours of heating than cooling are required, which makes space heating the better revenue producer to utilities.

Electricity is the heating energy source for 45% of new single-family homes (Figure 5) and is the preferred heating energy form in 65% of new multi-family dwellings (Figure 6). The key to its market share growth has been the heat pump (Figure 7,8). Underscoring the importance of the heat pump to electric utilities is the fact that the electric utility, not the manufacturer or dealer, gets the lion's share of the money paid out by a customer to own and operate a heat pump over its lifespan (Figure 9).

Clearly, electric utilities have a vital stake in energy-efficient and cost-effective heat pump technology.

EPRI Heat Pump Research Program

EPRI's heat pump research program covers a broad range of residential and commercial space heating, cooling and water heating applications. Although our primary goal is to accelerate the development of efficient, reliable and cost-effective equipment and systems to customers, we also have to consider the effect the heat pump will have on the utility's power demand characteristics and cost

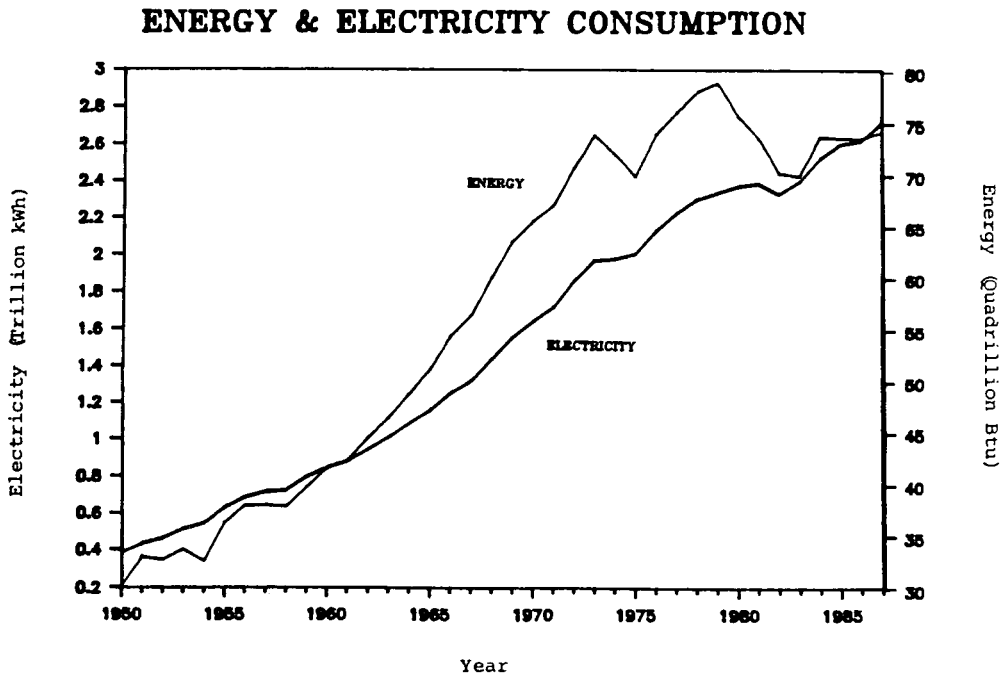

Source: EIA Figure 1

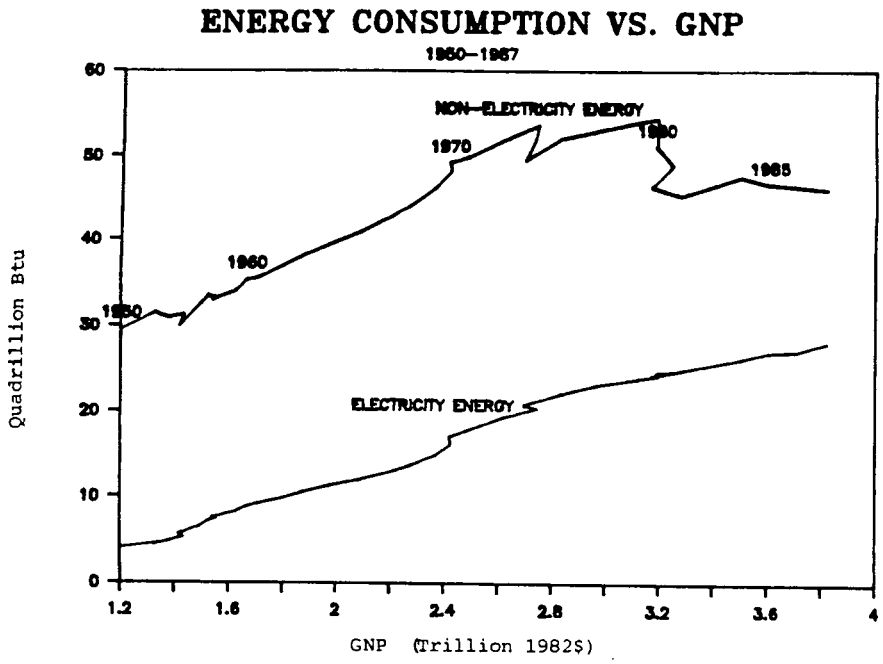

Source: EIA Figure 2

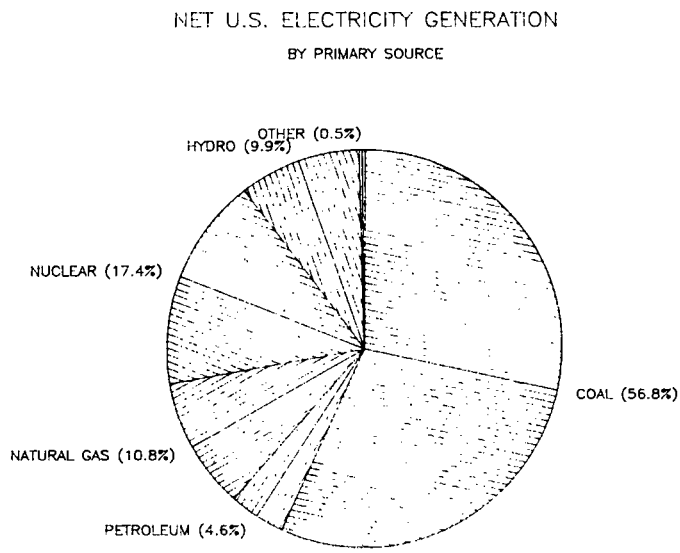

Source: EIA Data for 1987

Figure 3

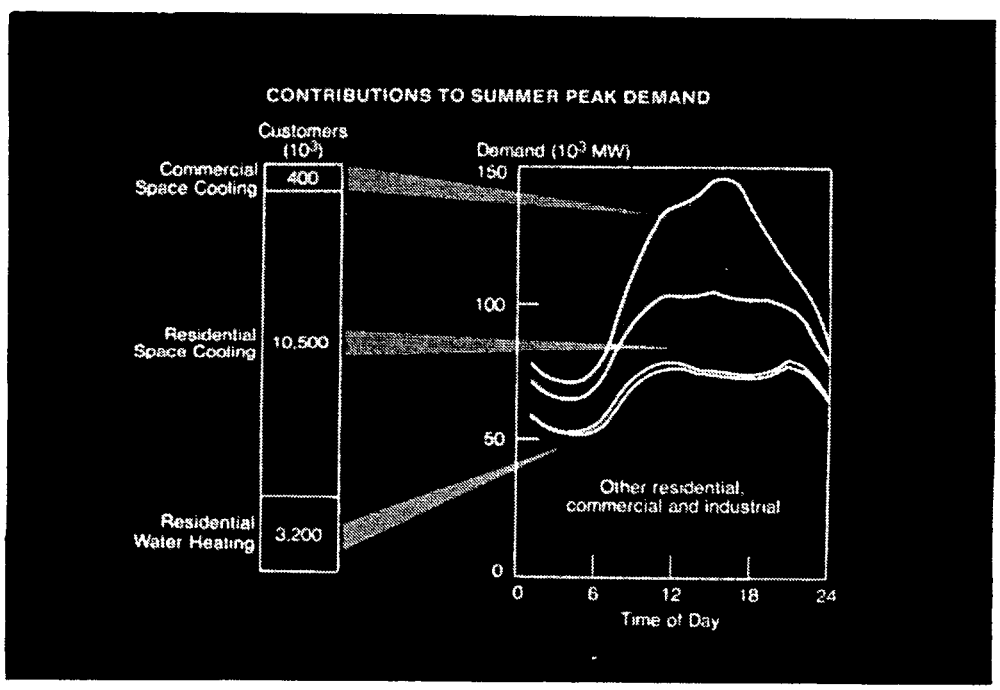

Figure 4

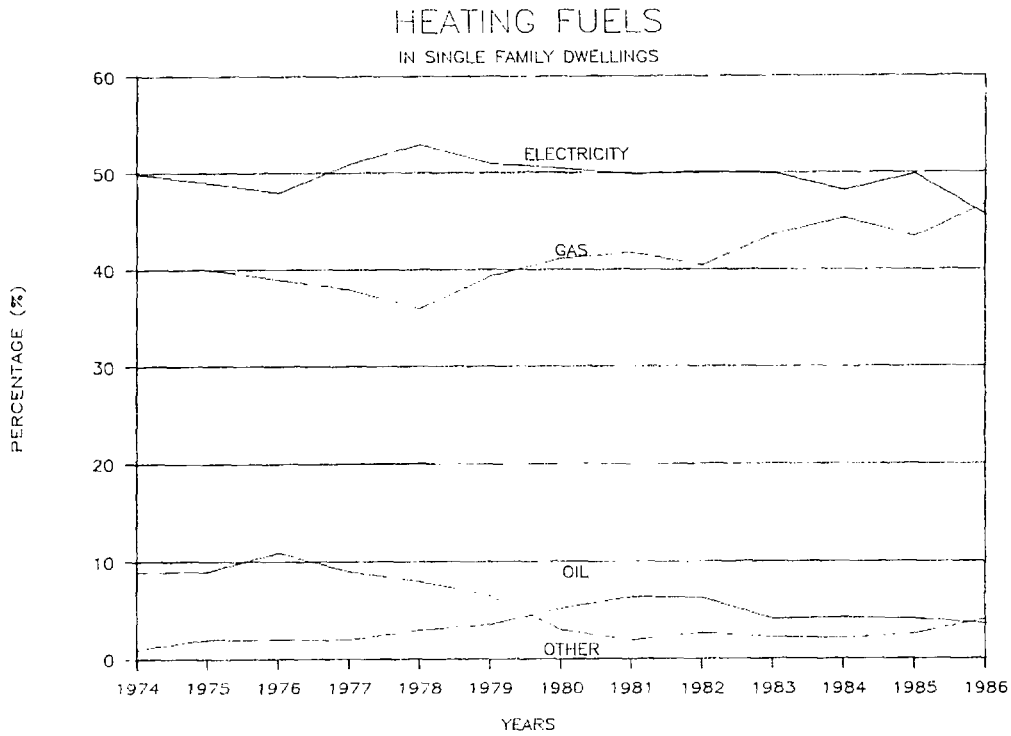

Figure 5

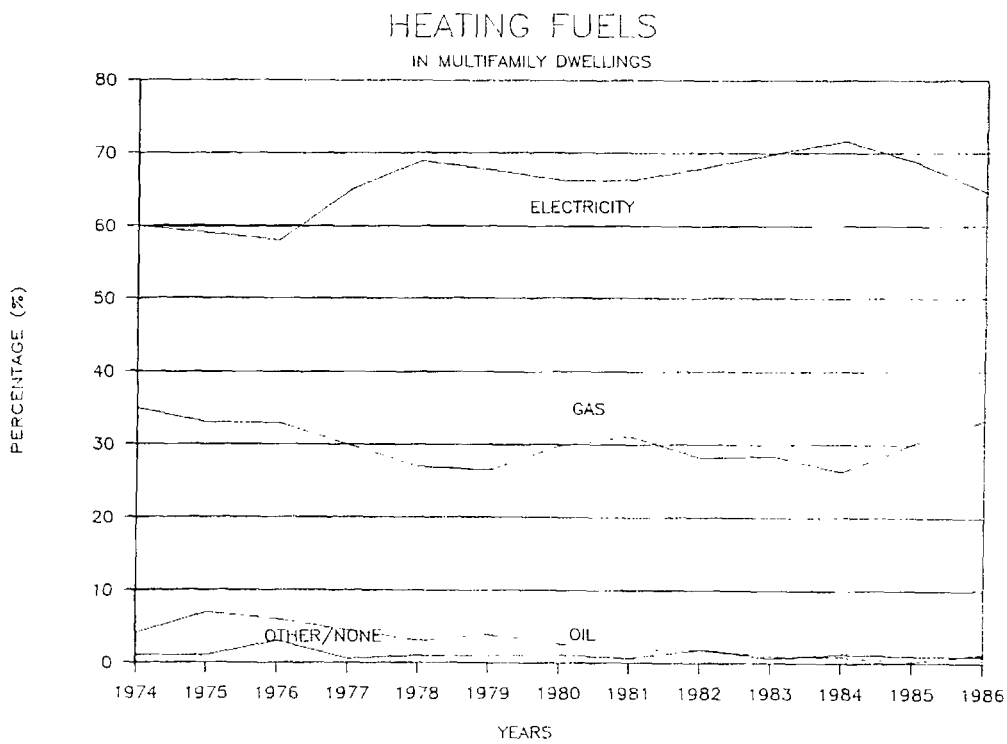

Figure 6

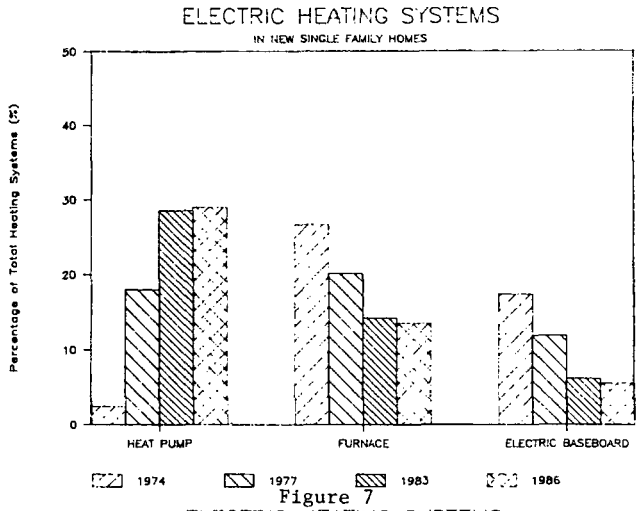

Figure 7

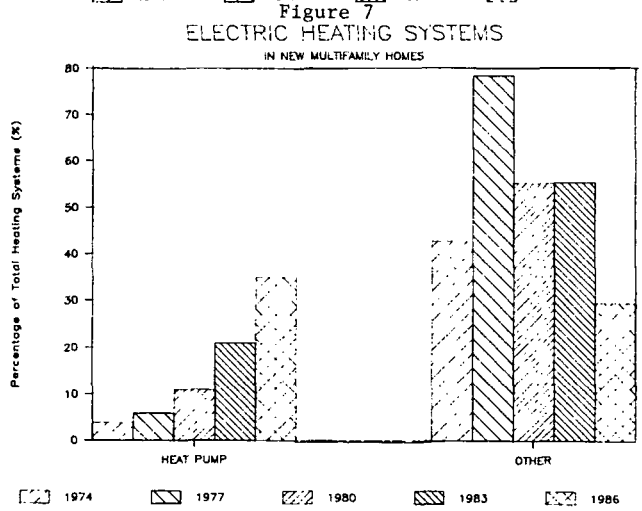

Figure 8

HEAT PUMP R&D:

ELECTRIC UTILITIES HAVE THE MOST AT STAKE

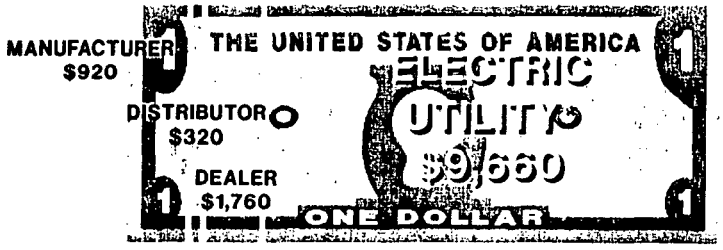

Revenue per Installation

*** 15-year present value at 12%**

7186.4 A

Figure 9

of service. A heat pump that saves energy for the customer, but imposes a high demand peak without the attendant kilowatthour revenue, will ultimately drive up energy costs to all customers. At the same time, time-of-use rates, providing significant economic incentive to a customer to reduce peak demand or shift his energy use to off-peak hours, are in place mostly for larger nonresidential customers. Because residential customers are charged for kilowatthour usage only, there is little incentive for customers to buy, and manufacturers to make, heat pump equipment with better power demand characteristics, without some inducement from the utility. EPRI's research is also aimed at developing the technology for utilities to do so economically and reliably.

Reliability and Field Performance

Our strategy in the near term is to emphasize projects that support utility programs in promoting efficient heat pumps. Given that the early heat pumps experienced high rates of failure in the 1950's and 1960's, questions about the reliability of heat pumps linger and have been the basis of strong counter-advertising by the electric utilities' competitors. To obtain and document the facts, EPRI has conducted a number of highly detailed surveys by tracking down heat pump and compressor maintenance and replacement records in two areas -- Alabama and Northern Illinois -- where it was possible to obtain a sufficiently large sample to draw statistically meaningful conclusions. Taken together, nearly 2400 heat pump customers were investigated by random sampling for total system service life data. Nearly 18,000 customers were in the heat pump compressor life survey.

The principal findings are as follows:

a. Median heat pump service life was in excess of 20 years in the Alabama sample and about 15.5 years in the Northern Illinois sample (Figure 10).

b. About half of the heat pumps removed from service were still functioning at the time of replacement, and were replaced due to perception of age or to take advantage of an incentive to buy higher efficiency equipment, not because of mechanical failure.

c. Between 84 and 91% of the heat pumps removed were replaced with other, newer heat pumps (range due to survey uncertainty); only 9% were converted to another heating system.

d. At the end of ten years, 59% of the units in Alabama and 69% of the units in Northern Illinois still had their original, factory-installed compressors. Because more than half of the original compressors were still in service at the end of ten years, it was not possible to determine the median life precisely, but an extrapolation puts it at about 13.5 years.

e. The median life of replacement compressors is at least 9 years and, possibly, more (the sample is biased toward equipment more prone to failure) -- only a few years shorter than the extrapolated median life of original, factory-installed compressors.

f. In-warranty maintenance cost data from Alabama show that in current dollars, heat pump maintenance cost has remained constant or decreased slightly. In constant dollars, it is clear that newer heat pumps are cheaper to maintain.

All of these studies have been published in EPRI research reports available to the public. The results have been summarized in several ASHRAE papers, hence having been subjected to detailed peer review.

EPRI studies of equipment field performance have found HSPF's in the 4.5-7.8 range with SEER's about 4.7-8.9. These studies have involved equipment of 1970's vintage design but did show that when local weather is taken into account, calculated and measured seasonal efficiencies were reasonably close, with occasional exceptions. Reports on these studies also have been published.

Our laboratory and field studies have shown that the DOE method for determining HSPF tends to underestimate defrost and overestimate cycling efficiency losses, at least for the equipment studied. However, these errors tend to compensate for each other and thus the overall agreement was within 4%. Improved algorithms, based on first principles, were developed for more precise calculation of seasonal efficiency.

Advanced Air-Source Heat Pump

An important project is a joint program with Carrier Corp. to develop a variable-speed air source heat pump with integrated water heating. The heat pump, designated 38QE (Figure 11), is aimed at the residential and light commercial add-on and replacement market, as well as the upscale new home market. The project is now in the final testing and component qualification stage. The original HSPF = 9 and SEER = 12 targets have been reached or exceeded in the laboratory. Moreover, integration of the water heating function is estimated to produce energy savings to the customer equivalent to that of a heat pump with an SEER about four points higher (and a correspondingly higher HSPF), when compared to electric resistance water heating instead. A joint project with NBS and DOE is planned to devise a rating scheme which accounts for water heating as well as space conditioning performance.

An important feature of the advanced heat pump is the optional demand-limiting control. This feature allows the utility to send a radio or power-line carrier signal to the heat pump

HEAT PUMP SERVICE LIFE

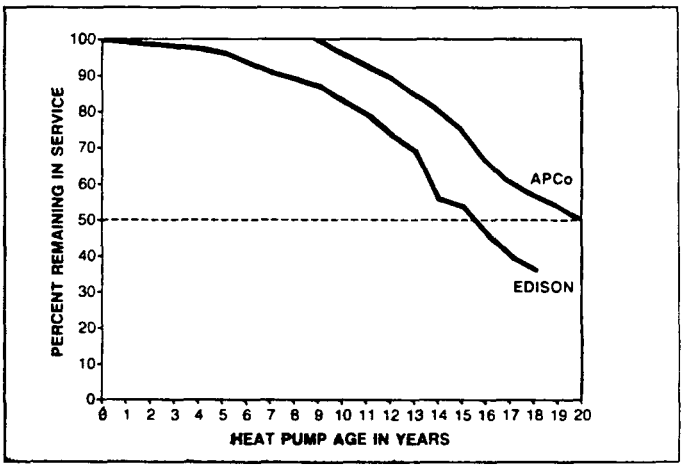

Figure 10

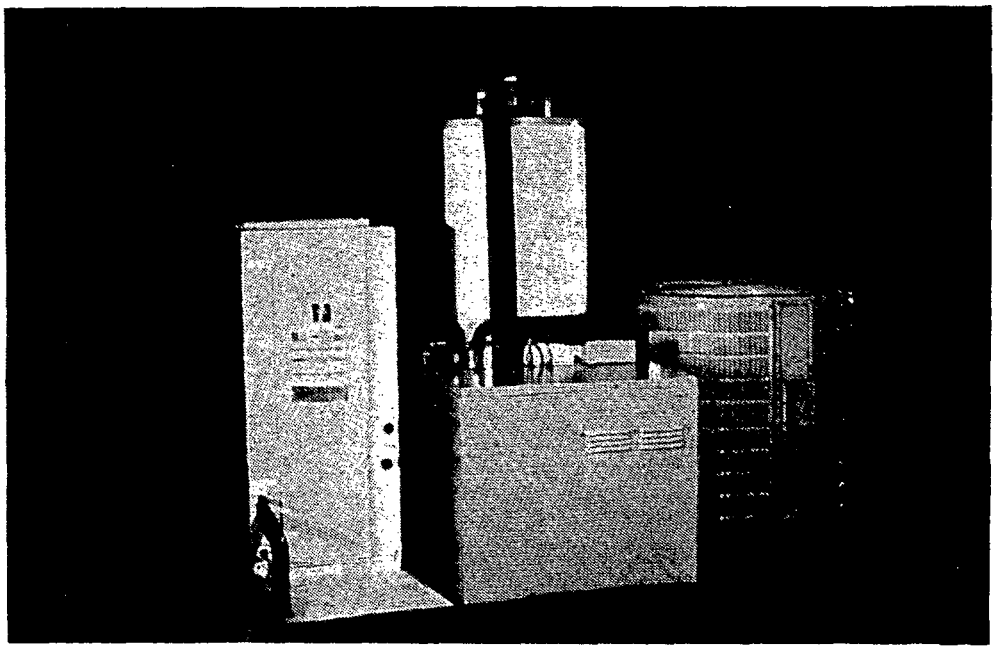

Figure 11

control system to limit the compressor speed and thereby the power demand (Figure 12). Resistance heating elements in the water tank are also disabled by the signal. The result is reduction in maximum power demand of about 2 kW in the summer and 3 kW in the winter and improvement in load factor. Naturally, the utility may have to provide an incentive to the customer to allow the utility to "load-manage" his heat pump, but features in the advanced heat pump make its load management more effective than the duty-cycling control practiced widely.

Outdoor noise level is about 7.1 to 7.2 bels, depending on model. A second-phase field test of ten units revealed some problems requiring design modifications, which have been made. Currently units are undergoing durability tests in the environmental chamber. Barring problems, production is to begin in about nine months.

Dual-Fuel Residential Heat Pump

Tecogen, Inc., with assistance from Goodman Manufacturing, have been working on a dual-fuel heat pump as an effort to develop an improved, furnace-supplemented heat pump for the fossil fuel furnace and air conditioner replacement market, especially in cold climates. Various schemes for putting supplemental heat into the heat pump cycle are being examined and, if any of them shows merit, will be tested in the laboratory.

Ground-Source Heat Pumps

EPRI also has a modest research program in ground-source heat pumps, closely coordinated with DOE, the National Rural Electric Cooperative Association and the recently-formed International Ground-Source Heat Pump Association. Typical projects being pursued include development of a classification scheme for the thermal properties of soil and rock and a joint project with ORNL to determine design criteria for direct-contact ground coils. Equipment improvement projects are also in our plans, but no work in this area is ongoing at the moment.

Closed-Loop Water-Source Heat Pumps

Turning now to heat pump research aimed at commercial buildings, a project is underway to instrument and monitor the operation of closed-loop water-source heat pumps. The objective is to obtain data on system performance, especially to optimize the control system to take maximum advantage of the excellent heat recovery capability of this type of system. Two projects to evaluate possible equipment improvements to water-to-air equipment itself have been started in partnership with manufacturers. EPRI views the potential of the closed-loop water-source heat pump system as an important and economically attractive alternative to the traditional variable air volume chiller-boiler based central plant.

Dual-Fuel Rooftop Heat Pumps

Another opportunity for the heat pump is as a replacement for the ubiquitous gas-electric rooftop HVAC unit or "year-round" air conditioner, as it is frequently called. The market for gas-electric units is about 146,000 units per year, single-package and split-system units combined, and many of these, installed fifteen to twenty years ago, are about due for replacement. The hours of operation of the commercial buildings (e.g. supermarkets, small retail stores) where gas-electrics are often applied would make the use of a heat pump for at least part of the heating requirements economically attractive, except for the cost of upgrading the power service panel to permit installation of supplemental resistance heat. EPRI is working with Lennox to test a dual-fuel heat pump (i.e. a unitary heat pump with gas supplemental heating) for retrofit and replacement applications. At the time of writing this paper, four of the five planned field-test units have been installed and are operating satisfactorily. Our plans (Figure 13) are to continue the field test into next winter to gather more operating data. W. S. Fleming is the field-test contractor.

Component Improvement and Advanced Concepts

Not all of EPRI's heat pump research is near- or medium-term. Projects are underway to examine the behavior of reciprocating compressors under variable speed operation, to understand better the limitations that current valve designs may impose on the compressor's ability to reach speeds greater than 90 and 120 Hz. Multipressure cycles are being examined in another, recently started, project.

Perhaps the most interesting area is the work on non-azeotropic fluids conducted by NBS with DOE cofunding. This work, begun in 1982, led to the Morrison-McLinden equation of state, as well as the Domanski computer code for modeling a heat pump charged with a refrigerant mixture. Current, EPRI-cofunded work at NBS is aimed at evaluating and testing one or more system designs employing a non-azeotropic mixture working fluid.

Whether this work will lead to a new heat pump technology for the mass market is not yet clear, but EPRI intends to continue to work with the DOE and national laboratories toward realizing the promise of this technology.

Summary

Research, by definition, sets its sights on the future and electricity is the energy of the future.

Because 99% of the customers and 69% of the revenue of the electric power industry come from residential and commercial customers, whose largest energy uses are heating and air conditioning, one key to utilities' future is,

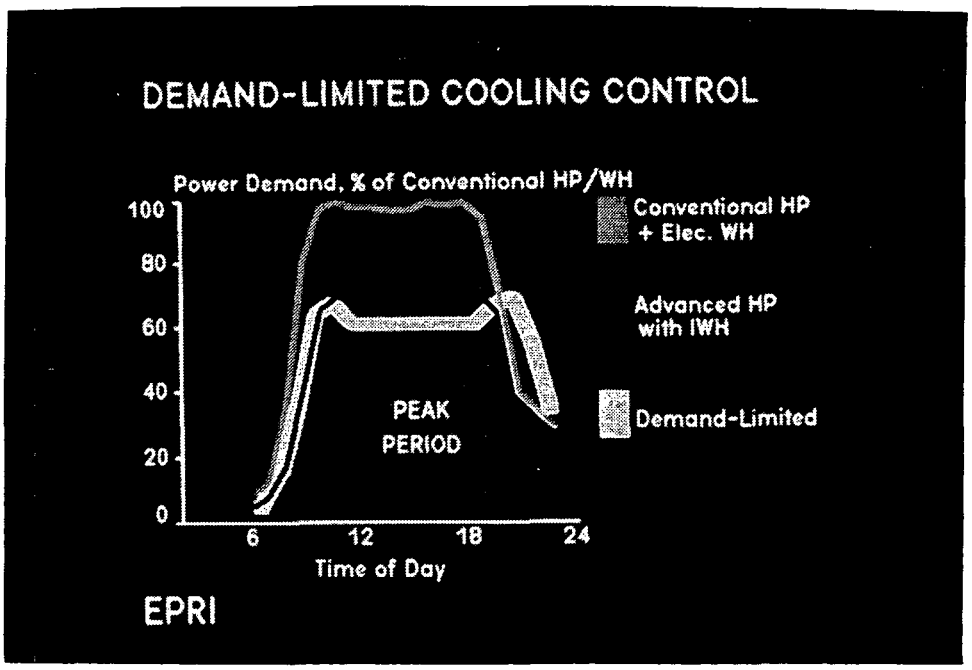

Figure 12

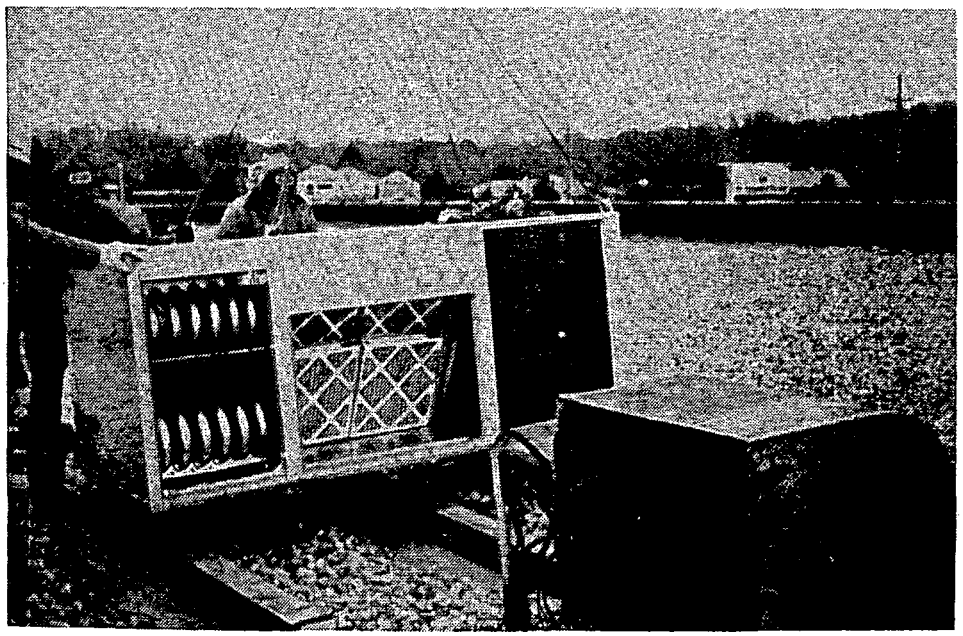

Figure 13

clearly, the electric heat pump. But, more important, an energy-efficient and cost-efficient heat pump is not only the best deal for the customer, but the most conserving of this Nation's economic resources -- capital and labor, as well as energy. Technical development programs that pursue thermodynamic efficiency for its own sake and ignore first cost, i.e. the efficient use of the customer's capital -- however much attention they focus on his energy dollars -- are, in the author's opinion, wasteful of the Nation's economic resources as well as liable to ultimate harsh judgment by the market-place.

EPRI's heat pump research and development program strives to maintain these considerations in their proper balance.

Overview of Ground-Coupled Heat Pump Research and Technology Transfer Activities

V. D. Baxter and *V. C. Mei*
Oak Ridge National Laboratory
Oak Ridge, TN 37831

Abstract

Highlights of DOE-sponsored ground coupled heat pump (GCHP) research at Oak Ridge National Laboratory (ORNL) are presented. ORNL, in co-operation with Niagara Mohawk Power Company, Climate Master, Inc., and Brookhaven National Laboratory developed and demonstrated an advanced GCHP design concept with shorter ground coils that can reduce installed costs for northern climates. In these areas it can also enhance the competitiveness of GCHP systems versus air-source heat pumps by lowering their payback from 6-7 years to 3-5 years. Ground coil heat exchanger models (based primarily on first principles) have been developed and used by others to generate less conservative ground coil sizing methods. An agressive technology transfer initiative was undertaken to publicize results of this research and make it available to the industry. Included in this effort were an international workshop, trade press releases and articles, and participation in a live teleconference on GCHP technology.

Introduction

Ground coupled heat pump (GCHP) research at ORNL has, since 1985, been focused on three areas. The first involves proof of concept testing of a GCHP system design optimized for northern climates. Second, we have wrapped up our ground coil heat exchanger (GCHX) modeling work. Finally, an active technology transfer effort has been undertaken dealing principally with the advanced design GCHP.

Optimized GCHP System Tests

The optimized design concept was developed from a joint analytical project between ORNL, Brookhaven National Laboratory (BNL), and Climate Master, Inc. The objective of this project was to minimize the life-cycle cost (LCC) for a GCHP system given the freedom to design the heat pump and the ground coil in concert. Details of this analytical project are reported elsewhere.[1] The results are summarized briefly in this paper.

Life cycle cost was calculated using three computer models which were developed or adapted for this purpose. They are:

Water-Source Heat Pump (WSHP) Model. A modification of the ORNL heat pump model[2] that uses experimentally validated water/refrigerant heat exchanger subroutines developed for this project.[3]

Ground Coil Model. A BNL-developed refinement of the GROCS/TRNSYS program that models the cycling behavior of buried pipe heat exchangers and does not require TRNSYS to simulate earth coils.[4]

Parameterized Heat Pump Cost Model. A program that calculates the manufacturer's cost for WSHPs in the 2- to 10-ton (7- to 35-kW) capacity range based on the same physical description as used by the WSHP model.[5]

Table 1 shows the results of the computer analysis. In the analysis were a base-case system, a fully optimized system, and a "buildable" optimized system. This buildable system was made

Table 1. Optimization Analysis Results

	Base-Case System	Fully Optimized System	Buildable Optimized System
Compressor Displacement, in.^{3}	3.27	3.419	3.27
Air Coil:			
Face Area, ft^3	3.33	5.19	5.00
Tube Rows	3	4	4
Water Coil:			
Shell I.D., in.	1.388	1.683	1.584
Length, in.	168	207.8	210
Ground Coil Length, ft	1500	766	750
Heat Pump Factory Cost	$608	$737	$717
System Installed Cost[a]	$4796	$3953	$3889
7-year LCC	$10723	$9151	$9132
System Performance			
SPFH	2.58	2.69	2.67
SPFC	3.29	3.69	3.63
APF	2.67	2.81	2.79

[a] Includes retail cost of WSHP unit plus ground coil cost at $1.50/ft ($4.92/m), excluding ductwork.

*Research sponsored by the Office of Buildings and Community Systems, U.S. Department of Energy, under Contract DE-AC05-84OR21400 with Martin Marietta Energy Systems, Inc.

up of currently available components to best approximate the fully optimized version. The analytical results show that the buildable version offers a first cost savings -- heat pump and ground coil installed -- of 19% over the base-case system. The WSHP for the buildable version can be constructed by adding about $110 in efficiency improvements to the commercially available base-case unit. These improvements allowed use of a ground coil only 50% as long as that of the base system.

Performance and costs of the buildable optimized system and two air-source heat pumps (ASHP) are compared in Table 2. The two ASHPs used in the comparison were (A) a standard mid-line system [heating COP = 2.7 at 47°F (8.3°C)], and (B) a high efficiency system [heating COP = 3.2 at 47°F (8.3°C)]. Compared to the A and B alternatives, the optimized GCHP system has lower 7-year LCCs and much higher annual efficiencies. Simple payback periods relative to both alternatives are under 3 years. Calculated LCCs represent the sum of the system first cost plus the annual electricity cost (at 8¢/kWh) multiplied by a present worth factor of 6.34. This present worth factor was calculated from U.S. Department of Energy electricity cost projections[6] using a discount rate (after-tax, after-inflation market interest rate) of 3.5%.

Results of the analytical phase of this project were sufficiently positive to warrant follow-on laboratory and field evaluations. Niagara Mohawk Power Company (NMPC) agreed to co-fund the field evaluations.

Two prototype WSHPs based on the buildable configuration from Table 1 were constructed by Climate Master, Inc., under subcontract to BNL. One of the prototypes was tested at ARI standard conditions by Climate Master, Inc. Rated performance from these tests is given in Table 3 with the model predictions. Test results and analyses showed reasonably good agreement. Agreement is similar to that achieved between test and analysis for ASHPs.[2]

The two prototypes were installed in locations near Syracuse, New York, and monitored over the 1985-86 heating season. Figures 1 and 2 illustrate the site layouts, the design heating loads, and the ground coil material and size. A monthly bin analysis method[7] (developed previously in work sponsored by NMPC, New York State Energy Research and Development Authority, and Rochester Gas and Electric Corporation) was utilized to size ground coils to the prototype units as applied to the two residences.

One site was designed with a one-pipe-per-trench horizontal ground coil, the other with a two-pipe-per-trench horizontal ground coil. In each case the coils were designed for a minimum source temperature of 25°F. The intent behind using two ground coil configurations was to verify that the prototype heat pump allows shorter single <u>and</u> multi-pipe coils.

Both ground coil designs represent about a 30% reduction in sizing as recommended for standard systems used in the New York area.[8] This reduction

Table 2. Performance and Cost Comparisons Between Buildable GCHP System and Two ASHP Systems

Cost (1984 $)		Annual Electricity Costs[c] (1984 $)	APF	7-year Life Cycle Cost (1984 $)	Simple Payback (years)
Heat Pump[a]	Ground Coil[b]				
Air-Source Heat Pump[d]					
A. 2984	----	1239	1.86	10839	----
B. 3460	----	983	2.34	9692	----
Ground-Coupled Heat Pump					
2764	1125	827	2.79	9132	vs A-2.20 vs B-2.75

[a] Installed cost excluding ductwork.

[b] Installed cost at $1.50/ft ($4.92/m).

[c] Electricity cost at $0.08/kWh.

[d] A. Standard mid-line system; heating COP = 2.7 at 47°F (8.3°C).
B. High efficiency system; heating COP = 3.2 at 47°F (8.3°C).

Table 3. Prototype WSHP Performance at ARI Rating Conditions.

Mode	Entering Water Temp[a] (F)	Entering Air Temp[b] (F)	Capacity (Btu/hr)		COP[c]	
			Measured	Predicted	Measured	Predicted
Heating	50	70	38,900	39,900	3.89	4.12
	70	70	49,000	50,100	4.34	4.44
Cooling	50	80	47,900	48,900	5.67	5.70
	70	80	44,500	45,100	4.48	4.50

[a] 9 gpm.

[b] 1200 cfm.

[c] Coefficient of Performance.

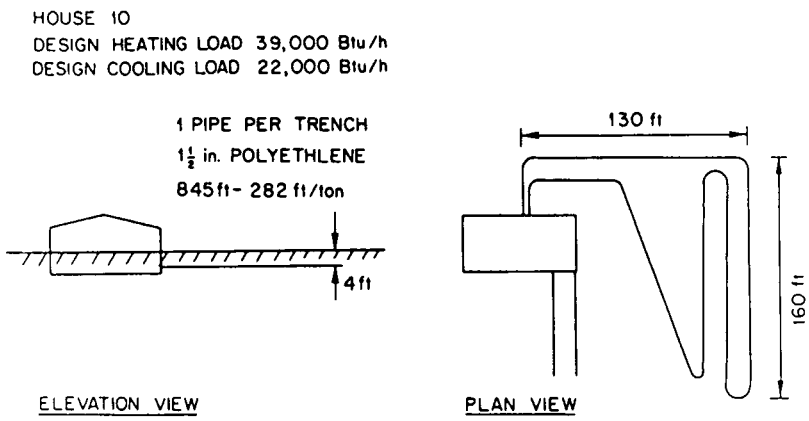

Fig. 1. Site 10 ground coil layout, size, and material

in ground coil length is estimated to reduce the cost of the optimized design GCHP by 10% over that of standard design GCHPs.

Reference 9 fully describes the field test results and analyses. Table 4 gives a summary of the performance at each site. Heating seasonal coefficients of performance (SCOPs) were 2.74 (Site 10) and 2.90 (Site 11). The lower value at Site 10 was the result of the unit operating with low refrigerant charge for a period of time. Heating seasonal performance factors (SPFHs) were 2.70 and 2.71. The unit with the higher SCOP (Site 11) had a higher thermal load and higher use of auxiliary electric resistance heat causing the equalization in SPFH. Cooling seasonal performance factors (SPFC) were 3.49 (Site 10) and 3.32 (Site 11).

Previous tests of existing technology based systems yielded SPFHs of 2.5 - 3.1 with ground coil sizes of 450 - 460 trench ft/ton (1 pipe per trench).[10] The advanced systems achieved heating SPFs of about 2.7 with ground coils of 282 trench ft/ton (1 pipe per trench) and 183 trench ft/ton (2 pipes per trench). Similarly, SPFCs for existing technology ranged from 3.1 -3.4 compared to 3.3-3.5 for the advanced systems.[10]

Normalized system performance analyses for a standard house under normal Syracuse weather with a given minimum source temperature indicated that the advanced WSHP design could achieve significantly higher performance than could current standard designs. This performance advantage can be sacrificed in favor of lower installed cost by reducing the ground coil length or by using a smaller WSHP. For equivalent SPFH, the advanced WSHP can be sized at 2 tons whereas a standard unit must be 3.5 tons. Under this condition, the advanced WSHP would require a ground coil only 40% as long as that needed by the standard WSHPs

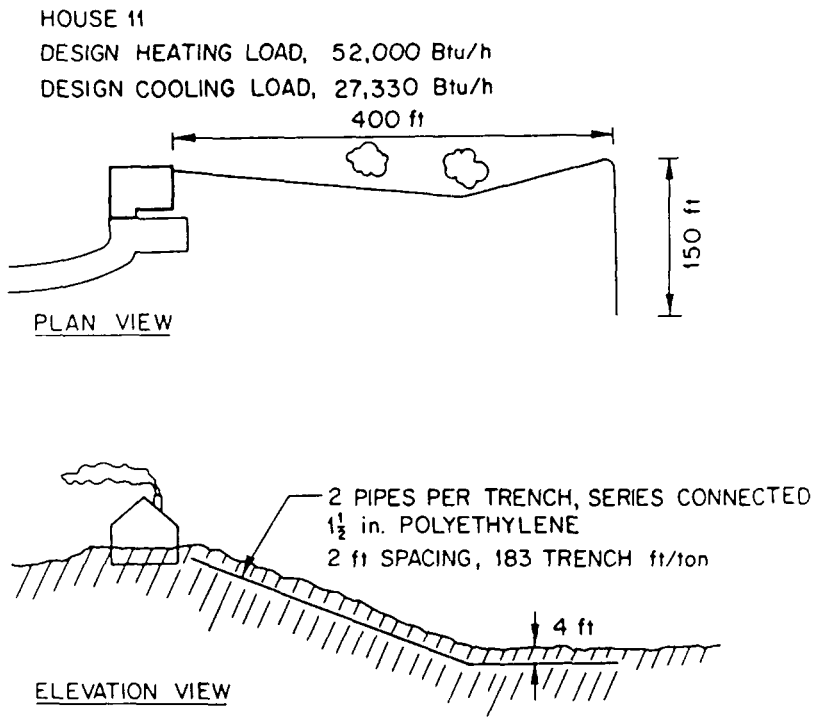

Fig. 2. Site 11 ground coil layout, size, and material.

Table 4. Field Performance Summary for Advanced Design GCHP Systems

	Site 10	Site 11
Heating Season		
Degree Days [°F days]	6,244	6,194
Load (kWh)	16,091	26,183
Energy Consumption (kWh)		
Heat Pump	5,881	9,012
Auxiliary	132	1,004
SPFH[a]		
Overall	2.70	2.71
Excluding auxiliary (SCOP)[b]	2.74	2.90
Cooling Season		
Degree Days [°F days]	189	271
Load (kWh)	422	4,000
Energy Consumption (kWh)	121	1,205
SPFC	3.49	3.32
Annual Performance Factor		
Overall	2.71	2.78
Excluding Auxiliary (ACOP)[c]	2.75	2.95

[a] Seasonal Performance Factor, heating.
[b] Seasonal Coefficient of Performance.
[c] Annual Coefficient of Performance.

(see Fig. 3). These analyses further indicated that the advanced WSHP enhances the competitiveness of GCHP systems versus ASHPs by lowering their payback from 6-7 years to 3-5 years.[9] This analysis is in agreement with the results from the earlier analytical project.[1]

It is important to note that *this advanced design with shorter ground coils is strictly applicable only in northern or heating-load-dominated climates.* For applications where the cooling load dominates, the shorter coil lengths of this design may result in excessively high water/brine temperatures entering the ground coil. The prototype WSHPs (used with longer, standard design ground coils) will yield higher GCHP system efficiencies for such applications, however.

GCHX Modeling

The ORNL GCHX modeling program began in 1980. The fundamental concept was to be more rigorous in the theoretical analysis underlying development of mathematical models for different types of ground coils. Only through the understanding of heat and mass transfer mechanisms between the fluid, coil wall, and soil can important design factors (many which are ignored by the line-source approach) be studied.

One vertical[11] and three horizontal[12] ground coil models were developed. The horizontal coil models included: (1) single coil with a radially symmetrical temperature profile and soil moisture freezing effect; (2) single coil with nonsymmetrical soil temperatures around the coil; and (3) double coils, one on top of the other in the same trench, with nonsymmetrical soil temperatures around the coils and with thermal interference effects.

The first horizontal coil model is designed to check the effect of soil moisture freezing around the coil. This model was used by W. S. Fleming and Associates to help develop the monthly bin analysis method described in reference 7. The second horizontal coil model enables simulation of the effect of ground surface heat transfer with the ambient air. The third is used to study the effect of two coils buried in the same trench.

All three models have been well validated with field experimental data provided by BNL and The University of Tennessee (UT). It is impossible to compare the ORNL models to line-source models on the basis of energy absorption/rejection, because this parameter is required input for line-source models. Comparison on the basis of predicted soil temperatures, however, reveals that ORNL models match the data better in spite of the fact that line-source models are given the exact heat rejection/absorption rate as input. Figure 4

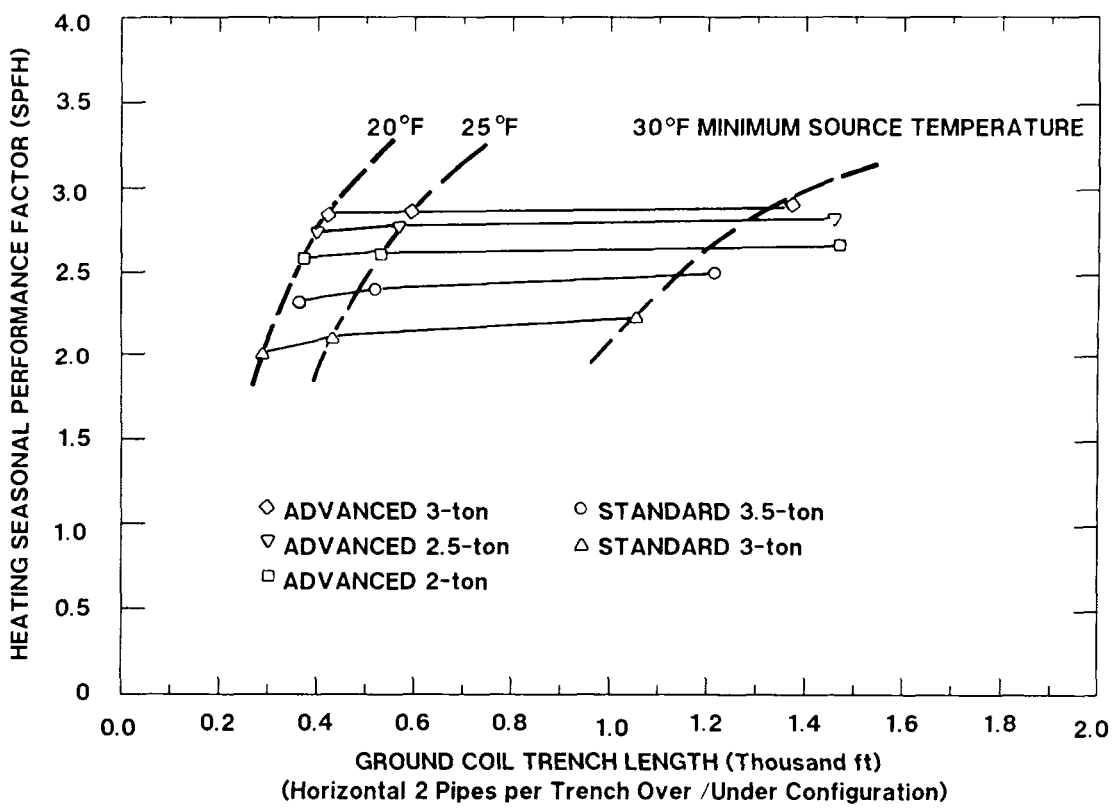

Fig. 3. SPFH vs ground coil length

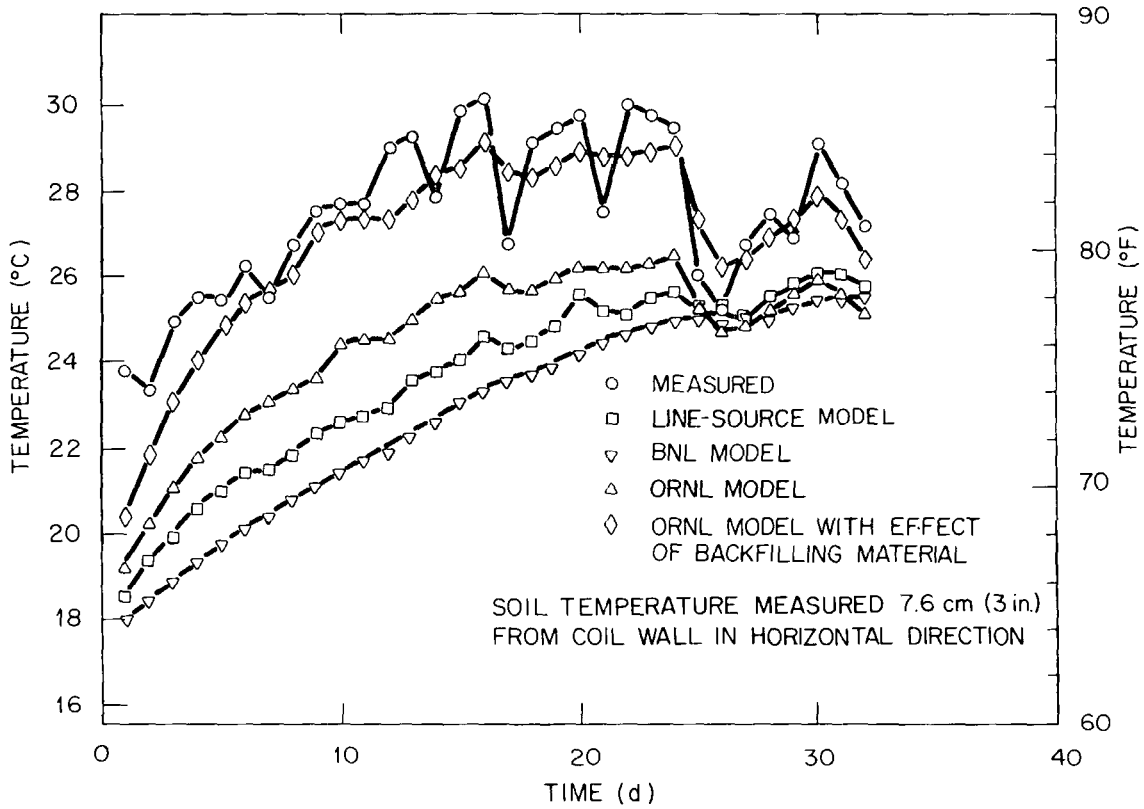

Fig. 4. Comparison of measured soil temperatures with those calculated by the line-source model, the BNL model, and ORNL model 2 (both with and without the effect of backfilling material).

shows soil temperature measured at UT[13] and as calculated by ORNL horizontal coil model 2, the BNL model,[4] and a simple line-source model[14]. All three models underpredict the experimental results, but the ORNL model comes closer than the other two. One reason for the underprediction is that the coil was backfilled with sand to eliminate possible contact resistance. At the beginning of the cooling season, the measured thermal conductivity of the sand was much higher than that of the clay.[13] Taking the sand into account in the ORNL model, the prediction is much closer to the test results. For the line-source and BNL models, to include the effect of the sand backfill region would have been very difficult and was not pursued due to time and budget constraints.

Computer codes for the models are listed in references 11 and 12. The codes are easy to use and do not require that users be adept at solving partial differential equations. All codes are available on floppy disks for personal computer (PC) application or on tape for mainframe computer application.

Although these models simulate ground-coil operation much more realistically than traditional line-source methods, they also require much more computer time to simulate coil operation. Therefore, at present, these models are probably more suitably used as references by which to check coil designs based on simpler methods. However, with anticipated improvements in PC speed, these models should be more practical for coil design purposes in the future.

Technology Transfer

The major emphasis of DOE-sponsored GCHP work at ORNL since fiscal year 1986 has been in the area of technology transfer. Various avenues employed have been a workshop, distribution of GCHX models, press releases, and teleconference participation. These are discussed below.

In October, 1986, an international workshop on GCHP technology was held in Albany, New York, to establish the current state of the technology development and to recommend areas for further research. This workshop, co-sponsored by the International Energy Agency (IEA), the Electric Power Research Institute, NMPC, and DOE, was attended by over 40 researchers from Europe, Canada, and the United States. Papers presented at the workshop and a summary of the recommended research topics were published in a Proceedings,[15]

which is available through the IEA. As a result of contacts made at the workshop, over 20 copies of our GCHX models were requested by various researchers.

A vigorous effort was undertaken in fiscal year 1987 to publicize the results of the optimized GCHP project to U.S. manufacturers, dealers, and installers. Sumner Rider and Associates, a public relations firm, was contracted to produce a series of press releases and a feature article for publication in the industry trade press. Press releases have appeared in several publications including the *Air Conditioning, Heating, and Refrigeration News*[16] and the *HVAC Product News*.[17] The feature article appeared in the April, 1988, issue of *Appliance* Magazine.[18]

In cooperation with ORNL and Climate Master, Inc., Richard O'Neil of NMPC produced an 11 minute video tape presentation on the optimized GCHP system. This video was telecast on September 4, 1987, as part of Oklahoma State University's second GCHP teleconference. An estimated 20,000 persons, mostly dealers and installers, saw this teleconference.

Over 250 requests for information on the advanced GCHP have been received, primarily as a result of the press releases. The major question asked is simply "Where can I buy one?". Unfortunately, we know of no available WSHPs that have the performance levels of the prototypes as listed in Table 3. A number of manufacturers have equipment available that has heating performance within 10% of the prototypes' level (see for instance references 19-21). Cooling performance of available WSHPs is about 20-25% lower than that of the prototype.

The primary objective of our technology transfer work has been to inform GCHP dealers and installers of the advantages of the advanced design system. In so doing, we hoped to stimulate demand for such systems earlier than it may otherwise have developed. How successful this effort will ultimately be is unclear at this time, but we have certainly sparked some interest in our target audience.

Conclusions

ORNL, in cooperation with NMPC, Climate Master, Inc., and BNL has developed and demonstrated an advanced GCHP system concept that for northern climates can lead to reduced system installation costs. Additionally, it can enhance GCHP competitiveness versus ASHPs in those regions by lowering paybacks from 6-7 years to 3-5 years. Some GCHX models have been developed that have been used by others to develop less conservative ground coil sizing methods. This technology has been publicized aggressively and has been made available to industry. The major remaining barrier to more wide-spread adoption of GCHP technology is the cost of the ground coil. Continued effort is needed to further reduce this cost.

References

1. M.A. Catan, and V.D. Baxter, "An optimized ground-coupled heat pump system design for northern climate application." *ASHRAE Trans.*, 91 (2B), 1185-1203 (1985).

2. S.K. Fischer, and C.K. Rice, "The Oak Ridge heat pump models I: A steady-state heat pump design model." ORNL/CON-80/R1, Oak Ridge National Laboratory, Oak Ridge, August 1983.

3. J.W. Andrews, M.A. Catan, P. LeDoux, P.D. Metz, and J.H. Saunders, "Optimized ground coupled heat pump design, Phase I final report." BNL 38869, October 1985.

4. J.W. Andrews, P.D. Metz, and J.H. Saunders, "A refined computer program for the transient simulation of ground coupled heat pump systems." BNL 34818, April 1984.

5. M. Hughes, "A parameterized cost model for ground coupled heat pumps." *ASHRAE Trans.*, 91 (2B), 1204-1215 (1985).

6. U.S. Department of Energy, Office of Policy, Planning, and Analysis. "Energy projections to the year 2010." DOE/PE-0029/2, October, pp. 3-5 (1983).

7. R.J. Hackner, P.J. Hughes, and R.A. O'Neil, "Design of ECHP systems in northern climates." *ASHRAE Trans.*, 93 (2), 1987.

8. P.J.Hughes, "Manual of acceptible practices for installation of residential earth-coupled heat pump systems." W. S. Fleming & Associates, E. Syracuse, N.Y., May 1986.

9. P.J. Hughes, and R.J. Hackner, "Field performance validation of an advanced design earth-coupled heat pump system." ORNL/Sub/85-22035/1, January 1988.

10. P.J. Hughes, R.A. O'Neil, L. Loomis, and J. Rizzuto, "Results of the residential earth-coupled heat pump demonstration in upstate New York." *ASHRAE Trans.*, 91 (2B), 1307-1325 (1985).

11. V.C. Mei, and S.K. Fischer, "A theoretical and experimental analysis of vertical, concentric-tube ground-coupled heat exchangers." ORNL/CON-153, October 1984.

12. V.C. Mei, "Horizontal ground coil heat exchanger theoretical and experimental analysis." ORNL/CON-193, December 1986.

13. W.S. Johnson, B. McGraw, R.N. Baugh, and W. Griffith, "TECH house I horizontal coil ground coupled heat pump: 1983-84 annual performance." ORNL/Sub/81-7685/3&92, Oak Ridge National Laboratory, August 1985.

14. M.D. Kalman, "Earth heat exchangers for ground source heat pumps," MS Thesis, Georgia Institute of Technology, Atlanta, 1980.

15. J.M. Calm, (ed.), *Proceedings of the IEA Workshop on Ground-Source Heat Pumps*, October 27-November 1, 1986, Albany, N.Y., September 1987.

16. *The Air Conditioning, Heating and Refrigeration News*, 171, (14), Serial No. 3043, p. 4, (August 3, 1987).

17. *HVAC Product News*, p. 21, July/August 1987.

18. V.D. Baxter, H.M. Hughes, P.J. Hughes, R.A. O'Neil, "Ground Coupled Heat Pumps for Northern Climates." *Appliance Magazine*, 45 (4), 69-76, (April 1988).

19. *WaterFurnace Liquid Source Heat Pumps Product Catalog*, 1986.

20. *GEOSystem Product Catalog*, Edition 286B, 1986.

21. Climate Master, Inc., *Geo-Thermal Heat Pump Product Catalog*, 1984.

Session 3

What Should Influence the Future Direction of the DOE/ORNL R&D Program?

Organizer: P. D. Fairchild
Oak Ridge National Laboratory
Chairman: T. Kapus
U. S. Department of Energy

Assessment of Japanese Variable-Speed Heat Pump Technology

Kenji Ushimaru
Energy International, Inc.
Bellevue, WA 98004

Abstract

An analysis of critical component technologies and design methodologies for Japanese variable speed heat pumps are presented. The market for variable speed heat pumps in Japan is predominantly residential split-type, between the fractional to 2.5 ton capacity range. Approximately 1.1 million residential inverter-driven heat pumps were sold in 1987. Based on the market trends, component technology and several advanced features are described. Similarities and differences between Japanese and U.S. system design methodologies are discussed. Finally, the outlook for future technology trends is briefly described.

Introduction

The present work focuses on the technology developments and market trends of Japanese variable speed heat pumps. The pace of technology advances and market growth of variable speed heat pumps in Japan since 1983 has been dramatic. The level of success attained by residential split-type heat pumps with variable speed capability compressors, inverters, low cost induction motors, microprocessor-based system controllers, and dynamic refrigerant control devices.

The purpose of this article is to evaluate the technical developments related to Japanese variable speed heat pumps and to provide a comprehensive view of the technical and market evolution. Specifically, the study reviews (1) the background environment in which the technology has evolved, (2) air conditioner and heat pump market trends which allowed the dramatic market penetration of the technology, and (3) a look into future application markets and new heat pump features for the next generation variable speed heat pumps.

In any residential appliance market, the development of a market-viable technology is greatly influenced by the regional culture, lifestyle, economic conditions, climate zone, and other available competing equipment. While Japan and the U.S. constitute the world's largest air conditioning and heat pump markets, the difference between the two countries in each of these factors is significant. In the present study, attention has been given to clearly identifying the background environment relative to design load conditions, economic parameters, customer preference, and design philosophy which motivated today's Japanese variable speed heat pump technology development.

This article consists of four essential elements designed to answer many questions arising from the success of variable speed heat pump technology in Japan (i.e., why is it that not anywhere else did this technology attain such a high degree of success?). The first is a brief description of the historical trends in heat pump market growth and economic conditions for the past ten years in Japan. The second section discusses the technology trends and the evolution of advanced technology features. The third section describes key component technologies in terms of design philosophy, customer requirements, market driving factors, and engineering know-how. The final section summarizes the analysis results so far, and provides a brief look at new features that are under consideration for the next generation of variable speed heat pump development in Japan.

Market Trends

In the past, the Japanese HVAC market experienced two stages of growth. The trend in shipments of residential air conditioning equipment (for domestic consumption) between 1975 and 1987 in Japan is illustrated in Figure 1. The first stage of significant growth in the domestic air conditioning equipment market came between 1975 and 1979. Aided by steady increases in both the standard of living and housing starts in Japan, residential air conditioning equipment shipments increased from 1.63 million units in 1975 to 2.87 million units in 1979 for cooling-only equipment; this represented a 75% increase. The heat pump market during the same period grew from 0.35 million units to 0.54 million units for a 54% increase. Industry experts attribute the dramatic increase in the domestic demand for air conditioning and heat pump equipment to the increase in the industrial and economic strength of Japan in the worldwide export market, which brought a higher standard of living to the average Japanese home. During the first growth period between 1975 and 1979, the demand for cooling-only air conditioning equipment dominated the residential market; heat pump type air conditioning equipment was still relatively unpopular.

The Japanese air conditioning equipment market collapsed along with many other appliance markets during the worldwide recession between 1980 and 1983. During this period, housing starts fell to a low level and Japan experienced some record-setting cool summers. Shipments for the cooling-only air conditioning equipment fell from the high of 2.87 million units in 1979 to 1.25 million units in 1982, representing a 56% decline. However, despite the unfavorable economic and cooling load conditions which characterized this time period, heat pump type air conditioning equipment showed remarkable strength. Stimulated by advances in

heat pump technology and efficient production know-how, Japanese manufacturers steadily shifted their price and performance competition in the area of heat pump air conditioners to compete more effectively against kerosene and gas heaters in winter and room air conditioners in summer. The growth picture indicates an increase from 0.51 million units of heat pump equipment shipped in 1980 to 1.16 million units in 1983 -- the market more than doubled in the recession-prone four-year period.

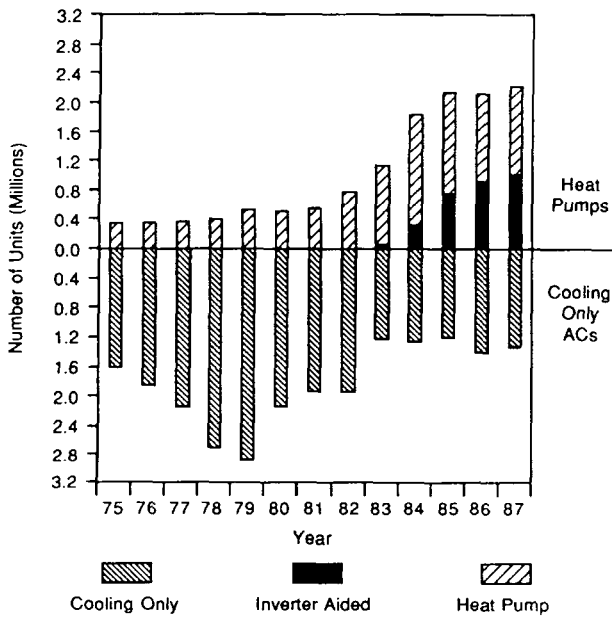

Figure 1. Shipments of Residential Air Conditioning Equipment in Japan 1975-1987

Coming out of the deep worldwide economic recession around 1983, the air conditioning equipment market entered the second stage of dramatic growth. Aided by the advent of the variable speed heat pump and increased consumer awareness of high efficiency residential appliances, the Japanese residential air conditioning market moved from the dominance of cooling-only equipment to the dramatic growth of heat pump equipment. In fact, the total heat pump market increased from 1.16 million units in 1983 to an estimated high of 2.2 million units in 1987 (a 90% increase over the five-year period). What is more remarkable is the increase in the demand for variable speed heat pump equipment. Since its introduction in 1983, the market share of this equipment increased from newcomer status to that of strong contender for the lead in domestic air conditioning equipment at over 1.1 million units in 1987. In 1987 the domestic shipment for residential air conditioning equipment reached 3.9 million units (JARN, 1988).

The Japan Refrigeration and Air Conditioning Industry Association (JRAIA) provided the following breakdown of residential equipment demand. JRAIA reported 1986 sales of 2.23 million heat pumps in Japan, of which:

- 1.1 million units were single room heat pumps with a variable speed compressor (49% of the total residential heat pump market),
- 1.0 million units were single room heat pumps with a fixed speed compressor (45% of the total),
- 30,000 units were multi-room heat pumps with a variable speed compressor (1% of the total), and
- 100,000 units were multi-room heat pumps with a fixed speed compressor (4% of the total).

Clearly, the Japanese air conditioning equipment market has transformed successfully from cooling-only to heat pump type equipment in the early 1980s. Furthermore, the heat pump market has evolved rapidly to the point that half of the heat pumps sold in Japan in 1987 were variable speed type.

Technology advances are numerous in the areas of compressors, inverter drives, controls, and system integration techniques. The Japanese manufacturers have committed their resources for research and development, manufacturing facilities, and marketing promotion to the development and sales of heat pump equipment. Advances in heat pump technology will be paid back over the cooling- and heating-cycle around the year, accelerating the payback period significantly when compared with cooling-only equipment.

Technology Trends

It is noteworthy to track the growth in equipment technology measured in terms of the cooling EER for Japanese heat pump units. Figure 2 shows the trend of these improvements (in metric EER -- kcal/watt = 0.25 Btu/watt) for a typical split-type, wall-mounted indoor unit with the cooling capacity of 2,240 kcal/hr (8,888 Btu/hr or 0.74 ton) at 60 Hz (JRAIA, 1987). As can be observed in the figure, typical EER for this popular split-type air conditioning equipment increased from 7.4 in 1973 to 11.2 in 1985, representing an increase of 50% over the 13-year period.

Figure 3 shows the trend in heating capacity and EER of the same 0.75 ton split-type equipment (Umezu and Suma, 1984). As can be noted from the figure, the high efficiency model had a claimed EER under the test conditions prescribed by the Japan Industrial Standards of 9.41 (Btu/watt) in 1975. Improvements came in 1979 using two new techniques: a microprocessor-based control system and a gas injection (supercharge) compressor (Mikawa et al., 1980). In 1982, some heat pump compressor operating systems were changed from the capacitor-start and capacitor-run system (CSR for capacitor start and run) to the solid-state relay-start and capacitor-system (PAS for posistor-aided start). The PAS system was widely used in cooling-only room air conditioners at the time. The PAS system did not need a starting relay or starting capacitor, and this reportedly contributed to simplification of electric parts and cost reduction. The PAS system was developed with the use of a smaller compressor motor in combination with a two-stage capacity compressor which had the full capacity mode and the "energy saver" mode using dual refrigerant injection ports. This mechanism essentially resulted in the advent of two-capacity heat pumps with claimed efficiency improvements from reduced cycling loss.

The highlight of the past developments in the Japanese heat pump market was the inverter-driven heat pump, first introduced by Toshiba in 1982. A brief description of the advanced technology features which characterize the popular Japanese split-type variable speed heat pumps and an assessment of inverters for heat pump applications is given in the following section.

Advanced Technology Features

Any analysis of space conditioning equipment, whether technically or market oriented, can be misleading unless the design load condition is prescribed. In order to give the proper perspective to how Japanese variable heat pump technology evolved in the last five years, it is important to understand the definition of Japanese space conditioning operating conditions, as well as the similarities and differences between typical Japanese and the U.S. design philosophies.

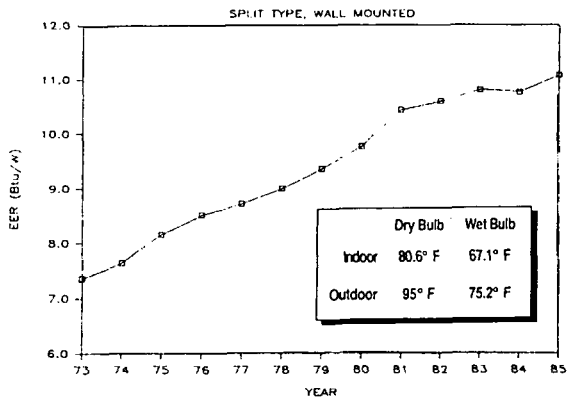

Figure 2. EER of Air Conditioners in Japan

Source: Japan Refrigeration and Air Conditioning Industry Association, 1987

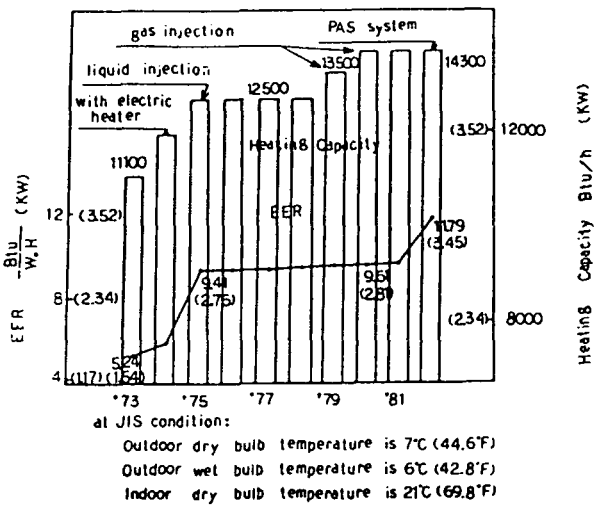

Figure 3. EER and Heating Capacity Improvement of Heat Pump Room Air Conditioners

Source: Umezu and Suma, 1984

Japanese Space Conditioning Operating Environment

The average low temperature range in Japan is between 0° and $-10^{o}C$ (32° and $14^{o}F$), except for extremely cold regions such as Hokkaido Prefecture (the northern-most island of Japan). In summer the average high temperature range in the Tokyo-Osaka corridor is from 25° to $35^{o}C$ (77° to $95^{o}F$). Under these typical operating conditions, an air-source heat pump room air conditioner is useful and viable for Japanese climates. When one considers the fact that over 60% of the country's population lives in the corridor between Tokyo and Osaka, and that almost 50% of Japanese families have room air conditioners, it makes sense that the competition for the greatest share of the popular space conditioning equipment market would take place in the climate range of this region.

Today, the market for central space conditioning systems (with central air ducts or hydronic systems) comprises approximately 2% of the Japanese residential market in most population centers except Hokkaido where the central type is quite common. It is interesting to note that the severe winter climate region (such as Hokkaido) is served by types of heating equipment that are similar to typical U.S. central style heating equipment in cold climate regions (regions defined by the U.S. DOE as between 4,000-5,500 degree days).

Figure 4 shows the average low temperature for a typical day in January in Japan. In Tokyo, the average low temperature is $0^{o}C$ ($32^{o}F$). Heat pumps are usually installed in a living room, and the average floor area of a Japanese living room is 13-17m^2 (140-183ft^2). Most Japanese construction is wood, except for concrete apartments, and heating loads are represented by the values specified by the Japanese Industrial Standards (JIS). Table 1 shows the heating load specified by JIS. The set temperatures for the calculation of the heating capacity are $21^{o}C$ ($70^{o}F$) indoor and $0^{o}C$ ($32^{o}F$) outdoor, which results in the heating load of 363-474 kW (12,390-16200 Btu/hr) for the range of the floor space.

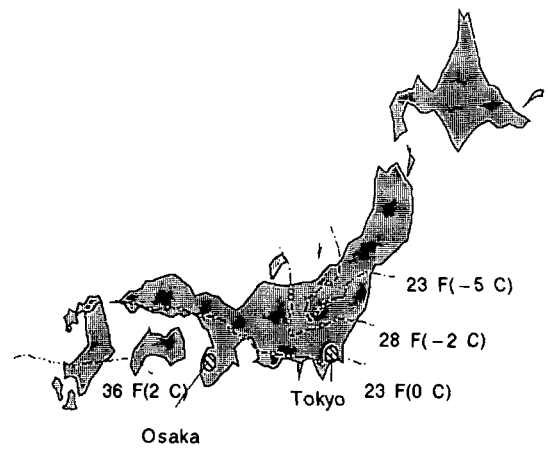

Figure 4. Average Low Temperature in Winter in Japan

The cooling load is estimated to be about 260 kW (8890 Btu/hr) for an average size room. Thus, the ratio of heating to cooling capacities would be more than 1.5. An air-source heat pump with a conventional (fixed speed) compressor, cannot attain this ratio unless supplemental heating is provided by auxiliary heating systems (in the conventional system, the capacity ratio is about 1.2).

This forms the basis for the dramatic evolution of variable speed heat pumps in the vast Japanese residential market. The market remains strong for the split-type room air conditioner (under 2.5 tons), with about 3.9 million units sold in 1987. Most industry experts agree that the level of 3.7 million units/year would be the peak domestic demand for this type of air conditioning equipment (1987 being an exceptionally strong year aided by higher-than-average cooling load hours during the year).

Compressor Developments

In Japan, refrigerant compressors have attained a high level of advancement and diversity. Supported primarily by private industry funding, compressor technology today is a result of design philosophy which is based on low noise, compactness, light weight, high efficiency, good reliability, and low cost.

Table 1. Heating Load Per Unit Floor Area (JIS, C9612)

Room Conditions			Heat load per unit floor area (W/m^2)	Ventilation times (times/h)	Window area / floor area (%)	Inhabits 10 m^2	Light W/m^2
Wooden house	Japanese style	face to south	291	1.5	40	3	0
		face to north	279	1.5	20	3	10
	European American style	face to south	279	1	30	3	0
		face to east	279	1	30	3	0
Concrete Apartment		up stairs	262	1	30	3	10
		middle stairs	233	1	30	3	10

*The heat load is enough to keep the room temperature at 21°C (70°F) with an outdoor temperature at 0°C (32°F). The value of heat load shown in Table 1 is measured at JIS condition (outdoor temperature is 7°C [45°F]).

Source: Umezu and Suma, 1984

During the 1960s in Japan, air conditioning was available almost exclusively for commercial buildings. Since the late 60s, the major Japanese electrical equipment and appliance manufacturers began an intensive development program to commercialize smaller and less expensive room air conditioners for the residential market. The impetus for such a development program was that the residential air conditioning equipment market was projected to grow rapidly into the 70s and Japanese precision manufacturing capability advanced well enough that fabrication of small-capacity rotary compressors for residential application became possible.

Key factors for the successful introduction of residential room air conditioners at the time were high efficiency, quiet operation, low cost, and compact size. There was an industry-wide consensus that (1) the projected growth in the residential air conditioning market would support a significant level of long term investment in fabrication facilities, personnel, and research and development, and (2) a new type of compressor technology needed to be developed to successfully move into the residential market for sizes ranging from fractional to 3 horsepower capacity.

It is noted here that the differences between the design requirements of residential air conditioners in Japan and the U.S. are: (1) typical Japanese room air conditioners are from 0.75 to 2 tons, where as popular U.S. residential air conditioners are of central type ranging from 2 to 4 tons; (2) Japanese usage patters would require a zone cooling with refrigerant piping whereas the central type was gaining momentum in the U.S. residential air conditioning market; and finally, (3) the high density residential structures in the Japanese urban areas required compact and quiet outdoor units in order to capture a large share of the lucrative apartment building and condominium markets.

From the first introduction of rolling-piston air conditioners in 1975, the refrigerant compressor market in Japan has completely turned over. Now, virtually 100% of residential refrigerators, room air conditioners, and heat pumps under 2.5 tons use rolling piston compressors. Rotary vane compressors found a market niche in passenger car air-conditioning, as did swash plate compressors because the capacity requirement in passenger car air-conditioning is above 3 tons -- a range in which rotary vane compressors would offer superior performance.

The highlight of the Japanese compressor development since the successful compact rolling piston program is perhaps the commercialization of scroll compressors. The impetus for the development of scroll compressors was the goal to improve the performance of air conditioning equipment from 3 to 6 horsepower. Traditionally, air conditioners in this capacity range used either reciprocating compressors or large multi-vane rotary compressors. Figure 5 illustrates a comparison of refrigerant compressor performance in terms of volumetric compression efficiency versus nominal compressor output for four different types of compressors. This figure, which has been widely employed to show the relative advantage of scroll compressors, is but a brief look at claimed efficiency. From the system design point of view, relative advantage or disadvantage of various compressors types must be compromised or improved by an iterative design process -- the process of design trade-off between compressor and the rest of the system. However, at a minimum this figure warrants a close look since it illustrates the initial motivation for the commitment by Japanese manufacturers to develop commercial scroll compressors for the global market.

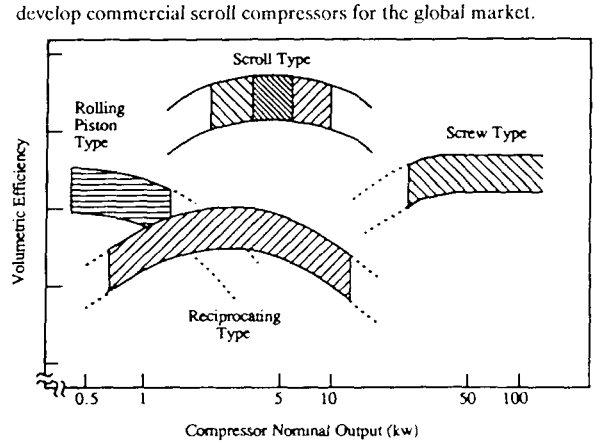

Figure 5. Comparison of Refrigerant Compressor Performance

Source: Hitachi, 1986

From an analysis of the data presented in the figure, it is noted that:

- o Rolling piston compressors exhibit good compression performance in the range of fraction-to-1kW. Rolling piston compressors larger than 3kW would be bulky and noisy (due to the higher vibration of the larger rotating piston). Some Japanese equipment in the medium size range had dual cylinder (two) rolling piston compressors to satisfy the capacity requirement prior to the advent of commercial scroll compressors.
- o Screw compressors are shown to exhibit excellent performance over 20kW with a wide range of stable operation. Screw compressors have been applied in large industrial installations for cryogenic cooling, helium compression, large chillers and refrigerators, and industrial heat pumps. Furthermore, a leading Japanese screw compressor manufacturer recently introduced a high performance 12kW screw compressor (for the capacity of 10 ton cooling). Thus, the level of technology is expanding application areas for the screw compressor to the range to be in direct competition with medium size reciprocating compressors. However, considering the manufacturing tolerance required for small screw compressors to avoid excessive tip losses from the rotor, the cost of fabrication appears to establish the market-acceptable limit of small screw compressors at around 10kW.
- o Reciprocating type compressors (in this figure only) exhibit a peak compressor efficiency at 4 kW with a steep decline in compression efficiency at less than 1 kW and greater than 10 kW. The characterization of the reciprocating compressor in a simple illustration like this figure is, of course, misleading. The reciprocating-type compressors are perhaps the most versatile compressors available today with many successful applications. Because this type of compressor shares basically the same mechanical configuration (of the main components) as the popular internal combustion engine, the reciprocating compressor has been successfully and cost-effectively applied to a range of applications far greater than what is shown in the figure.
- o Compared to rolling piston or screw compressors, reciprocating compressors tend to have a more complex design (a large parts count), higher vibration (due to high torque and discharge pulsation), lower efficiency (due to leakage, pressure drop across intake and discharge valves, and the top clearance volume at the cylinder top), and are bulkier (lower discharge power-to-weight ratio). Thus, the advent of commercial rolling piston compressors and screw compressors left a "performance gap" at the 1-10 kW range. This is the range of application the first scroll compressor was designed to fulfill. The scroll type compressor has high volumetric efficiency in the 3-8 kW range. Reportedly, this increase in performance is conceptually attributed to: (1) lower leakage rate of the refrigerant from the high pressure side to the low pressure side in the scroll compressor because of the crescent-shaped medium pressure areas between the high-pressure area and the low-pressure area; (2) no valve -- therefore no valve loss; and (3) zero top clearance volume. Although extremely high fabrication precision was required to manufacture a scroll compressor at a market-acceptable level of performance (and cost), the effort to commercialize scroll compressors was targeted at the replacement of reciprocating compressors in the 1-10 kW range.

Inverter Technology

The highly motivated Japanese market has driven the cost of inverter drives and custom Integrated Chips (ICs) low enough that they have been applied in a wide variety of residential and commercial equipment.

The current "state-of-the-market" inverter technology available in Japan for residential heat pumps (less than 2.5 tons) is predominantly the Pulse Width Modulation (PWM) type. Figure 6 shows the key features of a typical heat pump inverter, and its approximate performance ratings are described in the following.

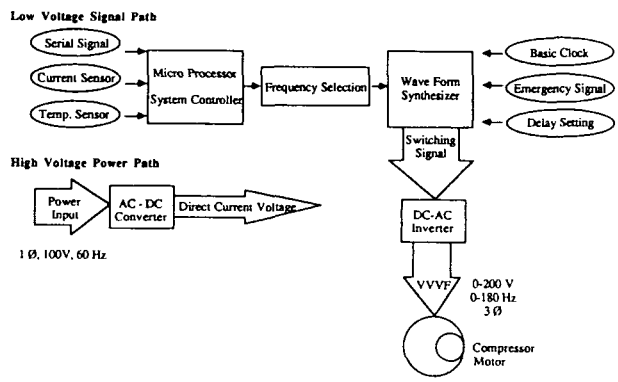

Figure 6. Key Features of a Typical Heat Pump Inverter

Typical residential inverter power rating is 100 V, 25 amp, single phase ac input. The ac input from the standard residential electric service is at 50 Hz in the Tokyo area (the Eastern region), and 60 Hz in the Osaka area (the Western region). The single phase ac input goes through a cd-link (an ac-dc converter) with maximum dc voltage of approximately 300 V. The dc output from the dc link module is fed into a dc-ac inverter. Popular Japanese inverters are predominantly of the PWM type for frequency and voltage control. For the particular type of torque-frequency required for the operation of a variable speed compressor (the exponential torque load, i.e., torque is proportional to square of speed), the PWM has been selected on the basis of low manufacturing cost and reliable performance.

The state-of-the-market inverter technology consists of a Darlington-type power transistor bridge with ratings of 0-300 V. The frequency range of commercial inverters is 35-115 Hz for medium size heat pumps to 30-180 Hz for the popular 0.75 ton units. The control module for inverter frequency selection is quite complex and is usually unique to each manufacturer. The low-voltage signal path is located in the indoor fan unit which interprets performance and ambient parameters from various sensors. These measured parameters are fed into a microprocessor system controller which selects the appropriate frequency. With today's technology, the frequency (and voltage) selection is a non-optimized data access into an 8-bit memory chip for PWM input.

It is anticipated that in the near future, Japanese HVAC manufacturers will be introducing Very Large Scale Integration (VLSI) chips for a fast PWM optimization scheme. If such a microprocessor were applied in residential heat pump control, it would mean a significant technology edge over other inverter technologies available elsewhere in the world. An optimized PWM is expected to result in much improved efficiency over the entire speed range, and at the same time insure a minimum harmonic distortion of output current and voltage. This technology, however, must be accompanied by a microprocessor which can perform fast real time calculations (at least fast enough to keep up with the PWM carrier wave frequency).

Current Japanese variable speed heat pump equipment is rich in other electronically driven convenience features. Examples of such features are wireless remote control, automatic discharge air control using variable louvers, humidity control, and programmable timers.

Although these convenience features are certainly useful and serve a good purpose in a typical household, they do not necessarily constitute essential ingredients in advanced heat pump technology development. Instead, the recent trend of critical component technology development in Japan appears to be motivated by the objective of increasing the functional value of the inverter. That is, to develop a heat pump unit that fits the Japanese residential market based on how critical components are designed around the inverter capability.

With the use of inverters, the heat pump unit can not only operate over a wide range of capacity modulation for load-following benefits, but can also achieve other important design goals. As an example, inverter-driven heat pumps can now attain the heating-to-cooling ratio of over 1.7 to better match the typical residential seasonal building load without the aid of auxiliary heating equipment. In another instance, other variable speed heat pump developments currently underway elsewhere in the world include the evaluation of simultaneous fan speed and compressor speed control using the ac output from the inverter concurrently between compressor motor, and outdoor fan motor for unitary equipment. Japanese designs do not use power output from outdoor inverters for the outdoor fan because the outdoor fan speed deviates over a wide range regardless of the compressor speed and thus the inverter does not drive the outdoor fan. The design philosophy here is that inverter technology will give the capability of precisely controlling the latent-to-sensible cooling ratio and allow more flexible control of temperature and humidity for enhanced comfortability.

In summary, Japanese inverter technology incorporates other key component features to provide enhanced comfort and a greater degree of temperature control between the indoor condenser and outdoor evaporator. This design significantly increases the inverter's functional value (i.e., being able to perform many functions with a single unit) to the point the associated premium can be justified.

Dynamic Refrigerant Control

The functional use of inverters in combination with electronic expansion valves provides an opportunity for dynamic refrigerant control. These critical components provide the potential for controlling the optimization of all the key operations of a heat pump. These operations include (1) defrost control, (2) compressor control, (3) fan control, and (4) refrigerant flow control. By controlling these operations, performance of the system can be optimized to provide (1) enhanced occupant comfort, (2) optimized efficiency over a range of operating conditions, and (3) increased system reliability.

Key measures of comfort include indoor and supply air temperatures and humidities. For single speed systems, indoor temperature is the only variable measured. However, humidity is also important. This is particularly true for a variable speed system because the temperature of the coil increases at low capacities, reducing latent cooling capability. Thus, control algorithms have been developed which control the supply air rate and indoor coil temperature so that the indoor air temperature and humidity are maintained at comfortable levels.

The system must also be able to sense when to vary system capacity to optimize efficiency. The method used depends on the sophistication of the system, the compressor type, and other system design features. A solid understanding of the heat pump operating characteristics is necessary to design a good control system. Key parameters to be measured include outdoor temperature and coil temperature. In addition, compressor discharge conditions are monitored. Because the compressor operates over a wide range of speeds, care must be taken to avoid overheating or other refrigerant conditions that might reduce compressor reliability. The temperature or electric current flow to the motors is monitored, and inlet and discharge refrigerant conditions to the compressor are measured and controlled. These data are fed into the control module in order to control the inverter operation to ensure system protection for improved reliability.

Electronic expansion valves used in combination with inverter drives and electronic control systems provide dynamic refrigerant control capability. Typically, electronic expansion valves consist of a pulse motor, a set of gears and driver, and the valve needle. The degree of valve opening is determined by the microprocessor control system. The control signals set the frequency of valve opening to allow varying rates of refrigerant flow.

A variable speed compressor can vary system capacity within a certain range to match system load. This creates a wide range of operating conditions which are difficult to handle using a conventional thermostatic expansion valve. A very complex refrigeration system is required when conventional valves are used with variable speed compressors (Itoh, 1986).

Japanese consumers further demand good occupant comfort during defrosting. In conventional reversing cycle defrosting, the heat pump unit switched to operate in the cooling mode to pull heat away from the room and route that energy to the outdoor coil. In this case, an auxiliary heater is employed to offset the cooling effect so as to maintain relative comfort in the room. However, the typical Japanese residential electric service does not allow a large current draw from the circuit breaker when a heat pump (and other residential appliances) are in full operation. Prior to the improved defrost technology development, the typical auxiliary heater was limited at 800 W at 100 V residential service. This created either occasional circuit breaker shut-off, or a cooling sensation during the defrosting cycle. These were considered to be the decided disadvantage of old style heat pumps.

Major manufacturers have now developed a variety of non-reversing cycle defrosting techniques using dynamic refrigerant control in combination with inverters (Murozono et al., 1986). The non-reversing cycle defrosting strategy is essentially derated heating operation. The compressor runs at full speed, refrigerant is piped to the indoor coil (in the heating mode), the indoor fan is set to minimum speed to maintain derated heating conditions, and the remaining energy available in the refrigerant is routed to the outdoor coil to complete the cycle. This defrosting strategy, which meets Japanese residential electrical service and solves consumer complaints, is enormously successful with today's equipment.

The important point in developments of various strategies to combine refrigerant control techniques to take further advantage of inverters is again increasing the functional value of inverter technology. This design philosophy to improve market-acceptance of variable speed heat pumps in the residential market by fully utilizing the compressor speed control (beyond the capacity modulation purpose) is a lesson which should be noted for the development of advanced heat pumps for the future.

Future Outlook

This article focused on the evolution and analysis of inverter-driven variable speed heat pump technology in Japan. In particular, the design philosophy of the current state-of-the-market equipment has been described in detail. It is evident that Japanese heat pump design is now built around how to best take advantage of inverter capability. This is clearly demonstrated by the component integration technique which emphasizes the ability to effectively control indoor and outdoor coil temperature over a wide range of operating conditions and occupant comfort requirements.

Because variable speed heat pumps are now widely accepted in the marketplace, and market conditions are relatively stable, future

market expansion will be driven by technological innovation. Considering the innovation opportunities and technical challenges facing the leading heat pump designers in Japan, it is noted that the near-term outlook will be based on the following themes:

- o Cold climate heat pump design.
- o Inverter performance improvement in medium capacity equipment (2.5 ton range).
- o Light weight scroll compressors.
- o Power electronics and inverter optimization for power quality improvement.

Before the inverter era in Japanese heat pump marketing, the public was rather reluctant to accept the equipment due to its poor reliability (particularly in heating cycle) and low comfort achievable in the peak heating season. The design theme of the current variable speed heat pumps appears to be (1) further improvement of heating capacity, (2) enhanced occupant comfort, and (3) seasonal efficiency improvements. The outlook for the next generation of heat pumps, at least for the near term, should be characterized by a similar trend.

The technical challenge facing heat pump manufacturers worldwide is the improvement of performance in cold climate applications. The success of heat pump air conditioners in the key residential market in Japan caused a decline in the cooling-only air conditioner market. In other words, the heat pump manufacturers enjoyed the success of their product sales at the expense of the loss of revenue from the cooling-only equipment market. Developing a market-viable system which can compete successfully in cold climate heating applications will give a new dimension to the marketing strategy for expanding the application area of variable speed heat pumps. For example, one of the major Japanese heat pump manufacturers has successfully developed a variable speed heat pump system using a nonazeotropic refrigerant mixture (Matsunaga et al., 1986). The conventional U.S. design philosophy on the use of nonazeotropic refrigerant mixtures is to provide capacity modulation. However, Japanese equipment is already capable of capacity modulation through the use of inverters. In contrast to the other design philosophies, Japanese manufacturers opted to use R-22 and low pressure additive refrigerants to improve heating capacity in low ambient temperature conditions.

Furthermore, the application of air-source heat pumps in cold region loads gives a unique opportunity to consolidate many innovative features of inverter and microelectronics into a single heat unit. This effort will be accompanied by experiments with hydrophilic film coatings to reduce frosting on outdoor coils (Mimaki, 1987).

In the area of inverters and motors, the technical challenge facing today's Japanese variable speed heat pump technology is the starting torque of the motor. The Japanese variable speed heat pump technology is predominantly induction motor based, and as such, generally suffers from the inherent shortcomings of induction motors (i.e., low starting torque generation). Fortunately, the dominant Japanese heat pump size is around 1 ton, requiring a relatively small motor starting torque. However, for mid-range equipment, which is targeted for new scroll compressors to replace reciprocating compressors, the starting torque problem may limit the application of low-cost inverters.

There are several techniques to solve the starting torque problems with induction motors. In large industrial applications, the so-called Field Orientation Control (FOC) is available to control the slip of induction motors to satisfy the requirement of either slip for maximum torque or slip for maximum efficiency. If a low cost FOC module could be made available, it would find many applications not limited to residential and commercial heat pump applications.

The continuing evaluation of brushless dc motors and their inherent advantage over induction motors will also be important. However, Japanese manufacturers whose low-cost inverter design emphasized induction motor applications appear to be less advanced than the U.S. dc motor designs for unitary heat pump applications.

The starting torque problem for induction motors becomes more serious for large size equipment. In the mid-range market for which scroll compressors are becoming popular, the perceived advantage of the scroll compressor is somewhat offset by the inability of the standard inverter to drive it efficiently. Today's scroll technology is based on cast iron construction. Even at starting condition, the inverter-induction motor combination must generate excess current to start. The heat generated around the surface of the rotor not only causes severe stress on the rotor bar, but in a hermetic compressor system it would translate to a significant loss in efficiency (at least in the cooling cycle).

Some manufacturers are considering cast aluminum construction for the next generation of compressors. The design goals are precision mass production, light weight, and improved reliability of future compressor designs.

The inverter performance will certainly improve as new power electronics devices and VLSI chips become available. In place of Darlington-type power transistors, the Insulated Gate Transistors (IGTs) are being used in experiments. The new power electronics devices will be designed to switch the input power faster and more efficiently (to synthesize variable frequency, variable voltage ac power) to further improve the system efficiency. The current 8-bit memory chips for inverter drives may be replaced by faster and more sophisticated 16-bit chips. The combination of power electronics devices and new logic chips can result in the capability to compute optimum PWM strategy over a wide range of operating conditions.

As more and more inverters of various sizes come on line, power distortion due to poor power factor and the effects of harmonics present in the synthesized ac power could severely degrade the quality of electrical power service. These factors will be increasingly important as inverter capacity becomes larger. Faster power electronic devices in combination with a PWM optimization algorithm could alleviate the problem by computing the PWM switching based on optimum efficiency and minimum harmonic distortion.

In conclusion, the future outlook for variable speed heat pump technology development is characterized by continuing effort to (1) penetrate cold climate markets, (2) further improve system performance, (3) develop high performance inverters and systems for unitary-size (2.5 ton range) equipment, and (4) improve the efficiency of PWM inverters. Regardless of other possible new developments, the trend of market and technology competition among major heat pump manufacturers (both Japanese and the U.S.) will continue to create an innovation-rich environment in which technology development will be the basis of future HVAC business worldwide.

References

1. Hitachi, Ltd., "Scroll Compressor Product Introduction," Hitachi, Ltd., Air Conditioning Technology Division, Tokyo, Japan, 1986.
2. Itoh, H., Improvement of a Heat Pump Room Air Conditioner by Use of Pulse-Motor-Driven Expansion Valve," *ASHRAE Transactions*, Vol. 92, Part 1, 1986.
3. Japan Air Conditioning, Heating and Refrigeration News (JARN), Private Communications, August, 1987.
4. Japan Refrigeration and Air Conditioning Industry Association (JRAIA), Private Communications, August, 1987.

5. Matsunaga, H., Hirao, H., Uchiyama, K., and K. Nakatani, "Characteristics of Compressor for a Room Air Conditioner Using a Non-Azeotropic Mixture of Refrigerants," *Proceedings of the 1986 International Compressor Engineering Conference,* Vol. 3, Purdue University, August 4-7, 1986.

6. Mimaki, M., "Effectiveness of Finned-Tube Heat Exchanger Coated in Hydrophilic-Type Film," *ASHRAE Transactions,* Vol. 93, Part 1, 1987.

7. Murozono, K., Wakabayashi, H., and M. Hori, "New Defrosting System for Residential Heat Pumps," *1986 International Institute of Refrigeration Meeting,* Purdue University, August 5-8, 1986.

8. Umezu, K, and S. Suma, "Heat Pump Room Air-Conditioner Using Variable Capacity Compressor," *ASHRAE Transactions,* Vol. 90, Part 1A, 1984.

CFC Restrictions: Energy Impacts and Technological Alternatives*

F. A. Creswick and *S. K. Fischer*
Oak Ridge National Laboratory
Oak Ridge, TN 37831

ABSTRACT

Recent international negotiations have resulted in an agreement to restrict the production and use of fully halogenated chloroflourocarbons. ORNL has conducted a study of technological alternatives to the use of restricted chloroflourocarbons in building applications and associated potential energy-use impacts. R-123 and R-134a have been identified as promising substitutes for R-11 and R-12. If these substitutes prove to be fully acceptable, energy-use impacts will be nominal. An urgent near-term need exists for information on the engineering properties of these fluids. If the use of substitutes does not prove to be acceptable, the energy-use impact would be an increase of about 1.0 quad per year if R-22 is available as a substitute and about 2.7 quads per year if not. The latter scenario is regarded as a serious consequence. The major impacts result from reduction in the R value of insulation for domestic refrigerator-freezers and in residential and commercial building insulation. In the long term, alternative technologies are available that could nullify any of the adverse energy-use impacts of chloroflourocarbons restrictions.

Introduction

Concern within the scientific and political communities about the possible effect of chlorofluorocarbon (CFC) compounds on the stratospheric ozone layer has been well documented in the scientific literature and popular press. Recently this concern has intensified as a result of growing scientific evidence that theories linking the release of CFCs into the atmosphere to the depletion of the ozone layer are basically correct even though the mechanisms are not yet completely understood.

In response to this apparent problem, the United States was one of the signatories of the United Nations Environmental Programme (UNEP) Montreal Protocol[1] imposing gradual reductions in the manufacture and use of CFCs over the next decade. The U. S. Environmental Protection Agency (EPA) has published proposed restrictions on the use of CFCs[2] under the provisions of Section 157 of the Clean Air Act to implement the terms of this treaty. These initiatives pertain to R-11, R-12, R-113, R-114, R-115, Halon-1301, Halon-1211, and Halon-2402 and call for a freeze on the aggregate ozone depleting potential (ODP) of these compounds at 1986 production levels by January 1989, a 20-percent reduction by July 1993, and a 50-percent reduction by July 1998.

Initial Activities

DOE/ORNL responded to the concern about the consequences of regulating CFCs by defining and conducting three tasks: a preliminary energy-use impact study, a survey of industry response to the problem and their perceptions of R&D needs, and formulation of a national R&D plan. The first two tasks generated information for use in drafting the R&D plan. These activities were complemented by a survey of trade associations, environmental advocacy groups, and selected industrial organizations conducted by Hagler, Bailly & Company.[3]

The scope of our investigations included building equipment, building insulation, and automotive air conditioning. We made use of relevant information generated by EPA and their contractors on the economic impact of various regulation scenarios, and we coordinated with the National Bureau of Standards (NBS) Center for Building Technology and staff members of the ORNL Building Thermal Envelope and Materials Program. The ORNL industry survey was conducted with the assistance of Kent Anderson, Joseph Pietsch, and Hans Spauschus.

A draft energy-use-impact report was completed in November 1987[4] and a draft document on an R&D plan was completed in December 1987.[5] These documents will pass ORNL and DOE review and be submitted for industry review and comment in the second quarter of 1988.

Applications Impacted

The principal uses of CFCs in the United States fall into four broad categories: (1)

*Research sponsored by the Office of Buildings and Community Systems, U.S. Department of Energy under contract DE-AC05-84OR21400 with Martin Marietta Energy Systems, Inc.

as refrigerants in vapor compression equipment, (2) as "blowing agents" for manufacturing rigid and flexible foam materials, (3) as solvents in cleaning electronic circuit boards, and (4) as fire extinguishing agents. The Department of Energy and ORNL are interested in the use of CFCs as refrigerants and in producing rigid foam for insulations for buildings and appliances because of their obvious links with national energy use. These applications will primarily be affected by controls on production of R-11, R-12, and R-115.

R-11 is used both in foam insulation and in refrigeration equipment, although its use in refrigeration is limited to centrifugal chillers. High R-value, polyurethane foams are made with R-11 for use in building insulation, domestic appliances (e.g., refrigerators, freezers, water heaters), and refrigerated trucks and railcars. Chillers using R-11 are manufactured in capacities ranging from 150 to 2,000 refrigeration tons.

R-12 is used to a small extent in polystyrene insulation, but its principal application is as the working fluid in vapor compression refrigeration equipment. A great deal of work will need to be done to develop alternative refrigerants for automobile air conditioners, household refrigerators and freezers, retail food store display cases, centrifugal chillers (R-12 is also used in this application as well as R-11 and R-114), and in the cooling system of soft drink vending machines. Substitute products will also need to be developed for the foam sheathings used in residential and commercial buildings and for foam boards used in subgrade foundation insulation.

R-115 is of interest primarily because it is a major constituent of the azeotropic mixture R-502. Use of R-502 has been increasing each year as it has gradually replaced R-12 as the refrigerant used in supermarket display cases. Although R-502 could be considered an alternative to R-12 (because of its low ODP, 0.3, and because its thermodynamic cycle efficiency is similar to that of R-12), its use in the future is uncertain because of the regulatory controls placed on R-115.

Energy-Use Impact

With the present technology used as base case, potential energy-use impacts were investigated in the ORNL study for four scenarios. These are the following:

(1) the availability of near-drop-in substitutes for R-11 and R-12, principally R-123 and R-134a;

(2) the need to revert to conventional fluids, principally R-22, because near-drop-in substitutes do not become available;

(3) the need to revert to fluids that are unconventional for these applications (such as ammonia or propane) because neither conventional nor alternative substitutes become available; and

(4) the use of alternative cycles and advanced technologies in the long term.

Table 1 is a matrix of the technologies assumed for each major application of R-11, R-12, and R-115 for each of the four scenarios given above.

The potential national energy-use impact was estimated for each application and each scenario by developing a per-unit impact and by assuming full penetration of the alternative technology into the existing equipment population. This methodology establishes an indication of the possible dimensions of the energy-use impact.

Table 2 presents the results of the analysis by application for each scenario. For the near-drop-in case, the potential energy penalty is a 0.22 quads per year (a quad is a quadrillion, or 10^{15}, Btu) increase in national energy use. Most of the impact results from a decrease in the R-value of the insulation used in the domestic refrigerator-freezers. Compared to the U.S. national energy consumption of about 75 quads for all uses, this level of impact would not be disruptive to the national economy or energy supply. If the near-drop-in substitutes do not become available, however, the estimated potential impact increases by a factor of 5 to about 1.0 quad per year, with domestic refrigerator-freezers, mobile air conditioning, and building insulation providing the major impacts.

If near drop-in substitute compounds do not become available and if R-22 cannot be considered an alternative (i.e., R-22 comes under scrutiny for federal regulation), then the estimated impact is about 2.7 quads per year. This is on the order of a 10% increase in energy use in the buildings sector. Centrifugal chillers contribute significant additional impact to this scenario.

There would, of course, be significant economic and social impacts associated with any of these scenarios, but they were not evaluated in the ORNL study. We recognize that these could be severe, or even devastating, to some industries as well as being disruptive to the economy in general. These social impacts have been omitted because they are beyond the scope of this work.

The negative numbers in the final column of Table 2 indicate a possible reduction in national energy use under this scenario. The impact of the advanced technology case was not fully evaluated in this study, and the benefit shown is largely the result of the

Table 1. Alternative technology scenarios

Application	Current practice	Near drop-in substitutes	Conventional fluids	Unconventional fluids	Advanced technologies
Refrigerator/freezer	R-12 with R-11 foam insulation	R-134a with with R-123 foam	R-22 with EPS[a]	Ammonia with fiberglass	Stirling cycle with vacuum panel insulation
Mobile a/c	R-12	R-134a	R-22	Ammonia	Stirling cycle
Beverage vending machines	R-12 with R-11 foam insulation	R-134a with R-123 foam insulation	R-22 with EPS	Ammonia with fiber-fiberglass	Stirling cycle with vacuum panel insulation
Retail refrigeration	R-502	R-502	R-22	Ammonia	Stirling cycle
Centrifugal chillers	R-11, R-12 R-114, R-22 and R-500	R-134a, R-123, and R-22	R-22 centri-fugal & screw compressors	Ammonia and current absorption	Advanced absorption and Stirling cycle
Refrigerated transport	R-11 foam	R-123 foam	EPS insulation	Fiberglass batts	Not considered
Water heaters	R-11 foam	R-123 foam	EPS insulation	Fiberglass batts	Vacuum panel insulation
Residential walls	R-11 and R-12 foams, EPS and fiberboard	R-123 and R-134a foams, EPS and fiberboard	EPS and fiberboard	Fiberboard	Not considered
Residential foundations	R-12 foam fiberglass	R-134a foam and fiberglass	Fiberglass	No substitute	Not considered
Commercial walls	R-11 and R-12 foam	R-123 and R-134a foams	EPS	EPS	Not considered
Commercial roofs	R-11 foam	EPS	EPS	EPS	Not considered

[a]Expanded polystyrene head board.

Table 2.
Potential national energy-use penalties (quads per year)

Application	Near drop-in substitute	Conventional fluids	Unconventional fluids	Advanced technologies
Refrigerator/freezer	0.11	0.56	0.89	-0.51
Mobile a/c	0	0.06	0.08	0.01
Beverage vending machines	0.01	0.03	0.06	-0.03
Retail refrigeration	0.01	0.01	0.02	-0.03
Centrifugal chillers	0.01	0.03	0.36	*
Refrigerated transport	0	0.01	0.02	*
Water heaters	0.03	0.04	0.09	-0.06
Residential walls	0.01	0.02	0.03	*
Residential foundations	0	0.11	a	*
Commercial walls	0.04	0.15	0.30	*
Commercial roofs	0	0	a	*
Total	0.22	1.00	1.85	-0.62

[a] estimate being revised

use of advanced insulation in domestic refrigerator-freezers. Further benefits could come in the applications that were omitted from this analysis. Existing concepts for advanced absorption heat pump equipment could provide a net annual energy saving as a substitute for centrifugal chillers. If Stirling refrigeration machinery can be developed to operate at 50% of Carnot efficiency, Stirling could substitute for vapor compression equipment with some energy saving.

It should be emphasized that this analysis did not deal with applications presently using R-22. If the use of R-22 were to be restricted, the impact would be much greater than that of the second scenario above.

Technological Alternatives

The search for alternative, or substitute, chemicals and technologies must begin with substances that are environmentally and socially acceptable (i.e., low ODP, nontoxic, nonflammable). The regulations on production of halogenated compounds recognize that they do not all pose the same threat to the environment. The accepted ODPs of the regulated CFCs and several compounds that might be used in place of the regulated ones are listed in Table 3. The first group of chemicals in this table are the refrigerants and blowing agents that are affected by the EPA regulations. The second group, with somewhat lower ODPs, lists some of the compounds that have been promoted as alternatives to the regulated CFCs. The third group, the Halons, are also covered under the Montreal agreement, although their primary application is in fire fighting equipment and is not of direct interest to the HVAC industry.

Table 3.
Ozone depleting potential of halogenated compounds

Compound	Formula	ODP
R-11	$CFCl_3$	1.0
R-12	CF_2Cl_2	1.0
R-114	$C_2F_4Cl_2$	1.0
R-113	$C_2F_3Cl_3$	0.8
R-115	C_2F_5Cl	0.6
R-22	$CHClF_2$	0.05
R-500	R-12/R-152a	low
R-502	R-22/R-115	0.3
R-134a	CF_3CH_2F	0.0
R-123	$CHCl_2CF_3$	low
R-141b	CCl_2FCH_3	low
Halon-1211	CF_2BrCl	3.0
Halon-1301	CF_3Br	10.0
Halon-2402	$C_2F_4Br_2$	TBD

An important point to note, however, is that even though the current agreement does not call for a complete phase-out of R-11 and R-12, this does not mean that sufficient supplies will be available for all applications. Manufacturers are free to shift production from one compound to another (within the constraints of the aggregate ODP ceiling), and they are likely to respond to price shifts in the marketplace. For instance, the Halons are perhaps irreplaceable in protecting valuable electronic equipment from fire damage, and, hence, might support high price increases. If more Halons are produced, there will be less R-11 and R-12 for heating, cooling, and insulation.

Alternative Pure Refrigerants

Promising substitute refrigerants have been identified for R-11 and R-12.[6] R-123, chemical formula $C_2HCl_2F_3$, is a close match for R-11 and is believed to have low ODP by virtue of its low chlorine content and the presence of a hydrogen atom in the molecule. The hydrogen atom is believed to make the molecule more susceptible to natural destruction and removal at low altitudes. R-123 is compatible with conventional refrigeration oils, although it has slightly less capacity per pound than does R-11. It may prove to be usable as a drop-in replacement for R-11 in centrifugal chillers.

R-134a, chemical formula $C_2H_2F_4$, is a promising replacement for R-12. It contains no chlorine and thus has an ODP of zero. R-134a is not miscible with conventional refrigeration oils but appears to be usable with some synthetic lubricants, so it could be used in place of R-12.

Both of these substitute refrigerants have been known for many years although no chemical company currently has a production scale plant for manufacturing them. Neither of them will be available in commercial quantities for at least 5 years, though, at which time the evaluation of their toxicities will be complete. Some preliminary data are available on the thermodynamic and engineering properties of R-123 and R-134a, but some uncertainty remains regarding their cycle efficiencies as substitutes for R-11 and R-12.

Work to date on the properties of R-123 and R-134a has been done mainly by the chemical companies with some recent work by a few automotive and HVAC equipment manufacturers. A cooperative industry or industry-government research is needed to develop required information in a timely manner.

Another alternative to R-11 and R-12 is the use of conventional refrigerants such as R-22, R-500, or R-502, which are already available and have lower ODPs than the designated CFCs. In general, this alternative will involve major product redesign, but little or no basic R&D is needed.

In searching for substitute refrigerants, the emphasis has been on methane and ethane derivatives, but propane derivatives, cyclic halocarbons, and other classes of compounds are potentially usable as refrigerants. Most alternatives can be ruled out on the basis of toxicity or flammability. Chemical companies say they have done extensive screening of substitute candidates; while this may be true, any individual or organization with the inclination can still consider it an appropriate task.

Refrigerant Mixtures

Some halocarbon compounds appear to have low ODP but are outside the volatility range of conventional refrigerants or are not suitable for use as pure refrigerants for some other reason. Mixtures of such compounds offer additional possibilities for alternatives. Depending on the properties of the constituents, the mixture may be azeotropic (discrete boiling point at any given pressure) or nonazeotropic (temperature changes during phase change). Mixtures may be binary, ternary, quaternary, etc. Chemical companies claim to have devoted considerable effort to evaluating mixtures; however, considering the large number of possibilities, it is doubtful that this work is complete. It is appropriate work for anyone with the inclination, but those having previously developed the analytical tools for working with mixtures will have a considerable advantage.

Both ORNL and DOE subcontractors (i.e., University of Illinois, Arthur D. Little, Inc., and NBS) have been engaged in research on nonazeotropic mixtures (NARMs) as refrigerants for several years.[7-10] NARMs offer potential of some basic cycle efficiency improvements over pure refrigerants as well as the possibility of modulating capacity by changing the composition of the active refrigerant charge. NARM technology is complex and U.S. equipment manufacturers have been reluctant to employ it. NARMs are used in some European and Japanese equipment.

Alternative Cycles

Up to this point in this paper we have been concerned with conventional vapor-compression refrigeration systems that are dominant in various applications. However unlikely, there is a possibility that neither new fluids nor refrigerant mixtures will prove to be acceptable alternatives for R-11 and R-12. There are competitive cycles like absorption, which are used to a lesser extent, and cycles like Stirling, which are used conventionally for cryogenic applications but which would be considered unconventional in food preservation or space conditioning. Evaluation of these cycles and proof of concept testing is needed as "insurance" in case the alternative refrigerants do not meet toxicity or efficiency requirements.

Absorption. Domestic refrigerators using an absorption cooling unit were widely used in the early part of this century and are still used for special applications such as recreational vehicles. While it is unlikely that the industry would return to this technology, it would be technically feasible to do so. Many large absorption chillers were installed for air conditioning applications in the 1950s and 60s, although sales volume has been low in the United States recently. These systems do not require CFC refrigerants.

Absorption heat pumps presently under development in the ORNL Building Equipment Research Program[11] will be capable of cooling-mode operation at primary-energy efficiency levels equivalent to those of present centrifugal chillers in addition to operating in the heating mode at more than twice the efficiency of a furnace or boiler. These systems can be expected to displace some chiller sales regardless of CFC restrictions; if necessary, they could be used instead of vapor compression systems for a wide range of space-conditioning applications.

Stirling Cycle. The use of electric-motor-driven Stirling refrigerators for domestic and commercial refrigeration is technically feasible. Stirling machines do not require CFCs and typically operate with hydrogen or helium as the working fluid. ORNL analytical studies of Stirling refrigerators have indicated that a reasonable level of efficiency could be obtained, although not as good as conventional vapor compression.[12] However, due to uncertainties in the validity of available analytical tools for Stirling cycle analysis, we believe that experimental work is now needed to fully explore the potential of this technology.

Desiccant Systems. Desiccant heating and cooling systems are technically feasible for a wide range of space-conditioning applications and additionally can offer the capability of removing indoor air pollutants. These systems operate with air and a desiccant bed of silica gel or zeolite or with a liquid desiccant solution.[13] The cost and durability of the desiccant bed are current R&D issues. While such systems have not been widely used in the past, they offer yet another alternative to CFC-based vapor compression systems.

Evaporative Cooling. Historically, "swamp coolers" have been a low-cost alternative cooling system in the southwest United States. Such systems do not employ CFCs and have low on-site energy requirements. Maintenance requirements due to fouling are the main deterrent to wide use of these systems, and there are also some potential health issues concerned in their use. This is a presently available alternative that additional R&D and product development could make more attractive.[14] Possible variations include direct and indirect, single-stage

and multistage systems, and hybrid evaporative-mechanical systems.

Alternative Blowing Agents

Foam insulation is commonly used in residential and commercial buildings, domestic and commercial appliances, and industrial applications. Most construction applications are in the form of polyurethane or extruded polystyrene panels used as building sheathing, although some commercial construction is done with "foamed-in-place" or sprayed on foam. The foamed-in-place technique is also widely used in appliance insulation where the ingredients for the foam are injected into the cavity between the inner and outer walls and the foaming action causes the insulation to completely fill the void in the shell. The sprayed on foam, which is common for irregular surfaces in industrial settings like tanks and pipes as well as the walls and roofs of metal buildings and warehouses, not only provides insulation but seals the wall from air infiltration.

R-11 and R-12 are particularly well suited to producing foam insulation. The low thermal conductivity of the gas entrapped within the foam helps to reduce heat flow through the insulation. The properties of these compounds are also such that "closed-cell" foams are formed so that the gases are retained for long periods, and, hence, their insulating value degrades slowly. Finally, these foams have structural properties that are important in their use in appliances where they actually contribute to the strength of the cabinet.

The alternative blowing agents that are being considered by industry for replacing R-11 and R-12 in manufacturing foam insulation are R-123 and R-141b for polyurethane foam and R-134a for polystyrene foam. None of these compounds has completed testing for toxicity nor are they available in large quantities. Some work has been done on blowing foam with each of these compounds, although a lot of development remains to be done. The foams produced to date have lower R-values per inch than R-11 and R-12 blown foams, and they age more rapidly. The compressive strengths of these boards is also lower than those for the foams they would be replacing, so appliances would have to be redesigned to include additional structural support.

Compact Vacuum Insulations

The DOE and ORNL have been looking at compact vacuum insulation panels for use in appliance insulation.[15] This emerging technology promises R-values in the range of 15-20 per inch for panels containing ultafine powders under a light vacuum or even 150-200 per inch for stainless steel panels under a hard vacuum (multiple layers of thin R-20 panels). These innovations could lead to significant reductions in the energy use for refrigerators, freezers, and hot water heaters. It is even possible that these materials will find applications in residential and commercial construction.

Conclusion

In the short term, there are no satisfactory substitutes for the restricted CFC fluids in buildings and automotive air conditioning applications. Switching to other conventional fluids would involve performance penalties and/or would require major product redesign.

In the medium term, there are technological alternatives available to accommodate any level of CFC restriction but not without adverse economic and energy-use impact. The least disruptive scenario is one in which R-123 and R-134a prove to be fully acceptable substitutes for R-11 and R-12 as refrigerants and R-123 or R-141b are acceptable as foam insulation blowing agents. The estimated energy-use penalty associated with this scenario is moderate - about 0.2 quads per year; most of this results from a decrease in the R value of domestic refrigerator/freezer insulation with the alternative blowing agents.

If R-134a and R-123 or R-141b do not become available and acceptable, the energy-use impact could increase to about 1.0 quads per year if R-22 is available as a substitute or to 2.7 quads per year if it is not. Domestic refrigerator-freezers, automobile air conditioning, centrifugal chillers, and building insulation would be the most extensively impacted applications.

A back-up alternative is the use of substitute refrigerant mixtures instead of pure refrigerants. In the long term, this alternative could prove to be advantageous over the use of substitute pure refrigerants.

It is likely that some alternative technologies, such as advanced absorption heat pumps, will begin to penetrate the markets considered here regardless of CFC restrictions. The use of these technologies could be expanded as alternatives to CFC systems, if necessary.

Possible impacts of R-22 restrictions have not been considered here because none have been proposed. R-22 is widely used for space conditioning applications and could be used as an alternative to R-12 in some applications. Such restrictions would be highly disruptive.

Although it is fortunate that there appear to be reasonable long-term alternatives to the use of R-11 and R-12, substantial R&D is required to implement them. Clearly, much of this work will appropriately be of a

proprietary nature that will bring economic rewards to those organizations that develop the superior alternatives. However, there is also an opportunity for cooperative industry-industry or industry-government R&D that will be mutually beneficial to the participants. Development of information on engineering properties of new refrigerants is an example of a research area in which cooperative R&D could reduce the time and cost of responding to CFC restrictions without compromising competition. Such cooperation could be in the form of information sharing, task sharing, or cost sharing. DOE and ORNL are keenly interested in working closely with U. S. industry to mitigate the energy, economic, and social impacts of CFC restrictions.

References

1. Montreal Protocol on Substances That Deplete the Ozone Layer, United Nations Environment Programme, Final Act, September 1987.

2. Protection of Stratospheric Ozone: Final Rule and Proposed Rule, 40 CFR Part 82, Fed. Regist. 52, 47486-47523, December 14, 1987.

3. "Alternatives to CFCs: Industry R&D Needs and DOE R&D Program Strategy," HBC 87-3035, Hagler, Bailly & Company, Washington, D.C., November 23, 1987.

4. S. K. Fischer, F. A. Creswick, and John Dieckmann, "Energy-Use Impact of Chlorofluorocarbon Restrictions in Refrigeration and Buildings Applications," draft report, Oak Ridge National Laboratory (to be published).

5. F. A. Creswick, P. D. Fairchild, and J. E. Christian, "A Plan for Research and Development on Chlorofluorocarbon Alternatives in Refrigeration and Buildings Applications," draft report, Oak Ridge National Laboratory (to be published).

6. U.S. Environmental Protection Agency, "Chlorofluorocarbon Chemical Substitutes," draft report, December 4, 1986.

7. E. A. Vineyard, "Laboratory Testing of a Heat Pump with Water-to-Water Counterflow Heat Exchangers Using Various Compositions of an R13B1/R152a Refrigerant Mixture," ASHRAE Trans. 94, 1988.

8. W. F. Stoecker, "Energy Characteristics of a Two-Evaporator Refrigerator Using a Refrigerant Mixture," ORNL/Sub/81-7762/2&01, Oak Ridge National Laboratory, March 1982.

9. R. L. Merriam and S. Mathias, "Evaluation of Advanced Vapor Compression Cycles for Use with Nonazeotropic Refrigerant Mixtures," ORNL/Sub/86-22000C/1 (draft report), Oak Ridge National Laboratory, January 1988.

10. M. Kauffeld et al., "An Experimental Evaluation of Two Nonazeotropic Mixtures in a Water-to-Water Breadboard Heat Pump," draft report, National Bureau of Standards, Gaithersburg, Md. (to be published).

11. R. C. DeVault, "Developments in Gas-Fired Heat Pumps in North America," Heat Pumps - Prospects in Heat Pump Technology and Marketing, Proceedings of the 1987 IEA Heat Pump Conference, Lewis Publishers, Chelsea, Mich., pp. 351-358, April 1987.

12. N. Domingo, "Comparative Analysis of a Stirling Heat Pump with Second- and Third-Order Computer Models," ORNL/CON-162, Oak Ridge National Laboratory, June 1985.

13. R. H. Turner, "Modeling a Thermally Activated Heat Pump with Desiccant Cooling," ASME Preprint 87-WA/AES-1, 1987.

14. R. H. Turner and F. C. Chen, "Research Requirements in the Evaporative Cooling Field," ASHRAE Trans. 93 (1), 1987.

15. D. W. Yarbrough, F. J. Weaver, R. S. Graves, and D. L. McElroy, "Development of Advanced Thermal Insulation for Appliances, Progress Report for the period of July 1984 - June 1985," ORNL/CON-199, Oak Ridge National Laboratories, May 1986.

International Cooperation in Heat Pump and Refrigeration Research Through the International Energy Agency

J. D. Ryan
U.S. Department of Energy
Washington, DC 20585

(See Appendix A)

Session 4

Thermally Activated Heat Pumps: Absorption Systems

Organizer : R. C. DeVault
Oak Ridge National Laboratory
Chairman: J. D. Ryan
U. S. Department of Energy

DOE Absorption Program Overview

R. C. DeVault
Oak Ridge National Laboratory
Oak Ridge, TN 37831

Abstract

Advanced technologies for gas-fired absorption heat pumps for building space conditioning (heating and/or air conditioning) are being developed with the U. S. Department of Energy support. Single-effect cycle absorption heat pumps for residental application were demonstrated in the 1970s but proved to be uneconomic and were not manufactured. Advanced technology absorption heat pumps with substantially higher efficiences are now being developed and have the potential to be economically competitive with existing HVAC equipment while saving energy.

Background

Residential and commercial buildings account for 37% of the total energy used in the United States. The primary energy uses in buildings are for heating, cooling, and the heating of water. Natural gas and oil are major fuel sources for building heating, and almost all air conditioning is done with electricity. Figure 1 shows by fuel type the energy consumed in the United States for heating and cooling.

Air conditioning is a major energy use in residential and commercial buildings. Currently in the United States, about 85% of all new houses are air conditioned, and about 30% of new houses use electric heat pumps for heating and air conditioning.[1]

Figure 2 shows the relative operating fuel cost to the consumer of electric heat pumps, gas furnaces, and gas fired heat pumps for a range of electricity to gas price ratios. As can be seen, with modestly efficient gas fired heat pumps [coefficient of performance (COP) > 1.4], heating fuel costs should be lower than for electric heat pumps for any credible electric-to-gas price ratio.

The U. S. Department of Energy (DOE) has been supporting research and development for absorption heat pump systems since the late 1970s. The goals for development of gas-fired absorption heat pumps are to produce equipment that, compared to existing technologies, will save primary energy, be economical to the customer to purchase and operate, and provide for the alternative use of natural gas for air conditioning.

*Research sponsored by the Office of Buildings and Community Systems, U.S. Department of Energy, under Contract DE-AC05-84OR21400 with Martin Marietta Energy Systems, Inc.

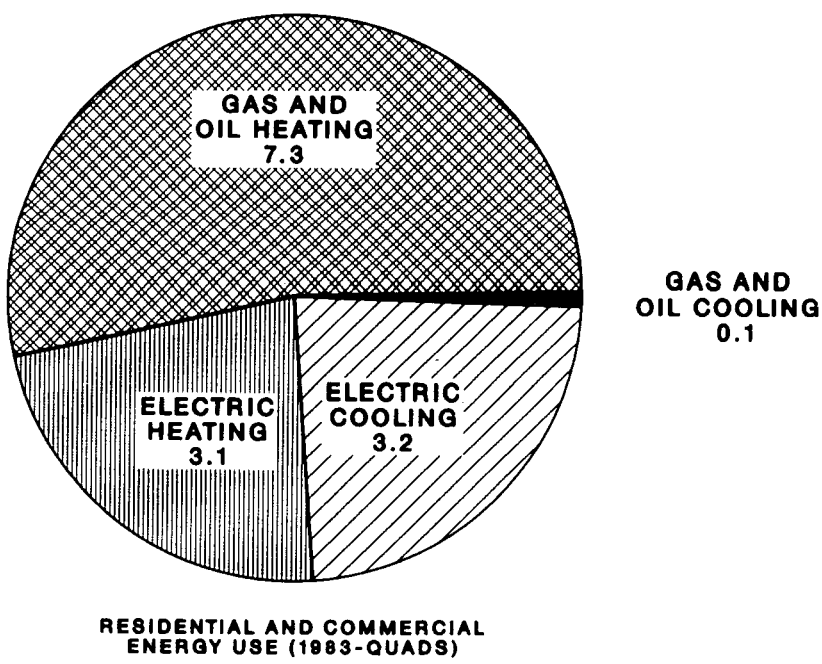

Fig. 1. Natural gas and oil are major fuel sources for building heating.

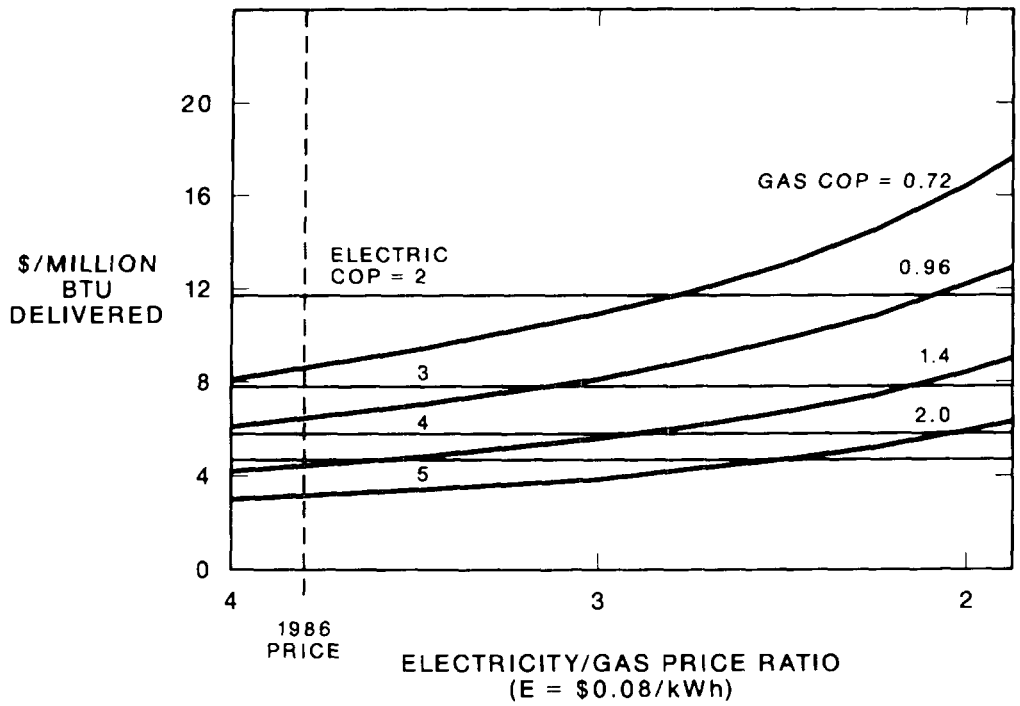

Fig. 2. Advanced absorption heat pumps will cost less to operate than electric heat pumps.

Project Summaries

Initial projects, first funded in the 1970s and now completed, were for the development of prototype single-effect absorption heat pumps for residential applications.

Arkla Industries, a manufacturer of ammonia-water air conditioners, developed a single-effect ammonia-water heat pump (for heating only) with steady state COPs of 1.25 at 8.3°C (47°F) and 1.12 at -8.3°C (17°F).[2] These performance levels are fuel based efficiencies including flue losses using the higher heating value of natural gas.

Allied Corporation, under sponsorship of DOE, the American Gas Association, and the Gas Research Institute, developed a single-effect heat pump for both heating and cooling for residential applications, using a fluorocarbon refrigerant and an organic absorbent. Prototype heat pumps were developed to achieve a heating COP of 1.2 at 8.3°C (47°F) and a cooling COP of 0.5 at 35°C (95°F).[3] The prototype development used R-123a (1,2-dichloro-1,2,2-trifluoroethane) for the refrigerant and ETFE (ethyl tetrahydrofurfuryl ether) for the absorbent. Further refinement of the Allied prototype, including a condensing flue, showed potential for about a 1.5 heating COP and a 0.6 cooling COP.

Both the Arkla and Allied heat pump prototypes were successfully operated and achieved their performance goals. However, the single-effect performance levels were not sufficient to offer reasonable economic incentive for customer acceptance, so neither machine was further developed or manufactured.

Based on the achieved performance results of the Arkla and Allied single-effect cycle prototypes and the need to provide economic payback to customers of less than 3 years as opposed to conventional heating and air conditioning systems, the DOE absorption heat pump program goals were re-evaluated in late 1981. The decision was made to evaluate advanced absorption cycles capable of producing higher efficiency heat pumps than conventional single-effect cycles while still using existing absorption fluid combinations. Higher efficiency levels were needed, especially for air-conditioning operation, in order to save enough money in fuel costs to offset the assumed high initial cost of absorption machines.

In 1982, the DOE absorption program, managed by Oak Ridge National Laboratory's (ORNL) Building Equipment Research Program, issued a Request for Proposal (RFP) for the development of advanced absorption cycles with performance goals of COPs of 1.6 in heating and 0.7 in

cooling, as compared with current state-of-the-art single-effect values of 1.2 and 0.5. The RFP was distributed to more than 50 potential bidders within the United States. Three contractors were selected for the work under the advanced cycles program, and work was started in late 1982 and early 1983. The three contractors are Carrier Corporation, the Trane Company, and Phillips Engineering Company.

The work in the advanced absorption cycles program is divided into three phases. Phase I is the analytical evaluation of advanced cycles, with a preferred advanced cycle being selected for further development. Phase II is the development and testing of a laboratory breadboard prototype of the selected advanced cycle. Phase III is the development and testing of a packaged proof-of-concept prototype after successful completion of Phase II.

The goal of the Phase I selection of a preferred advanced cycle was not necessarily to pick the highest efficiency cycle but rather to select cycles with a combination of features, such as high efficiency, low manufacturing cost, high inherent reliability, etc., that appeared to offer the most likely path to a manufactured product by the 1990s.

Each of these projects is reported on at this conference, so I will not go into detail on project results. Each contractor completed Phase I analysis and selected a "preferred" advanced cycle.[4-6]

Each of these advanced cycles selected by Carrier, Trane, and Phillips offers potential for a rated heating COP in the range of 1.8 to 2.0 and cooling COP in the range of 0.8 to 1.2, significantly exceeding the original program goals set in 1982.

Phase II of the projects, the laboratory breadboard demonstration of the cycles identified as most promising, has been completed at Trane and at Phillips and is well advanced at Carrier.

During 1985, Phillips successfully operated a proof-of-principle breadboard prototype of a residential-sized unit with performance exceeding the original advanced cycle RFP goals. The Generator Absorber Heat Exchange Cycle (GAX) breadboard achieved COPs of over 1.8 in heating at 8.3°C (47°F) and 0.8 in cooling at 35°C (95°F). An independent cost analysis of the Phillips prototype concept has predicted a customer-installed cost equal to that of existing mid-line gas furnace/electric air-conditioner combinations or to that of electric heat pumps, indicating the potential for advanced absorption cycle residential heat pumps to become a major consumer product in the future.
DOE has also sponsored the development of a modular user-oriented absorption cycle computer model for use in evaluating advanced absorption cycles for heat pumps and heat transformers. The basic model has been completed and is available for use on main-frame computers and on IBM compatible personal computers.[7]

The Institute of Gas Technology (IGT), under DOE sponsorship, has undertaken the cataloging of absorption fluids properties data and references for all available U.S. data[8] and also for available foreign data.[9]

In support of the advanced heat pump work, ORNL has developed a unique instrument using fiber optics to measure precisely the refrigerant concentration in the refrigerant-absorbent mixture in an operating absorption device.[10] This fiber-optic refrigeration cycle monitor measures the refractive index of fluids. Because most refrigerant-absorption fluids are binary mixtures, the refractive index of the fluid is directly related to the concentration of its individual components. In tests with $LiBr/H_2O$, the instrument has demonstrated the ability to measure local refrigerant concentration to an accuracy of 0.1% inside an operating absorber. Combining measurements of local concentration and temperature allows on-line monitoring and control of the refrigeration system, as well as a detailed study of heat and mass transfer processes occurring within absorption systems. This new measurement capability should help in the design of new absorption systems for increased operating efficiency.

Figure 3 shows primary energy consumption in heating and cooling for existing technologies, the prior single-effect cycles, and the current advanced cycle concepts. Based on recent progress in the DOE program, advanced absorption cycle heat pumps show the potential for significant energy savings with acceptable consumer economics for both residential and commercial applications.

As noted earlier in this paper, the current advanced absorption cycles heat pump program was started in 1982 and has made steady progress toward potential products. The Phase II laboratory proof-of-principle demonstrations are now complete at two of the three contractors and well advanced at the third. As shown in Fig. 3, these advanced absorption projects have demonstrated very high heating performance compared to all existing HVAC products. These advanced absorption cycles have also demonstrated the potential for acceptable cooling performance, although by no means as good as presently available electric air- conditioning efficiency levels.

Further, as a result of the Phase I efforts of the three DOE contractors and independent work performed at ORNL, it became apparent that the advanced cycles selected in Phase I for heat pump applications have only "scratched the surface" of the long-term potential for absorption technology.

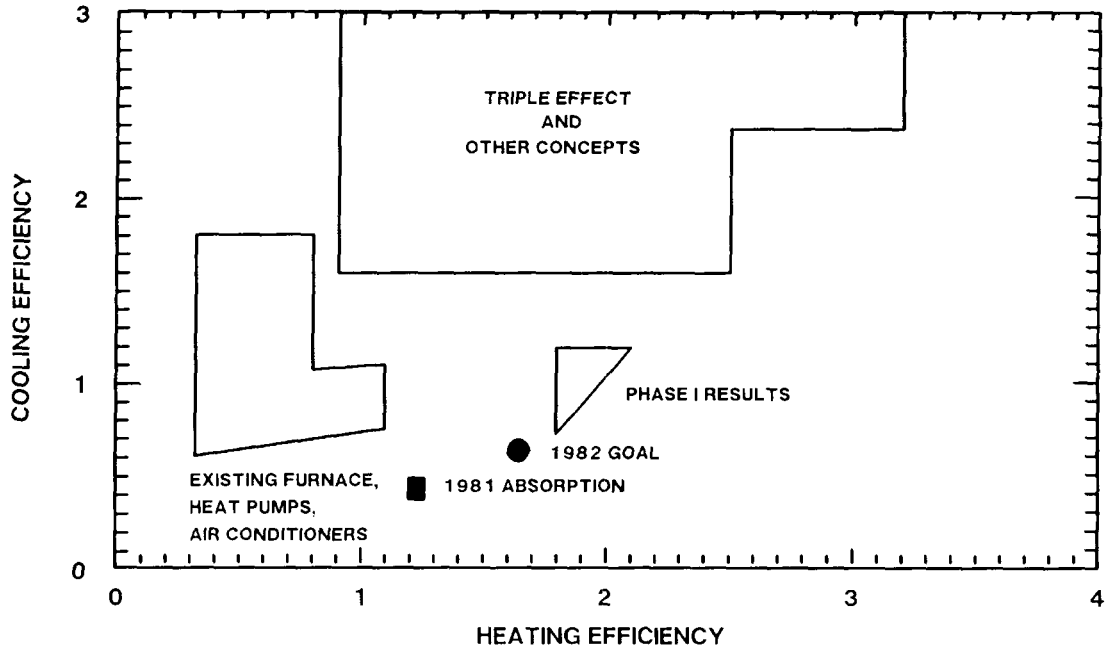

Fig. 3. Absorption cycles have been identified with performance potential well beyond current technology.

Accordingly, since 1983 DOE has supported further work on additional advanced absorption cycles and on advanced absorption fluids. This work has included a large number of potential applications, including but not limited to, building air conditioning and heating. As a result, the DOE program has expanded far beyond the 1982 advanced cycles program. I will now briefly describe one of these program directions.

Since air-conditioning performance of even double-effect cycles is at best marginal for U. S. applications, one of the programs supported by DOE is the development of the basic technology to substantially improve absorption's air-conditioning efficiency.

More than one hundred absorption cycles have been patented during the present century, including an absorption cycle conceived by Albert Einstein. It is well known to those actively involved in absorption research that there are many hundreds, perhaps thousands, of technically possible absorption cycles.

With DOE sponsorship, a particular triple-effect cycle[11] has been conceived that has the potential for low cost while simultaneously offering much higher efficiency than double-effect cycles.

The triple-effect chiller is 30 to 60% higher in efficiency than a double-effect cycle using equivalent heat exchangers. Because the triple-effect chiller can use several existing absorption fluids, uses only conventional heat exchangers, and needs less total heat exchange per unit of capacity than any single-effect or double-effect cycle; the triple-effect chiller has the potential to be no more, and possibly less, expensive than existing double-effect absorption chillers.

Other advanced cycles, in addition to the triple-effect chiller, are also being developed.

Figure 3 shows the efficiency potential for the "Third Generation" absorption technology (advanced cycles and advanced fluids) now being developed.

REFERENCES

1. "1986 Statistical Panorama," The Air Conditioning, Heating and Refrigeration News, April 7, 1986.

2. R. H. Merrick and D. Kuhlenschmidt, "Development and Demonstration of an Ammonia-Water Absorption Heat Pump," ARKLA Industries, Inc., ORNL/sub/86X-61603C, Proc. DOE Heat Pump Contractor's Program Integration Meeting, June 1982.

3. K. P. Murphy, R. Simon, B. Phillips, J. Marsala, and E. Whitlow, "Development of a Residential Gas-Fired Absorption Heat Pump - Physical and Thermodynamic Properties of R123a/ETFE, System Development and Testing and Economic

Analysis," prepared for ORNL by Allied Corporation, ORNL/sub/79-24610/4, August 1985.

4. B. A. Phillips, "Advanced Residential Absorption Heat Pumps Cycle Analyses-Construction of a Test Model," Proc. DOE/ORNL Heat Pump Conference, December 11-13, 1984, Washington, DC.

5. F. C. Hayes, "Evaluation of Advanced Design Concepts for Absorption Heat Pumps," Proc. DOE/ORNL Heat Pump Conference, December 11-13, 1984, Washington, DC.

6. R. C. Reimann, "Advanced Absorption Heat Pump Cycles," Proc. DOE/ORNL Heat Pump Conference, December 11-13, 1984, Washington, DC.

7. G. Grossman and E. Michelson, "A Modular Computer Simulation of Absorption Systems," ASHRAE Trans. 91, Pt. 2, 1985.

8. R. A. Macriss and T. S. Zawacki, Absorption Fluids Data Survey-Final Report on U.S. Data, ORNL/sub/84-47989/1, 1986.

9. R. A. Macriss, J. M. Gutroj, and T. S. Zawacki, "Absorption Fluids Data Survey-Final Report on Foreign Data," ORNL/sub/84-47989/2, April 1987.

10. D. T. Bostick, L. N. Klatt, and H. Perez-Blanco, "Real-Time In-Situ Refractometer for Concentration Measurements in Absorption Machines," ASHRAE Trans., PO-86-04, no. 3, 1986.

11. R. C. DeVault, U. S. Patent 4,732,008, "Triple-Effect Absorption Chiller Utilizing Two Refrigeration Circuits."

Development of an Advanced-Cycle Absorption Heat Pump for Residential Applications

B. A. Phillips
Phillips Engineering Company
St. Joseph, MI 49085

Introduction

This paper is a second report on a program funded by the Department of Energy under contract 86X-17497C from the Oak Ridge National Laboratory which has the purpose of developing residential thermally activated heat pumps based on an advanced absorption cycle. The first report (1) referred to Phase I and the start of Phase II of the program. The present report covers Phase II and the part of Phase III now under way. The overall objectives of the program are to develop a gas-fired absorption residential heat pump with air to air operation and having coefficients of performance greater than 0.7 in cooling mode and 1.6 in heating mode at the ARI rating conditions.

Phase I was an analytical study for the selection of the absorption cycle and working fluids best suited to the residential application.

The known absorption working fluids were evaluated for ability to operate to -20°F evaporator temperatures, for long term stability at boiler temperatures up to 400°F, and for ability to meet code requirements. The ammonia/water pair was the only fluid combination with a proven record of meeting those requirements over periods of 20 years or more. It was therefore chosen for the cycle evaluations and for later system development. However, the recently proposed ternary combination of ammonia, water and lithium bromide had been shown to have potentials for lower rectifier losses and for usage to higher boiler temperatures. (2) Although its corrosion characteristics could be expected to be worse than ammonia/water, it was also suggested for investigation. With both of these fluid combinations the code requirements are that a secondary fluid be used to transfer the heat to or from the home. The necessary temperature differentials for the two heat transfer steps thus required were included in the heat and mass balances used in calculating the cycle coefficients of performance.

The known absorption cycles were then screened for ability to meet the COP objectives and the low cost and simplicity required for the residential market. The second screening reduced the number of cycles to six, all of which were expected to produce coefficients of performance significantly above the project COP objectives. Those cycles were the Double Effect, the Resorber Augmented, the Generator Absorber Heat Exchange, the Variable Effect, the Two Stage GAX, and the Regenerative Double Effect. The criteria used in comparing the cycles were: the coefficients of performance, the pumping power requirements, the total heat transfer required (as a major factor in the total system cost), the operating pressure levels, the number of major components, the number of solution pumps, and the range of temperature over which the cycle could operate.

All the cycles other than the Resorber Augmented cycle were found to have cycle COP's from 1.03 to 1.11 in cooling mode and 2.03 to 2.11 in heating mode. The COP's of the Resorber Augmented cycle were below those levels but above the project requirements. Comparison of the cycles on the bases of the other criteria and the individual cycle characteristics found during the analyses showed the Generator Absorber Heat Exchange Cycle, Figure 1, to be better than the other cycles for the application. It was therefore selected for development in Phase II.

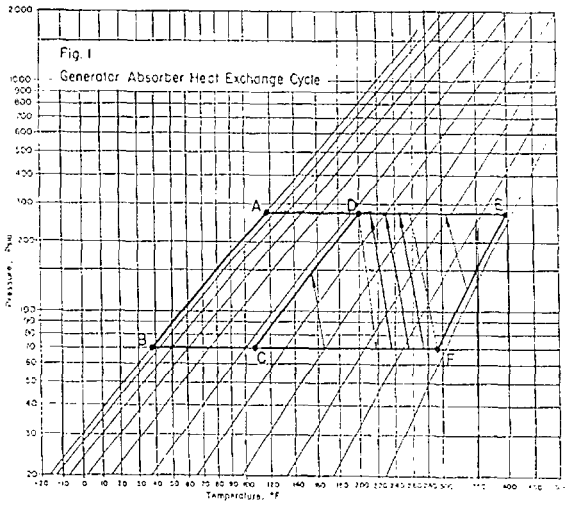

Drawings of a potential ultimate heat pump design were made and supplied to an independent engineering and manufacturing company for a factory cost estimate. The normal multipliers for other corporate costs and for distributor and dealer mark-ups were then applied to that material, labor and factory burden estimate to arrive at an estimated retail cost. That retail cost figure was found to be near the mid-point of the range of residential heating plus cooling equipment at the time.

Phase II

Phase II had the objectives of experimentally demonstrating operation of the GAX cycle and of achieving first the project performance goals and then a target established for Phase II, of a cycle COP of 1.9 in heating mode, using an ammonia/water test unit. A second objective was to investigate the NH_3/H_2O-LiBr ternary fluid for corrosion and heat transfer characteristics and for performance in a GAX cycle unit.

A laboratory test unit of the GAX absorption cycle was designed and built (1). Figure 2 is a schematic diagram of the unit. The unit was tested using electric resistance heat input to eliminate burner and flue loss uncertainties. The generator and the absorber of the test unit were both made tall to allow sufficient transfer surface and to improve the accuracy of measuring the heat and mass transfer performance along the lengths of the two components. The localized determinations proved valuable in optimizing the overall performance of both the components. All components in the system were developed and improved until the heating and cooling cycle COP's reached 1.78 and 0.78. At 90% flue efficiencies those cycle COP's equal the basic RFP project objectives of gas fired COP's of 1.6 in heating mode and 0.7 in cooling mode.

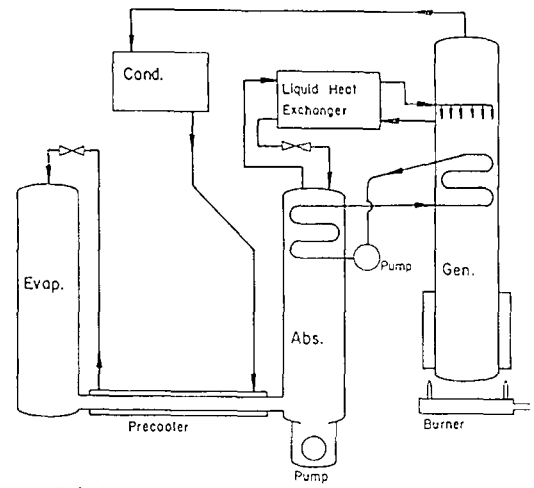

Fig.2 Generator - Absorber Heat Exchange Unit.

After those COP's were reached the component developments were continued, until performance equivalent to a cycle COP in heating mode of 1.9 was reached at the 47°F rating conditions. The test unit was then operated over a range of transfer fluid temperatures representative of outdoor ambient temperatures above and below the ARI rating conditions. The results of these tests are shown in Figure 3. The solid lines in Figure 3 represent the performance objectives for the ultimate product. The cycle COP's calculated in Phase I (1) are slightly higher than the solid lines in this diagram. The dotted lines and the test points shown were calculated from the raw data by correcting for measured heat losses plus conservative estimates of insulation losses.

The test results also indicated the areas in which further improvements to individual components could be made. The possible improvements were sufficient to reach the solid lines in Figure 3.

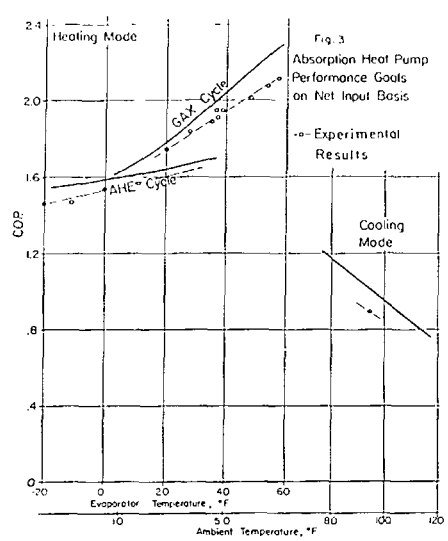

Ternary Fluid Investigations

The second part of Phase II involved investigations of the ternary working fluid composed of ammonia/water-Lithium Bromide (2). The absorbent was 40% water and 60% Lithium Bromide. The program consisted of corrosion studies of the ternary fluid in steel and stainless steel cells, and of tests of the fluid in a GAX cycle breadboard test unit. The corrosion program utilized corrosion test cells 3 inches in diameter and 4 inches long operated at boiler temperatures and pressures. A bank of the test cells in shown in Figure 4. The cells contained coupons of sheet metal having 2 square feet of surface area and coiled to fit within the cell. The corrosion rates were determined in terms of the rate of formation of hydrogen gas. Preliminary tests of mild steel and 316 stainless steel cells were made at 300°F, with and without lithium chromate as inhibitor. The uninhibited mild steel cell produced large quantities of gas and the inhibited 316 SS cell produced none. The inhibited mild steel cell and the uninhibited 316 SS cell produced intermediate quantities.

A test program with a series of 316/316L stainless steel cells was then initiated, operating with chromate inhibitor at 400°F. Stress corrosion cracking was found to occur in as little as six hours of operation. The cracks were located above a cylindrical weld just above the liquid level. Attempts to prevent cracking by improvements in the welding process and stress relieving only lengthened the time before cracking to a maximum of 24 hours. The chromate was concluded to be the primary cause of the cracking. Plans to investigate the traces of chloride ion in the chromates were cancelled when test cells with other inhibitors did not crack at 400°F and 500°F. Molybdates were investigated first, followed by arsenates and arsenites. All three reduced hydrogen generation to less than 10 ml per day in the stainless steel cells but did not stop it completely. Molybdate was chosen for use in the test unit constructed of 316/316L stainless steel. Six molybdate cells were continued in operation at 500°F. At about five months of operation stress corrosion cracks began to appear in a different location, and all cells cracked within seven months. Four arsenate cells

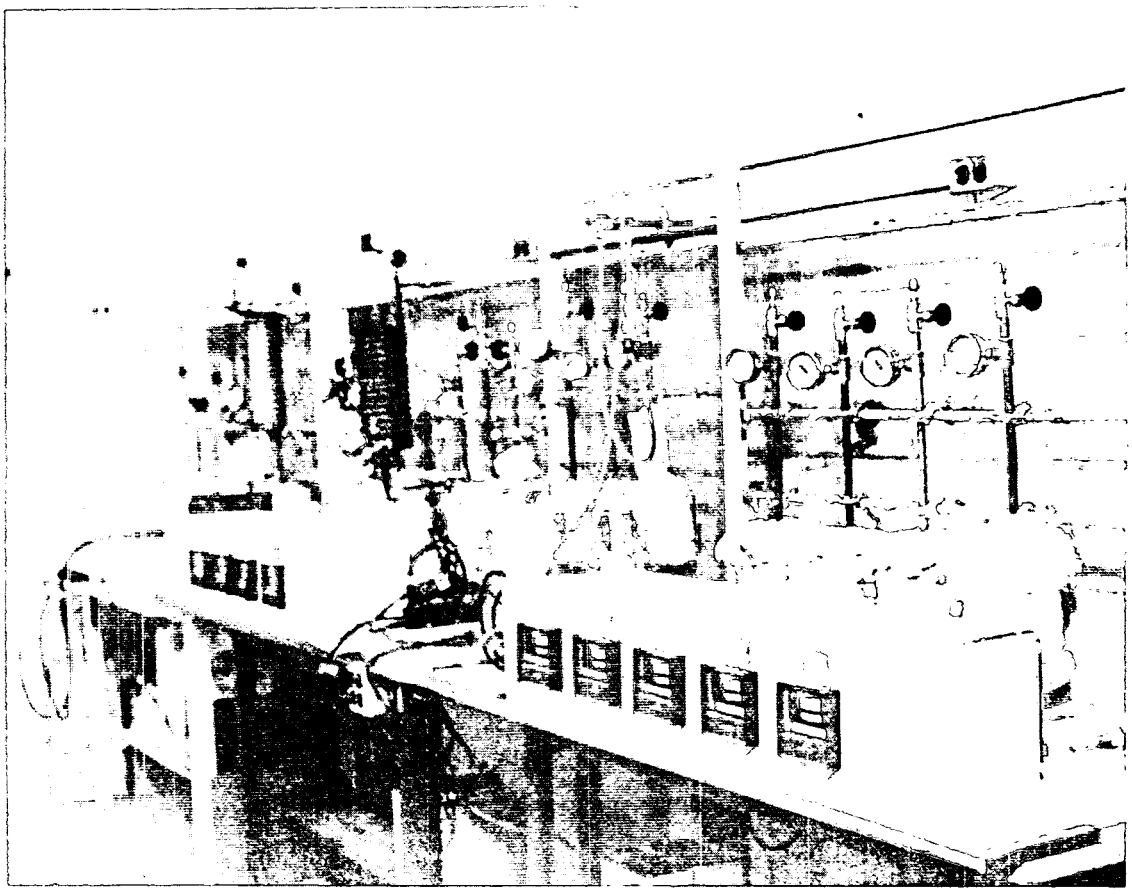

Figure 4 - Photograph of a Rack of Corrosion Test Cells

were operated and one arsenite. No cracking occurred on those cells. The hydrogen generation rates were as stated above, the arsenates slightly less than the molybdates and the arsenite perhaps a little higher.

Breadboard Test Unit

The breadboard test unit was similar to the ammonia/water test unit but with somewhat higher heat and mass transfer surface, to compensate for the higher viscosity of the ternary solutions. This unit was also electrically heated. A photograph of the test unit with associated power supply, instrumentation and controls is shown in Figure 5. In operation, hydrogen was generated at much higher rates than had been expected from the test cell results. After a few days of testing it settled down to about 150 ml per hour. The hydrogen was collected in a chamber seperate from the working fluid circuit. Although it was vented every half hour, it undoubtedly affected the heat and mass transfer in the absorber and the condenser. It was determined the rate of gas generated was reduced essentially linearly on turning off heaters. Most of the hydrogen generation was therefore associated with the heat input surfaces, but the evidence was not conclusive that it was only due to over temperature.

Overall heat transfer rates in the absorber were found up to 200 to 300 Btu/Hr Sq Ft/°F. They were somewhat less than those for ammonia/water, but comparisons were questionable due to differences in the conditions. They were higher than expected, considering the higher liquid viscosities and the probable hydrogen blanketing conditions.

The unit performance was also good under the conditions. At equivalent stages of development the ternary fluid unit performed to higher COP's than the ammonia water unit had. Coefficients of performance up to 1.83 were reached in heating mode operation. At that stage of the development the cracking of the molybdate inhibited corrosion test cells produced concerns about the safety of the operation. The potential hazards of a sudden large crack in the six inch diameter boiler could be significant. The testing and development of the ternary fluid unit was therefore stopped at that point. When the tested generator and absorber were cut open, all surfaces wetted by the ternary solution were found to be covered by a thick

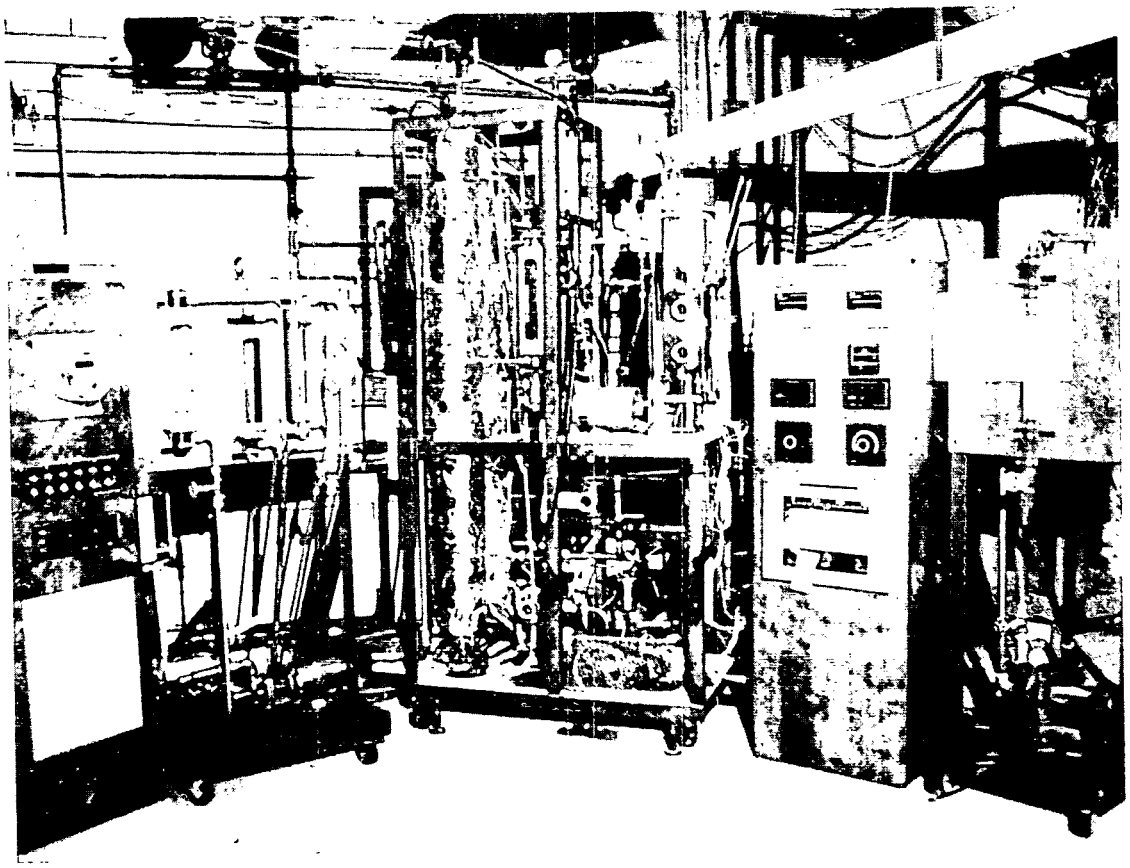

Figure 5 - Photograph of Ternary Fluid Test Unit with Instrumentation & Controls

coating of a black powder, containing much, if not all, magnetite. This soft coating, up to a 1/2 millimeter in thickness was undoubtedly also a significant factor in reducing the heat transfer rates.

The corrosion characteristcs of this ternary fluid combination are thus discouraging. Yet the potential performance advantages of ternary solutions is substantial. Therefore investigations of ammonia/water combinations with other salts are continuing under a Department of Energy SBIR project.

Phase III

Phase III of the development of the ammonia/water heat pump has been under way for over a year. The objectives are to continue development to improve the performance to COP's of 0.9 in cooling mode and 1.8 in heating mode under gas fired conditions and to develop a prototype unit of that performance to a size, weight, and cost suited to the residential market. The objectives are being pursued in parallel paths. One is the development of compact heat and mass transfer surfaces to reduce the size of the major absorption system components, the generator, absorber, evaporator and condenser, and to also improve their performance. A second step has been the design and construction of an outdoor test heat pump using absorption system components similar to those tested in the breadboard test unit. That heat pump, shown in Figure 6 has been operating outdoors for almost a year. The purpose was to investigate the operation of the GAX cycle under changing outdoor conditions through winter and summer. 4,500 hours of operating time have been accumulated. The outdoor testing has been very valuable. Differences in the reactions of the GAX cycle and those of single effect and absorber heat exchange cycles to variations in their environments have been significant. It has become evident that the control systems will require modification from those used in our past developments.

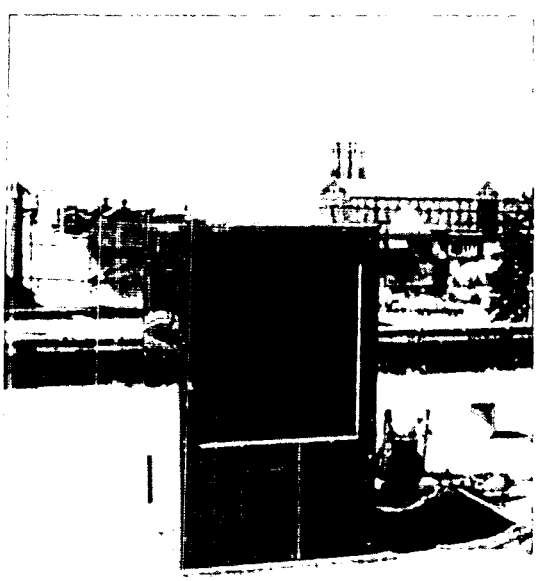

Figure 6 - Photograph of Outdoor GAX Test Unit

A third parallel path is the development of the prototype heat pump. A first model of the outdoor system has been designed and constructed. Figure 7 shows the dimensions and general configuration. The absorption components are located in the fully enclosed end on the left of the drawing. The location of the outdoor finned coil, fan and motor are as shown. The water pumps, eight way valves, solution pump motor, and controls are in the compartment below the finned coil. Figure 8 is a photograph of the prototype as first constructed.

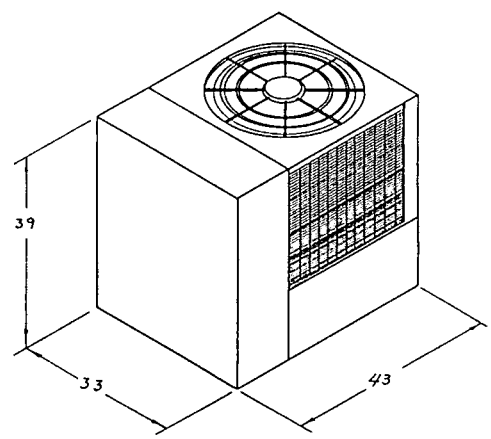

Fig.7 Three RTon Prototype

An intensive program of testing and developing the absorption system and individual components is underway. The solution pump is a key component of sufficient importance to have a program of its own. Due to its crucial importance to the system, the pump program includes the development of three types of pumps. Two of them are direct pumping hermetic pumps to be magnetically driven by an external motor. The third pump represents a fall-back position in case development of the sealed pumps cannot be completed in time. The latter development is directed toward correcting the problems of the diaphragm pumps and extending their operating range to the low pressures at evaporator temperatures below zero Fahrenheit.

The sealed pumps are a vane pump and a gear pump. Wear and operating life are major concerns. The Metals and Ceramics Division of Oak Ridge National Laboratory has joined in developing the new materials required to solve those and related problems. Important advances have been made. A test pump has operated 3000 hours with no significant wear. In other developments the pump performance has been improved. Although much work remains to be done the results to date are very encouraging.

References

1. B. A. Phillips, Analysis of Advanced Residential Absorption Heat Pump Cycles, Proceedings of DOE/ORNL Heat Pump Conference, Washington DC, December 1984, p. 265.

2. R. Radermacher, Working Substance Combinations for Absorption Heat Pumps, Ph.D Thesis, Tech. Univ. of Munich, (1981)

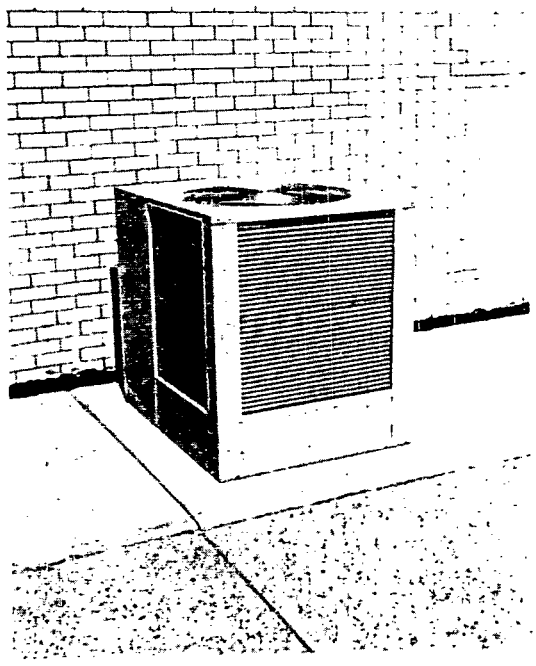

Figure 8 - Photograph of 3 R Ton Prototype

Evaluation of a Commercial Advanced Absorption Heat Pump Breadboard

R. J. Modahl and *F. C. Hayes*
The Trane Company
La Crosse, WI 54601

Introduction

An advanced absorption heat pump program is being conducted by The Trane Company, with support from the U.S. Department of Energy. The overall objective of the program is the evaluation, development, and proof testing of advanced absorption refrigeration cycles which are applicable to residential and commercial heat pumps for space conditioning. The heat pump system is to be direct fired with natural gas, and to use working fluids whose properties are known. Target COP's are 1.6 at 47°F and 1.2 at 17°F in the heating mode, and 0.7 at 95°F in the cooling mode, including the effect of flue losses.

The overall project is divided into three phases. Phase I was the analytical evaluation of advanced cycles, and included selection of preferred concepts for further development. Phase II involved the development and testing of critical components and breadboard version of the selected system. Phase III is the development of a prototype unit and is contingent on successful completion of Phase II.

Phase I was completed in late 1984 and the results were presented at the DOE/ORNL Heat Pump Conference, Washington, D.C., Dec. 11-13,1984. This paper summarizes the results of the Phase II work.

Review of Phase I Results

In Phase I, 24 cycle/fluids combinations were evaluated. Computer models were developed to predict system performance. COP, theoretical pump power, and internal heat exchange were calculated for each system. These results were used as indicators of operating and installed costs to rank the relative promise of each system. The highest ranking systems involved the cycle concepts absorber/generator heat exchange, absorber heat exchange and generator heat exchange, regeneration, and resorption/desorption, in combination with the NH_3-H_2O-LiBr ternary or the NH_3-H_2O binary solution. User economics analyses showed Simple Payback and Internal Rate of Return to be about the same for a highly complicated advanced cycle using the ternary solution and for a relatively simple advanced cycle using the binary solution when compared to a conventional gas boiler and air cooled reciprocating compressor chiller. Therefore, the simpler cycle, which involved absorber heat exchange, absorber/generator heat exchange, and generator heat exchange using NH_3-H_2O was chosen for initial breadboard testing in Phase II. It was planned that the NH_3-H_2O-LiBr ternary and other advanced cycle features, which offer the potential of higher COP but probably at a higher first cost, would be considered later.

Breadboard System Design

A schematic diagram and a Duhring plot of the cycle chosen for Phase II testing are shown as Figs. 1 and 2. A CAD drawing of the breadboard system used to evaluate this cycle is shown as Fig. 3. The advanced components of the cycle are the absorber (Q_{AHE}), absorber/generator (Q_{AG}), and generator (Q_{GHE}) heat exchangers. Fig. 4 is a picture of the breadboard system.

Referring to Figs. 1-3, the direct fired generator is a single burner, 2-pass, fire tube boiler. It is connected through a top opening to the rectifier/stripper column which contains a commercial packing and special liquid re-distributers. A vapor/liquid mixture from the generator heat exchanger is

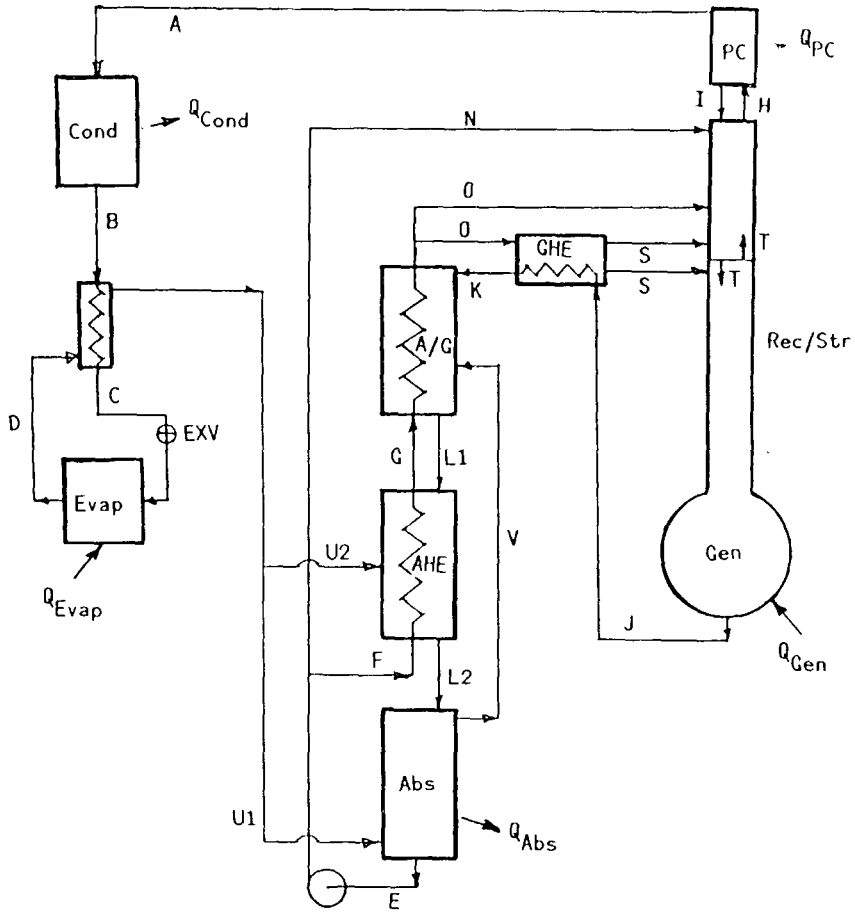

FIG. 1: SCHEMATIC DIAGRAM OF THE TEST CYCLE

fed at a mid-point to the rectifier/stripper column. Additional liquid, rich in NH_3, is fed to the top of the column. Vapor from the top of the column goes to the partial condenser for further enrichment before passing to the total condenser.

The total condenser, refrigerant heat exchanger, and evaporator are not shown in Figure 3 (in the interest of simplicity), although they were installed later in the program. Their designs were not included in the critical objectives of this project.

The hot solution, lean in NH_3, leaves the bottom of the gas fired generator and passes to the generator heat exchanger, which is a counterflow tube-in-tube design. In the generator heat exchanger, heat from the lean solution is used to boil off NH_3 from the solution leaving the absorber/generator heat exchanger.

The cooled lean solution then goes to the absorber/generator exchanger where it absorbs refrigerant as it flows over and down the outside surfaces of helically coiled tubes. The heat of absorption is used to boil off more NH_3 from the rich solution flowing inside the tubes.

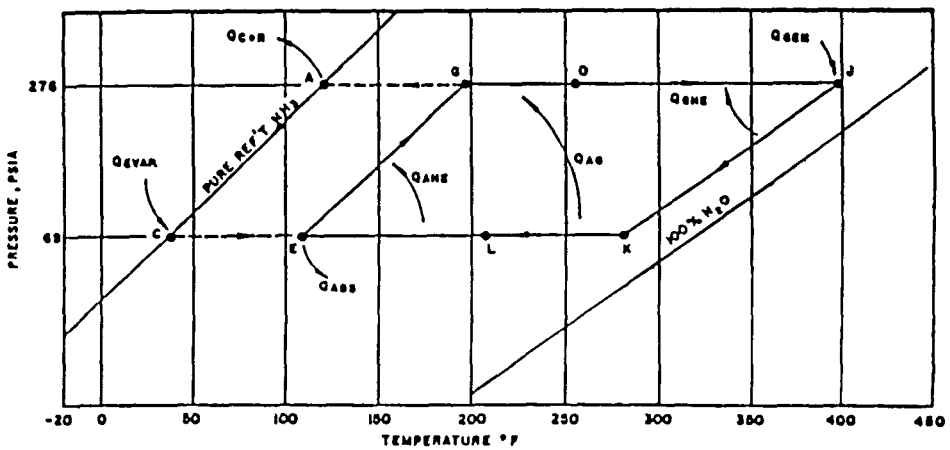

FIG. 2: DUHRING PLOT OF THE TEST CYCLE

The solution leaving at the bottom of the absorber/generator heat exchanger enters at top of the absorber heat exchanger and then flows in series to the water cooled absorber, absorbing refrigerant in each of these exchangers as it flows down the outside of the helically coiled tubes.

Rich solution from the bottom of the water cooled absorber goes to the solution pump where it's pressure is raised to the cycle high side pressure. Some of this solution is sent to the top of the rectifier/stripper column to provide cooling required in the rectification process. The remainder is heated to saturation as it passes up through the absorber heat exchanger. It then passes in series through the absorber/generator and generator heat exchangers where vaporization of refrigerant occurs. This vapor, generated by internal heat exchange, reduces the heating requirements of the gas fired generator and therefore improves the efficiency of the cycle. The resulting vapor-liquid mixture enters at a mid-point of the rectifier/stripper column to complete the solution flow paths.

The nominal design capacity of the breadboard system was 180,000 Btuh cooling (15 tons), and 400,000 Btuh heating. Although this may seem to be rather large for a breadboard, the idea of the rather large capacity was to minimize scale-up problems in Step III prototype designs of commercial equipment.

The water cooled absorber and the absorber/generator heat exchangers were designed and built to conform to the ASME pressure vessel code, Section VIII. Mild carbon steels were used. The generator was designed to conform to Section I. Because Section I does not permit use of stainless steels, acceptable boiler steels were used in the generator build. The basic decision was to accept the potential for higher levels of corrosion in the breadboard direct fired generator rather than going to the problems of obtaining an exemption for some type of Stainless at this time. The tube-in-tube heat exchangers were purchased from vendors and were made from 316 Stainless steels and the packing in the rectifier/stripper column was 316 Stainless as well.

Phase II Test Plan

The approach taken in the test program was to build and test components and the overall breadboard system in a stepwise manner. Selected components were built, installed, and tested for satisfactory performance before more components were added. Separate tests were run on the water cooled absorber, absorber/generator heat exchanger, and the direct fired generator. The main goals of the test program were to confirm our computer predictions of Phase I, demonstrate workable component and system designs, and obtain fundamental data for subsequent product design concept work.

In parallel with the breadboard system design work, limited stability and corrosion testing was done to determine suitable materials for the breadboard system.

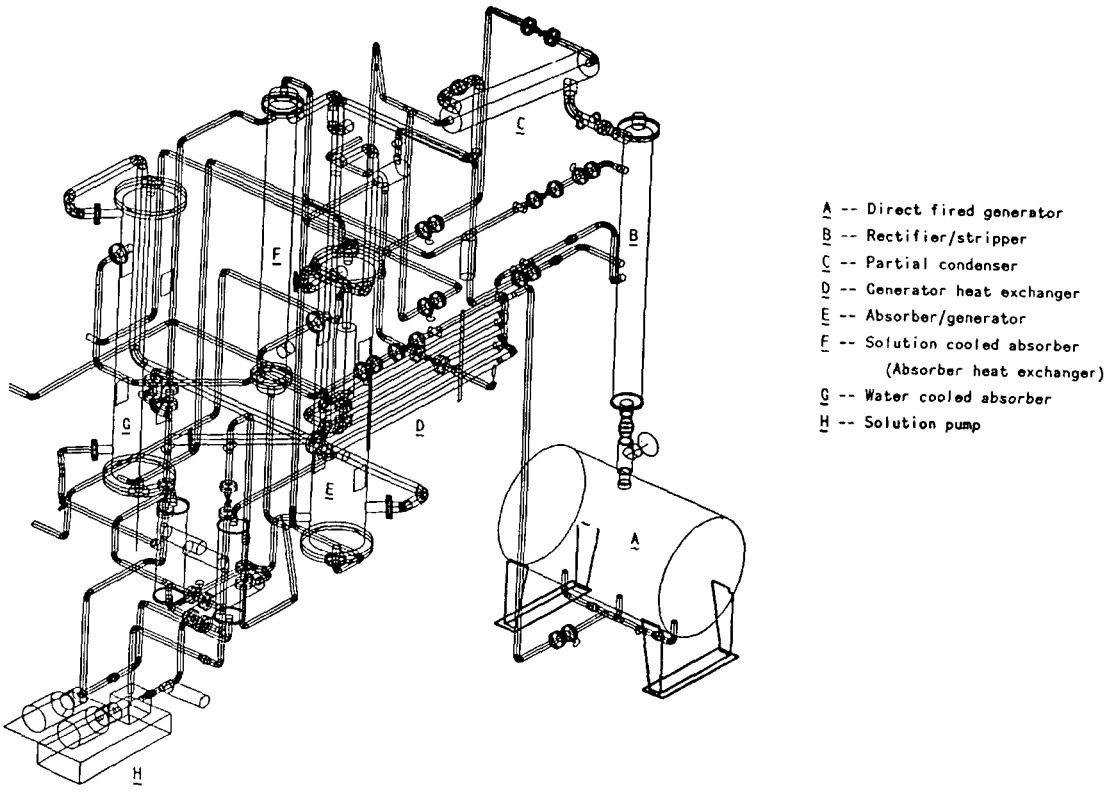

FIG. 3: CAD DRAWING OF THE BREADBOARD SYSTEM

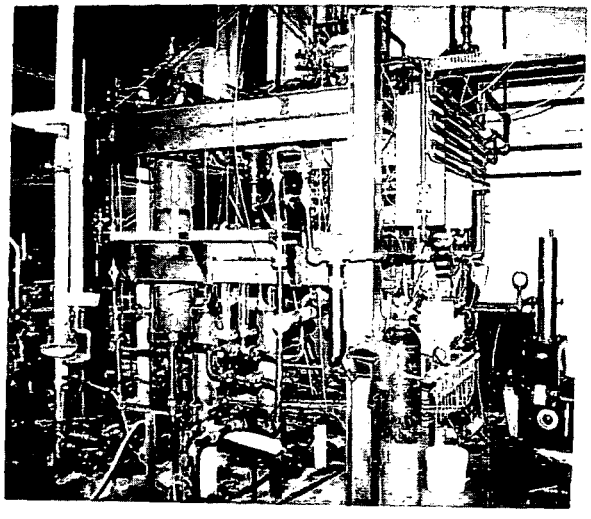

FIG. 4: PICTURE OF THE BREADBOARD SYSTEM

Test Results

Stability and Corrosion Tests

Selected test results are shown in Table 1. Mild carbon steel and Stainless steel showed very low corrosion rates in the ternary NH_3-H_2O-LiBr solution liquid phase at 425°F with Chromate and Arsenite inhibitors and no air present. Both of these metals showed evidence of pitting or blistering when exposed to the vapor phase. Titanium coupons showed no corrosion in either phase. The inhibitors were depleted after 700 hours in the 425/70°F cycling tests with the ternary solution, so periodic replenishment may be needed. Stressed mild steel and weld samples showed no evidence of corrosion or stress corrosion cracking in either the ternary or the binary NH_3-H_2O liquid phases at 350°F. In one test, 11% of a presently used absorption rate additive charge was recovered after cycling at 428°F/70°F for 700 hours. At lower temperatures (212/70°F), virtually all the additive charge was recovered.

Table 1

STABILITY/CORROSION TEST CONDITIONS/RESULTS

	Run No.							
TEST CONDITIONS	14	16	20	32	38	41	43	44
Solution								
NH_3-H_2O-LiBr	x(1)	x	x	x	x	x	x	-(2)
NH_3-H_2O	-	-	-	-	-	-	-	x
Metal coupons								
35 Titanium	-	x	x	-	-	-	-	-
316 SS (3)	x	-	x	x	x	-	-	-
1020 Steel	x(4)	-	-	x(4)	x(4)	-	x(5)	x(5)
Inhibitors								
Chromate	-	x	x	-	x	-	x	x
Arsenite	x	-	-	x	-	-	-	-
Abs. additive	-	-	-	x	x	x	-	-
Test Temps, °F								
Cycled 425/70	x	x	x	x	x	-	-	-
Cycled 212/70	-	-	-	-	-	x	-	-
Continuous 350	-	-	-	-	-	-	x	x
Total time								
Hours	800	800	800	700	700	50	438	438
TEST RESULTS								
Corrosion rates								
Mpy (1020 Steel)	.19	-	-	*(6)	.003	-	0	0
Mpy (316 SS)	.07	-	.001	*	*	-	-	-
Additive								
% recovered	-	-	-	2	11	97	-	-

NOTES

(1) 'x' denotes sol'n, metals, temps, etc involved in the test

(2) '-' denotes non-involvement

(3) in all cases the test vessels were 303 or 316 Stainless Steel with Teflon O-ring gaskets

(4) Steel coupons cut from 'as recieved' material

(5) 'As rec'd', 'stressed', and 'welded' steel samples were all included

(6) Asterisk (*) indicates corrosion not detected; coupons gained weight

Component Tests

The water cooled absorber, absorber/generator heat exchanger, and direct fired generator were tested separately to confirm satisfactory performance before completion of the overall breadboard system. For both the component and overall system tests, three secondary water (or Glycol) loops were built and used to provide the required component and system loadings.

The most critical component of the advanced cycle concept is the absorber/generator heat exchanger. In the breadboard, the same heat exchanger configuration was used for the water cooled absorber. The absorption side heat transfer coefficient was determined from the water cooled absorber tests because water side coefficients were reasonably well known and also larger than absorber side coefficients. The absorption side coefficients thus determined are correlated in the form of Nusselt vs. Reynolds numbers in Fig. 5. Design Reynolds Number was 300 to 500 for the NH_3-H_2O breadboard cycle. The measured absorption side heat transfer coefficients agreed closely with predicted values.

The absorption side correlation shown in Fig. 5 was used to reduce the data from the absorber/generator heat exchanger tests. The resulting generator side heat transfer coefficients are correlated in the form of j-factor vs. Reynolds Number in Fig. 6 where Reynolds Number is based on the generator side inlet conditions. The generator side Reynolds Number at nominal design capacity for the NH_3-H_2O breadboard cycle was about 2500 and about 700 for the ternary cycle. The experimental j-factors shown in Fig. 6 are well below predicted values; about 35% low at nominal design capacity for the NH_3-H_2O breadboard cycle. As a result, the overall heat transfer coefficient for the absorber/generator exchanger at the design point was more than 25% below design value.

A possible explanation for the low performance of the absorber/generator exchanger is that some of the tubes were ineffective due to solution recirculation resulting from low velocities and unfavorable hydrostatics. The exchanger design consisted of several helically wound tubes in parallel through which the generator side solution flowed upwardly. In operation, heat transferred from the absorber side acted to sensibly heat the generator side solution and vaporize some refrigerant. But at the low design solution flowrates, the hydrostatic pressure difference on the tubeside exceeded the velocity pressure drop so that liquid solution could have flowed downward (recirculated) in some of the tubes. Hence, only a fraction of the tubes may have been effective on the generator side. In a proposed redesign, longer lengths of fewer coiled tubes in parallel would be used to increase velocity and improve the heat

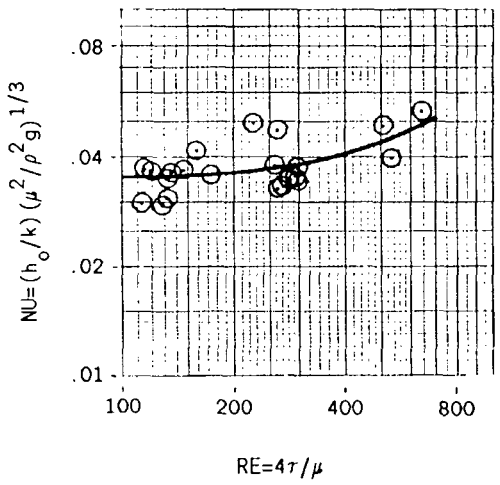

FIG. 5: CORRELATION OF ABSORPTION SIDE HEAT TRANSFER COEFFICIENTS

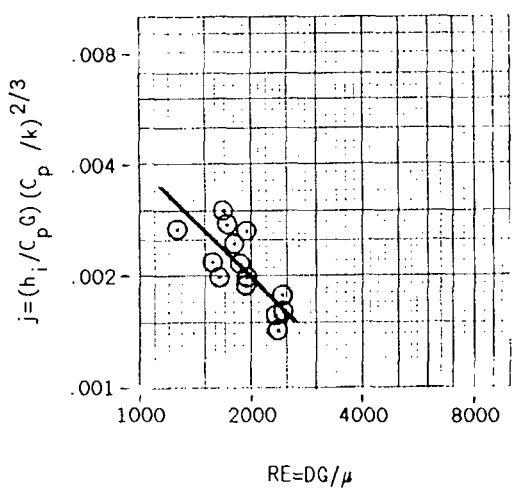

FIG. 6: CORRELATION OF GENERATOR SIDE HEAT TRANSFER COEFFICIENTS

transfer coefficient. Means would also be incorporated to assure velocity pressure drop exceeds hydrostatic pressure difference over the range of design flow conditions.

Although the absorber/generator exchanger performance was well below expectations, it was decided to proceed with overall system assembly and test. It was considered better to proceed with overall breadboard tests using the existing absorber/generator exchanger, than to accept the time delay and expense required to redesign (meeting ASME pressure vessel code), build, and install an improved component. The other components and overall cycle performance could still be measured and compared with computer predictions.

Separate tests on the direct fired generator before installation in the breadboad involved primarily burner adjustment to get proper gas and air flowrates for good combustion efficiency. During build of the direct fired generator, thermocouples were attached to the solution side of the firetube wall at potential hot spots. The generator was designed with liberal firetube surface area so that the maximum difference between wall temperature and leaving solution temperature would not exceed 25°F. Measurements made during breadboard system tests showed the average difference between the highest measured wall temperature and the leaving solution temperature was about 5°F, with the maximum difference recorded being 5.6°F. The measured experimental combustion efficiency ranged from 81 to 84%. A combustion air pre-heater was installed late in the test program which was planned to raise the efficiency to about 87%. Test problems prevented confirmation of the 87% efficiency level.

Overall Breadboard System Tests

Design capacities were not achieved with the breadboard system because flooding problems in the rectifier/stripper limited solution circulation rates to about 2/3 of design rates. This limited heating capacity to about 60 to 70% of nominal design. Furthermore, rectifier modifications designed to reduce flooding at the expense of COP were of little benefit in increasing capacity, and prevented demonstration of design COP in later testing at 2/3 design capacity.

Typical breadboard cycle test results are shown in Table 2. Test conditions varied considerably due to control problems discussed later, but were reasonably close to design rating conditions. The table shows good agreement between experimentally determined COP's and computer model predictions at the lower generator temperatures (Runs 3-19, 3-25, & 3-27). The computer predictions were based on a model that represented the cycle after rectifier modifications had been made to reduce flooding. At higher generator temperatures, corrosion product non-condensables reduced cycle efficiency to about 85% of computer predictions (Runs 3-28 & 3-35). The non-condensables are believed to have originated in the vapor phase areas of the direct fired generator. At high operating temperatures, the rate of non-condensables production was too high to be successfully removed by the breadboard purge equipment.

Computer simulations were also made with a model representing the original breadboard configuration. The model assumes no rectifier flooding or non-condensable problems. With these assumptions and the use of component

TABLE 2

TYPICAL BREADBOARD CYCLE TEST RESULTS

Run No.	3-19	3-25	3-27	3-28	3-35
Cond. Sat'n Temp., °F	100	93	101	102	103
Evap. Sat'n Temp.	25	33	10	31	38
Abs. Lvg Sol'n Temp.	101	104	109	107	107
Gen. Lvg Sol'n Temp.	326	342	339	360	360
Thermal COP, test	1.63	1.87	1.59	1.54	1.54
COP, Comp. model	1.70	1.86	1.55	1.76	1.83
COP(test)/COP(model)	.96	1.0	1.03	.87	.84

performances based on actual test data, the model predicts project COP goals could have been achieved at 2/3 design capacity. The absorber/generator heat exchanger is the limiting component in these simulations.

Because of corrosion problems with the binary solution, it was decided to not test the ternary in this set-up.

Problems

The major problems encountered in the experimental program were rectifier flooding, system control, and boiler corrosion at the high temperature operating conditions.

As indicated previously, rectifier flooding limited solution circulation rates to about 2/3 of design values. Correcting this problem would have required a complete redesign and build of the rectifier/stripper component, requiring several months of time. The decision was made not to make this modification because sufficient fundamental data could be obtained on the components and overall system with the existing rectifier/stripper for later product design concept work.

The system was designed with automated control of the three glycol loops to facilitate obtaining steady state operating conditions at specified test conditions. However, the control problem was more difficult than originally anticipated and efforts to achieve automatic control of the system were eventually abandoned. Manual setting of test conditions was quite time consuming and limited the amount of data which could be taken.

Non-condensables (principally hydrogen corrosion product) required frequent purging of the system and further delayed testing. The non-condensables are believed to have originated primarily from the direct fired generator, and redesign using stainless steels should reduce this problem.

Modified Product Design and Performance Prediction

The preliminary Phase I product design was modified based on the findings of Phase II. This included a change in the basic cycle so that the solution flows in series through the absorber heat exchanger and the water cooled absorber instead of in parallel. This provided a larger mean temperature driving force so that less surface area was required in the absorber heat exchanger. The experimental tests showed that, except for the absorber/generator heat exchanger, the breadboard component's overall heat transfer coefficients were as good or better than had been predicted in Phase I. This allowed a reduction in the heat transfer surface area required for some cycle components. The effect of these changes was a 50% reduction in estimated amount of absorption side component heat transfer surface area required in the modified design. However, the corresponding material savings was partially offset by more rectifier material required to avoid flooding. The net result was that a modified design with the same predicted COP's and parasitics required less heat transfer surface and less overall material.

User Economics Update

An update of the user economics analysis conducted in Phase I is summarized in the following.

* The Phase II modified product design provides the same COP's and requires the same parasitics, so it's energy requirements are the same as reported in Phase I.

* Manufacturing costs for the absorption side components and accessories (materials, labor, and overhead) have increased 30% since the time of the Phase I estimate. Coil costs (for air-to-glycol secondary loops) have increased 10% in this time. The combined effect of these cost increases and the material reductions described in the previous section is a reduction of about 10% in estimated product cost for the modified design.

* The first cost and operating cost of competing equipment is improving.

* To show the effect of energy cost changes, the results of an up-date of the user economics analysis conducted in Phase I for the Chicago apartment application are shown in Table 3. For this example electric demand charges are up 77%, off-peak electricity is down 37%, and natural gas is down 22% since the time of the Phase I analysis. The effect of these changes had a negligible effect on simple pay-back, reducing it from 2.2 years in the original analysis to 2.15 now.

* On balance, user economics predictions for the absorption heat pump have not changed significantly since the Phase I analysis.

Conclusions

The primary conclusions of this investigation were as follows:

* The absorption cycle incorporating absorber heat exchange, generator heat exchange, and absorber/generator heat exchange and NH_3-H_2O as the working fluid can achieve the efficiency goals of the

TABLE 3

RESULTS OF USER ECONOMICS ANALYSIS

BASIS: Apartment building in Chicago with Commonwealth Edison rate structure, 1987 energy costs.

INPUT

System	Conventional	ABS4
Size, tons cooling	155	155
Installed cost, $/ton	490	678
Heating COP, 47F	.8	1.61
, 17F	.8	1.37
Cooling COP, 95F	3.0	.80
, 115F	-	.64
Parasitics, KW/Ton	.18	.283

OUTPUT(1)

Ann. elec. consump., 10^3 KWH	1022	1017
Ann. gas consump., 10^3 therms	83.1	64.5
Elect cost, energy, 10^3 $	42.3	40.4
, demand, 10^3 $	26.6	22.8
Gas cost, 10^3 $	35.5	27.6
Total utility cost, 10^3 $	104.3	90.8
SPB, yrs.	-	2.15

(1) The annual electric consumption numbers include everything for the building, not just HVAC equipment.

project for commercial product applications. Although operational problems prevented demonstrating the project goals with the breadboard system, enough data was obtained on component performance to assure that design goals could be achieved with breadboard redesign.

* A feasible design was demonstrated for the most critical component of the cycle, the absorber/generator heat exchanger.

* Absorption Heat Pump economics continue to show promise in Northern climate applications.

Future Development Work

The results of our Phase II work has provided the information required to develop good product design concepts. The next step in the overall project is a product design concept and market study to provide justification for product development.

Development and Proof-Testing of Advanced Absorption Refrigeration-Cycle Concepts—Phase II

R. C. Reimann
United Technologies-Carrier
Syracuse, NY 13221

Gorken Melikian
United Technologies Research
East Hartford, CT 06108

Background

Under contract with the U.S. Department of Energy, Carrier Corporation has been investigating the feasibility of a gas-fired, advanced cycle absorption heat pump with the ultimate goal of developing equipment for the commercial market.

In Phase I of the contract an optimum cycle and working fluid pairs were identified. A patented Carrier enhanced dual loop (CEDL) was identified with two separate fluid systems. Lithium bromide/water would be employed in the upper, high temperature loop and several new ternary and conventional fluids were identified for the lower loop. The cycle (Fig. 1) is unique in that the two loops are double coupled at two intermediate temperatures yielding high efficiencies while maintaining the flexibility to meet a variety of applications.

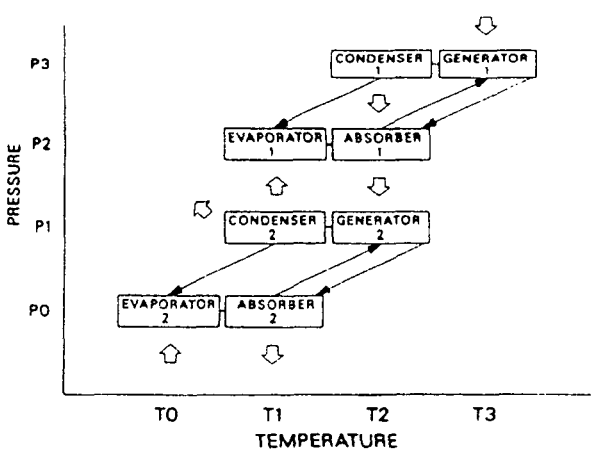

Figure 1. CEDL AHP cycle

Figure 2 illustrates a suggested machine configuration consisting of five shells and the thermal communication between the two separate fluid loops.

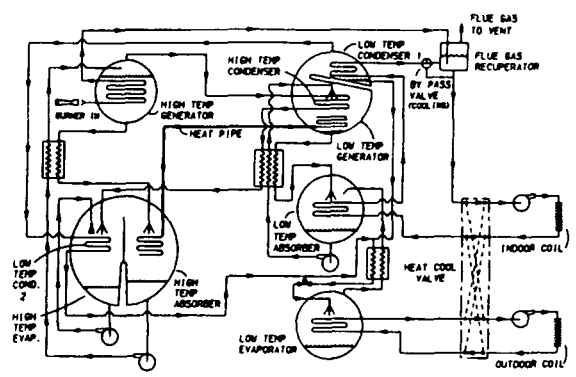

Figure 2. CEDL schematic

This paper summarizes the results of the work performed to date under Phase II of the DOE program. The Phase II objective is to design, fabricate, and proof-test a natural gas-fired absorption heat pump (AHP) with an efficiency level substantially higher than present day state-of-the-art equipment. To achieve these objectives, Carrier investigated the performance of the candidate Phase I fluids (lithium bromide:zinc bromide/methyl alcohol-MEOH or lithium bromide:water methylamine-MMA) as well as high concentration formulations of the conventional LiBr/H20 mixture for high temperature, upper loop use. These results were compared with several existing fluid candidates including ammonia/water.

The objective of the work completed to date is to provide currently unavailable technical data on the (1) coupled heat and mass transfer process in the AHP absorber; (2) fire tube wall temperature distribution in the gas-fired generator; (3) chemical and thermal stability of the selected refrigerant-absorbent fluid systems; (4) design optimization of the CEDL system for selected applications; and (5) fabrication of a breadboard system.

Absorber Studies

Absorber tests were conducted to determine the heat and mass transfer performance of selected fluids and absorber geometries. In order to obtain this information, a test facility was designed to emulate the operation of an absorber of predetermined design. The baseline approach was to test a "small-scale" version of a full size absorber and to extrapolate these test results. This approach was augmented by a combined experimental/analytical procedure based on an absorber performance model developed by UTC.

The small scale absorber (minisorber, shown in Fig. 3) simulates a full size machine tube diameter, spacing and bundle depth. Refrigerant vapor and strong absorbent were supplied on a continuous basis from an electrically heated vapor generator (desorber). Instrumentation and regulated cooling water provided a means to obtain heat and mass transfer rates. A glass front panel enabled observation of the absorption process and characterization of the tube wetting, distribution, presence of noncondensibles, etc.

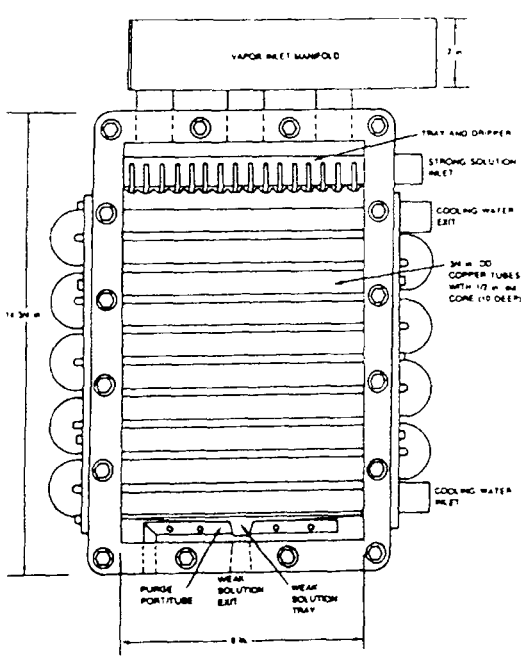

Figure 3. Minisorber apparatus

LiBr/H20 Tests

Testing was organized into two efforts; (1) calibration of the minisorber apparatus and the UTC absorber performance model and (2) measurement of absorber performance for the fluids of interest. The purpose of calibrating the minisorber with a commercial LiBr/H20 fluid system (LiBr with appropriate corrosion inhibitors and a heat/mass transfer enhancement additive) was to demonstrate the ability of the minisorber to duplicate the performance levels achieved with full scale commercial equipment. A second objective was to provide absorber performance test data over a wide range of operating conditions with which a statistically meaningful correlation can be made. These data were used to confirm and validate the UTC absorber model (AAPPP) and to subsequently establish the effective solution diffusivity enhancement for the LiBr/H20 fluid system with additives.

Performance correlation. The diffusivity enhancement factor (Em) which "best" represents enhanced LiBr/H20 fluid performance was established as that value which minimizes the error between measured and calculated heat transfer. Figure 4 shows the results of this effort and indicates that the standard deviation of the heat transfer error ((Q Measured - Q Calculated)/Q Calculated) is minimized at an Em of 3 (Em = 1 represents solution diffusivity without heat/mass transfer additives). This result implies that the enhanced LiBr/H20 fluid diffusivity was increased by a factor of three due to the additive. This result is consistent with previous Carrier data, unrecorded minisorber test data and visual observation of the minisorber performance with unenhanced (pure) LiBr/H20.

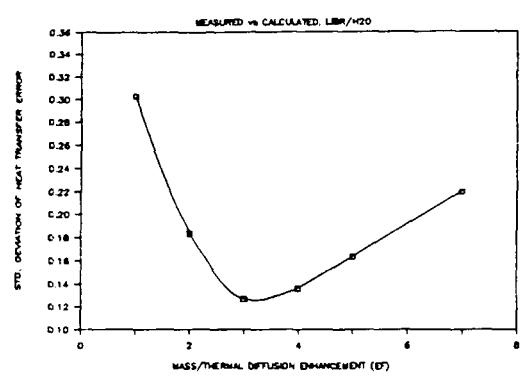

Figure 4. Standard deviation of absorber heat transfer error

The comparison of measured data and model predictions was made for cooling water temperature change (shown in Fig. 5), heat transferred, mass transferred, and absorber outlet solution subcooling.

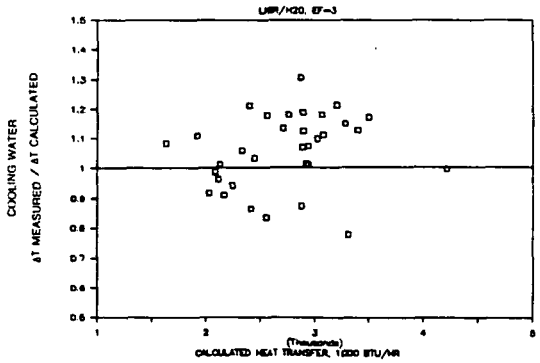

Figure 5. A comparison of measured and calculated absorber cooling water temperature increase

Typical measured values of absorber performance expressed in terms of the weak solution subcooling were 2-10 C and mass transfer effectiveness were 80 to 90 percent. Heat transfer film coefficients ranged from 200 to 550 Btu/hr/ft2/F. Overall, the ability of the UTC absorber model to predict enhanced LiBr/H20 absorber performance was within the experimental data error and considered acceptable for use as an absorber design tool.

Ternary Fluid Tests

The second part of the testing was directed at establishing the absorption characteristics of two alternative ternary fluids: lithium bromide:water/monomethylamine (MMA) and lithium bromide:zinc bromide/methanol (MEOH).

Minisorber tests were conducted over a range of operating conditions, surfactants and tube surface variations. The mass/transfer rates achieved were considerably lower than those for enhanced LiBr/H20. Accordingly, the use of these fluids is a falling film absorber would require unacceptably large surfaces. Although other direct contact absorber configurations may be designed, there are several alternative fluids with acceptable absorber performance (e.g., NH3/H20). Thus, detailed design of a breadboard CEDL with MMA and MEOH was discontinued. Detailed absorber model (AAPPP) calculations indicate a comparison of the performance of different absorber fluids cannot be made without evaluation of the overall cycle in which the fluid is utilized. Nevertheless, an absorber heat transfer film coefficient (Ho) is often used in simplified absorber design procedures. Thus, a comparison of the familiar Ho values achieved in all of the minisorber tests conducted in this program indicates Ho values for MEOH are less than half that of LiBr/H20 and Ho values for MMA are less than one-fifth that of LiBr/H20.

Generator Studies

Small scale generator (minigenerator) tests were conducted with an apparatus which simulates the operating conditions of an AHP vapor generator. Specifically, this apparatus (shown schematically in Fig. 6) provided controlled solution and hot gas flows to the fire tube-in-shell type generator. The test apparatus includes a two-pass fire tube in counterflow with the absorbent solution. A small water-cooled condenser provided the vapor removal load along with a water-cooled solution heat exchanger to maintain generator inlet conditions. The objectives of the tests were to: (1) determine wall temperature uniformity of the generator fire tube, (2) record maximum wall and solution temperatures, (3) measure heat transfer performance, and (4) validate the UTC generator design procedure.

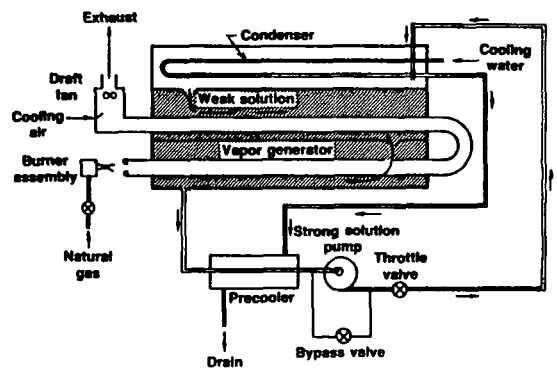

Figure 6. Minigenerator test apparatus schematic

In order to provide baseline performance estimates for the generator, a series of tests were performed over a range of fuel input rates with bare tubes (unenhanced) in each pass. From these data, the bare tube heat transfer characteristics could be modeled using well known heat transfer techniques. As a complement to the bare tube data, tests were also conducted to provide gas-side enhancement effects by installing twisted metal tapes (turbulators) to increase inside turbulence, a technique used extensively by Carrier.

Tube wall uniformity was measured by thermocouples placed longitudinally over the first 32 inches of the 48 inch first pass fire tube. The measured temperature profiles showed no sharp peaks (hot spots) with a maximum temperature of less than 15 F above the outlet bulk strong solution. Accordingly, solution maximum temperatures can be approximately 15 F below the maximum allowable temperature determined from thermal stability and metal corrosion tests.

An important aspect of the generator test program was to calibrate and validate the UTC gas-fired generator prediction model (GASGEN). Confirmation of the validity of this model is illustrated in Fig. 7 wherein a comparison is made of the measured heat transferred with that calculated for the same conditions. Agreement within 10 percent for both bare tube and enhanced tube tests was demonstrated thereby promoting confidence in the use of the GASGEN model as a design tool for full scale generators.

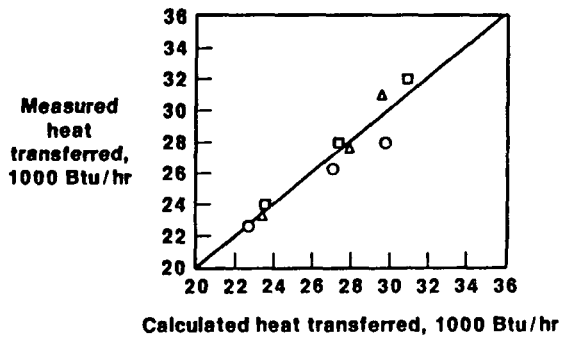

Figure 7. A comparison of measured and calculated generator heat transfer for LiBr/H20
bare tubes
2/3 turn/ft turbulator
1 turn/ft turbulator

Overall heat transfer coefficients for each test indicate bare tube gas film coefficients were on the order of 4 Btu/hr/ft2/F, while those tests having turbulators showed 50 percent higher performance. Accordingly, the use of a simple metal tape twisted turbulator will significantly reduce generator area.

Chemical/Thermal Stability Studies

The achievement of a stable absorption system (fluid/materials) requires prevention and control of (1) direct chemical attack on the containing vessel material, (2) catalytic acceleration of absorbent-refrigerant breakdown by vessel materials, (3) galvanic reactions between vessl components due to fluid interactions, and (4) concentration cell corrosion of vessel components due to peculiar fluid compositional changes.

Although some fluid/vessel material combinations have natural high stability, many combinations of interest for advanced AHP systems require inhibition by addition of a corrosion suppressant. Therefore, the corrosion test undertaken included evaluation of corrosion stabilizing inhibitors. Additionally, it is known that heat transfer additives (surfactants) are frequently required to improve the absorber performance, therefore measurement of their stability was made.

Fluid/materials compatibility and corrosion tests were conducted for three absorbent/refrigerant fluid systems: (1) LiBr/H20, (2) LiBr:ZnBr2/CH3OH and (3) LiBr:H20/CH3NH2.

Corrosion Tests

The materials of construction selected in this study were DHP copper, 90-10 CuNi, 304 SS, A414 mild steel, and Duplex SS 2205. Corrosion rates of these materials were evaluated at typical generator operating conditions by measuring the weight loss of metal coupons mounted in special corrosion test vessels and also by electrochemical methods.

For purposes of comparison, corrosion rates of 100 mdd (milligrams/dm/day) or greater are generally considered excessive. In commercial LiBr systems, corrosion rates of 10 to 100 mdd for mild steel can be obtained by controlling the alkalinity of the fluid system. Addition of commercial (chromate) inhibitors can reduce the corrosion rate to less than 10 mdd. For the dual loop AHP system under consideration, temperatures and concentrations are much higher than any previously considered commercial LiBr/H20 system; therefore, higher corrosion rates are expected and improved corrosion control will be required.

LiBr/H20 tests. Two LiBr/H20 corrosion tests were performed, (1) short term tests of up to seven days duration, and (2) long term tests of up to 46 days. The short term tests (conducted with two inhibitors and five materials of construction) were used to identify appropriate test procedures and acceptable inhibitor/material combinations.

The seven day corrosion studies, demonstrated that the corrosion rate of mild steel could be controlled to 65 mdd in 75 percent LiBr at 225 C using a proprietary fluid system, designated as Carrier Carrene 16 DL. Often, in cases where an inhibitor is used, the initial corrosion rate will be high and then drop off as a protective coating builds up on the surface of the steel.

To investigate this effect, several long term tests were conducted with mild steel coupons. A composite of these long term corrosion data results and previous Carrier test data are presented in Fig. 8. These results show the corrosion rate generally decreases with test duration and increases with the temperature/concentration levels. For the most severe conditions of 227 C/75 percent LiBr a corrosion rate of approximately 30 mdd was measured after 46 days and a correlation of the test data indicates corrosion rate should continue to decrease with time. Accordingly, the Carrene 16 DL inhibitor solution system appears to acceptably reduce mild steel corrosion rates for use in the dual loop AHP generator.

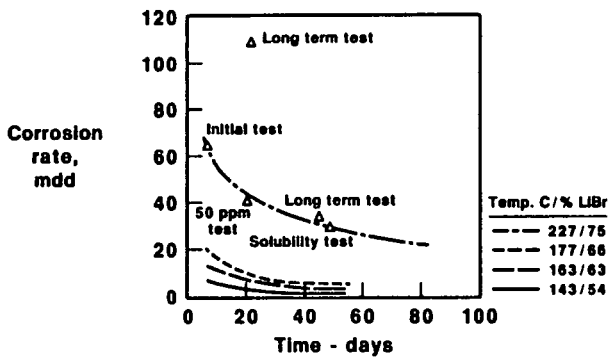

Figure 8. The corrosion rate of mild steel in Carrene 16 DL (inhibited LiBr solution)

Ternary tests. The corrosion tests for the MEOH system were conducted for a mixture of 35 percent LiBr/ZnBr2 in a 2:1 mole ratio and 65 percent CH3OH on a weight basis. These tests, conducted at 150 C for seven days, indicated corrosion rates of all the metals tested were below 30 mdd and therefore this fluid system is acceptable without any inhibitor.

The corrosion tests for MMA system were conducted for a mixture of 70 percent LiBr/H2O (in a 3:2 mole ratio) and 30 percent CH3NH2 on a weight basis. These tests, conducted for mild steel, 90-10 CuNi, 304 SS, DHP, Cu, and 2205 SS at 125 C for seven days, indicated corrosion rates were below 20 mdd and therefore this fluid system is acceptable without any inhibitor.

Fluid Stability Tests

Fluid stability evaluations were conducted for the fluids known to be susceptible to decomposition at the conditions encountered in the advanced AHP application. Specifically, breakdown rates were measured for the mass/heat additives and the alcohol containing LiBr:ZnBr2/CH3OH fluid system.

Mass/heat transfer additives. Mass and heat transfer enhancing additives significantly improve the commercial viability of LiBr absorption systems and have been found to be necessary in the Carrier advanced dual loop AHP. However, the additives may be unstable at extreme temperatures. To identify an acceptable additive, the stability characteristics of two known mass transfer additives were measured at the extreme operating conditions projected for the dual loop AHP. The two compounds tested were 2-ethyl-1-hexanol (referred to herein as hexanol) and phenyl methyl carbonal (referred to herein as PMC).

Previous Carrier tests indicate that hexanol begins to decompose somewhere between 167 C and 232 C forming both 2-ethyl-1-hexaldehyde and 2-ethyl-1-hexene. A mixture of 0.5 percent hexanol in the Carrier Carrene 16 DL solution system was heated for seven days at 227 C in a Ni plated steel vessel containing coupons of A414 steel, Cu, 90/10 Cu/Ni and 304 SS, in both the liquid and vapor phases. Approximately 7 percent of the original hexanol charge decomposed into 2-ethyl-1-hexaldehyde. Accordingly, the acceptability of hexanol for the dual loop AHP application will depend on the final AHP design (generator peak temperature, materials selected, and time at temperature) and the effect of 2-ethyl-1-hexaldehyde on system performance. These issues will be evaluated in a later task of the program.

Phenyl methyl carbinol, an alternative to hexanol, was tested in the same fashion as hexanol. Analysis of the reaction products of PMC indicated that PMC decomposed completely at 227 C and therefore is unacceptable for use at the extreme conditions encountered in the dual loop AHP.

The stability tests to date indicate acceptable dual loop AHP systems with LiBr/H2O systems can be designed with hexanol as the additive by proper selection of the generator material and purging of the decomposition products.

Methanol. The LiBr:ZnBr2/CH3OH system was tested for thermal stabiity at 100 C, 130 C and 150 C. In each case the formation of dimethyl ether, which results from a dehydration of CH3OH, was seen in the gas phase analysis after four days. Although the loss of methanol is not a problem, the formation of ether which has a high vapor pressure can be a concern.

The test data indicate methanol decomposition rates become unacceptable (over 0.1 percent/yr) at temperatures above 130 C. This result is consistent with the other research findings. Although a maximum generator temperature of 130 C would not significantly limit the use of MEOH in lower temperature cycles, this fluid has poor mass transfer performance in a falling film absorber (described earlier). Accordingly, MEOH systems would require cycle compromises necessitated by incorporation of high pressure loss absorber configurations.

CEDL Design

Concurrently with the previously described fluid physical and chemical studies, a computer design code was developed enabling the performance evaluation of the various fluid combinations at the DOE target points (47 F, 17 F heating and 95 F cooling) in the dual loop configuration. The results of the previous

testing and thermodynamic property data, were used to develop design specifications for both a breadboard and commercial machine configurations.

Using a combination of analytical and experimental tools, optimum CEDL designs have been identified for alternate applications such as building heating and cooling, industrial process heating and cooling, refrigeration and space cooling. The resulting projected performance levels for these CEDL's are substantially above the DOE targets as shown below.

CEDL Fuel COP

	DOE Target	Dual Loop
Heating		
47 F (8.3 C)	1.6	1.8-2.1
17 F (-8.3 C)	1.2	1.7-1.8
Cooling		
95 F (35 C)	0.7	0.9-1.5

CEDL fuel COP's assume combustion air preheating and flue gas recuperation. In addition to the higher performance potential, the CEDL cycle has unmatched design flexibility which allows its adaptation to numerous alternative applications by appropriate selections of fluid pairs and adjustment of operating conditions.

Breadboard AHP Fabrication

The upper, or high temperature loop of the CEDL, is being fabricated as a stand alone breadboard (Fig. 9) in order to facilitate testing, modification, and burner evaluation.

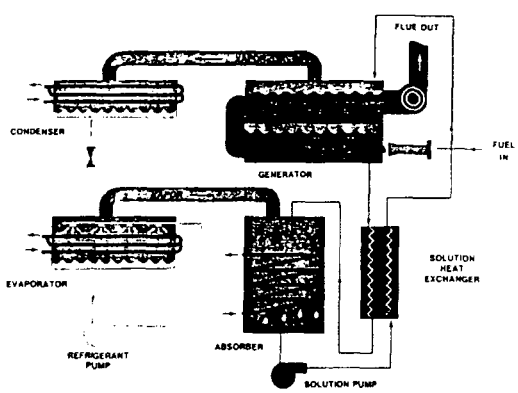

Figure 9. CEDL upper stage breadboard unit

Secondary fluids communicate with the evaporator, absorber and condenser and allow independent control of inlet conditions thus eliminating the influence of lower loop design on the testing and evaluation of the upper loop. Once the upper loop has been qualified and fully characterized, the lower loop will be added to complete the CEDL configuration. The major CEDL breadboard components have been fabricated.

The generator is a shell-tube configuration with a forced draft exhaust blower and either an "in shot" or radiant burner. As in the minigenerator study, the lithium bromide solution flows counterflow to the flue gas.

The absorber is a multiple row, helical coil with a single spray nozzle distributing solution in a falling film over the tubes. This design was chosen in order to more closely scale down a commercial size absorber bundle while maintaining the proper tube wetting and flow.

The absorber is close-coupled to the evaporator which is also a sprayed, falling film design. The condenser, normally would be inside of the lower stage generator, however, for the breadboard unit, a separate shell and tube bundle was employed to allow stand alone testing of the upper stage.

The remaining upper loop components including a flat plate-frame solution heat exchanger (selected on the basis of its low pressure drop and high effectiveness) and appropriate accessories, such as the solution dilution purge circuiting have also been fabricated. Testing of the CEDL components has been completed. Testing of the upper loop breadboard over a range of conditions which simulate a variety of applications and configurations will be initiated in early 1988. Future activities shall include fabrication of a lower loop of the CEDL, integration of the two loops, and testing of the complete CEDL.

Absorption Enhancement Research and Related Diagnostics*

H. Perez-Blanco, M. R. Patterson, D. T. Bostick
and *L. N. Klatt*
Oak Ridge National Laboratory
Oak Ridge, TN 37831

Abstract

An understanding of the absorption process and of the techniques that can be employed for its enhancement is an important step in the development of the technology. This paper reports on ongoing experimental efforts toward developing that understanding, as well as on related research already completed in the area. The experimental apparatus under construction is described, with the techniques to be employed. Absorber performance data analysis requires accurate property values in the form of computer routines. The routines developed to date are described here. A brief status report of the development of a fiber optics instrument, which will monitor concentration at different absorber locations, is also included.

Introduction

Absorption machines are essentially a combination of heat/mass exchangers.[1] The effectiveness of those exchangers determines the capacity and operating temperatures of the machine. One component in particular, the absorber, often has a strong bearing on the overall performance of the units. This is so, because the function of the absorber is to draw refrigerant vapor from the evaporator into the working solution, rejecting heat in the process. Thus, the operating temperature (and consequently the pressure) of an adequately sized evaporator, for which considerable design experience exists, is a function of the capacity of the absorber. Unless the absorber can handle the design refrigerant flow, the evaporating temperature will raise until all the refrigerant can be absorbed, thus hampering machine performance. This is not to say that other components do not offer challenging design and development problems. However, the temperature gradients available for heat transfer tend to be lower in the absorber than in the generator or the condenser, and the lower temperature levels tend to increase the viscosity of the solution in the absorber. In relative terms, the absorption process tends to be the most difficult transport operation taking place in absorption machinery.

Over the years, designers have dealt with absorber performance (or lack thereof) in various ways. Initially, the problem has been to downsize physically large absorbers to meet aesthetic and cost reduction requirements. Thus, ejectors driven by hot solution have been installed to boost the refrigerant pressure in the absorber;[2] a variety of absorber configurations, ranging from falling film[3] to premixing followed by absorption inside vertical tubes,[1] has been proposed or adopted. The most persistent problems seem to have arisen in lithium-bromide units at high salt concentrations, with absorbers in the falling film configuration. Special tube surfaces,[4] as well as additives,[5] have been proposed or employed to enhance the transport process.

The development of advanced cycles[6] has forced a redefinition of the problems as operating ranges unexplored before come into use. Advanced cycles generally have stringent capacity requirements over well-defined temperature ranges. These requirements multiply the designer's challenges, as he must deal with indefinite transport properties without benefit of past experience.

This background suggests that an understanding of absorber performance and of a means to enhance the absorption process is a worthwhile long-term undertaking. To gain this understanding, it was deemed appropriate to study the absorption process experimentally under conditions as close as possible to real operating ones. To this end, two experimental apparatus, one for ammonia-water and one for lithium-bromide water solutions, have been designed and are under construction. Private industry expert consultation was sought and incorporated into the design apparatus.[7] This paper outlines the design, as well as the techniques for data analysis that have been developed so far.

Very early in this effort it was ascertained that two broad areas needed attention for the successful completion of the study. One was that of transport and equilibrium properties, and the other was that of instrumentation. Data analysis of experiments requires knowledge of the property values of the working fluids. Computer routines giving these values are being developed. The property values given in the routines reflect the latest findings of Macriss et al.[8,9] In the area of instrumentation, a concentration measuring device requiring no removal of fluid for sampling was deemed useful for the work. The status of that instrument, which employs fiber optics and advanced electronics, is summarized here.

Experimental Apparatus

The intent of the experiment is to study absorber performance under realistic conditions, such as those encountered in actual operation of the machines. To this end, the experimental loops have the components shown in Fig. 1. Powered by electric heaters, the generator serves to boil off refrigerant, which is then expanded

*Research sponsored by the Office of Buildings and Community Systems, U.S. Department of Energy under Contract DE-AC05-84OR21400 with Martin Marietta Energy Systems, Inc.

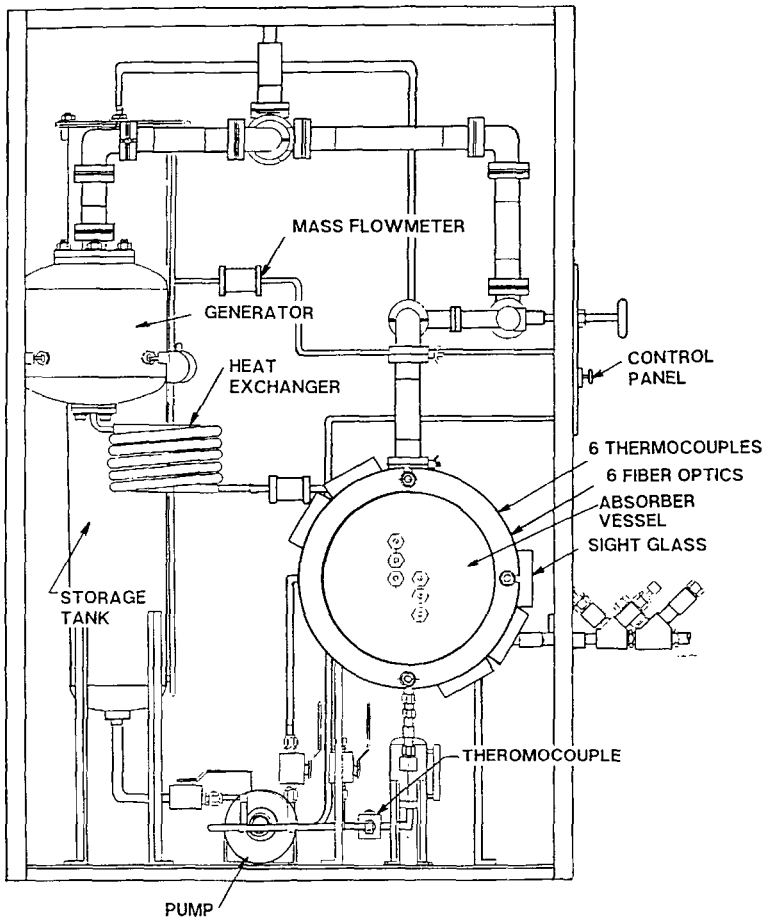

Fig. 1. Schematic of heat and mass transfer test apparatus.

into the absorber, where it is absorbed into the solution. The solution exiting the generator goes through a heat exchanger, where the solution temperature can be reduced to a desired value. From the generator the solution flows into the absorber, is collected in a small sump tank, and is returned to the generator by a pump. High generator pressure is relied upon to drive the solution from the generator to the absorber, as opposed to gravity. This solution was adopted to overcome the high pressure drop of the mass flowmeters. The storage tank serves to accumulate solution and or refrigerant for concentration control and during periods when the absorber is down. A summary of the operating conditions is shown in Table 1, with characteristics of the instrumentation for the ammonia-water loop. Similar characteristics apply to the lithium-bromide-water loop, and in both cases construction is 304L stainless steel.[10]

The absorber vessel is designed so that heat exchangers can be replaced and or modified expediently. There is easy access to the absorber coils, which can be dismounted easily. The coils are thermally and electrically insulated from the vessel itself to minimize both heat losses to the vessel and potential corrosion problems. Initially, both absorbers will be of the falling film type, although they can be modified easily to test other types. The absorber coil for the lithium-bromide-water loop consists of eight tubes 1/2-in. diam, and for the ammonia water consists of a 30-in.-long coil, wound in a 4.5 diam, made of 1/2-in. tube.

The Absorption Process

A technique for determining the effectiveness of different absorbers is required. To develop that technique, consider the schematic of Fig. 2, which shows in highly idealized form the three phases and four substances present typically in any absorber. When the absorber works as intended, the refrigerant vapor, dm, is absorbed into the liquid solution, and the heat generated, dQ, is dissipated to the cooling fluid across a metallic wall. The coolant is assumed to be water in this case.

A simple model of the absorption process is now formulated to determine which parameters are important for experimental characterization. Let

Table 1. Operating conditions and instrumentation

	Generator	Absorber
Operating conditions		
Pressure, psia	80-100	60-70
Temperature, °F	300-230	270-100
Concentration, %NH_3	5-20	5-50
Solution flow rates out, lb/h	20-150	>20->150
Power rating, kW	0.5-2.5	0.5-2.5
Instrumentation		
Type T, precision grade thermocouples, ±1 °F	1	10
Solution mass flowmeters 1% of reading accuracy	0	2
Densitometers, ±0.0005 g/cc	0	2
Cooling water volume flow rate 1% of reading accuracy	0	1
NBS traceable thermometers 0.1 °F (cooling water)	0	2
Fiber optics	0	6
Pressure transducer, 1% reading accuracy	0	1

us concentrate on a differential of length, dz, along the absorber. It is assumed that the mass transfer operation from vapor to the solution can be described by an equation of the form:

$$dm = K\,(xv - x)\,dA \quad , \qquad (1)$$

where dA denotes the product of H·dz. (The symbols are explained in the nomenclature at the back of the paper.) A heat balance on the control volume of thickness, dz, and on that enclosing the vapor, solution, and cooling water reads:

$$hv\,dm - cp\,d(Tm) - mc\,cpc\,dTc = 0 \quad , \qquad (2)$$

where the heat exchanged by the solution and vapor has been neglected, and coflow has been assumed for the purposes of illustration. Note that also the solution specific heat has been assumed to be constant, which is a suitable approximation for the purposes of the present analysis.

It is assumed that an overall heat transfer coefficient, U, characterizes the transfer of heat from the solution to the cooling water in an equation of the form:

$$dQ = U\,(T - Tc)\,dA \quad . \qquad (3)$$

Then, a heat balance on the control volume containing the solution and the vapor phase gives:

$$m\,cp\,dT = U\,(T - Tc)\,dA - (hv - cpT)\,dm \qquad (4)$$

If Eq. (2) is integrated between the inlet of the heat exchanger and a generic point, z, and the subscript $\underline{i}$ is used to denote inlet conditions, the following is obtained:

$$mc\,cpc\,(Tc - Tc_i) = hv\,(m - m_i) - cp\,(Tm - T_i m_i) \quad . \qquad (5)$$

Equations (1) through (5) characterize the absorber performance, albeit under a number of simplifying assumptions. It is noteworthy that at least two parameters are required, namely, a mass transfer coefficient and an overall heat transfer one. To establish the relative importance of each in describing how the absorber works, the equations are made dimensionless by choosing as suitable reference values the inlet cooling water variables. The inlet cooling water temperature, mass flow rate, and specific heat are the reference values. The length over which the solution is distributed is adopted as the reference length H.

Substitution of Tc from Eq. (5) into Eq. (4) and replacement of dm in Eq. (4) by Eq. (1),

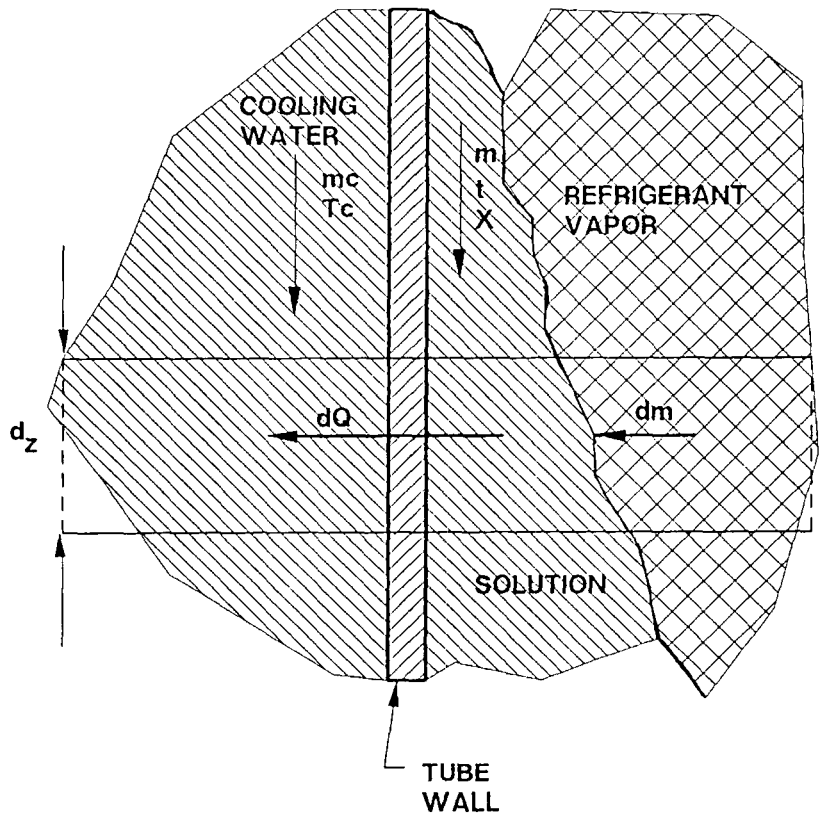

Fig. 2. The absorption process.

after making the equations nondimensional, gives the following for the derivative of the solution temperature along the absorber:

$$\frac{dT^*}{dA^*} = \frac{1}{M^*}\left\{\left(\frac{UH^2}{mc\ cpc}\right) 1 + M_i^* T_i^* - T^*(1 + M^*) + hv^*(m^* - m_i^*) + \left(\frac{KH^2}{mc}\right)(hv^* - cp^*\ T^*)\ (xv - x)\right\} \quad (6)$$

Equation (6) employs two dimensionless parameters, *one for heat transfer and one for mass transfer*, given by:

$$U^* = \frac{UH^2}{mc\ cpc} \quad . \quad (7)$$

$$K^* = \frac{KH^2}{mc} \quad . \quad (8)$$

When no absorption takes place, Eq. (6) reduces to the equation corresponding to pure heat transfer in a coflow configuration.

To study the influence of mass transfer on the temperature profile, the mass transfer coefficient was increased progressively, and Eq. (6) was integrated by employing a standard second-order Runge Kutta method.[11] Other values chosen for this analysis were: $xv = 0.8$, $m_i^* = 0.25$, $cp^* = 0.5$, $U^* = 10$, and $T_i^* = 1.5$. The cooling water temperature was determined from a heat balance, and the temperature profiles are shown in Fig. 3. The curves with K^* equal to zero correspond to pure heat transfer. As the mass transfer coefficient is increased, the solution temperatures increase progressively to a point that it becomes impossible to approach the pure heat transfer temperature values at the outlet of the absorber. In fact, for the case of K^* equal to 0.5, the solution temperature profile is very different from the one corresponding to pure heat transfer. The cases of Fig. 4 show that when mass transfer effects are important compared with the ability of the absorber to dissipate heat, the solution temperature could increase monotonically.

The analysis presented so far is relatively simple. It does not include an equation of state

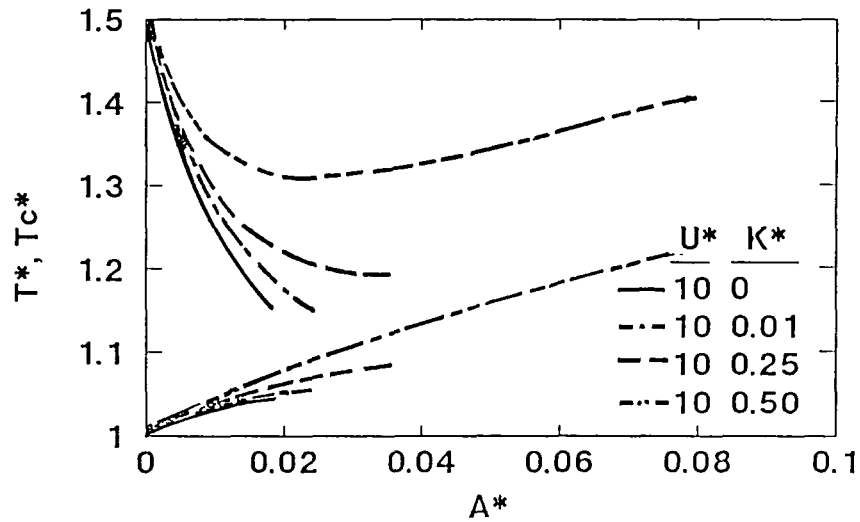

Fig. 3. Temperature profiles for increasing mass transfer in the coflow case.

for the solution, which would serve to incorporate equilibrium considerations and, depending on the inlet conditions, limit the solution temperature increases of Fig. 4 by limiting the absorption rate. However, it does include two parameters intended to describe two transport operations, one activated by concentration gradients and the other by temperature gradients. The controlling resistance to the mass transfer operation takes place at one of the two sides of the vapor-solution interface. The controlling resistance to heat transfer may be located in either of the two liquid sublaminar boundary layers, or, perhaps more unlikely, at the solid wall.

Experimental Technique

The experimental characterization of the two different phenomena described above that take place at different interfaces is a challenging proposition. Yet, such characterization is needed to determine which enhancement technique works best. Different approaches have been undertaken in the past, such as measuring the rate of decay of pressure in a static absorber[12] or calculating an overall heat transfer coefficient.[13] In the present experiments, it is intended to follow simple approaches, increasing the complexity only as required to get consistent, repeatable results.

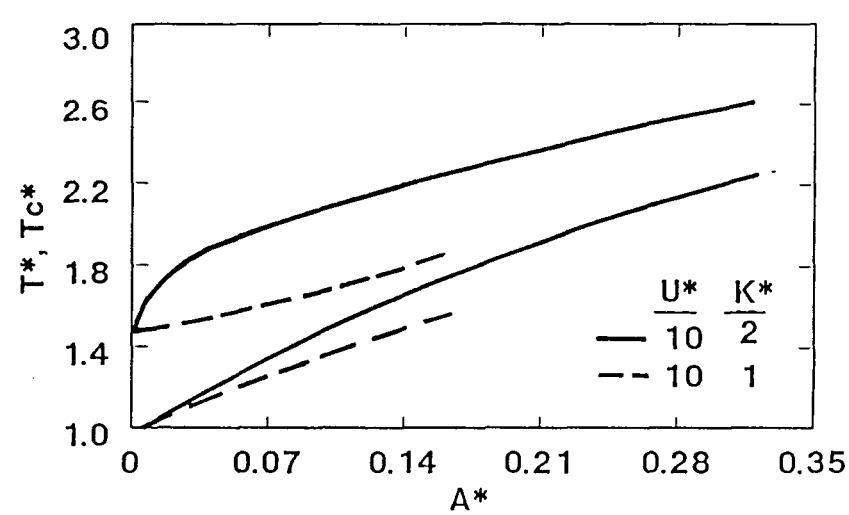

Fig. 4. Temperature profiles for high mass transfer rates in the coflow case.

For a given heater setting, the heat load on the absorber should be nearly constant. Under those conditions, an effective enhancement technique should decrease the absorber pressure level. Subtle steady-state pressure level differences may be hard to measure accurately, however. Furthermore, repeating steady-state conditions accurately from one experiment to the next may not be possible. Thus, the determination of an overall performance parameter, describing both heat and mass transfer may be called for. Such a parameter is called the absorber heat transfer coefficient, and it is a catch-all parameter that is different from the overall heat transfer coefficient of Eq. (3). The absorber heat transfer coefficient (UF) is given by

$$UF = \frac{Q}{A \ T \ \ln} \quad . \tag{9}$$

At constant heater setting, UF turns out to be an exclusive function of the logarithmic mean temperature difference. Thus, lack of equilibrium between the vapor and liquid phases may cloud the resolution offered by this approach. It has been so widely used, however, that in conjunction with concentration measurements at the outlet of the absorber to determine subcooling, it may serve as a useful technique. It would, however, require extremely well-defined and repeatable inlet conditions.

In terms of complexity, measuring an overall heat transfer coefficient and a mass transfer coefficient (K) may be the next step. It is hoped that this approach will not require the repeatability criterion of steady-state conditions. That requirement would employ integrated versions of Eqs. (1) and (3), namely

$$K = \frac{1}{A} \int_{\text{inlet}}^{\text{outlet}} \frac{dm}{(xv - x)} \ , \tag{10}$$

$$U = \frac{1}{A} \int_{\text{inlet}}^{\text{outlet}} \frac{dQ}{(T - Tc)} \ . \tag{11}$$

Experimental determinations by the above equations call for values of temperatures and concentrations along the absorber, which can be obtained with the present instrumentation if some thermocouples are added to the cooling-water side. Other approaches for determining U and K exist, but they require further analysis at this point in time.

New approaches to evaluate enhancement depend heavily on the fiber optic concentration measuring device. A brief description of the status of this development is included below. At this point, it may suffice to point out that the high-response speed of the fibers and their accuracy allow the determination of time lags between pressure changes and concentration changes in thin solution films. The shorter the lag time, the more effective is an enhancement strategy. An experiment consisting of a well-defined step or ramp pressure increase in the absorber allows the measurement of time lags under realistic absorber conditions, thus adding a new experimental technique for evaluating absorber performance.

Property Data

Computer subroutines with thermodynamic and transport properties are required for data analysis and correlation. In addition, it is expected that the routines will be useful to other researchers if Computer Aided Design (CAD) of absorption units becomes more widespread. The relevant data for the working fluids were extracted from the literature, compiled, screened in terms of their scattering, and fitted. Standard polynomials were employed for the fits, with enough terms to minimize the fit standard deviation.

The fits completed for ammonia-water are summarized in Table 2, which indicates the properties correlated, the range of the independent variables for which the fit is valid, the standard deviation for the fit, the mean value of the property being fitted, the ratio of standard deviation to mean value, and the number of points employed for the fit. (The sources of data points for the fit are refs. 14 and 15.) Two other needed transport properties of this solution, namely, thermal conductivity and viscosity, are already in hand.[16] The values of molecular diffusivity have not yet been found, and they will have to be estimated if they are not available in the near future.

The status of the fits for lithium-bromide-water is shown in Table 3, which has the same format as Table 2. (The sources for the property data are refs. 16 and 17.) The values of molecular diffusivity still remain to be found or calculated.

Concentration Measurements

Current effort in this area is concentrated on developing a fiber optics sensor for measuring the concentration of ammonia-water solutions. This effort follows the development of a quartz fiber optic sensor for measurements in lithium-bromide-water solutions. The instrument relies on the measurement of light loss in a portion of the fiber that is stripped of its coating and in contact with a thin film of solution. This instrument allowed the determination of solution concentrations below each tube in a miniabsorber.[18] Furthermore, it allowed the determination of temporal correlations between pressure and concentration fluctuations and temperature and concentration fluctuations in a thin solution film in a falling film miniabsorber.[19] The speed and resolution of the fibers were instrumental for producing those correlations. The time lags between pressure and concentration fluctuations are a clear indication of the effectiveness of any enhancement technique, since the concentration should faster approach equilibrium with the value

Table 2. Summary of property routines for ammonia water

Variable [unit]	Routine name	Range	Standard deviation Sd	Mean Mn	Sd/Mn	Number of data points
P(x,T) [atm]	PJOINT(x,T)	0<x<100 40<T<338°C	0.108	2.857	0.0378	1375
x(T,P) [%]	XCON(T,P)	Obtained by inversion of P(x,T)				
H(x,T) [kj/kg]	$HFNH_3$(x,T)	0<x<100% 40<T<338°C	0.041	1.409	0.0291	1679
x(T,P) [%]	HTP(T,P)	Obtained by inversion of H(x,T)				
D(x,T) [kg/l]	DENS(x,T)	0<x<80% 0<T<150°C	0.012	0.825	0.0145	629

Table 3. Summary of properties for lithium-bromide water

Variable [unit]	Routine name	Range	Standard deviation Sd	Mean Mn	Sd/Mn (%)
E(x,T) (kj/kg)	HLIBR(x,T)	0<x<70% 0<T<180°C	1.0	252.1	0.40
TW(x,T) [°C]	TDEW(x,T)	58<x<64% 74<T<121°C	0.20	32.46	0.60
P(x,T) [Pas]	PRESS(x,T)				
k(x,T) $\frac{kcal}{m\ hr^{o}C}$	TCON(x,T)	5<x<65 wt % 0<T<100°C	0.0018	0.4447	0.40
Mu(x,T) [cp]	VISCOS(x,T)	5<x<60 wt % 9<T<90°C	0.115	1.970	5.80
D(x,T) [kg/l]	SPMASS(x,T)	10<x<60 wt % 0<T<100°C	0.001	1.339	0.10
ST(x,T) (dyn/cm)	STEN(x,T)	5<x<60 wt % 0<T<90°C	0.257	77.644	0.33

corresponding to the pressure the more effective the technique. An example of the concentration autocorrelation determined with the fiber optics is shown in Fig. 5. The pressure autocorrelation is shown for reference,[19] and it can be seen that the concentration lags behind the pressure. The upper limit of the concentration range for these fibers needs to be raised from 56 to 65%. Glass fibers or other materials may serve this purpose, but it remains to be determined.

Whereas the fiber developed for lithium bromide-water solutions can measure indexes of refraction ranging from 1.42 to 1.465, the range for ammonia-water solutions in typical absorbers is from 1.33 to 1.37. In practical terms, this means that not enough light is lost in the stripped portion of the fiber. To increase the light loss, a microbend has been introduced in the sensing portion of the fiber, following recent developments in this area by other researchers. The results obtained with a quartz fiber, employing a light emitting diode as the source and a silicon photocell as a detector, are given in Fig. 6. Ammonia concentrations from 1 to 60% can be determined, but the sensitivity is limited to +/- 2% of reading, because not enough light is transmitted through the fiber.

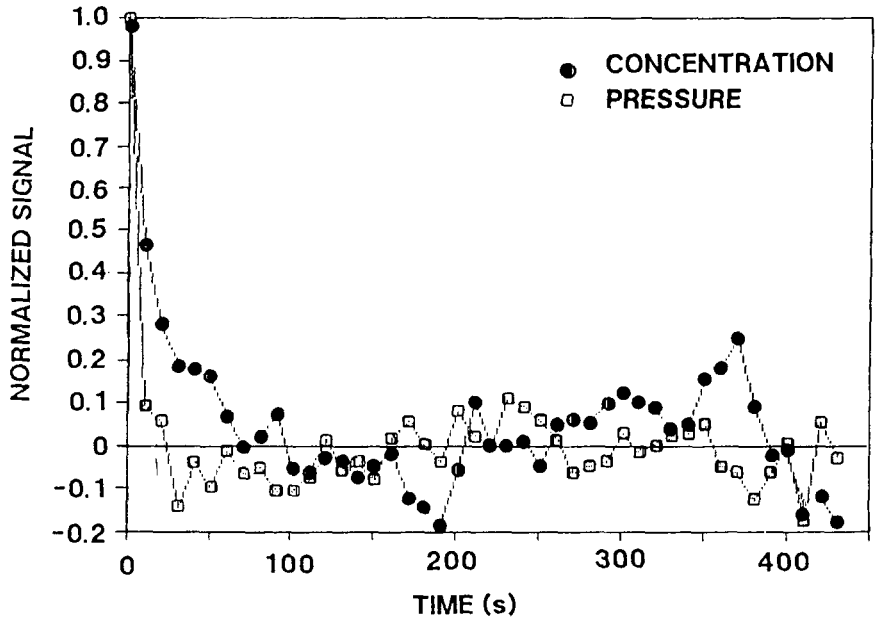

Fig. 5. Autocorrelation of concentration measured with fiber optics. The pressure autocorrelation is included for reference.

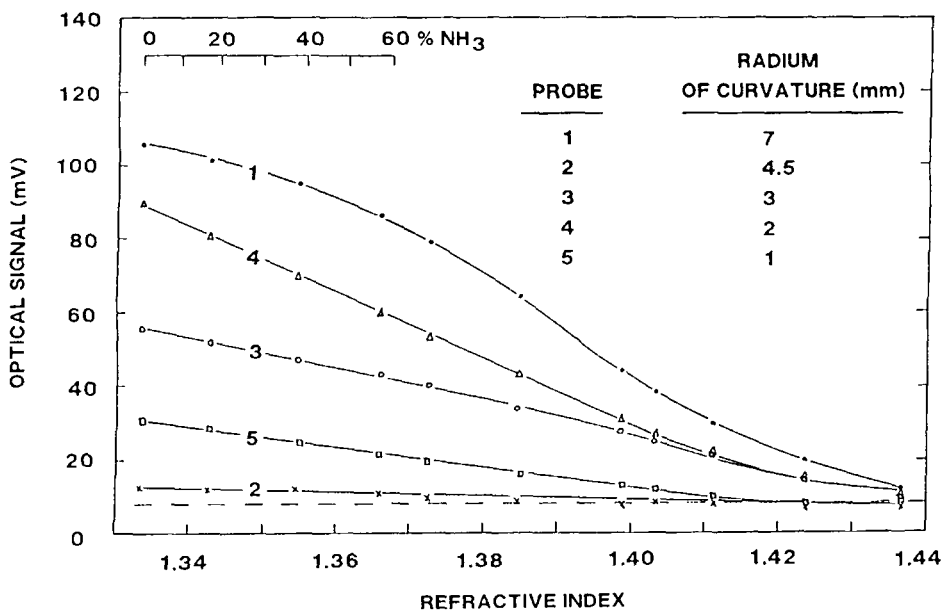

Fig. 6. Optical signals for refractive indexes in the range corresponding to ammonia water, for varying bend ratios.

To increase the intensity of the light going through, narrow the wavelength, and, hence, improve the sensitivity; a continuous wave laser diode will be employed. The laser diode emits at 850 nm, which is a wavelength that closely matches the peak wavelength of the silicon detector. A laser diode can be obtained with collimating optics and fiber optic connectors, allowing fiber-diode connections that are expedient and reproducible. A photocell diode is incorporated into the laser package to measure the intensity of the emitted light. The current from the monitor is fed into a feedback loop to control the forward current of the laser and to stabilize its output. The laser optical output powers at 2, 5, and 10 mW are one to two orders of magnitude above the intensity of any LED. As a side note, these laser diodes are common components in fiber optics communication systems and CD players.

With the sensitivity problem thus resolved, it becomes necessary to study the stability of the laser diode, feedback circuitry, and detector diode. With no cooling of the circuitry, drifts of the optical output of up to 20% in 30 min were observed. Cooling the circuitry with a fan reduced the fluctuations to 2% of the mean signal over a 1-hour period. To further reduce the uncertainty associated with the drift, the current output of the monitor diode was converted to voltage and used as a reference of the laser light output measured by the silicon detector. This mode of operation eliminated the effect of the drift.

In the near future, the laser diode will be coupled to a fiber optic that has a microbend. After calibration, the fiber will be tested in a solution of ammonia water over an extended period of time to determine stability and durability characteristics of the whole assembly. The test bed will be a small container built on 2-inch stainless steel pipe tees that are welded together. The solution temperature will be manually controlled with a heater and a cooling coil. Figure 7 is a schematic of the assembly. Subsequent plans are to use the fiber in the absorber test loop.

Conclusions

Experimental test beds for different absorber configurations have been designed, and construction of the ammonia-water apparatus has begun. How to measure the effectiveness of enhancement techniques in a general and repeatable way is the main experimental challenge now. The different measurement strategies outlined here will be used as needed in order of increasing complexity. The thermodynamic and transport property data required for analysis and reduction of the experimental data have been gathered, and many properties have been fitted. The lack of molecular diffusivity information, as well as some discrepancies in the ammonia-water vapor phase data, still need to be resolved. The fiber optic concentration monitoring device for ammonia is under development, and indications are that if the fiber can stand the ammonia-water environment, a viable instrument will result.

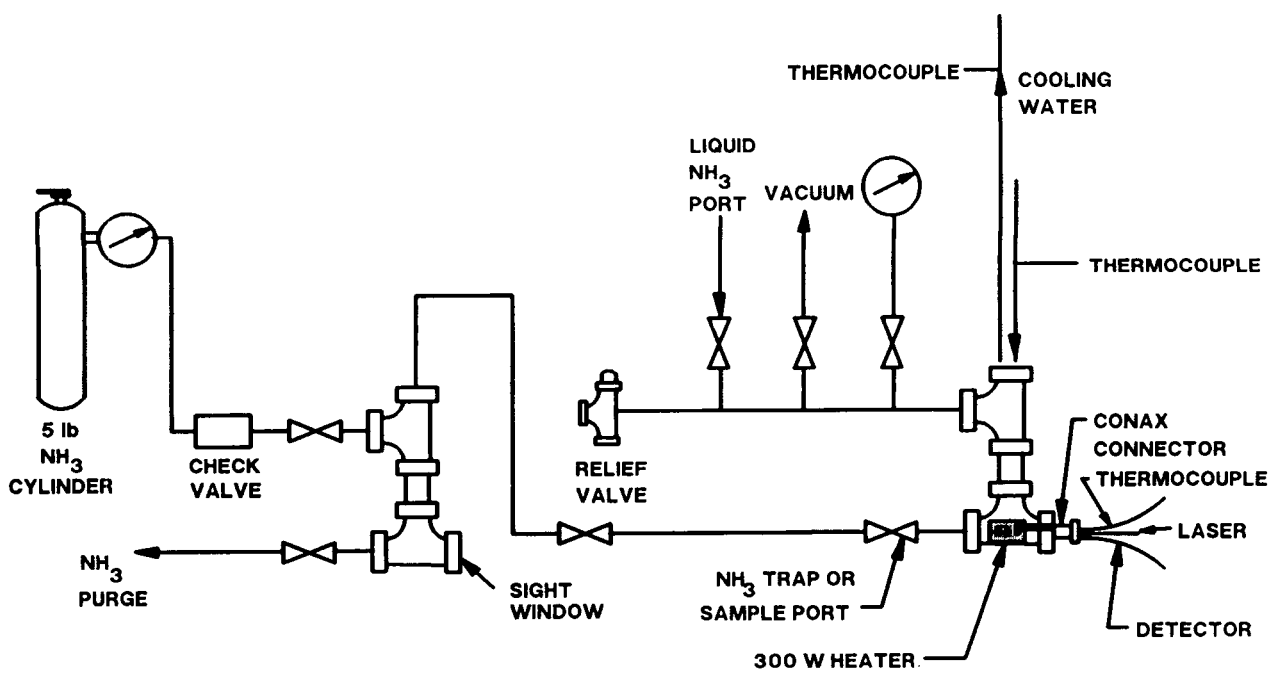

Fig. 7. Schematic of test bed for fiber optic in ammonia-water solutions.

Nomenclature

A	area (m^2)
cp	specific heat of solution (kJ/kg c)
cpc	specific heat of cooling water (Btu)
D	density (kg/liter)
E	enthalpy (kJ/kg)
H	depth of heat exchanger (m)
hv	enthalpy of the refrigerant vapor (kJ/kg)
k	thermal conductivity (kcal/m hr °C)
K	mass transfer coefficient (kg/s m^2)
M	solution heat capacity, M = m cp (kJ/s)
Mn	mean
Mu	viscosity (cp)
m	solution mass flow rate (kg/s)
mc	cooling water flow rate (kg/s)
TW	dewpoint of lithium-bromide water solutions (°C)
T	solution temperature (°C)
Tc	cooling water temperature (°C)
ΔT ln	logarithmic mean temperature difference (°C)
P	pressure (atm, Pascal)
Q	heat flow rate (kW)
Sd	standard deviation
ST	surface tension (dyn/cm)
U	overall heat transfer coefficient (kW/m^2C)
UF	absorber heat transfer coefficient (Btu)
x	concentration of refrigerant in solution (%)
xv	concentration of refrigerant in solution in equilibrium with the vapor concentration (%)
i	inlet (when used as a subscript)
*	dimensionless (when used as a superscript)

References

1. M. Bogart, Ammonia Absorption Refrigeration in Industrial Processes. Gulf Publ. Co., Houston, Texas, 1981.
2. H. Chung, M. H. Hour, M. Prevost, and R. Bugarel, "Domestic Heating Application of an Absorption Heat Pump," Proc. of Int. Conf. on Directly Fired Heat Pumps, Bristol, England, September 1984.
3. ASHRAE Handbook, 1983 Equipment Volume, ASHRAE, Atlanta, Georgia, 1983.
4. R. L. Webb and L. J. Mougin, "Apparatus and Method for Absorbing a Vapor in a Liquid and Absorption Refrigeration System Incorporating Same," U.S. Patent 4,223,539, 1980.
5. N. E. Hopkins, "Absorption Refrigeration System Using a Heat Transfer Additive," U.S. Patent 3,593,540, 1971.
6. B. A. Phillips, "A New Future for Absorption?" ASHRAE Journ. **28**(11), pp. 38-40, 1986.
7. W. J. Biermann, B. A. Phillips, and E. P. Whitlow, Consulting meetings held on September 28 (Biermann) and October 2, 1987 (Phillips and Whitlow).
8. R. A. Macriss and T. S. Zawacki, "Absorption Data Fluids Survey: Final Report on USA Data," Institute of Gas Technology Rep., ORNL/Sub/84-47989/1, May 1986.
9. R. A. Macriss, J. M. Gutraj, and T. S. Zawacki, "Absorption Data Fluids Survey: Final Report on Foreign Data," Institute of Gas Technology Rep., ORNL/Sub/84-47989/2. April 1987.
10. J. C. Griess, J. H. DeVan, and H. Perez-Blanco, "Corrosion of Materials in Absorption Heating and Refrigeration Fluids," ORNL/TM-9646, Oak Ridge National Laboratory, Oak Ridge, Tennessee, 1985.
11. T. M. Creese and R. M. Haralick, Differential Equations for Engineers, McGraw-Hill, New York, New York, 1978.
12. C. W. Chi, "Effect of Additives on Properties of LiBr Solutions," Proc. of Symp. on Air-Conditioning Systems, Sponsored by American Gas Assoc., Chicago, Illinois, 1968.
13. R. C. Reimann and W. J. Biermann, "Development of a Single-Family Absorption Chiller for Use in a Solar Heating and Cooling System," DOE/CS/31587-T3-Vol.2, 1984.

14. T. S. Zawacki and R. A. Macriss, "Recommended Values for the Ammonia- Water Absorption Fluid Properties," Institute of Gas Technology Project No. 65062 for Oak Ridge National Laboratory, 1987.

15. B. H. Jennings, "The Thermodynamic Properties of Ammonia Water Mixtures: an Assessment in Tabular Format," ASHRAE Paper No. 2662.

16. T. Uemura, "Properties of Refrigerant-Absorbent Systems used for Absorption Type Refrigeration Machines," Reito, Vol. 52, No. 600, 1975, Translated from Japanese into English at Oak Ridge National Laboratory, ORNL/TR-87/9, 1987.

17. L. A. McNeely, "Thermodynamic Properties of Aqueous Solutions of Lithium Bromide," ASHRAE Trans. Vol. 85 (part 2) pp. 413-434, 1979.

18. D. T. Bostick, L. N. Klatt, J. E. Strain, and H. Perez-Blanco, "Real Time in Situ Refractometer for Concentration Measurements in Absorption Machines," ASHRAE Trans., Vol. 92, Part 2b, pp. 174-186, 1986.

19. D. A. Bostick, L. N. Klatt, and H. Perez-Blanco, "Fiber Optics Refractometer for Absorption Machines," Proc. of Symp. in honor of B. T. Chao, Urbana, Illinois, 1987.

Worldwide Survey of Absorption Fluids Data

R. A. Macriss and *T. S. Zawacki*
Institute of Gas Technology
Chicago, IL 60632

Objectives

The overall objective of this study is to develop improved data for the thermodynamic, transport and physical properties of absorption fluids. A specific objective of this phase of the study is to compile, catalog and coarse-screen the available worldwide data of known absorption fluid systems and publish it as a reference document to be distributed to manufacturers, researchers and others active in absorption heat pump activities.

Introduction

Over the past 90 years, a wealth of physical and thermodynamic property data has been developed for fluid systems potentially applicable to the absorption refrigeration/heat pump cycle. A significant portion of the data is available in the literature, some still remain confined to in-house files for various reasons and other are proprietary.

Generally, published data have been generated in regions of temperature, pressure and composition of interest to designers of absorption chillers and heat pumps. Recent research has focused on developing efficient cycle configurations, using multi-effect or multi-stage concepts, for both space heating and cooling. These new designs operate at temperatures and pressures significantly higher than encountered in the conventional absorption cooling cycle. Other new concepts are based on the addition of a third component to the binary solutions normally used in the conventional cycle.

In an effort to define the availability and quality of existing data and, thereby, assist in the determination of needs for new data useful to advanced concepts, the Institute of Gas Technology (IGT) has performed a comprehensive literature search and a coarse and fine screening of existing literature data in order to identify potential conflicts or gaps in the data, with particular emphasis on certain key fluid systems. Assisted by Oak Ridge National Lab (ORNL), IGT has carried out liaison activities with foreign researchers at the Universities of Essen and Stuttgart (Federal Republic of Germany), French Petroleum Institute and Graz de France, Kansai University (Japan) and Ben Gurion University (Israel), known to possess other unpublished data that may be useful to this program.

These activities have helped to further demonstrate the importance of a centralized and well documented source of the available data to the timely development and introduction of advanced absorption heat pump technology for space conditioning and temperature boosting. Clear benefits are thought to be the identification of unresolved conflicts in data of known, important fluid systems, of data gaps for key fluids and properties, and of new, potentially useful fluid systems.

A first compilation covering data developed in the USA over the past 60 years has been published (ORNL/Sub/84-4798/1). A second compilation covering mainly European and Japanese data has also been published (ORNL/Sub/84-4798/2). The information and data in this paper are presented in a format utilized in the two earlier published reports mentioned above.

Methodology

Both in-house-file and literature searches were undertaken to obtain available worldwide publications, dating back to the 1900's, with pertinent physical, thermodynamic and transport properties data for absorption fluids. Cross-checks of literature searches were also made, using available published bibliographies and literature review articles, to eliminate secondary sources for the data and only include original sources and manuscripts.

Fluid Properties and Data

The properties of these fluids relate to the liquid and/or vapor state, as encountered in normal operation of absorption equipment employing such fluids, and to the crystallization boundary of the liquid phase, where applicable. The actual data were systematically classified according to the type of fluid and property, as well as temperature, pressure and concentration ranges over which data were available. Data were sought for the 17 different properties listed below:

Mixture Properties

1. Vapor-Liquid Equilibria
2. Crystallization Temperature
3. Corrosion Characteristics
4. Heat of Mixing
5. Liquid-Phase-Densities
6. Vapor-Liquid-Phase Enthalpies
7. Specific Heat
8. Stability
9. Viscosity
10. Mass Transfer Rate
11. Heat Transfer Rate
12. Thermal Conductivity
13. Refractive Index
14. Entropy
15. Surface Tension
16. Toxicity
17. Flammability

The type of available data was of importance, with raw experimental data considered to be highly desirable for use in actual process and equipment design and sizing, and for process design correlation development. For this reason, raw tabulated experimental data were given the highest possible ranking, with other forms of data following in importance, as shown below:

Data Rank

Form of Data	Symbol
RAW EXPERIMENTAL	(E)
• Tabular	(T)
• Graphical	(G)
SMOOTHED EXPERIMENTAL	(S)
• Tabular	(T)
• Graphical	(G)
EMPIRICAL POLYNOMIAL	(P)
EQUATIONS OF STATE	(C)

Empirical polynomial relationships based on raw or smoothed experimental data are often reported. Such correlations are at best as good as the experimental data and can help facilitate the use of the data in performance and design calculations through automation (computer software & terminals). In the absence of data, reliable methods of prediction were sought (equations of state, generalized correlations). These methods are expected to possess greater uncertainties than the previous forms of data.

Coarse-Screening of Literature Data

Several approaches have been used in carrying out quality review and coarse screening of data from multiple sources, for each of several key or highest priority binary and ternary fluids. These alternative approaches include:

- Consideration of the authors' statements concerning data quality
- Assessment of the measurement technique and apparatus used in obtaining the data
- Consideration of a given authors' reputation for measuring data, where a single authors' data were the only available for a fluid system.

A more reliable method used to compare data from various sources, for a given fluid and property, has been the plotting of data on a common basis. Such plots have also served to reveal the amount of scatter or internal consistency of a given author's data and, therefore, its quality.

Accomplishments

Over 450 different worldwide publications were identified with data relating to properties of binary, ternary and multicomponent absorption fluids. After elimination of duplication through cross-checking, a total of 200 primary sources of data were selected (see References) and the actual documents acquired, dating as far back as 1901, with nearly 90% of the documents published between 1960 and 1987. The texts of these manscripts are mainly in English, German, Japanese, Russian or French.

The absorption fluids covered in the 200 documents are combinations of 32 different "refrigerant" compounds with 97 single, 37 binary and 10 ternary "absorbent" compounds. Generally, the 32 refrigerants are divided among the following categories of chemical compounds:

Refrigerants

INORGANIC	3
ORGANIC	29
• Amines	3
• Alcohols	5
• Halogenated	20
• Hydrocarbons	1

Likewise, the single absorbent compounds are generally subdivided as follows:

Absorbents

INORGANIC	34
ORGANIC	63
• Alcohols	9
• Ethers	5
• Alcohol-Ethers	3
• Amides	8
• Amines	4
• Amine-Alcohol	1
• Esters	13
• Ketones	5
• Acids	4
• Aldehyde	1
• Others	10

The binary and ternary absorbents are various mixtures of 2 or more single absorbent compounds. Figure 1 below presents examples of absorption fluid systems and the number of references that contain vapor-liquid equilibrium data for each fluid system. Similar charts have been prepared to cover other fluids, properties and relevant references.

In terms of absorption fluids properties, for which data are available in the 200 primary documents, the list shown in the next column reveals that vapor-liquid equilibrium is the predominant property, reported in almost 60% of the documents. Toxicity and flammability of fluids, on the other hand, is reported in only two documents.

Thermodynamic, Transport, and Other Data

Fluid Property	No. of References*
Vapor-Liquid Equilibrium	132
Enthalpy	53
Specific Heat	33
Viscosity	44
Heat of Mixing	49
Density	46
Crystallization	66
Surface Tension	13
Corrosion (and Inhibitors)	17
Thermal Conductivity	9
Entropy	4
Stability	25
Refractive Index	7
Heat Transfer	7
Mass Transfer	6
Toxicity	1
Flammability	1

* A given document may contain data relating to more than one property; therefore, the sum of the references is larger than 200.

For each fluid and property in this study, the type of data and the temperature, pressure and concentration ranges, to which the data correspond, and the reference access number,

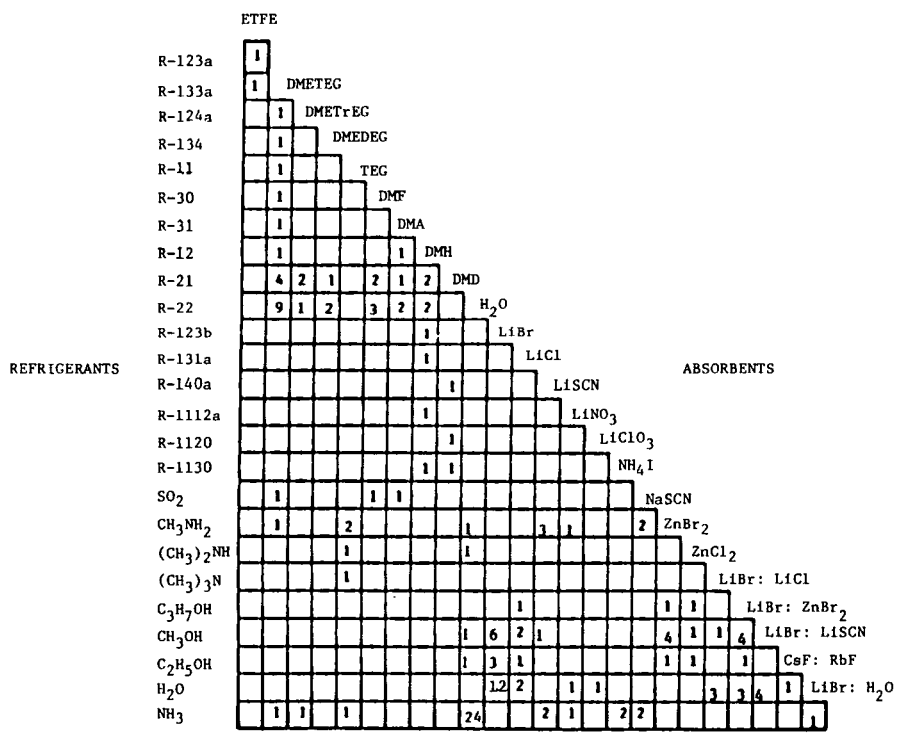

Figure 1. NUMBER OF REFERENCES FOR VAPOR-LIQUID EQUILIBRIUM DATA

first author, year of publication and text language, are all included in tables as shown in the example of Table 1.0 attached below.

Several key absorption fluids, currently of interest to researchers of advanced absorption heat pumps, are shown below:

Key Fluids

NH_3-H_2O	CH_3OH-LiBr-$ZnBr_2$
NH_3-H_2O-LiBr	TFE-NMP
NH_3-H_2O-$LiNO_3$	TFE-DMEDEG
NH_3-NaSCN	TFE-DMETEG
H_2O-LiBr	CH_3NH_2-H_2O-LiBr
H_2O-LiBr-LiCl	R21-DMETEG
H_2O-LiBr-LiSCN	R22-DMEDEG
H_2O-LiBr-$ZnBr_2$	R22-DMETEG
H_2O-NaOH-KOH-CsOH	R22-DMF
H_2O-$LiNO_3$-$NaNO_3$-KNO_3	R123a-ETFE
CH_3OH-LiBr	R124-ETFE
CH_3OH-$ZnBr_2$	R133a-NMP

Data coarse-screening and evaluations were carried out for the selected or key absorption fluids. The data screening indicated that the plethora of references for NH_3/H_2O may be misleading for the following reasons:

- Most current research with the NH_3/H_2O fluid is concentrated in advanced cycle designs, with operating conditions (temperature, pressure) covered by data developed in the past 2-3 years.
- Data for several important properties (heat and mass transfer rates, stability), and for operating conditions beyond present limits for other properties, are not available.

Unresolved conflicts in important data of various fluids and data gaps for key fluids were summarized. Figure 2 is an example of conflicting data for the vapor phase composition of the NH_3 + H_2O system at various temperatures. Data conflicts, lack of data for known key fluids at conditions beyond the limits of present data, and new fluids without property data constitute these summaries.

Figure 3 presents an example of absorption fluid systems with prioritized gaps in crystallization temperature data.

With extremely few exceptions among key fluids and their properties, and with emphasis toward the current development activities dealing with advanced absorption heat pump concepts, most all candidate fluids have data gaps that need to be addressed in the near future.

1.0. Vapor-Liquid Equilibrium

Fluid System	Data Type	Temp. Range, °C	Press. Range, atm	Weight, % X (R) Y (R)	Reference No.	Author	Year	Country	Text
H_2O + LiBr	TEP	0-72	0.42-53 (1)	42.2-55.6	98	Matsuda	1980	Japan	Japanese
H_2O + LiBr	GEP	0-72	0.6-60 (1)	44.8-54.6	98	Matsuda	1980	Japan	Japanese
H_2O + LiBr	GP	0-80	0.4-100 (1)	35.0-60.0	98	Matsuda	1980	Japan	Japanese
H_2O + LiBr	GEP	20-160	2-800 (1)	35.5-77.2	171	Uemura	1964	Japan	English
H_2O + LiBr	GP	30-160	1-800 (1)	40.0-65.0	171	Uemura	1964	Japan	English
H_2O + LiBr	P	NA	NA	NA	155	Uemura	1977	Japan	Japanese
H_2O + LiBr	GEP	0-150	3-800 (1)	35.5-100.0	49	Hasaba	1959	Japan	Japanese
H_2O + LiBr	TGP	0-180	1-800 (1)	40.0-80.0	49	Hasaba	1959	Japan	Japanese
H_2O + LiBr	GE	30-100	3.16-160 (1)	NA	71	Iyoki	1977	Japan	Japanese
H_2O + LiBr	GS	-20-190	0.1-1000 (1)	30.0-100.0	116	Oouchi	1985	Japan	Japanese
H_2O + LiBr	TEP	20-175	5-950 (2)	30.0-75.0	130	Renz	1981	Germany	German
H_2O + LiBr	GS	0-180	1-1000 (2)	30.0-100.0	130	Renz	1981	Germany	German

X - Liquid Phase
Y - Vapor Phase
(1) - mmHg
R - Refrigerant
A - Absorbent(s)
(2) - mbar
c - ppm by weight of A in Vapor Phase
m - mole, W = Weight
NA - Not Available

Table 1.0. WATER BINARY AND MULTICOMPONENT ABSORPTION FLUIDS PROPERTIES DATA

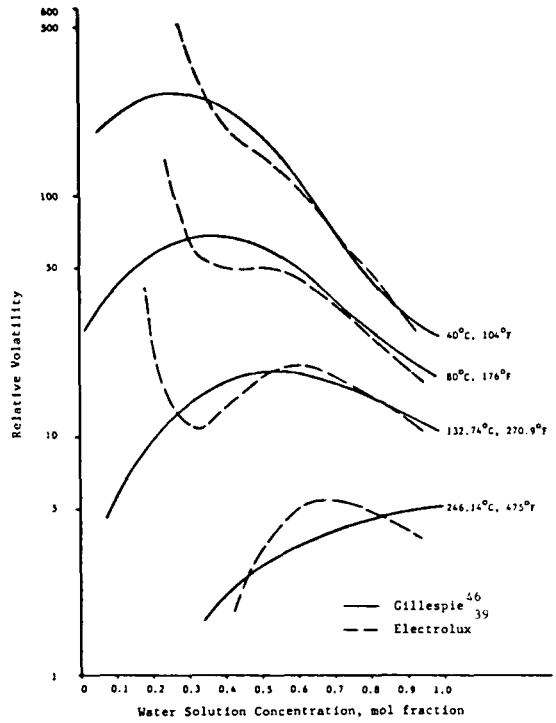

Figure 2. COMPARISON OF AMMONIA-WATER RELATIVE VOLATILITIES

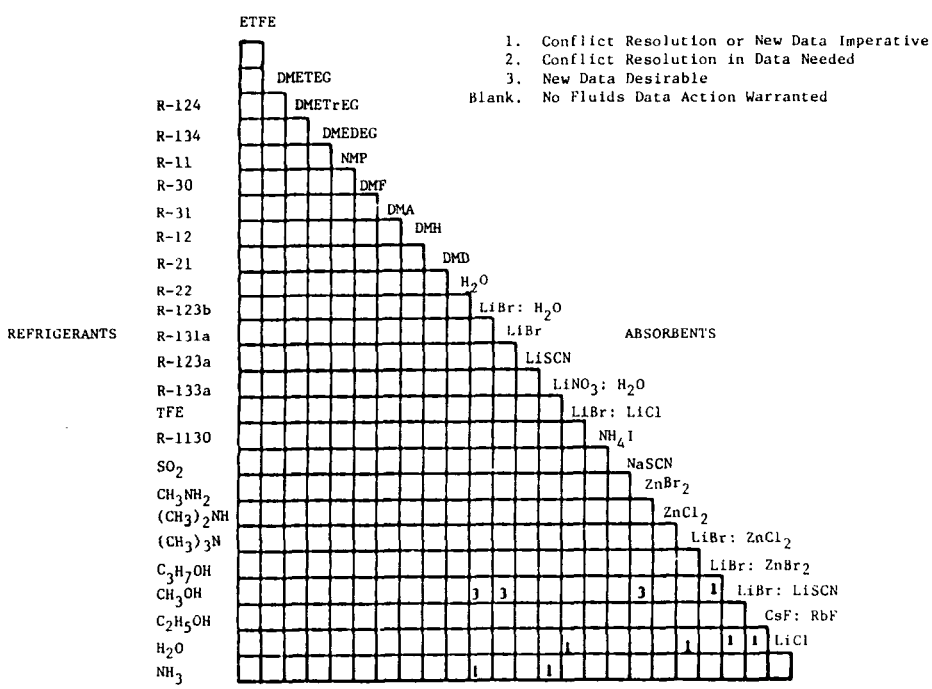

Figure 3. GAPS IN CRYSTALLIZATION TEMPERATURE DATA

References

1. Macriss, R. A. and Zawacki, T. S., "Absorption Fluids Data Survey: Final Report on USA Data," Institute of Gas Technology, Chicago, Illinois, May 1986.

2. Macriss, R. A., Gutraj, J. M., and Zawacki, T. S., "Absorption Fluids Data Survey: Final Report on Foreign Data," Institute of Gas Technology, Chicago, Illinois, April 1987.

3. Complete list of 200 references available in ORNL/Sub reports.

Session 5

Heat-Actuated Heat Pumps: Engine-Driven Heat Pumps

Organizer and Chairman:
G. T. Privon
Oak Ridge National Laboratory

GRI Heat Pump R&D Program Overview

A. R. Maret
Gas Research Institute
Chicago, IL 60631

(Paper not supplied in time for publication)

Engine-Driven Heat Pump Program Overview

G. T. Privon
Oak Ridge National Laboratory
Oak Ridge, TN 37831

A. T. Braun
Tectonics Engineering Corporation
Minneapolis, MN 55431

Abstract

This overview presentation is a brief summary of the efforts that have taken place in the small commercial-sized internal combustion engine-driven heat pump project being carried out by the Oak Ridge National Laboratory for the Department of Energy. Aspects of the project discussed are: objectives and effort scope, the engine-compressor-seal concept, early results, recent developments, current status, and future plans.

Introduction[1]

If one were considering the development of a gas fired heat pump, the most obvious approach would be to take a standard unit and to replace the electric driven compressor with an internal combustion (IC) engine-driven compressor. The IC engine in one form or another, has been tried either in air conditioning or heat pump application for some 30 years. Conventional engines have not proven to be broadly acceptable in this service because of problems associated with limited life, reliability, maintenance, and cost. With the opportunity presented by DOE for development of high-efficiency equipment under a high-risk long-term scenario, there was potential for new engine concepts. For heat pump application the development goals are: high thermal efficiency, life and reliability comparable to that of existing electric systems (i.e., 15-year design life), and reasonable maintenance needs (once a year servicing and one major overhaul every 5 years).

Of the IC engine proposals received, the Braun linear engine was selected and its development has been supported by the Department of Energy (DOE) and the Oak Ridge National Laboratory since 1980. The attributes that make the engine-compressor concept attractive are inherent in its design and consist of simplicity, low manufacturing cost potential, dynamic balanced operation, high efficiency, durability, high-reliability potential, and capacity modulation capability. Engine durability and reliability had been demonstrated and documented earlier by Tectonics Research, Inc., in industrial gas application.[2] The selection of the 15-ton to 20-ton class heat pump equipment for development was predicated on existing air compression technology at Tectonics as developed by A. Braun. Additionally, entry into the market with small commercial equipment was judged to be more likely because other engine niche market opportunities were identified for those engine models. In the 8 years since project inception these premises are still true.

Braun Engine-Compressor-Seal Concept[2-4]

The Braun engine-compressor-seal assembly has few major components (Fig. 1). The piston motion is linear--back and forth in a straight line; hence, no rotating cranks or rocking connecting rods are present. The one-cylinder engine operates in a two-cycle mode rather than in the conventional four-cycle automotive mode. Thus, the engine has no valves, valve-train gear, fly wheel, or distributor. However, like a conventional IC engine, it has a spark plug, battery, and generator. The lubricant to the engine piston is metered by drops, as in the rotary automotive engine, to ensure long piston-ring life and low exhaust emissions. Thus, no oil changes are necessary.

The engine assembly consists of two moving subassemblies, a piston and rod, and

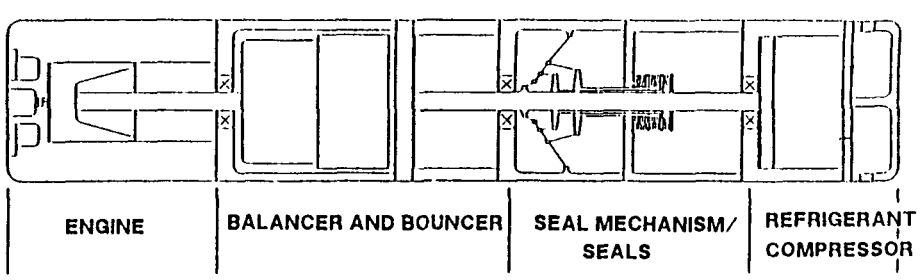

Fig. 1. Layout of Braun BR-105R model (breadboard) engine compressor.

a balancing counterweight. The balance mechanism, between the engine and compressor, results in smooth vibration-free operation.

A bounce space and piston are in an adjacent position on the assembly and assist in operation and control of the engine. The bounce space acts as a gas spring that helps to control the motion of the entire piston rod assembly.

Once started, the engine operates at a natural resonant speed determined by the combined effects of the compressor load and the bounce-space pressures. The piston stroke length varies with load conditions. Thus, by controlling the bounce-space pressures and fuel quantity, the stroke can be varied to respond to load change.

To prevent refrigerant leakage from the sliding rod that connects the engine and compressor pistons, a unique patented hermetic-seal assembly was developed at Tectonics. The assembly consists of metal bellows, a mechanism to limit bellows travel, and a means of controlling the pressure across the bellows.

Project Objectives and Scope

As part of the DOE-funded thermally activated heat pump program, the IC engine project shares its objective to advance the technology needed to accelerate the development and commercialization of energy efficient, gas and oil-fueled nonelectric equipment for space heating and cooling of buildings.

IC engine heat pump related activities, other than the early A. D. Little Inc., assessment study[5] on IC engines as drivers for heat pumps, have centered on the Braun engine-compressor-seal technology. The scope of these activities has included analysis and design, hardware development, and test at Tectonics, followed by in-unit laboratory test by an HVAC manufacturer and further engine-compressor refinements. With these efforts nearing successful completion, the intent is to co-fund preprototype unit development and to proceed with field site demonstration and evaluation. The preprototype unit development is intended to produce a viable design that includes engine waste heat recovery, appropriate muffling and acoustic treatment, system controls for unattended efficient operation, and that meets existing standards for safety, emissions, etc.

Early Results (1980-1984)

Initial development started after early analysis predicted a heating COP value in excess of 1.4 for a Braun engine heat pump at the 47°F rating condition. Efforts consisted of fabrication of a laboratory test rig (20 ton breadboard system), design and test of a hermetic seal (based on available components), design and test of a compatible single-cylinder R-22 compressor, modification of a Tectonics 20 BHP BR-105 standard carbureted linear engine, and successful proof of concept test of the complete breadboard assembly. These early tests of the carburetor engine compressor with propane fuel confirmed that the system could operate over the required range of heat pump conditions. In this time frame a fuel-injected BR-105 engine was tested (on propane) by an independent laboratory, which confirmed a previously attained engine brake thermal efficiency of 34% lower heating value (LHV).[3] The test results lent credence to expectations of higher efficiencies as the fuel injection system was improved. Together with acceptable emissions test results, this led to discarding the carbureted system.

Figure 2 shows the Braun engine-compressor (on the left) and the breadboard test rig (on the right) in the Tectonics laboratory as prepared for test.

Figure 3 shows Coefficient of Performance (COP) projections for an air-to-air heat pump, based on engine brake thermal efficiencies as derived from test and projections of 11.7, 30, and 34% for higher heating value (HHV) and 13, 33, and 37% for LHV.[6]

Recent Developments (since mid-1984)

During this period the earlier results were improved upon and design optimization of the seal, engine, and compressor occurred. Specifically:

- The seal was redesigned for low cost manufacture and longevity, and the engine/compressor design was changed accordingly.
- As of March 1987 a bellows subassembly, on accelerated life test, had accumulated 2.5 billion cycles before removal. At the nominal engine speed of 1000 cpm and 4000 hours of system operation per year, this result is equivalent to 10 years of operation.
- An engine with fuel injection was adapted to natural gas and successfully tested on the breadboard.
- Reliability testing of hermetic seal and engine-compressor assemblies was started.
- In late 1986 and early 1987 a natural gas fuel-injected engine with packing seals was tested in an air-to-air heat pump unit in a laboratory test system by Mammoth* (now a division of Nortek).

*Effort co-funded with Minnegasco, Northern Natural Gas, and Mammoth.

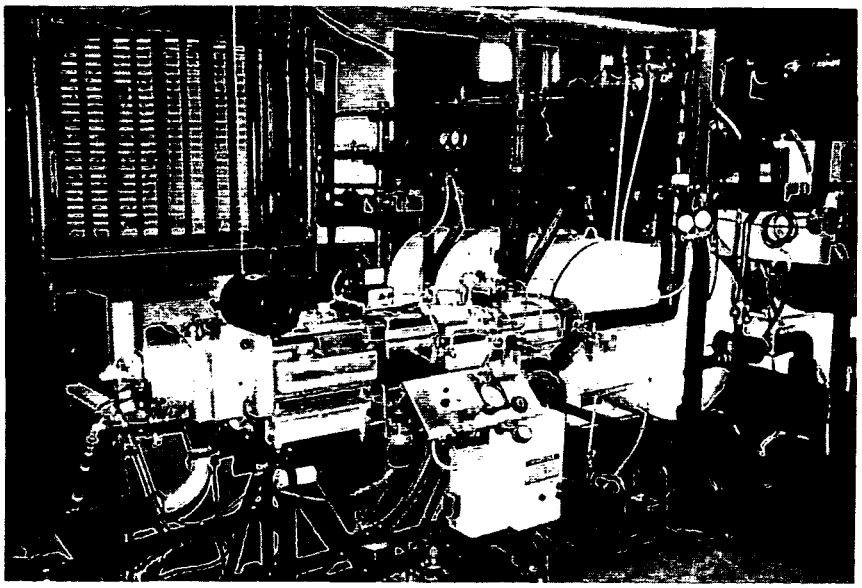

Fig. 2. Braun linear engine heat pump test setup.

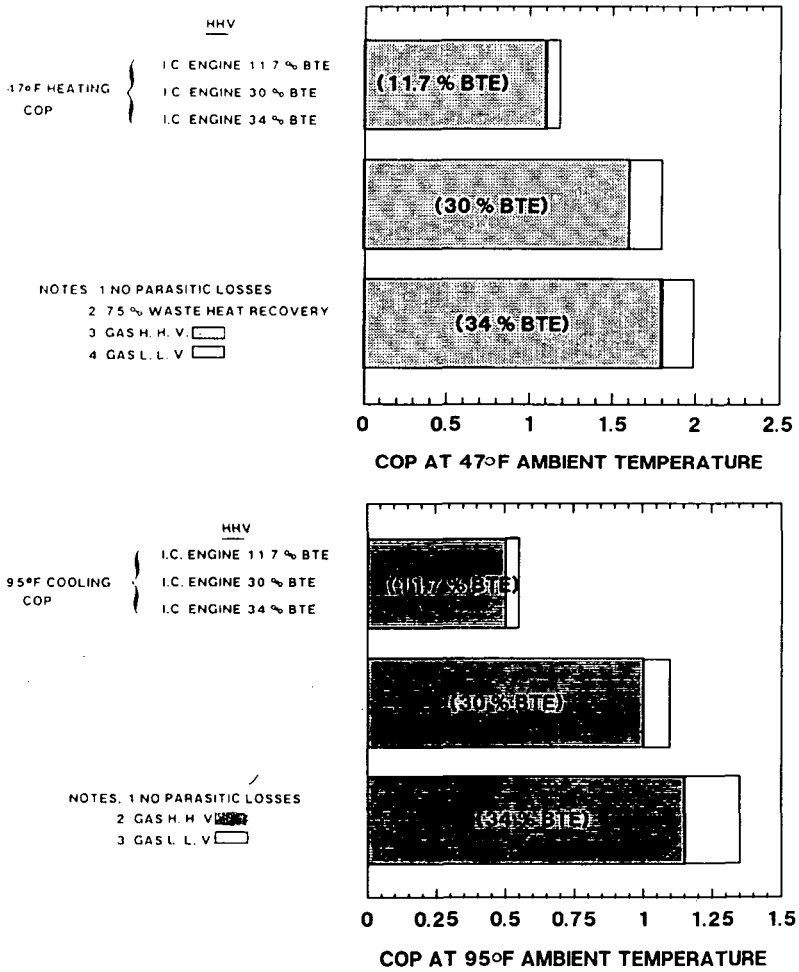

Fig. 3. COP projection for air-to-air heat pump.

- Manufacturing and marketing analyses were completed. Using 1987 rates (labor and energy) and performance figures comparable to those attained on the breadboard and assuming a simple 3-year payback, the results indicated that a competitive unit could be built and sold in select markets.+

Figure 4 shows the Mammoth unit, with engine and compressor enclosed, in the Mammoth laboratory prior to test.

In Fig. 5 the results of the natural gas fuel-injected engine-compressor tests in the Tectonics breadboard and the Mammoth air-to-air heat pump unit are presented. The tests were conducted in accordance to ARI and ASHRAE standards. COP values for heating and cooling are plotted against outdoor ambient temperature. The values are based on HHV but do not include electric parastics; and in the case of heating, the values include 75% recovery of engine exhaust and cooling jacket heat energy. The results, though preliminary, do confirm the potential of the concept and do provide expectations that steady-state COPs of 2.0 in heating and 1.0 in cooling can be realistically targeted for fully developed equipment.

*Effort co-funded with Minnegasco, Northern Natural Gas, and Mammoth.

+Marketing assessment co-funded with Minnegasco.

Current Status

Control development, part-load rating effort, and reliability testing are in progress. Upon final selection of controls, breadboard testing at Tectonics Research, Inc., will be conducted to demonstrate correctness of operation. These efforts are expected to continue through 1988.

Planned Activities

Pending availability of funding and continued success in the current efforts, it is expected that the following will take place as early as 1989:

An in-unit laboratory test of updated engine-compressor-seal assembly with controls for unattended operation to establish correctness of operation.

A 15-ton heat pump preprototype unit development and test.

A field test of one or more of the units.

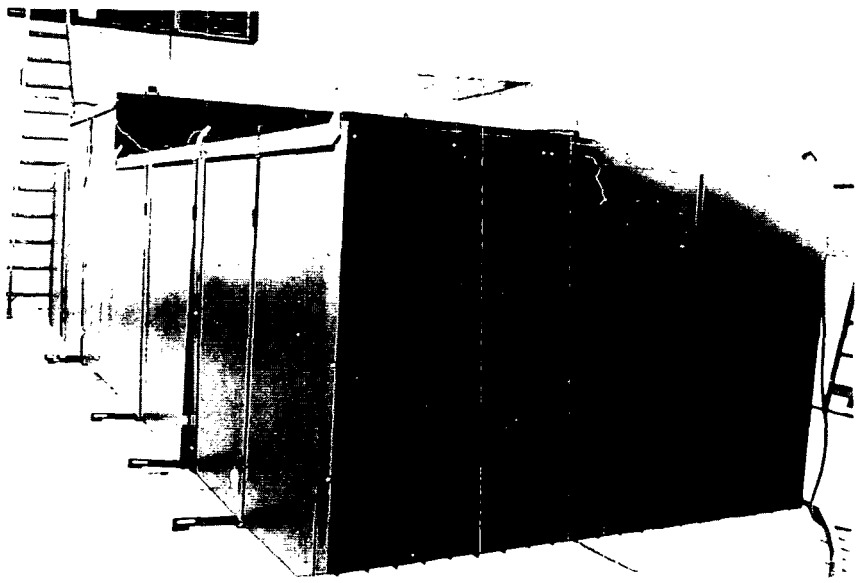

Fig. 4. Mammoth rooftop heat pump unit in test chamber.

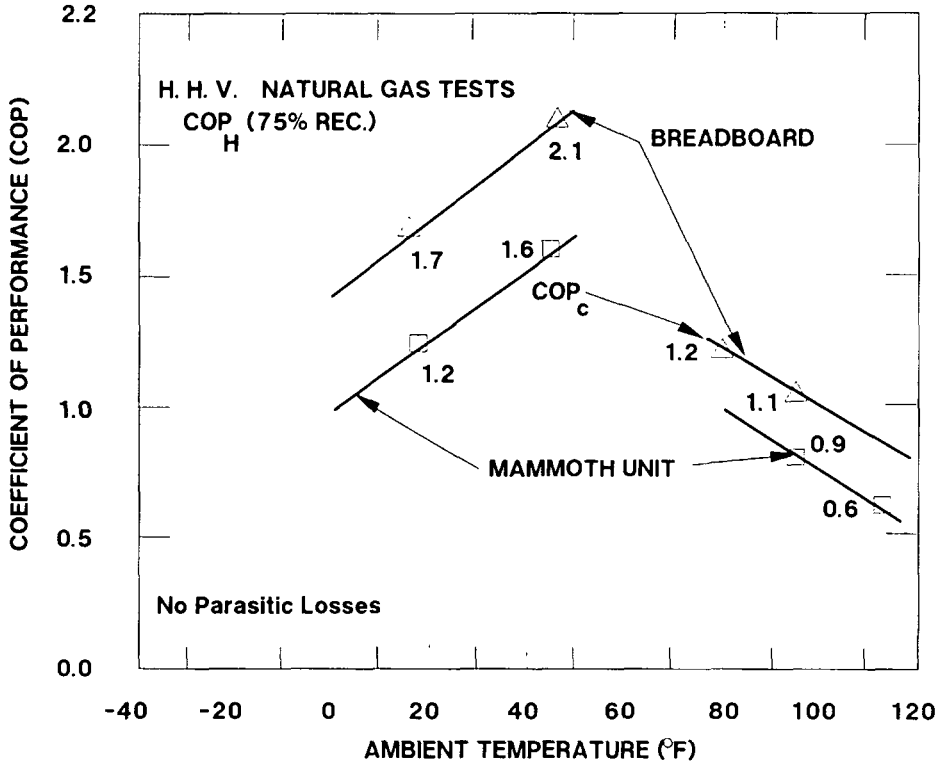

Fig. 5. Results of natural gas heat pump tests.

References

1. A. T. Braun (Tectonics Research, Inc.), "Test and Demonstration of a Hermetic Compressor Seal and Phase I, Development of a Braun Linear Engine-Driven Heat-Actuated Heat Pump," Conf-810672, Proceedings of the DOE Heat Pump Contractors' Program Integration Meeting, June 1981.

2. A. D. Little, "Assessment of Internal Combustion Engines as Drivers for Heat Pumps," ORNL/Sub/80-13836/1&2, Final Report, January 1984.

3. G. T. Privon, "Engine-Driven and Absorption Heat Pump Programs," Conf-841231, Proc. of the DOE/ORNL Heat Pump Conference: Research and Development on Heat Pumps for Space Conditioning Applications, December 1984.

4. A. T. Braun (Tectonics Research, Inc.) "Status of the Braun Free-Piston Engine Driven Heat Pump," Conf-841231, Proc. of the DOE/ORNL Heat Pump Conference; Research and Development on Heat Pump for Space Conditioning Applications, December 11-13, 1984.

5. Tectonics Research, Inc., "Development of a Braun Linear Engine-Driven, Heat Actuated Heat Pump," ORNL/Sub/80-61619/1, Final Report, July 1985.

6. F. A. Creswick, R. C. DeVault, F. Chen, G. T. Privon, "The Promise of Gas-Fired Heat Pumps for Buildings," Oak Ridge National Laboratory Review Publication, Number 3, pp. 14-18, 1987.

Status of the Braun Engine-Driven Heat Pump Development

A. T. Braun
Tectonics Engineering Corporation
Minneapolis, MN 55431

R. J. Prekker and *A. P. Schneeberger*
Mammoth, a Nortek Company

(Paper not supplied in time for publication)

An Analytical Study of Hybrid Ejector/Internal Combustion Engine-Driven Heat Pumps*

R. W. Murphy
Oak Ridge National Laboratory
Oak Ridge, TN 37831

Abstract

Because ejectors can combine high reliability with low maintenance cost in a package requiring little capital investment, they may provide attractive heat pumping capability in situations where the importance of their inefficiencies is minimized. One such concept, a hybrid system in which an ejector driven by engine reject heat is used to increase the performance of an internal combustion engine-driven heat pump, was analyzed by modifying an existing ejector heat pump model and combining it with generic compressor and internal combustion engine models. Under the model assumptions for nominal cooling mode conditions, the results showed that hybrid systems could provide substantial performance augmentation--up to 17% increase in system coefficient of performance for a parallel arrangement of an enhanced ejector with the engine-driven compressor.

Nomenclature

C	coefficient of performance
f	engine energy fraction
L	lower heating value
Q	cooling load
R	engine energy stream fraction
w	mass flow

Subscripts

e	ejector
f	fuel
i	engine/compressor
j	jacket
r	refrigeration cycle
s	system
x	exhaust

Introduction

Ejectors are extremely versatile devices. They can accommodate all three material phases and can accomplish two primary functions, mixing and pumping/compressing, which have many practical applications. Under the mixing category, ejectors can be employed for direct heating/cooling, blending/suspending, reacting, and dissipating purposes. Related specific uses include chemical processes, thermal signature reduction, pollution dilution, combustion control, and noise reduction. Within the pumping/compressing category, ejectors may be used for slurry pumping, ventilation, heat pumping, noncondensable removal, process drying, vacuum maintenance, and thrust augmentation.

In addition to its versatility, the ejector often combines high reliability with low maintenance cost in a package requiring little capital investment. For any particular application, these positive attributes must be carefully weighed against possible disadvantages such as low efficiency, control difficulty, or excessive noise.

The ejector application of interest for this session is, of course, the heat-actuated heat pump. When employed in a heat pump system such as that illustrated in Fig. 1, the ejector essentially replaces other types of compressors used in more conventional systems. In this situation, the ejector uses a high-pressure (primary) fluid stream to compress the low-pressure (secondary) fluid stream by (a) accelerating the primary stream, (b) entraining and accelerating the secondary stream, and (c) decelerating the combined primary and secondary streams to an intermediate pressure. The energy required to accomplish the compression is provided by heat input to a pump-fed boiler on the primary fluid stream. The other components of the heat pump system (that is, evaporator, condenser, and expansion valve) remain essentially the same, with the possible exception of size variations, as those in conventional systems. Such devices have long been employed in industrial heat pumping applications where the availability of service steam from central fired boilers made it the fluid of choice.

In a previous study, Hsu[1] used an analysis derived by Elrod[2] and thermodynamic property equations for fluorocarbons developed by Downing[3] to estimate performance for ejector heat pumps operating with Refrigerants 11, 113, and 114. For Refrigerant 11 with boiler, condenser, and evaporator temperatures at 200°F (93.3°C), 110°F (43.3°C), and 50°F (10.0°C), respectively, calculated coefficients of performance were 0.3 for the cooling mode (C_e) and 1.3 for the heating mode.

Although the performance calculated by Hsu was not especially impressive when compared with other heat-actuated heat pump options, the ejector advantages noted above are considerable. In a situation where relatively low-temperature "waste" heat is available, a combined or hybrid system may be attractive, particularly if ejector performance can be enhanced to levels substantially above model estimates. Based on simple internal combustion engine, compressor, and ejector component

*Research sponsored by the Office of Buildings and Community Systems, U.S. Department of Energy under Contract DE-AC05-84OR21400 with Martin Marietta Energy Systems, Inc.

ORNL-DWG 86-7998R

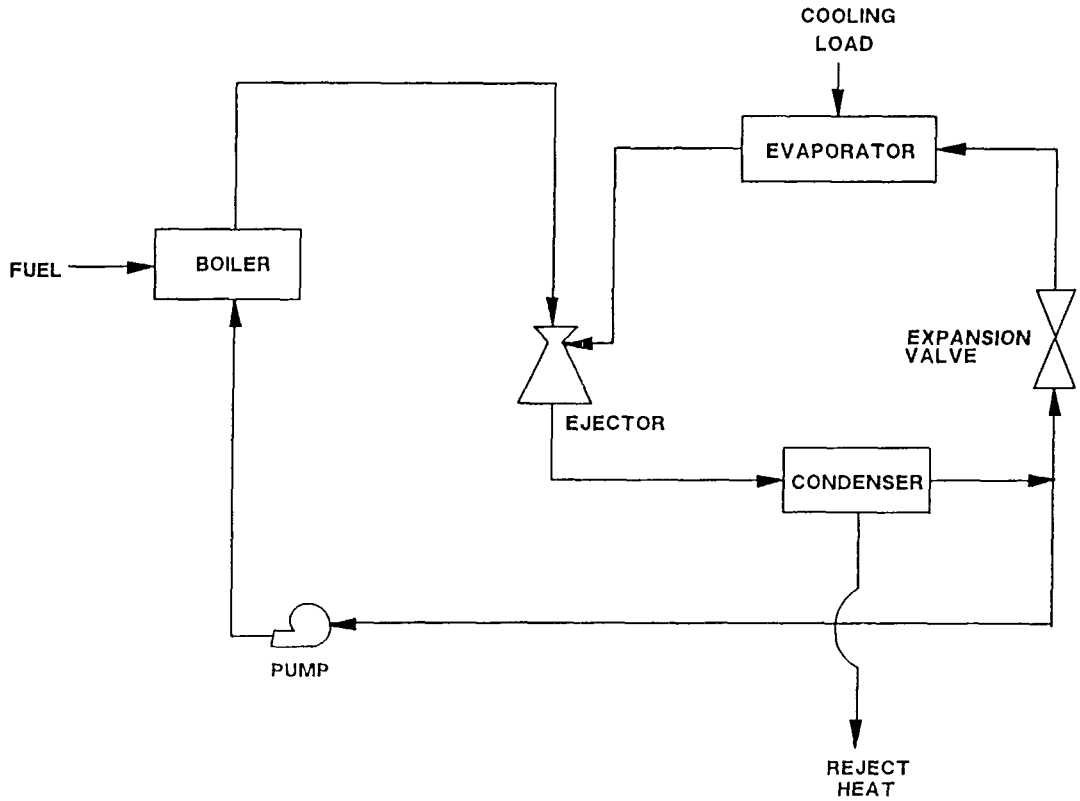

Fig. 1. Ejector heat pump.

models, this paper examines the performance potential of selected hybrid systems and ejector enhancement levels and makes comparisons with the associated baseline system.

System Selection

As the base for the hybrid systems considered here, a combustion-engine-driven vapor-compression heat pump with given cooling capacity was selected as shown schematically in Fig. 2. As candidate hybrid systems to provide the given cooling capacity, both parallel and series configurations of the ejector with the engine-driven compressor were evaluated (see Table 1). In the parallel arrangement illustrated in Fig. 3, the engine-driven compressor and the ejector work across the entire pressure difference between the condenser and the evaporator, with the ejector entraining and compressing (as a secondary stream) part of the evaporator refrigerant mass flow and thereby reducing the refrigerant mass flow through the compressor, the power required by the compressor, and the fuel usage by the engine. In the series arrangement with ejector downstream (illustrated in Fig. 4), both the compressor and the ejector handle the full refrigerant mass flow from the evaporator, but the ejector reduces the compressor power requirement and fuel usage by providing part of the pressure rise required to bring the refrigerant from the evaporator pressure to the condenser pressure.

Modeling

A generic internal combustion engine model by Segaser[4] was combined with a generic heat pump model (fixed efficiency compressor) to establish fuel usage and coefficients of performance. Brake thermal efficiency (f_i), jacket heat fraction (f_j), and exhaust heat fraction (f_x) values were based on the lower heating value of the fuel and were taken to be those for a liquid-cooled, naturally aspirated, spark-ignition gas engine operating at 75% of rated load (see Table 2). The compressor was assumed to have a fixed efficiency of 65.0%, which, for the baseline case of Refrigerant 11 operation with a 50°F (10.0°C) evaporator and 110°F (43.3°C) condenser, gives a refrigeration cycle coefficient of performance (C_r) of 5.00.

All heat transfer processes were modeled as isobaric. The refrigerant vapor leaving the evaporator and the refrigerant liquid leaving the

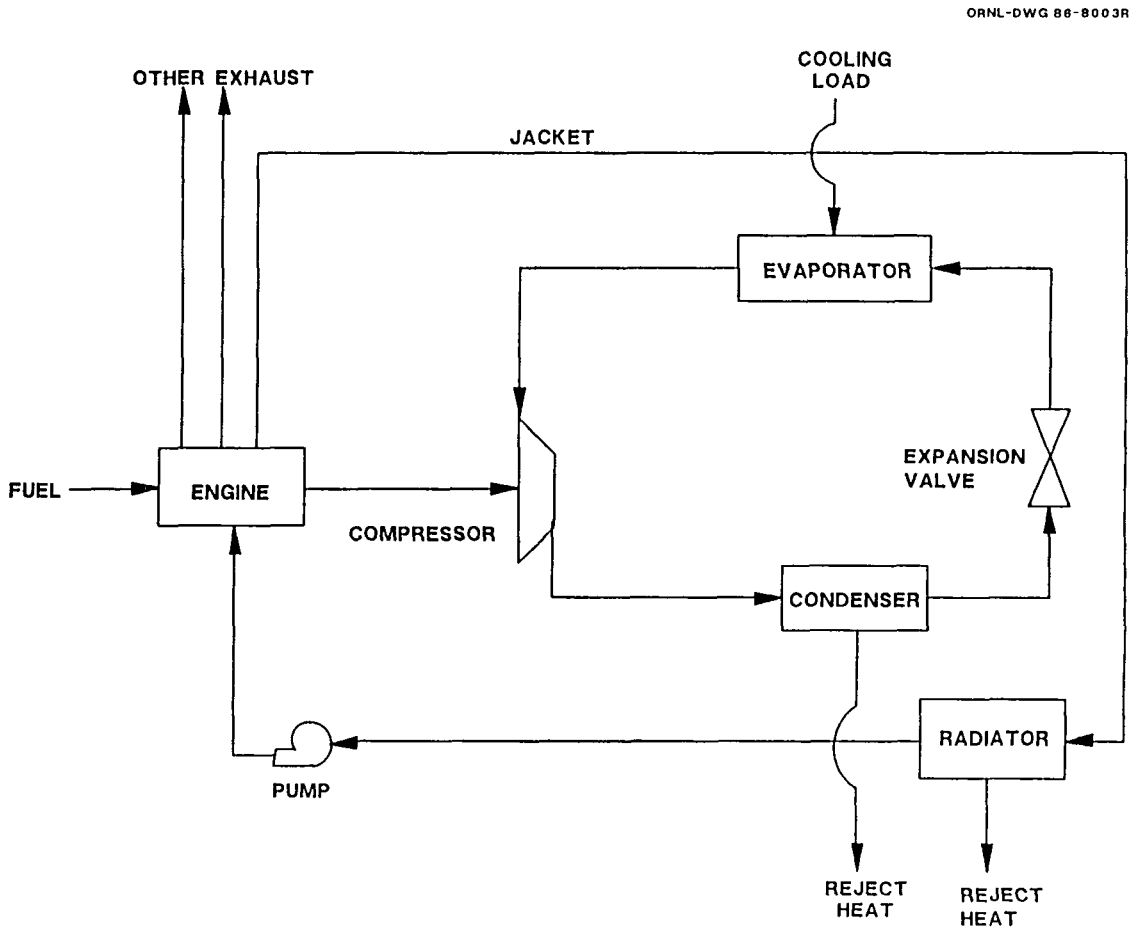

Fig. 2. Internal combustion engine-driven heat pump.

Table 1. System configurations

System	Configuration
1	Baseline engine-driven
2	Hybrid with parallel ejector
3	Hybrid with series ejector downstream
4	Hybrid with enhanced parallel ejector
5	Hybrid with enhanced series ejector downstream

Table 2. Generic engine characteristics at 75% of rated load (energy flows based on fuel lower heating value)

Brake thermal efficiency	30.7%
Jacket coolant heat rejection	27.8%
Exhaust gas heat rejection	26.7%
Lube oil heat rejection	5.3%
Radiation and other losses	9.5%
	100.0%

ORNL-DWG 86-7999R

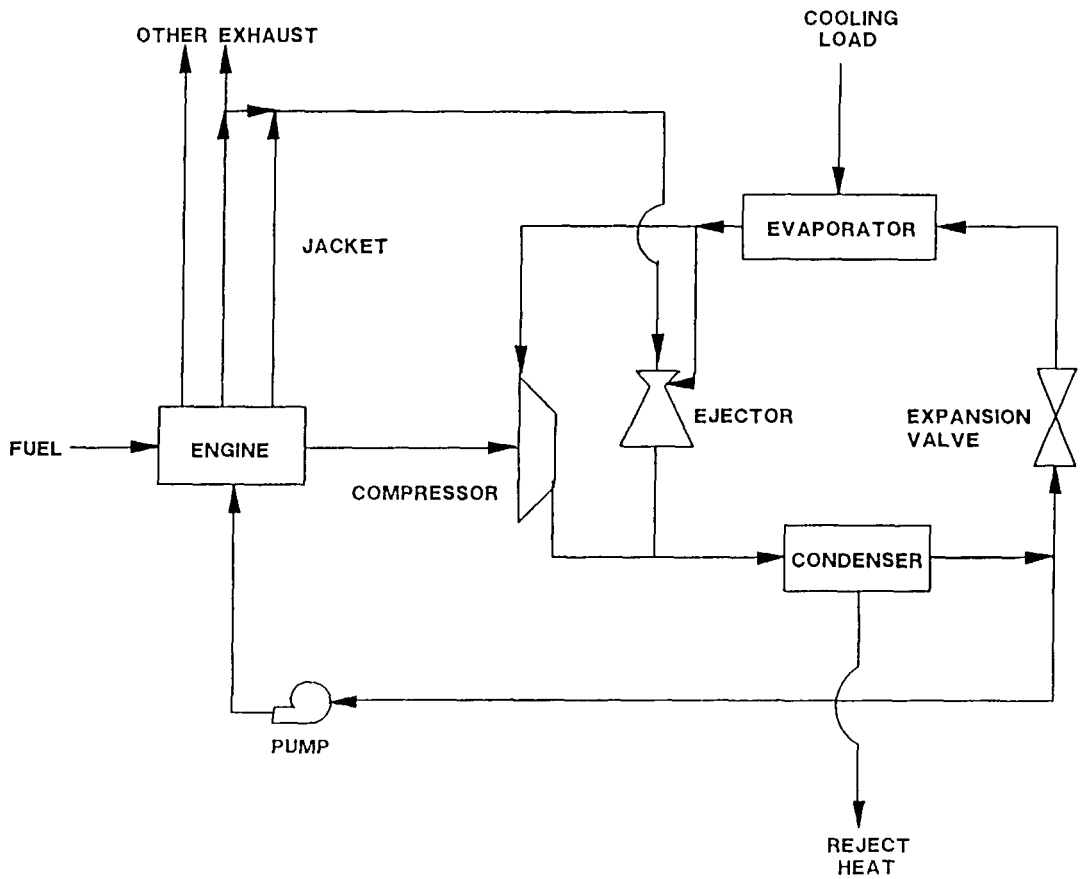

Fig. 3. Combined internal combustion engine-driven and ejector heat pump (parallel arrangement).

condenser were assumed to be saturated at the evaporator and condenser temperatures, respectively. The refrigerant expansion process was assumed to be isenthalpic.

Heat to drive the primary ejector stream was derived from only the engine jacket and engine exhaust. It was assumed that 100% of the former (R_j) and 50% of the latter (R_x) could be recovered by heat transfer from the jacket and exhaust to boil refrigerant in the pumped system feeding the ejector primary nozzle. Consistent with the earlier work by Hsu, primary nozzle efficiency for the ejector was assumed to be 97% and diffuser efficiency to be 75%. Based on the assumption of improved device design for the acceleration, entrainment, and deceleration processes, an enhanced ejector was modeled as providing twice the ejector heat pump cooling coefficient of performance determined by the Hsu model for the given exit pressure and inlet temperatures and pressures. Heat pump cycle conditions were set at the Hsu baseline values as indicated in Table 3.

Table 3. Heat pump cycle conditions

Working fluid	Refrigerant 11
Evaporator saturation temp. pressure	50°F (10.0°C) 8.78 psia (60.55 kPa)
Condenser saturation temp. pressure	110°F (43.3°C) 27.89 psia (192.29 kPa)
Boiler saturation temp. pressure	200°F (93.3°C) 102.52 psia (706.85 kPa)

Solution Methods

As defined here, fuel consumption (w_f) and system cooling coefficient of performance (C_s) are inversely related figures of merit for a fixed cooling load (Q) and fixed fuel lower heating value (L_f) according to the relation

$$C_s = \frac{Q}{w_f L_f} .$$

For the parallel arrangement of Fig. 3, the exit pressure and inlet temperatures and pressures to the compressor and ejector are fixed such that the engine-driven compressor and ejector models can be solved separately for the required operating points. Therefore, the total cooling load to be accommodated must be composed of the individual cooling loads (Q_i and Q_e) associated with each component operating separately between these fixed conditions, that is,

$$Q = Q_i + Q_e ,$$

where

$$Q_i = f_i w_f L_f C_r$$

and

$$Q_e = (R_j f_j + R_x f_x)\ w_f L_f C_e .$$

The resulting hybrid system cooling coefficient of performance is given by

$$C_s = f_i C_r + (R_j f_j + R_x f_x)\ C_e .$$

For the series arrangement of Fig. 4, an iterative solution is required because the compressor exit/ejector secondary inlet condition is not known a priori. The calculation sequence employed was as follows:

(1) Assume a value for the exit pressure of the compressor.

(2) Combine with the given compressor inlet evaporator exit conditions and the compressor model to calculate the compressor exit state.

(3) Employing this state as the inlet state for the ejector secondary stream, the given primary stream inlet (boiler exit) conditions, and the given condenser pressure, use the ejector model to determine the ejector exit conditions and mass flow (entrainment) ratio.

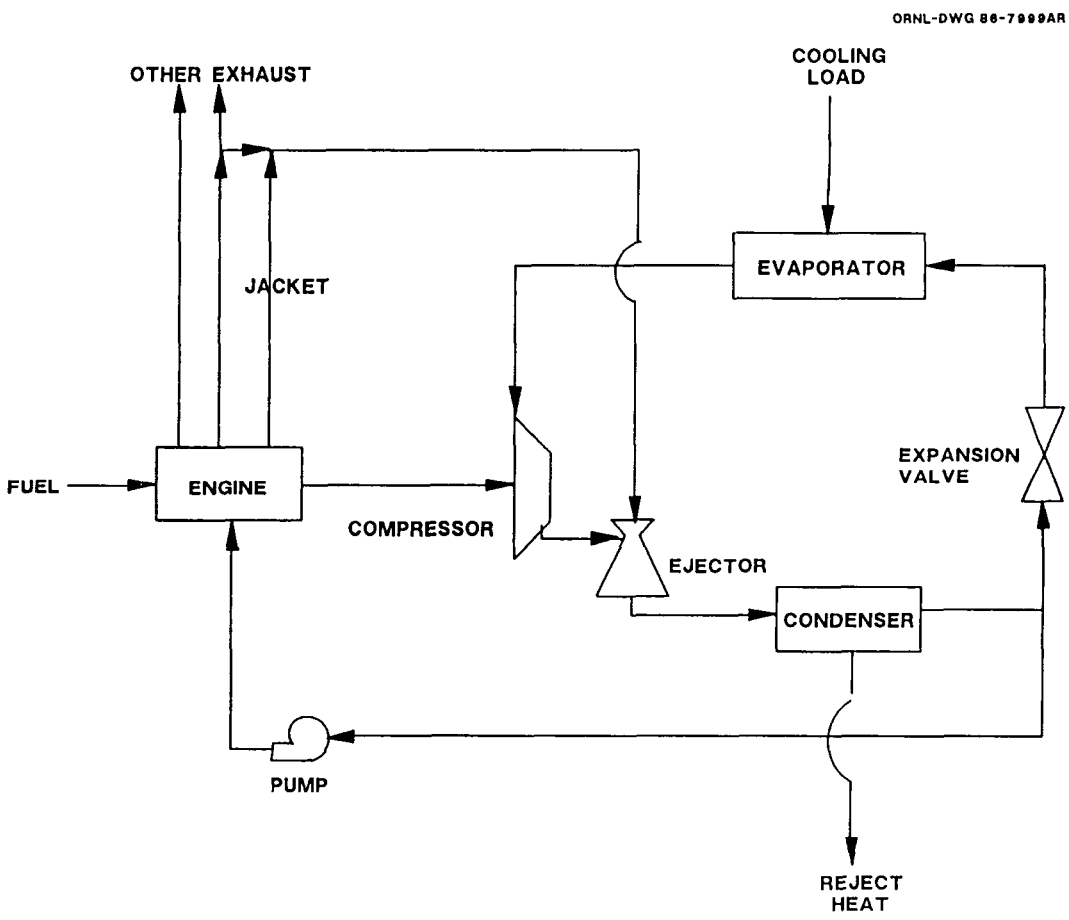

Fig. 4. Combined internal combustion engine-driven and ejector heat pump (series arrangement with ejector downstream).

(4) Using the state properties and mass flow ratio, determine the power required by the compressor.

(5) Using the state properties and engine model, calculate the shaft power available to the compressor.

(6) If the power required exceeds the power available, reduce the assumed compressor exit pressure and thereby reduce the compressor enthalpy rise and power requirement while reducing the ejector entrainment ratio and increasing the rejected heat and power available from the engine.

(7) Continue the iteration until convergence is achieved.

Results

All performance results are referenced to the baseline engine-driven configuration denoted in Table 1 as System 1. For the generic engine characterized in Table 2 and the heat pump cycle conditions specified in Table 3, System 1 had a cooling coefficient of performance of 1.535. For convenience, the engine fuel consumption for this case was assigned a value of 10.00 (lower heating value) energy units, establishing a cooling load of 15.35 energy units to be accommodated by all the competing hybrid systems. Of necessity, the compressor of System 1 must encounter both the full mass flow from the evaporator and the full pressure difference between the evaporator and the condenser.

As shown in Table 4, the parallel ejector arrangement of System 2 uses the "waste" heat from the engine to drive an ejector which compresses 8% of the required evaporator mass flow. The net effect is to reduce the compressor power requirement and engine fuel consumption by 8% and to increase the system cooling coefficient of performance to 1.66.

System 3, employing the series ejector arrangement, uses the recovered engine heat to accomplish the last 7% of the required pressure rise. Making somewhat less effective use of the ejector, this configuration achieves a system cooling coefficient of performance of 1.61 by reducing the compressor power requirement and engine fuel consumption by 5%.

Incorporation of an enhanced ejector into the parallel arrangement (System 4) increases the portion of the evaporator mass flow handled by the ejector to 14%, reduces the compressor power and fuel consumption to 86% of the System 1 value, and increases the system cooling coefficient of performance to 1.79 (17% greater than the value for System 1).

If such an enhanced ejector were implemented in the series configuration (System 5), the ejector could provide 18% of the pressure rise, requiring 88% of the System 1 compressor power and fuel consumption and providing a system cooling coefficient of performance of 1.74. By way of comparison, if such performance were to be achieved by System 1 using engine improvements alone, an increase in brake thermal efficiency from 30.7% to 34.9% would be required.

Conclusions

With the given assumptions, the analysis predicts that the performance of a heat pump driven by an internal combustion engine can be substantially improved when an ejector driven by engine reject heat is combined in selected hybrid configurations. Estimated increases in system coefficient of performance ranged from 5 to 8% at baseline ejector conditions and from 14 to 17% under enhanced ejector assumptions. Corresponding reductions in engine fuel consumption apply. For a given level of ejector performance, arrangements placing the ejector in parallel with the engine-driven compressor gave calculated system performance superior to that for those using a series configuration.

References

1. Hsu, C. T., Investigation of an Ejector Heat Pump by Analytical Methods, ORNL/CON-144, Oak Ridge National Laboratory, July 1984.

2. Elrod, H. G., Jr., "The Theory of Ejectors," J. of Appl. Mech., Trans. ASME, A170-A174, Sept. 1945.

3. Downing, R. C., "Refrigerant Equations," ASHRAE Trans. 80(2), 158-169, 1974.

4. Segaser, C. L., Internal Combustion Piston Engines, ANL/CES/TE 77-1, Oak Ridge National Laboratory, July 1977.

Table 4. Performance calculations for selected systems

System	Compressor mass flow as percent of evaporator mass flow	Compressor pressure difference as percent of total	Cooling coefficient of performance	Relative engine fuel consumption
1	100	100	1.54	10.00
2	92	100	1.66	9.24
3	100	93	1.61	9.52
4	86	100	1.79	8.58
5	100	82	1.74	8.80

Entrainment Enhancement of a Supersonic Jet for Advanced Ejectors

W-H. Jou and *G. S. Knoke*
Flow Research Company
Kent, WA 98032

C-M. Ho
University of California
Berkeley, CA 94720

Abstract

Improved ejector performance is required for heat-actuated heat pump applications. Laboratory experiments were conducted to investigate the use of a new rectangular supersonic nozzle configuration for mixing enhancement. Noncircular nozzles were previously found to increase substantially the jet entrainment in subsonic flow. Both flow visualization using schlieren photographs and pitot measurements in the far field indicate that the improvement in mixing for a supersonic jet is as good as that for a subsonic jet if not better. Mixing enhancement using a rectangular jet provides a technology basis for the development of the desired ejectors for heat pump applications.

Introduction

For many years, steam ejectors have been used to operate heat pumps for certain applications. Increased interest in fuel conservation, waste heat utilization, and cost reductions has stimulated the development of heat pump systems employing gas ejectors using fluorocarbon refrigerants.[1] Such systems are attractive for applications employing low-temperature waste heat or for augmenting more conventional heat pump cycles.

Using a jet ejector to compress a working fluid to higher pressure is a known technology (see, for example, Elrod[2]). Compared to mechanical compressors, which have the lowest reliability of any component on a conventional heat pump system, the ejector offers the advantages of being simple in construction with no moving parts and, hence, inexpensive and highly reliable. As illustrated in Figure 1 (from Murphy[3]), the motive power in a jet ejector heating system is provided by heating the working fluid in a boiler. The resulting hot, pressurized fluid drives the ejector to compress the vapor from the evaporator to the pressure required in the condenser. Some of the condensed fluid is pumped back to the boiler; the rest is bled through the expansion valve to the evaporator.

Ejectors operating over practical temperature ranges with conventional heat pump working fluids will require supersonic primary nozzles. Unfortunately, the mixing characteristics of a supersonic jet are inherently inferior to a subsonic jet. Therefore, mixing enhancement for a supersonic jet using newly developed technologies is crucial to the successful application of the ejector-based heat pump system.

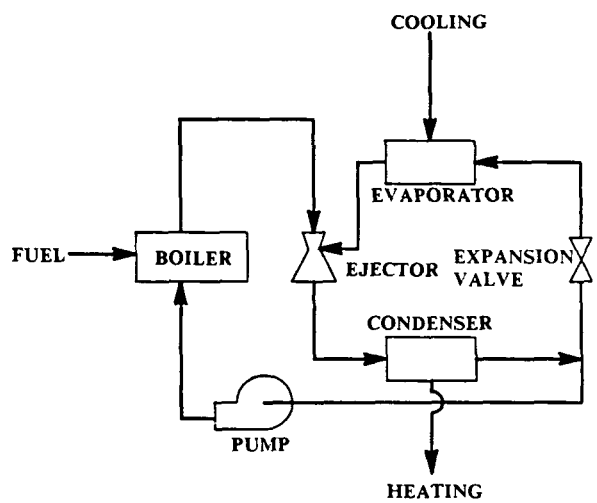

Figure 1. Jet-Ejector Heating System (from Murphy[3])

In recent years, a new level of understanding of turbulent mixing mechanisms has been achieved through the discovery of coherent structures in turbulent flows. These are large vortices produced by the hydrodynamic instability of a shear layer between two streams. These vortices engulf the surrounding fluid into the jet by induction. Since the nature of the interaction between these vortices is now well understood,[4] mixing enhancement can be achieved by actively or passively manipulating the vortex dynamics. For example, Ho and Huang showed experimentally that, by forcing a shear layer at different frequencies, dramatic differences in the merging process may result.[5] When the shear layer is forced at a frequency in the neighborhood of the most probable frequency, the shear layer rolls up into a train of vortices, and the merging of these vortices is suppressed for a large distance. When the frequency is decreased, the frequency of the response switches to the so-called "mode II" merging, in which two rolled up vortices merge at a fixed location where the mixing layer spreads quickly. With further decrease in forcing frequency, the response switches to "mode III" and "mode IV," in which three and four vortices merge to form a single structure,

a. Mode I

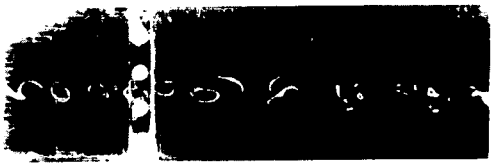

b. Mode II

c. Mode III

d. Mode IV

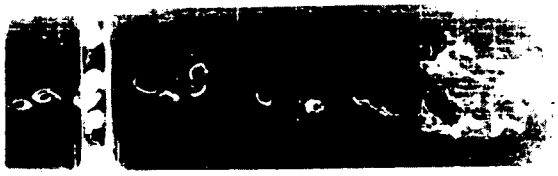

e. Collective interaction

Figure 2. Modes of Vortex Merging (from Ho and Huang[5])

respectively. The most dramatic "collective interaction," in which a large number of vortices merge simultaneously to form a large structure, can be observed when a very low frequency and an increased amplitude of forcing are applied. These complex vortex merging processes are shown in Figure 2 (from Ho and Huang[5]). These methods of manipulating vortex dynamics can be utilized in an advanced ejector to improve its performance.

For mechanical simplicity and reliability of the ejector, a passive mixing control strategy is much preferred over an active control device. The most successful passive control device for subsonic jet mixing was found to be a noncircular nozzle cross section, such as an elliptical or rectangular shape with an aspect ratio of approximately 2 to 4.[6,7] The entrained fluid within 5 nozzle diameters downstream of the nozzle can be increased to as much as 5 times that of a nozzle with a circular cross section. This increased entrainment is caused by the high degree of contortion of the vortex rings at the edge of the jet and the resulting complex vortex-induced flow. As shown in Figure 3 (from Ho and Gutmark[7]), a ring vortex emerging from an elliptic nozzle is first warped out of its own plane, then high azimuthal modes are excited to make a wrinkled vortex ring. This high contortion of the vortex ring causes its breakdown into turbulence downstream. This is in contrast to the more axisymmetric evolution of the vortex rings downstream of a circular nozzle. This new technology, if proven applicable to a supersonic flow, can be employed for the development of an advanced ejector to be used in a heat-actuated heat pump.

The present paper reports the results of our laboratory experiments, which were designed to demonstrate that the mixing enhancement of a supersonic jet can also be achieved by using a nozzle with a noncircular cross section. This experimental investigation is the first stage of an attempt to develop an advanced supersonic ejector for heat pump applications using this new technology.

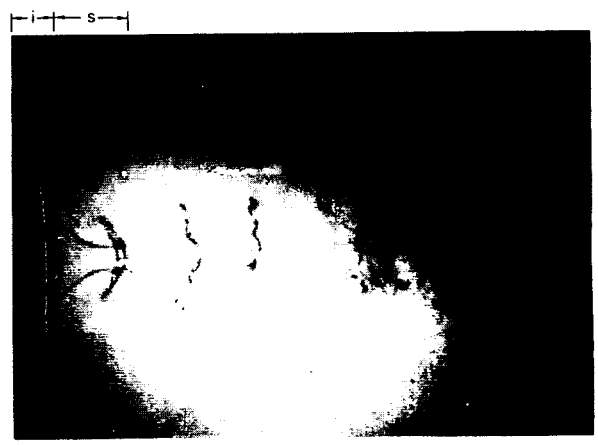

a. Major axis plane

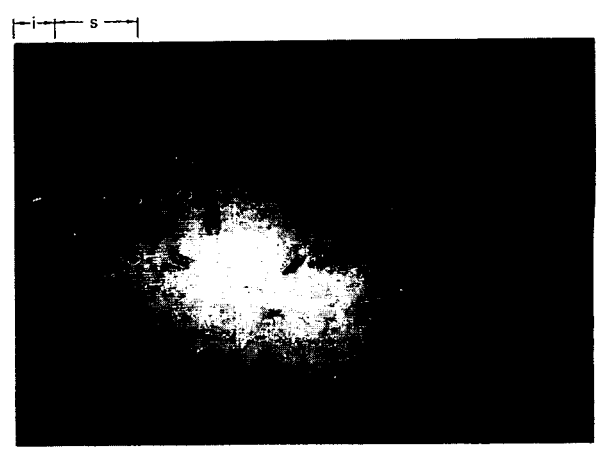

b. Minor axis plane

Figure 3. Contortion of Vortex Rings of an Elliptic Jet (from Ho and Gutmark[7])

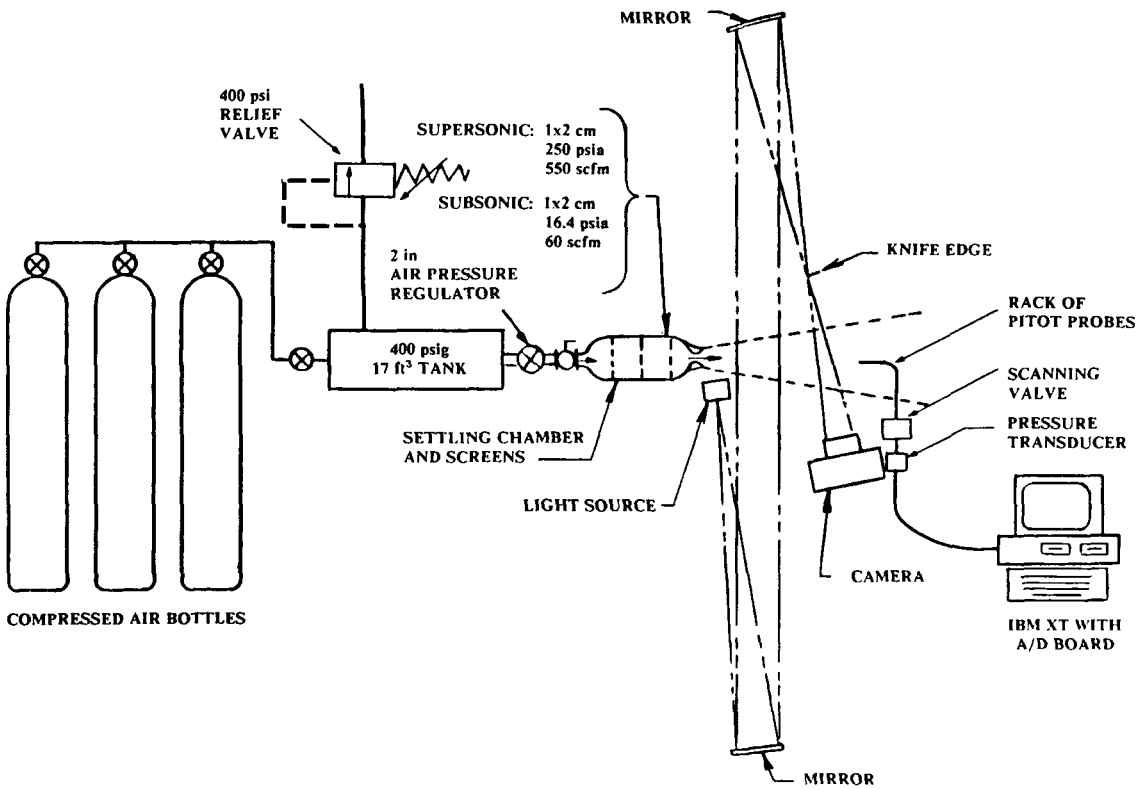

Figure 4. Air Simulation Ejector Test Apparatus

Experimental Apparatus and Procedures

To study jet entrainment using both flow measurements and flow visualization, we constructed a free-jet experimental facility that could provide air flows through subsonic and supersonic nozzles. The facility was sized to allow quantitative measurements of jet entrainment as well as flow visualization for studying the various subsonic and supersonic mixing flows.

As illustrated in Figure 4, the test facility consisted of bottles of compressed air, a large high-pressure tank, pressure regulators, control valves, the nozzle apparatus, a schlieren system, the pitot probe apparatus, and the data acquisition system. The 0.5-m^3 (17-ft^3) tank had a working pressure of 2.8 MPa (400 psi). At the outlet of the tank was a pressure regulator to control the nozzle stagnation pressure at 1.6 MPa (235 psia) for the supersonic tests and about 12 kPa above atmospheric pressure (1.7 psig) for the subsonic tests. On-off control was provided by a large ball valve to minimize flow constriction. The air then flowed into a small settling chamber with a honeycomb for removing flow nonuniformities and into the nozzle, which exited into the laboratory. Four interchangeable nozzles were designed and fabricated that attached to the settling chamber: a rectangular subsonic nozzle, a circular subsonic nozzle, a rectangular converging-diverging supersonic nozzle, and a circular converging-diverging supersonic nozzle. The rectangular nozzles had exit dimensions of 1x2 cm, with Mach numbers of 0.4 and 2.5 for the subsonic and supersonic nozzles, respectively. The circular nozzles for the reference tests had an exit diameter of 1.60 cm to provide the identical flow area as the rectangular nozzle. The stagnation temperatures were essentially room temperature.

The exit pressure of the nozzle was carefully adjusted to match the ambient pressure. Under- or over-expansion causes expansion fan or shockwaves to form outside of the exit. The streamline at the edge of the jet will be deflected as a result giving erroneous visual results of increased or decreased mass flux. This carefully matched pressure at the exit ensures that the mass flux entrainment is faithfully represented by the visual increase in the jet cross-sectional area.

Schlieren photographs of the jet flow from two directions provided good evidence of the differences in the initial mixing rate of the turbulent jet flow. Contrast was provided by the low temperature of the supersonic jet and by the addition of CO_2 for the subsonic jet. The schlieren system consisted of a spark source with a power supply, two 15-cm (6-inch) spherical first surface mirrors with a 110-cm (48-inch) focal length to form the parallel light passing through the turbulent flow, a knife edge, and a 35-mm camera with a doubler and a zoom lens placed about 25 cm (10 inches) from the knife edge to achieve the desired image size.

A special part of the apparatus was the light source for flow visualization. To provide high-quality flow visualization, we used the Xenon Nanolamp system, consisting of a power source, a lens and filter assembly, and a 20-ns pulsed light source. The pulse generation circuit is a capacitive discharge type that uses a ceramic thyratron as a switch. The light pulse has a radiation spectrum extending from radio frequencies to shortwave ultraviolet; a lens and filter assembly was used to reduce radio frequency noise from the arc and focus the light for sharper photographs.

Pitot probe measurements at 10 to 30 diameters downstream of the nozzle were also taken. The data were reduced

to give a first-order estimate of the mass flux entrained. These measurements have provided valuable information on the mixing enhancement in the near field, as will be discussed later.

Test procedures were developed for obtaining the schlieren photographs and the pitot measurements. For photographs, the schlieren system was always aligned first, with the zoom lens focused on the plane of the jet. The high-speed light source was triggered by the camera using the cable normally connected to a flash attachment; thus, the schlieren system operated in normal room-lighting conditions. The storage tank was filled, the pressure regulators were set, and the control valve was opened to start the run. With the auto-wind camera, there was no difficulty in taking two or more photographs on each test run.

For the pitot measurements, the procedure was more complicated. The pitot rack first had to be set at the appropriate standoff distance with the tube spacing adjusted to survey the whole jet. Then the traverse speed of the rack had to be set and its starting position established. The standoff distance, tube spacing, and traverse speed also had to be entered into the computer, which was then preset for the test run. The gas flow and the traverse mechanism were started together and, one second later, the computer was triggered to rotate the scanning valve and read the pressure transducer.

The data from the pressure transducer were fed into the data reduction software for computing the estimated mass flux. The data from the schlieren photographs were also used to estimate the mass entrainment rate. Since the stagnation pressure of the supersonic nozzle was set to provide exact pressure matching between the jet and the room air to prevent under- or over-expansion, the visual spreading angle measured in two directions was used to estimate the mass entrainment.

Results and Discussion

For ejector applications, standoff distances may be in the range of 2 to 8 nozzle diameters. Therefore, the entrainment characteristics in the "near field" are of the most interest. Hence, we shall concentrate on comparing the near-field entrainment of a supersonic rectangular jet with that of the supersonic circular jet. In the process, the subsonic results will also be discussed to emphasize the distinctive nature of supersonic mixing. Far-field measurements can also be used as auxiliary information to confirm the near-field results. The mixing characteristics will be analyzed in terms of flow visualization and the mass flux in the jet cross sections.

Figures 5a and 6a show schlieren photographs of the subsonic (Mach 0.4) and supersonic (Mach 2.5) flows downstream of a circular nozzle, respectively. The edges of the turbulent

a. Circular

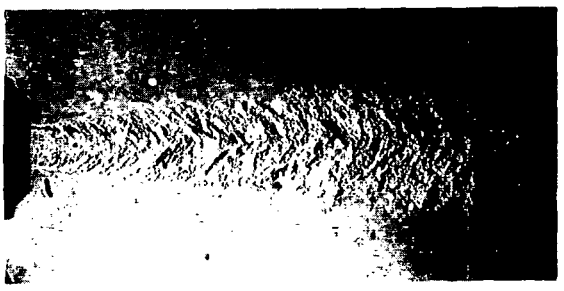

b. Horizontal rectangular

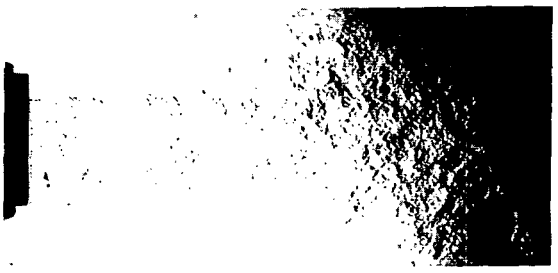

c. Vertical rectangular

Figure 5. Subsonic Schlieren Photographs

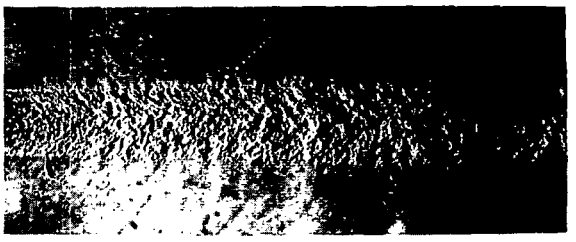

a. Circular

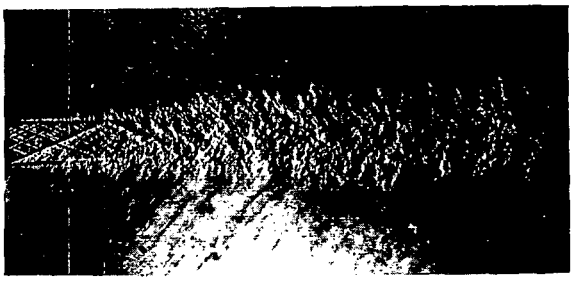

b. Horizontal rectangular

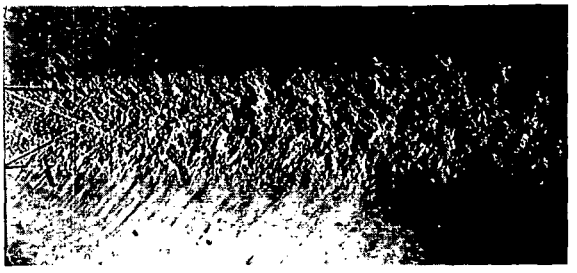

c. Vertical rectangular

Figure 6. Supersonic Schlieren Photographs

flow region represent the boundaries of the jet, since the turbulent motion of the fluid is the main mechanism for entrainment of the surrounding fluid. It is clear by comparing these photographs that the spreading angle of the subsonic jet is substantially larger than that of the supersonic jet. This result is consistent with recent experiments for a two-stream supersonic mixing layer in which the spreading angle of a supersonic mixing layer was found to grow at only 25% of that of a subsonic mixing layer.[8] This conclusion is also supported by the stability analysis of a supersonic mixing layer in which the growth rate of the hydrodynamic instability waves is shown to be very small in the supersonic regime. These visual results of the spreading of a circular jet serve as baseline cases for comparison with the performance of jets with noncircular cross sections.

The superior mixing characteristics of a rectangular subsonic jet are demonstrated in Figures 5a through 5c. At a downstream location, the cross-sectional area of the rectangular jet is clearly larger than that of the circular jet. In particular, the spreading angle of the "wide side," i.e., viewing parallel to the major axis, far exceeds that of the circular jet. This result agrees well with previous results of Ho and Gutmark.[6] They also measured the mass flux at various locations and found that the entrained mass flux of an elliptic jet can be as high as 5 times that of a circular jet 2 hydraulic diameters downstream of the nozzle exit. If a similar improvement in entrainment can be achieved for a supersonic jet, the noncircular jet can be used as the basis for developing an advanced ejector.

Figures 6a through 6c are schlieren photographs comparing a Mach 2.5 circular jet to a rectangular jet with the same Mach number. Indeed, the visual spreading rate of the rectangular jet is substantially higher than that of the circular jet. This high spreading rate is evident not only for the "wide side" but also for the "narrow side."

To illustrate the mixing enhancement of a rectangular jet, the ratio between the visual cross-sectional areas of a rectangular jet and a circular jet was plotted against the nondimensionalized streamwise distance from the jet exit in Figure 7. For a subsonic jet, the ratio attains its maximum value of approximately 1.9 at approximately 5 diameters downstream.

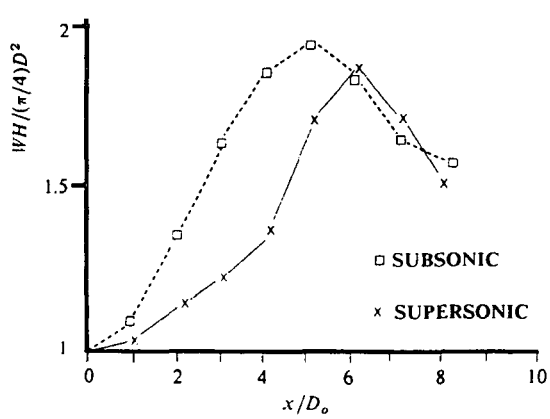

Figure 7. Rectangular/Circular Jet Area Ratio Versus Nondimensional Standoff Distance

For a supersonic jet, the location of the maximum is slightly further downstream at 6 diameters. The maximum value of this ratio is comparable to that of the subsonic jet.

In the far field 10 to 30 jet diameters downstream of the nozzle exit, the pitot pressure measurements provide some quantitative data on the mass flux of the jet. Figure 8 shows the entrained mass fluxes as functions of the axial distance for both the subsonic and supersonic flows and for the circular and rectangular jets. The slope of the curve represents the change in the entrainment ratio per the number of jet diameters downstream. In the far field, the behavior of the jet is relatively insensitive to the geometry of the nozzle. Hence, the slope is independent of the nozzle shape as expected and as shown in Figure 8. However, the enhanced near-field entrainment of a rectangular nozzle leaves a permanent "scar" far downstream. This "scar" reflects itself by shifting the origin of the entrainment curve, as can be seen in Figure 8. This shift is much stronger for a supersonic jet than for a subsonic jet. This evidence in the far field strongly supports near-field flow visualization results in suggesting the substantial near-field mixing enhancement of a rectangular jet at supersonic speeds.

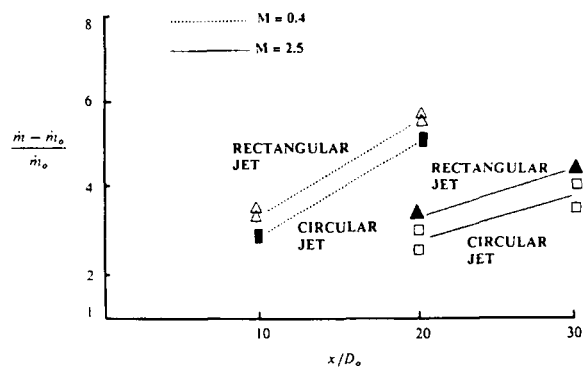

Figure 8. Far Field Entrainment in the Jet

Conclusions

A heat pump system using an ejector is simple in construction and has no moving parts. Hence, it is inexpensive to build and is highly reliable. The successful development of such a system critically depends on the development of a high-performance ejector. A supersonic ejector will provide the necessary compression ratio for the system. Unfortunately, the mixing characteristics of a conventional circular supersonic ejector are poor. Mixing enhancement is required for successful applications to a practical system.

The goal of the present investigation is to demonstrate that a passive mixing enhancement method using an ejector with noncircular cross sections, originally developed for a subsonic jet, is also effective when applied to a supersonic free jet. The experimental results shown here are very encouraging. In a free-jet configuration, the near-field entrainment of a rectangular supersonic jet is shown to increase substantially over the conventional circular jet.

However, this is only the first step in a series of investigations to establish the technological basis for the development of a practical ejector. The logical path for transferring this new technology to the proposed applications would next call for a demonstration that this mixing enhancement can also be applied to a confined jet, i.e., an ejector configuration, as we

are currently in the process of doing. In contrast to free-jet entrainment, the geometric configurations of the enclosing mixing chamber and diffuser may have strong effects on the entrainment. For example, it is still not clear whether the mixing chamber should have a rectangular or a circular cross section for effective mixing. With this resolved, the pressure recovery of the ejector will be investigated.

Various diffuser configurations will be considered. It is not immediately obvious how the confining mixing chamber for a rectangular ejector should be designed to minimize the pressure loss. Also, two potential basic configurations for the diffuser need to be considered. A shockless diffuser is very long and thus suffers from high friction losses, while a shock-compression diffuser has shock losses but is short and thus has less friction losses. Depending on the entrainment and the operating Mach number, the trade-off between the shock loss and the friction loss must be considered carefully.

Finally, the ejector parameters must be varied to maximize the performance, i.e., to obtain a high entrainment rate and high pressure recovery, under the constraint of the required compression ratio. Practical considerations for the development of a commercial product, such as size, manufacturing, and assembly requirements, must be recognized. In summary, we have taken a successful first step along the path of an investigation to develop an efficient supersonic ejector for heat pump applications.

Acknowledgment

This work was performed under a prime contract with the Department of Energy through subcontract 86X-95917V from Oak Ridge National Laboratory. The authors would like to thank Dr. Fang C. Chen and Mr. Richard Murphy of Oak Ridge National Laboratory for several stimulating discussions.

References

1. Chen, F. C. (1986) "On the Vertical Integration of Thermally Activated Heat Pump," *Technical Economics. Synfuels and Coal Energy - 1986. Proceedings of the Ninth Annual Energy-Sources Technology Conferences* (New Orleans, LA, Engineers), New York, p. 145.

2. Elrod, H. G. Jr. (1945) "The Theory of Ejectors," *Journal of Applied Mechanics. Transactions of the ASME*, p. A-170, September.

3. Murphy, R. W. (1986) "Ejector-Coupled Heat Pumps," Presentation to Energy Division, Oak Ridge National Laboratory, March 14.

4. Ho, C.-M., and Huerre, P. (1984) *Annual Review of Fluid Mechanics*, Vol. 16.

5. Ho, C.-M., and Huang, L.-S. (1982) "Subharmonics and Vortex Merging in Mixing Layers," *Journal of Fluid Mechanics*, Vol. 119 pp. 443-473.

6. Ho, C.-M., and Gutmark, E. (1986) "Visualization of a Forced Elliptic Jet," *AIAA Journal*, Vol. 24, No. 4, p. 684, April.

7. Ho, C.-M., and Gutmark, E. (1987) "Vortex Induction and Mass Entrainment in a Small-Aspect-Ratio Elliptic Jet," *Journal of Fluid Mechanics*, Vol. 179, p. 383, June.

8. Papamoschou, D., and Roshko, A. (1986) "Observations of Supersonic Free Shear Layer," AIAA Paper No. 86-0162.

9. Miles, J. W. (1958) "On the Disturbed Motion of a Plan Vortex Sheet," *Journal of Fluid Mechanics*, Vol. 4, Part 5, pp. 538-552.

Session 6

Thermally Activated Heat Pumps: Stirling Engine-Driven Heat Pumps

Organizer : F. C. Chen
Oak Ridge National Laboratory
Chairman: F. A. Creswick
Oak Ridge National Laboratory

An Overview of the Stirling Engine Heat Pump Program*

F. C. Chen
Oak Ridge National Laboratory
Oak Ridge, TN 37831

Abstract

This paper summarizes the recent developments in the Stirling engine-driven heat pump program activities sponsored by theDepartment of Energy (DOE) through Oak Ridge National Laboratory (ORNL). This technology has displayed its ability to meet the thermal performance objectives. Enhanced technology options guided by value engineering principles are being pursued toward the development of an economically viable household engine-driven heat pump.

Objective

The objective of this program is to advance the technology needed for the development of Stirling engine-driven heat pumps that will lead to more efficient use of fossil fuels in the space conditioning of residential and commercial buildings.

Introduction

A Stirling engine driven heat pump is a type of thermally activated heat pump (TAHP), providing high thermal efficiency, multifuel capability, and quiet operation. Among several Stirling engine variations, the free-piston type represents the most promising concept for residential applications because of its mechanical simplicity, its potential for long life and high reliability, and its compatibility with hermetic heat pump compressor design.

The primary benefits from free piston Stirling engine (FPSE) heat pumps[1] (HP) include energy savings, improved utility load utilization, increased elasticity in energy supply, better thermal comfort, increased resistance to foreign competition in the HVAC industry, and possible spinoffs in generic Stirling technology. Recognizing these needs, DOE initiated a program for the development of FPSE heat pump technology several years ago. While the technology continues to be viewed as a long-term, high-risk option, recent progress has enhanced its commercial potential, with possible product introduction in the 1990s.

The Market

The heat pump is unique in today's residential equipment market in providing both heating and cooling. An FPSEHP can replace a furnace and a conventional air conditioner concurrently. Virtually all U.S. residential buildings may use cooling at some time of the year (almost all new housing units <u>everywhere</u> in this country have air conditioning); therefore, examining present heating equipment types (Fig. 1) and energy usage by fuel type (Fig. 2) provides useful information on the scope of the potential residential use of Stirling engine-driven heat pumps.

The nation's 85 million residential units use about 15 quads of primary energy per year or 21% of the nation's total. Over half of all U.S. residences are heated by warm-air furnaces, and about 75% of all residences are heated with fossil fuels, primarily gas or oil.

In the commercial sector, the variety of heating equipment is considerable, because buildings vary greatly in size and purpose. Small and mid-size retail and office (known as light commercial) buildings are well suited to the use of Stirling engine-driven heat pumps; in fact a prototype of such a machine is currently under development by the Gas Research Institute (GRI). Light commercial buildings could use the FPSEHPs developed in this plan just as electric heat pumps were first developed for residences. The light commercial sector consumes about 6 quads of primary energy per year. Fuel use for space conditioning light commercial (<5000 sq ft) buildings in the United States is given in Fig. 3. Over 1.3 million of these units are served by oil and natural gas. Presently, almost all have furnaces or boilers.

The future market of FPSEHP vis-a-vis conventional fossil-fuel-fired heating technology is difficult to assess, based as it is on so many local variables (i.e., climate, local codes, utility availability, pricing, and policies), as well as on regional and national influences (i.e., energy costs). However,

*Research sponsored by the Office of Buildings and Community Systems, U.S. Department of Energy, under Contract DE-AC05-84OR21400 with Martin Marietta Energy Systems, Inc.

ORNL-DWG 88-7632

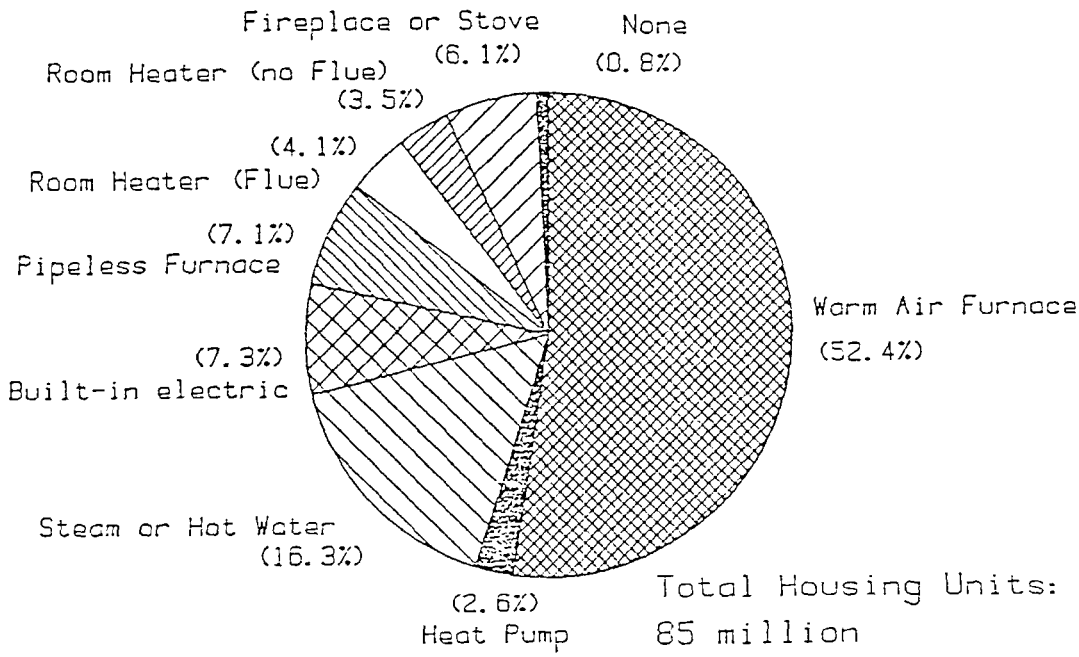

Fig. 1. National residential heating equipment distribution.

ORNL-DWG 88-7631

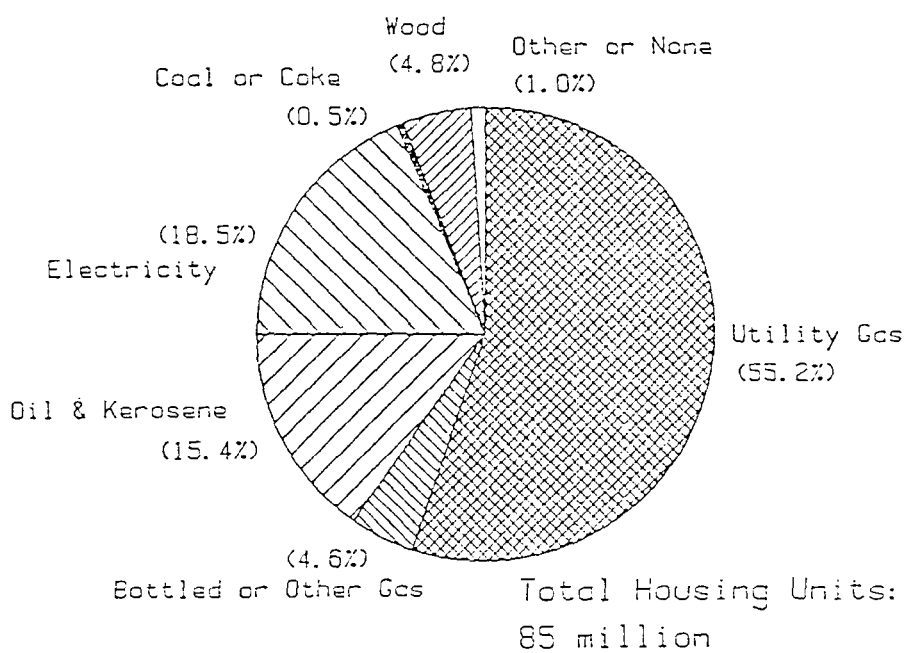

Fig. 2. Residential energy usage by fuel types.

ORNL-DWG 88-7633

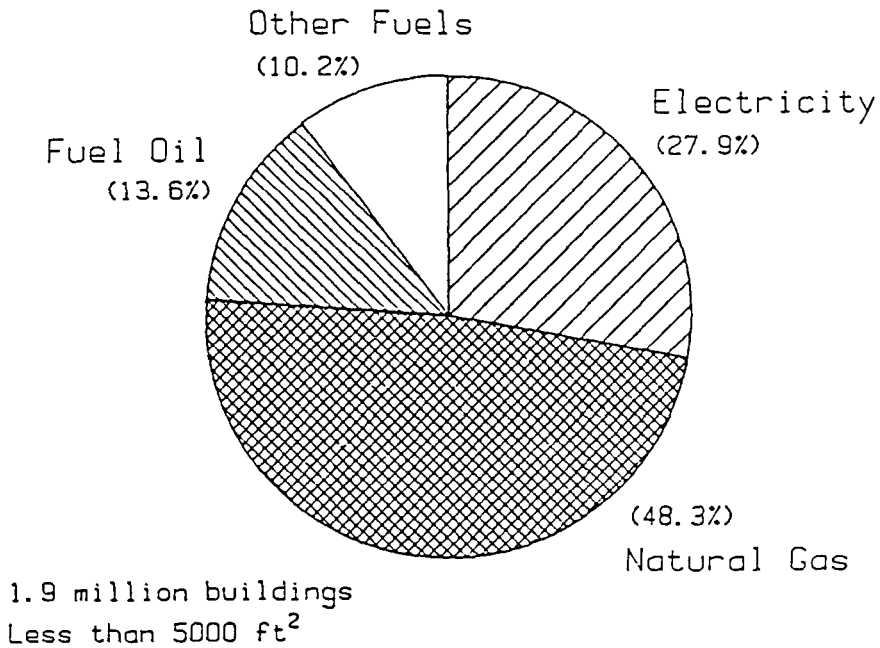

Fig. 3. Fuel types for heating light commercial buildings.

the 55.2% of total U.S. housing units (47 million units) and the 48% of light commercial buildings (1.3 million) currently dependent on gas will be the potential initial market for FPSEHPs.

Program Strategy

The general strategy to develop a viable FPSEHP technology may be divided into five steps: 1) novel concept evaluation, 2) laboratory experimentation, 3) engineering design, 4) prototype development, and 5) technology transfer. Each of the R&D stages treats particular aspects of the development problem, and all may require some types of supporting fundamental research or technical economic assessment.

In the first phase, novel component and system concepts are evaluated and from these the most promising concepts are selected for further evaluation. In the second phase, the laboratory work necessary for advanced component development and supporting research of a basic and applied nature is carried out. Advanced component concepts are developed and separately tested to ensure their viability within a full system. A full breadboard system is developed and can be tested and iterated as necessary. This phase of development focuses primarily on FPSE and transmission/compressor (T/C) performance. Third phase efforts will focus on the design and development of prototype systems resulting from information and data obtained from laboratory testing of breadboard systems in the second phase. This third phase focuses on system reliability, performance, and manufacturability. In the fourth phase, units will be fabricated for field test and evaluation, with cost sharing coming from the private sector. Industrial participants are brought to the program as early as possible, hence, the technology transfer phase, to some degree, is ongoing throughout FPSEHP development.

Background

In recent years, many FPSEHP approaches have been conceived, including duplex Stirling[2], resonance tube[3] (Fig. 4), Rankine cycle inertia compressor, hydraulic T/C (Fig. 5), direct connecting, and magnetic coupling concepts. Only a few have been examined, notably the the FPSE/Rankine inertia compressor[4] and hydraulic T/C[5] concepts and more recently the magnetic coupling concept.

ORNL-DWG 88-7636

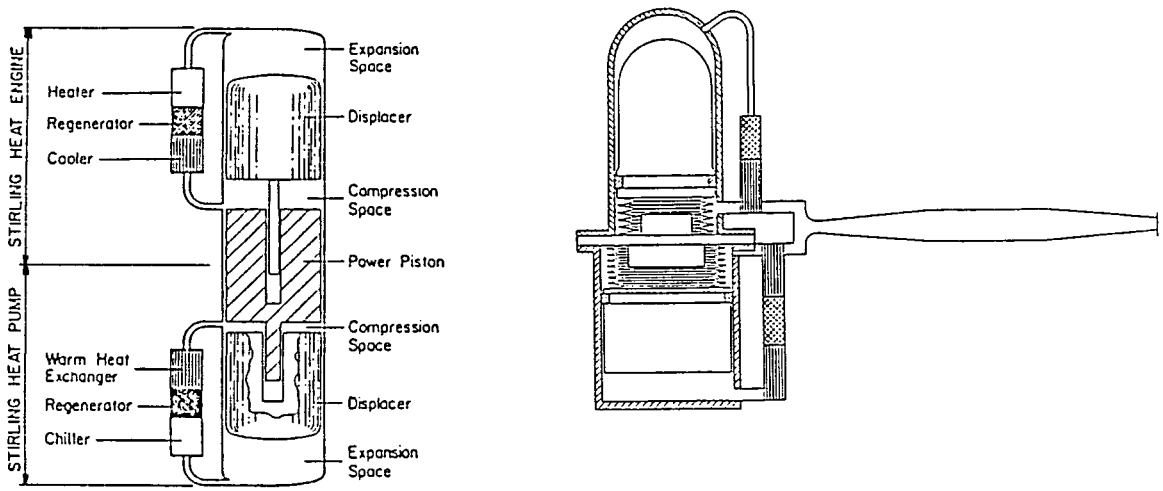

(A) FREE PISTON TYPE

(B) RESONANCE TUBE TYPE

Fig. 4. Duplex Stirling heat pumps.

ORNL-DWG 88-7637

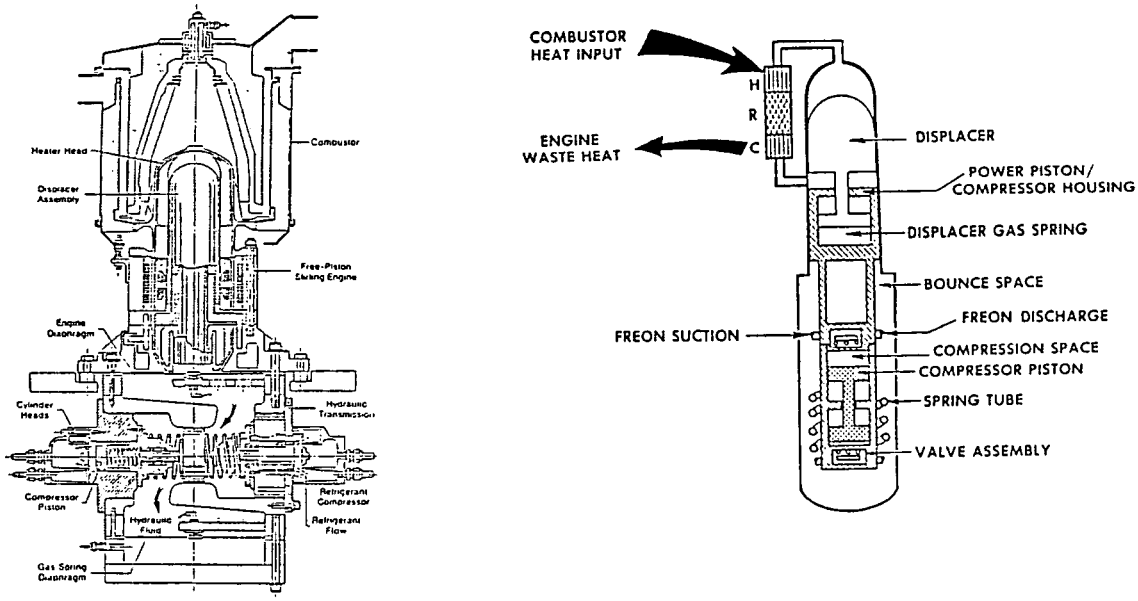

(A) HYDRAULIC-COUPLED STIRLING/RANKINE HEAT PUMP

(B) HYDRAULIC-COUPLED STIRLING/RANKINE HEAT PUMP

Fig. 5. FPSE with Rankine cycle heat pumps.

Technical challenges include design of effective hermetic coupling of the engine and the vapor compressor, control of a tuned resonant system over a wide range of loads, and demonstration of a basic capability to achieve the performance targets.

The program is oriented toward systems development projects, and the GRI has been a major co-sponsor of the hardware development efforts with DOE/ORNL. The program has also accommodated a limited level of supporting research, international cooperation, and technology assessment. These have contributed to advancing the state of technology on issues such as load matching, cyclic heat transfer, research needs, and engine options. Cooperative efforts with NASA and DOE-Energy Conservation Utilization Technology, and projects with university researchers have played important roles in these supporting technology activities. A schematic of the program activities is shown in Fig. 6.

The technology feasibility and acceptable thermal performance have been verified (Table 1). As far as the technology transfer is concerned, questions still remain on the life, reliability, market, and economics of the system.

Technical Status

Currently DOE/ORNL is funding five subcontracted technology development activities as shown in Table 2. These projects are in addition to the in-house technical support and cooperative work through the participation in the International Energy Agency (IEA) Annex XI--Stirling technology for applications in buildings. Two of the subcontractors, MTI and Sunpower, Inc. are systems development related. The other three (NASA, MIT, and ADL) are in supporting research and assessment activities that address the three more important technical issues identified during the course of the hardware development work. Many other issues remain to be examined.

Hydraulically Coupled FPSE/Heat Pump Development (Subcontractor: MTI)

The objective of this project is to develop a commercially viable hydraulically coupled T/C module that can be driven hermetically by existing and/or advanced FPSEs. The combined Stirling/Rankine HP system will have a targeted capacity of 3-ton cooling and coefficient of performances (COPs) of 1.7 (heating) and 1.0 (cooling).

ORNL-DWG 88-7639

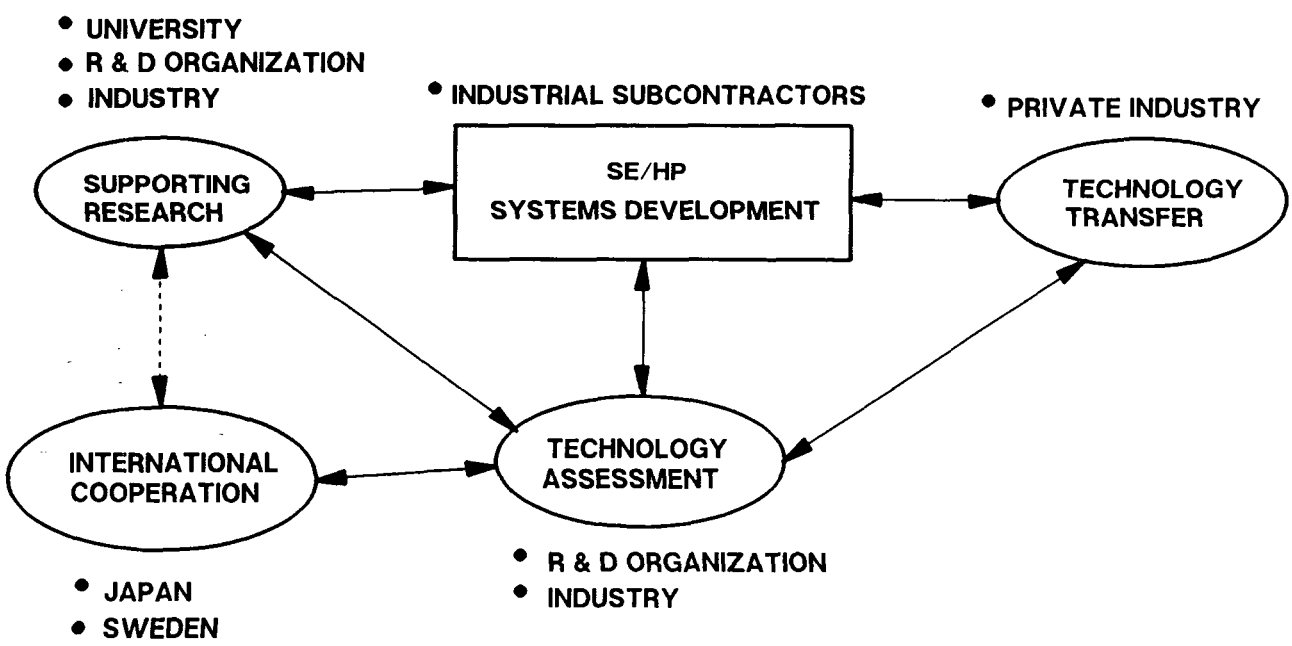

Fig. 6. Schematic of Stirling engine heat pump activities.

TABLE 1
FPSE HEAT PUMP PROGRAM GOALS

Parameter		Commercial Targets	Proof-of-Concept Targets	Present Status Mark I Heat Pump
Unit Capacity:				
Heating, 47°F	(Btu/hr)	70,000	70,000	60,000
17°F	(Btu/hr)	—	—	35,000
Cooling, 95°F	(RT)	3	3	3.2
COP (HHV)				
Heating, 47°F		1.70	1.50	1.61
17°F		—	—	1.20
Cooling, 95°F		1.10	1.00	0.98

RT — Refrigeration Tons

TABLE 2
FPSEHP PROGRAM ACTIVITIES

- **ADVANCED HYDRAULICALLY COUPLED FPSEHP**
- **MAGNETICALLY COUPLED FPSEHP**
- **INHOUSE TECHNICAL AND MANAGEMENT SUPPORT**
- **INVESTIGATION OF FPSE POWER AND LOAD COUPLING**
- **INTEGRATION OF ANALYSIS AND EXPERIMENTS FOR STIRLING SYSTEMS**
- **COMPARATIVE ASSESSMENT OF KINEMATIC AND FREE-PISTON STIRLING TECHNOLOGY**

As one of the first of the FPSE/Rankine systems concepts investigated by DOE for residential applications and a major hardware development effort on Stirling engine heat pump technology until recently, this concept is cosponsored by GRI in the FPSE development. Power produced from a FPSE is transferred through a hermetically sealed engine diaphragm to a hydraulic transmission device. In turn, this device passes the engine power to a refrigerant compressor through deflection of the engine diaphragm and deformation of the hydraulic fluid.

The technology development effort has gone through a couple of hardware modifications, which have overcome engine instability and load matching problems and improved heat pump performance and power transmission. The demonstrated capacity to date has surpassed

the proof-of-concept (POC) target of 3 refrigeration tons. The technical results achieved and the progress made to date on the heat pump power module are the subject of a paper to be given by MTI in this conference[6]. At present, the project effort is concentrated on the value engineering, long life, and reliability requirements needed for an advanced design. This concept and technology could provide the first entry of fuel-efficient and super-quiet next generation gas-fired packaged residential heat pumps.

Magnetically coupled FPSE Heat Pump (Subcontractor: Sunpower, Inc.)

This project will utilize state-of-the-art magnetic materials in conjunction with component optimization and innovative systems design and development to provide a mid-term engine-driven heat pump. The Sunpower FPSE for the heat pump applications is a derivative of the military ground power unit. It has a power output range of 3-7 kW that is suitable for heat pumping in residential and small commercial buildings. Since the initial project effort last summer, a magnetic transmission test rig (Fig. 7) has been assembled. The rig is intended to test and characterize the critical component leading to the design and development of a magnetically coupled FPSEHP module. To date, the magnetic coupling/compressor test rig has been successfully operated at a frequency of 60 Hz with a compressor force load of 1400 Newtons and a power transmission of 3 kW. The technical progress and status of this project will be given by Sunpower[7] during this conference.

Inhouse Technical Support (ORNL)

The inhouse technical support by ORNL is an integral part of the Stirling engine heat pump program which is one element of the DOE TAHP program. This project is closely related to the other projects in the Stirling engine heat pump area. As such it disseminates the technical data generated in systems and component testing and analysis projects for overall technology development. It analyzes the technical progress made in other projects to identify the needs and to resolve them in the advancement of the technology.

Early in the project, the poor performance obtained and the lack of understanding of the free-piston engine tests were identified. An inhouse technical effort was focused on the development of a computer code[8] to simulate the performance of a free-piston Stirling engine (Fig. 8) and to improve our understanding of the engine dynamics and its interaction with a heat pump. By utilizing this computer code and through the inhouse supporting research, we at ORNL were able to assist MTI in identifying the cause of the engine instability experienced during the heat pump test. Based on suggestions derived from our inhouse analysis, stable engine operations were achieved. Our analysis of the hydraulic transmission has pinpointed design requirements for high efficiency that have improved the power transmission efficiency from 35% to better than 80%. The combination of a stable engine, improved power transmission, and good engineering practice, as exercised

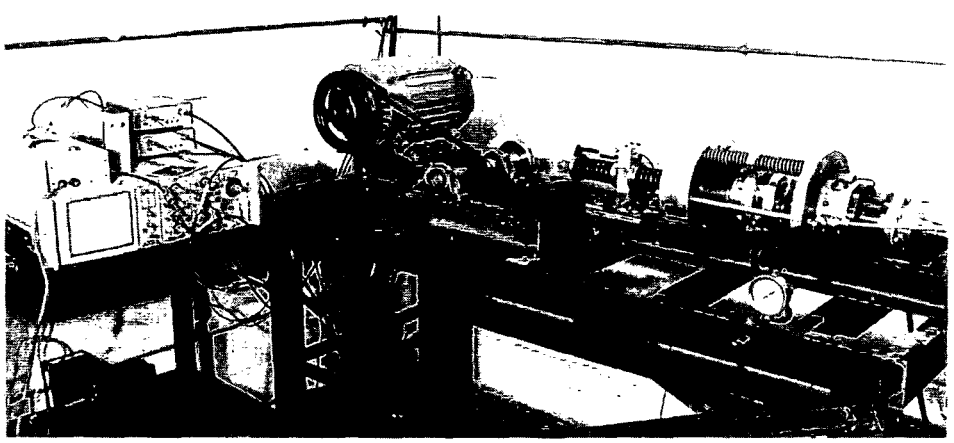

Fig. 7. Magnetic coupling/double acting compressor test rig.

ORNL-DWG 88-7630

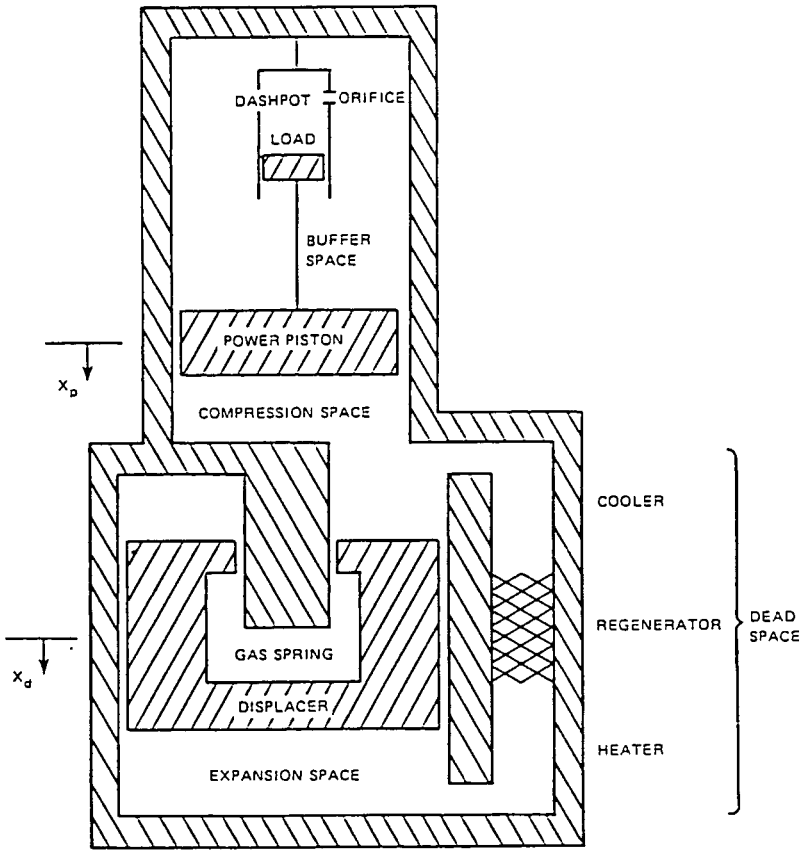

Fig. 8. Simplified schematic of RE-1000 free-piston Stirling engine.

by MTI has resulted in elevation of the Stirling engine heat pump module cooling capacity from 1.0 to 3.2 refrigeration tons surpassing the POC target.

After achieving the steady-state performance targets, the supporting research effort was shifted to the capacity control strategies to take full advantage of the variable capacity that an FPSE heat pump (Fig. 9) can offer. An evaluation of engine control[9] was performed and six control options were examined. The option of a displacer alternator control was found to be an effective way to modulate the heat pump capacity, although the engine average pressure or compressor clearance volume controls would yield better thermal efficiency at part load.

This supporting research will continue to analyze the technical progress made in an effort to assist in the successful development of the technology.

In the international cooperative effort, ORNL is active in the strategic assessment of Stirling technology for applications in buildings and is cosponsored by Japan and Sweden. Current activities include technology assessment workshops, comparative analysis of technology options, and development of joint R&D projects. Upon completion of the current effort in late 1988, it is anticipated that a better perspective can be derived of the Stirling technology and its applicability in different parts of the globe, and increased international cooperation on common R&D needs can be jointly sponsored.

Investigation of FPSE Power and Load Coupling (NASA, Lewis Research Center)

Development of FPSE for space power generation has been a NASA project for quite some time. The common interest in making an efficient FPSE has led to the cooperative project to

ORNL-DWG 88-7634

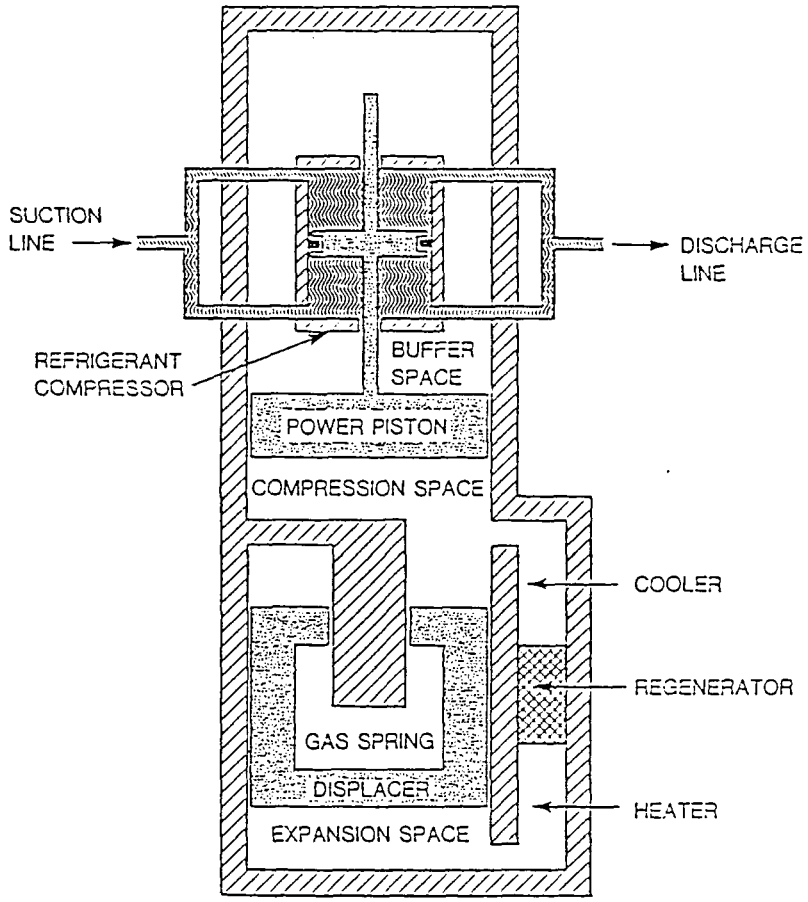

Fig. 9. Schematic of RE-1000 FPSE with compressor.

investigate some of the generic problems in the technology, such as engine characterization, dynamic load interaction, and life expectancies of key engine components.

This project is intended to address technology issues early in the systems' development. It is to provide test data that will increase fundamental understanding of the behavior of an FPSE and its intended applications in building equipment and to be used to update and validate an engine performance simulation code for engine systems design analysis.

In the early 1980s, under an Inter Agency Agreement between NASA and DOE, Lewis Research Center (LeRC) undertook the development of generic FPSE technology applicable to TAHP and to space power. Activities include FPSE characterization, computer code verification, 1000-hour engine endurance test, and load matching. The test engine was an existing RE-1000 1-kW FPSE.

To date, the performance of the RE-1000 FPSE has been characterized with a dash pot load using two types of displacers[10]. Using the test data, an FPSE performance simulation computer code has been validated. A 1000-hour engine endurance test under electric generator load had been completed without any major component failure. The tests showed that an FPSE has the potential of long life and high reliability. A continuation of the endurance test to 10000 hours is being pursued, without the assistance of DOE.

Currently, a hydraulic load simulator has been connected to the FPSE (Fig. 10) for conducting engine/load interaction tests. It is anticipated that the test results will

ORNL-DWG 88-7635

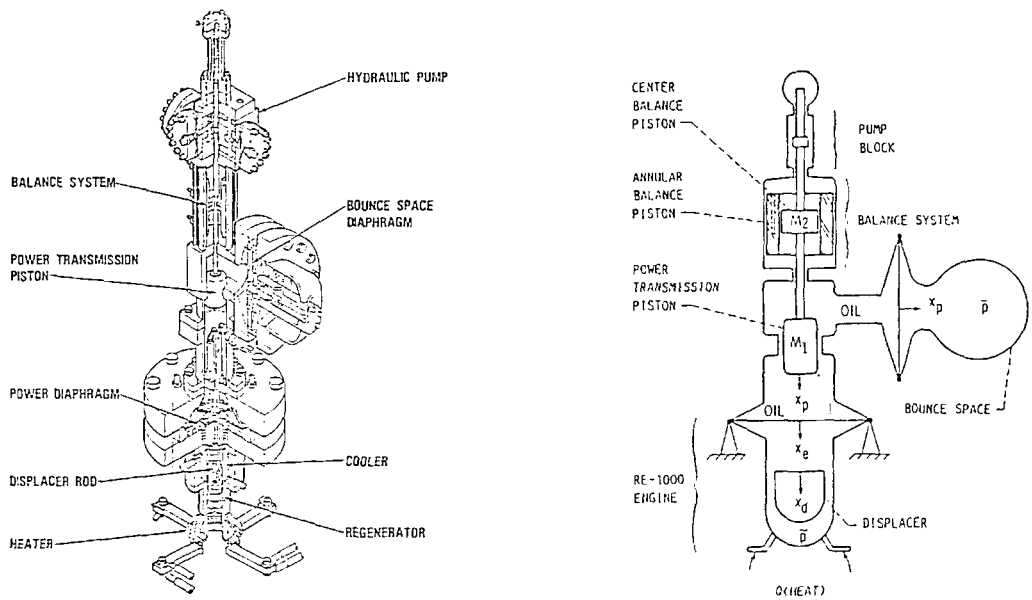

(A) CUTAWAY VIEW OF THE RE-1000 FREE-PISTON STIRLING ENGINE WITH HYDRAULIC LOAD

(B) SCHEMATIC OF HYDRAULIC OUTPUT DEVICE

Fig. 10. Schematic of RE-1000 test rigs.

be very useful in the development of control strategy for future generations of FPSEHPs.

Integration of Analysis and Experiments for Stirling Cycle (Subcontractor: MIT)

This project is to develop an integrated rational design methodology for Stirling machines to minimize errors between engine test results and computer performance predictions.

An accurate computer performance prediction code is almost a must in a modern systems design methodology. Previous Stirling code work has been aimed at prediction of overall performance, and the validity of the modeling of the individual components and processes has been assumed. In the early development work of this program, significant discrepancies existed between engine test results and computer predictions. These were often attributed to a lack of understanding and inadequate modeling of cyclic heat transfer in a Stirling engine. This project is part of the supporting research, and the intent is to analyze the cyclic heat transfer and to devise an integrated approach for the development of a better design simulation code.

The project began in late 1985 and is a 3-year effort to investigate the cyclic heat transfer in a Stirling machine, both experimentally and analytically, and to develop methodology to simulate performance. The initial work of the cyclic heat transfer in a cylinder (Phase I) has been completed, and the heat transfer in a combined cylinder and heat exchanger is in progress. The technical progress of the project, especially the heat transfer power loss correlation developed for gas spring design analysis, is presented in the paper[11] given by MIT.

Comparative Assessment of Kinematic and Free-Piston Stirling Technology (Subcontractor: A.D. Little, Inc.)

This project is a technology assessment activity. Its purpose is to expedite our effort in the delineation of the attributes of free-piston and kinematic Stirling engines (KSE) as heat pump drives for applications in buildings. The FPSE and the KSE are the major technology options in external combustion

engines that can be used for heat pump drives. KSE technology is more developed than that of FPSE and is more vigorously pursued by the Japanese and the Swedish for applications in buildings. However, an FPSEHP can be packaged with relative ease into a hermetically sealed unit. Partly for this reason, DOE/ORNL has been concentrating on the development of an FPSEHP for the residential market. As part of the IEA activities and utilizing the expertise of the Japanese and the Swedish in KSE and the United States in FPSE, this project will provide a strategic assessment and data on the state of the Stirling technology in general for applications in buildings.

This effort is a continuation of the assessment of FPSEs as heat pump drives. It is a 2-year effort to be completed by mid-1988. Its technical progress will be presented in the paper[12] to be given by A.D. Little in this conference.

ACKNOWLEDGMENTS

This work was sponsored by the Office of Buildings and Community Systems, U.S. Department of Energy under contract DE-AC05-84OR21400 with Martin Marietta Energy Systems, Inc. The author appreciates the reviewers' comments and the editorial effort provided by E. Rodgers.

REFERENCES

1. R. Hutchinson, B. Ross, and F. C. Chen, "Free-Piston Stirling Engine Heat Pump Program Plan," Revised Draft, June 1987.

2. Sunpower, Inc., "Duplex Stirling Heating-Only Gas-Fired Heat Pump," Phase II, GRI Contract 5081-341-0464, Gas Research Institute, Chicago, March 1983.

3. J. Budliger, "New Concept for a Stirling-Stirling Heat Pump System," ASME Paper, 87-WA/AES-5, December 1987.

4. General Electric Co., "Development and Demonstration of a Stirling/Rankine Heat Activated Heat Pump," ORNL/sub/82-17485/1, November 1984.

5. R. A. Ackermann, "Free-Piston Stirling Engine Diaphragm-coupled Heat-Activated Heat Pump Component Technology Program," Phase 1C, ORNL/sub/86-47985/1, July 1987.

6. R. A. Ackermann, "Development of a Hydraulically Coupled Free-Piston Stirling Engine Heat Pump Compressor," Proc. 1988 DOE/ORNL Heat Pump Conf., April 1988.

7. W. Beale, "Preliminary Assessment of a Magnetically Coupled Free-Piston Stirling Engine Heat Pump Compressor," Proc. 1988 DOE/ORNL Heat Pump Conf., April 1988.

8. N. C. J. Chen and F. P. Griffin, "Linear Harmonic Analysis of Piston Stirling Engines," ORNL/CON-172, June 1986.

9. F. P. Griffin, N. Domingo, and F. C. Chen, "Evaluation of Power Control Methods for Free-piston Stirling Engine Driven Heat Pumps," Proc. 22nd IECEC, August 1987.

10. J. Schreiber and S. Geng, "RE-1000 Free-piston Stirling Engine Hydraulic Output System Description," NASA/TM-100185, October 1987.

11. A. A. Kornhauser and J. L. Smith, "Integration of Analysis and Experiments for Stirling Cycle Processes, Part 1--Experimental Study of Gas Spring Hysteresis Loss," Proc. 1988 DOE/ORNL Heat Pump Conf., April 1988.

12. W. P. Teagan, "Comparative Assessment of Free-piston vs. Kinematic Stirling Engines as Heat Pump Drives," Proc. 1988 DOE/ ORNL Heat Pump Conf., April 1988.

Development of a Residential Free-Piston Stirling Engine Heat Pump

R. A. Ackermann
Mechanical Technology, Inc.
Latham, NY 12110

Abstract

After several years of development, the free-piston Stirling engine heat pump (FPSE/HP)* has successfully demonstrated proof-of-concept targets. The performance targets were achieved during an off-site test and evaluation program conducted at the Lennox Industries Engineering Center. The performance achieved for the module was a cooling thermal coefficient of performance (COP) of 0.91 and a heating thermal COP of 1.62. In addition to its performance achievement, the FPSE/HP module demonstrated good reliability in over 60 days of operation and ran stably and repeatably over a range of ambient conditions from 0 to 105°F.

This paper will provide a description of the FPSE/HP module tested at Lennox, describe the developmental history of the FPSE/HP at Mechanical Technology Incorporated (MTI), and present the results of the Lennox tests. This work has been a collaborative effort between MTI, Oak Ridge National Laboratory (ORNL), the Department of Energy (DOE), and the Gas Research Institute (GRI). The financial and technical support provided by ORNL, DOE, and GRI was responsible for the successes achieved.

Historical Developments

In 1981, MTI was awarded a contract by DOE/ORNL to design and fabricate a lower end, transmission and compressor, to mate with an existing MTI FPSE. The objective of this program was to demonstrate the performance potential of an FPSE/HP. The lower end was designed for a residential application requiring 3.0 tons of cooling at the 95°F ambient temperature conditions. A second goal was to demonstrate stable, reliable operation over a range of ambient temperature conditions from 17 to 95°F. Prior to the program, researchers were unable to demonstrate stable performance with an FPSE/HP, and there was concern that it was inherently unstable.

The lower end design for this program is shown in Figure 1. The existing MTI FPSE, the engineering model engine proposed as the driver for the lower end, is shown in Figure 2. To distinguish the lower end components, it is assumed that the lower end consists of two primary elements: the hydraulic transmission and the refrigerant compressor. The hydraulic transmission is designed to transfer power from the engine to the compressor through the deflection of the engine diaphragm. Referring to Figure 1, the deflection of the engine diaphragm creates a force unbalance across the counterweight forcing it to move. Because the oil is incompressible, the compressor piston (plunger) is also acted upon, but in the opposite direction to the counterweight. Through this reverse motion of the counterweight and compressor piston, the lateral vibration of the system is eliminated. The lower

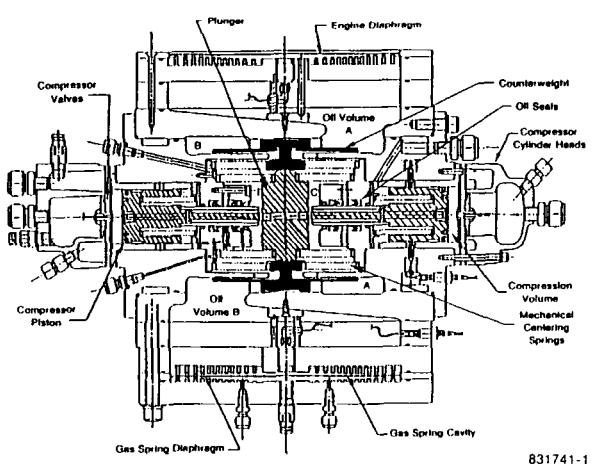

Fig. 1 Compressor and Hydraulic Transmission Layout

*Engine/transmission/compressor assembly.

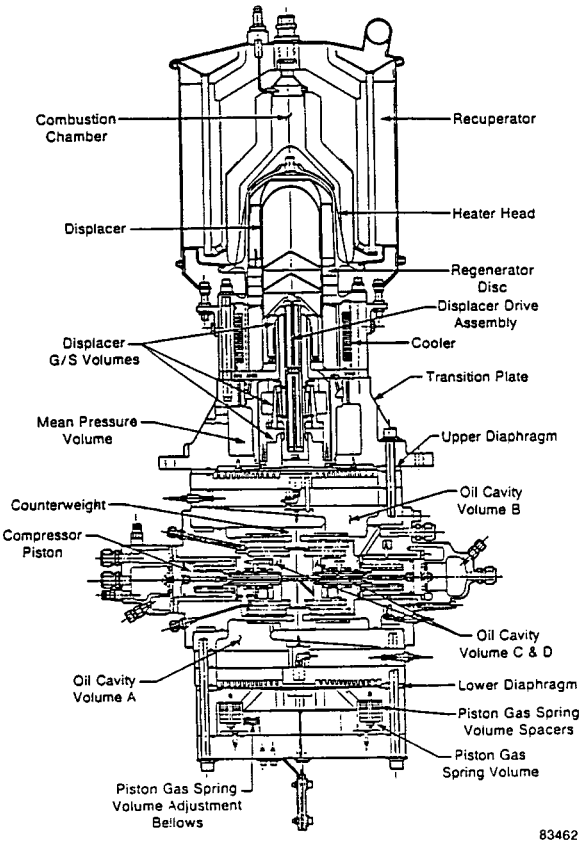

Fig. 2 Engineering Model FPSE/HP

gas spring diaphragm and the gas spring developed in the compressor volumes provide the restoring force for the plunger.

The compressor consists of the compression volumes located on either side of the compressor pistons, the valve plate assemblies, and the compressor cylinder heads. A conventional refrigerant compressor design was followed for the compressor components, and an opposed, two-cylinder compressor, where the compression and expansion processes are 180° out of phase in each cylinder volume, was selected to balance the cyclic forces on the plunger.

The engineering model FPSE driver is shown in Figure 2. It consists of an external heater system: a natural gas combustor and monolithic engine heater head; thermal components: a regenerator, cooler, and a displacer which shuttles the working fluid (helium) through the thermal components between the expansion (hot) and compression (cold) volumes in the engine. Two unique features of this engine are that the displacer is supported by a gas bearing and employs close-clearance seals to eliminate rubbing of the moving elements, and the use of a linear drive motor to control and modulate the displacer stroke.

The breadboard system described above was first assembled in March 1983 and tested through the completion of Phase I in September 1983. During this initial testing, the breadboard system was operated at four ambient temperature points: 95, 80, 47, and 17°F, and demonstrated:

- Stable operation at each of the four conditions
- Mechanical integrity of the system and the longevity of the metal diaphragms
- Workability of the hydraulic transmission and its potential as an efficient coupling between the engine and the compressor.

The major shortfall of the breadboard system was that it did not achieve the rated 3.0 tons of refrigeration at the 95°F ambient conditions. Instead, only 1.0 ton was achieved. A follow-on program (Phase IA) was initiated in November 1983 to determine the reasons for the shortfall.

Analysis of test data and computer simulation performed during Phase IA showed that the compressor and hydraulic transmission losses were significantly larger than originally predicted. This resulted in a load stiffness that prevented the engine from achieving its rated output power. This is shown in Figure 3, in which the hydraulic transmission and compressor load characteristics are plotted along with the engine's power output characteristics. The intersection of these two curves represents the operating point for the system. As shown in the figure, the increased transmission losses raise the load line of the transmission and compressor, which produces a lower piston stroke and a reduced engine PV power output. This result is analogous to a rotary prime mover in which too high a starting load will prevent the machine from reaching its full speed. By reducing the load, the speed will increase and the machine will produce its rated power.

A subsequent matching analysis based on the engine load matching criteria presented identified two major areas for improvement. First, the hydraulic losses had to be reduced to reduce the starting load on the engine. Second, the transition plate required to adapt the engineering model engine to the lower end produced excessive dead volume and restrictive flow passages that were degrading the engine performance. Based on these

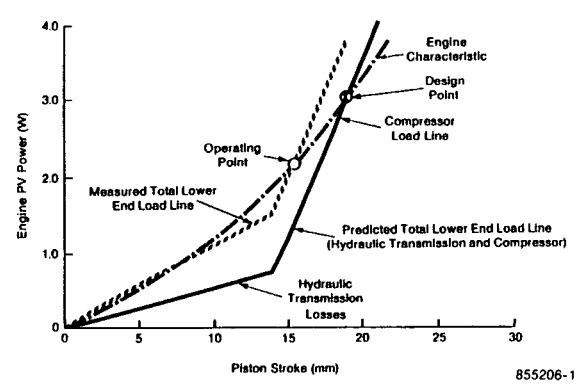

Fig. 3 Representative Lower End and Engineering Model FPSE Power Characteristics

results, a program was formulated to address the lower end losses. Under a parallel program supported by GRI, it was decided that the displacer drive system in the engineering model engine should be redesigned to improve the engine performance by improving the transition plate design. This redesign was begun in 1983, with plans to mate the new engine to the breadboard lower end prior to the Lennox evaluation.

During the next phase of the program (IB), several of the more important losses identified in Phase IA were investigated experimentally. In particular, the compressor piston seals and the hardware associated with the critical clearance seals in the hydraulic transmission were modified, and several different hydraulic transmission fluids were tried. The results obtained were encouraging in that the improvements made produced a capacity increase from 1.0 to 2.0 tons of cooling. However, the increase to 3.0 tons was not achieved, but the testing did show that the internal counterweight was responsible for the largest loss in the hydraulic transmission. In order to achieve a large reduction in the losses, therefore, the internal counterweight would have to be removed. The internal counterweight was removed from the hydraulic transmission by replacing it with an external vibration absorber. Several absorber designs were considered, and a tuned spring mass system that could easily be mounted to the compressor housing was selected. The design of the absorber is schematically shown in Figure 4, and the modified lower end with the internal counterweight removed is shown in Figure 5.

Figure 6 shows the occurrence of events described above and relates the major milestones to the dates they occurred. As shown, the modified lower end was integrated with the advanced displacer drive (the Mark I) in 1986 to form the Mark I FPSE/HP shown in Figure 7. The Mark I FPSE/HP proved very successful in achieving its

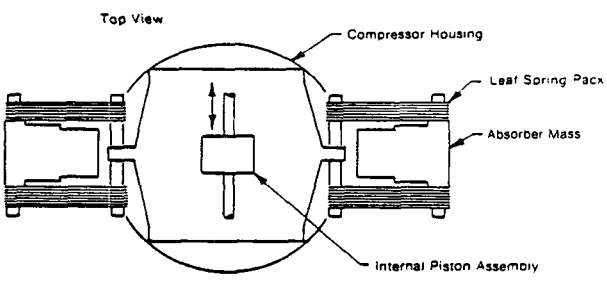

Absorber Specifications

Absorber Dynamic Mass	38 lb_m (each side)
Housing Effective Mass	285 lb_m
Unbalance Force	2442 lb_f – 57.8 Hz. Due to 16.5 lb_m Piston at 22-mm Stroke
Leaf Springs	13 Springs Per Pack: 17-7 PH, 0.071-in Sheet
Maximum Bending Stress	35 ksi at Maximum Stroke = 0.204 in.

852947-3

Fig. 4 Vibration Absorbers

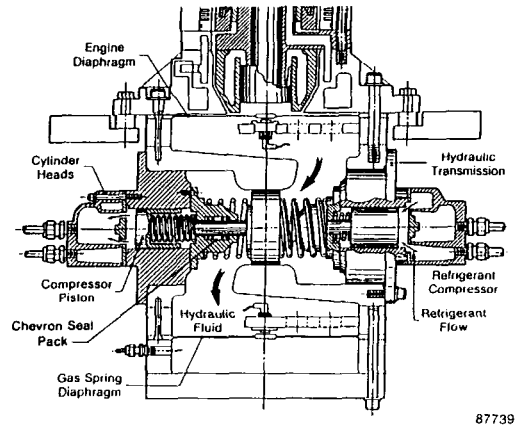

Fig. 5 Hydraulic Transmission Showing Chevron Seal Pack Location

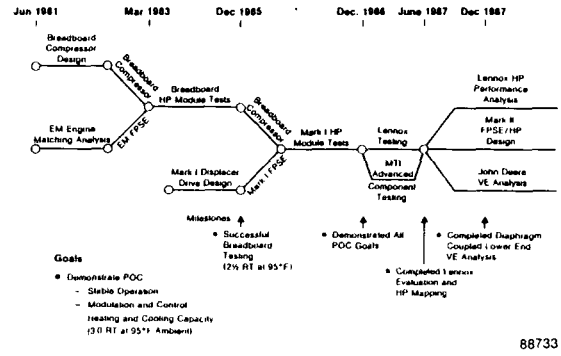

Fig. 6 FPSE/HP Historical Development

original performance goals of 3.0 RT* capacity at the 95°F ambient temperature conditions, an overall lower end efficiency of 68%, and an engine efficiency of 25%. With this success, it was decided that the unit was ready for shipment to Lennox Industries for their evaluation.

Lennox Testing

Testing of the Mark I heat pump module was performed at the Lennox Industries engineering facility during the period of 1 April 1987 through 29 May 1987. The results presented herein were obtained from the Lennox testing using their laboratory calorimeter test setup. The testing had two major objectives:

1. To verify the reported performance of the Mark I over a range of ambient conditions from 0 to 95°F

2. To map the performance of the heat pump module over a broad range of evaporator and condenser conditions and compressor piston strokes.

*RT = Refrigeration Tons = 12,000 Btu/hr.

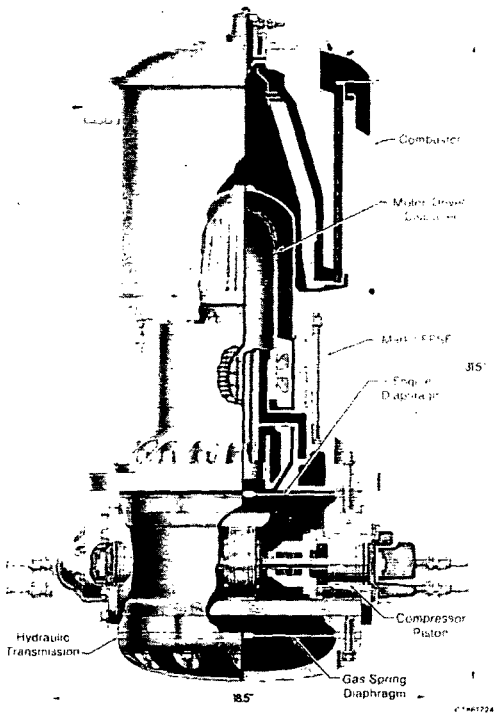

Fig. 7 Mark I FPSE Heat Pump Module

The Mark I heat pump module performed very well at Lennox. The module accumulated over 140 hr of operating time during the test period and provided performance data at 72 test points ranging from evaporator and condenser conditions equivalent to ambient temperature conditions from 0 to 105°F.

The Lennox Test Plan prescribed four series of tests that were designed to meet the objectives. These were:

- Verification testing
- Qualification testing
- Parametric mapping tests
- Variable cooler temperature testing.

The verification testing consisted of a single operating point test that was run periodically to ensure that the unit was performing consistently and the data were repeatable. Typically, this test was run at the beginning of each new series of tests or whenever there was a concern that the unit's performance might be changing. The qualification testing consisted of running the specified ambient temperature conditions given in Table 1, and measuring heating and cooling capacity at these points and the unit's thermal COP. The parametric mapping tests were performed to describe the unit's performance over a wide range of evaporator and condenser saturation temperature. Table 2 presents all of the proposed mapping points, as well as the operating

Table 1

Heat Pump Test Conditions for R-22 Refrigerant

	Ambient Temperature								
	Cooling				Heating				
Test Parameter	95°F	87°F	80°F	Test Point 2	47°F	32°F	17°F	0°F	Test Point 1
Discharge Pressure, psia	277.4	225.4	196.5	311.5	210.6	202.1	196.5	183.1	241.0
Saturation Temperature, °F	121	105	95	130	100	97	95	90	110
Suction Pressure, psia	90.7	94.7	98.7	90.7	76.2	57.7	42.9	29.8	69.6
Saturation Temperature, °F	45	47.5	50	45	35	20	5	-12	30
Suction Temperature, °F	55	57.5	60	55	45	30	15	-2	40
Pressure Ratio	3.06	2.38	1.99	3.43	2.76	3.50	4.58	6.14	3.46

*Includes at least 10°F superheat.

Table 2

Planned Test Matrix

Test Condition Number	Discharge Pressure (psig)	Suction Pressure (psig)	Liquid Temperature at Flowrator (°F)	Suction Temperature (°F)	Number of Compressor Strokes	Comments
Verification Testing						
1	261.0	75.6	106.0	51.2	1	See notes
Qualification Testing - Cooling						
2	296.8	76.0	115.0	65.0	2	ARI rating point
3	262.7	76.0	106.0	55.0	2	95°F OD point
4	210.8	80.0	90.0	60.0	3	87°F OD point
5	181.8	84.0	80.0	65.0	4	80°F OD point
Qualification Testing - Heating						
6	226.3	54.9	95.0	50.0	4	ARI rating point
7	195.9	61.5	85.0	45.0	4	47°F OD point
8	187.4	43.0	82.0	30.0	3	32°F OD point
9	181.8	28.2	80.0	15.0	2	17°F OD point
10	168.4	15.1	75.0	-2.0	1	0°F OD point
Parametric Testing						
11	143.6	10.1	70.0	0.0	3	80°F condition/-20°F suction
12	143.6	24.0	70.0	20.0	3	80°F condition/0°F suction
13	143.6	43.0	70.0	40.0	3	80°F condition/20°F suction
14	168.4	10.1	80.0	0.0	3	90°F condition/-20°F suction
15	168.4	24.0	80.0	20.0	3	90°F condition/0°F suction
16	168.4	43.0	80.0	40.0	3	90°F condition/20°F suction
17	195.9	24.0	90.0	20.0	3	100°F condition/0°F suction
18	195.9	61.5	90.0	55.0	3	100°F condition/35°F suction
19	195.9	84.0	90.0	70.0	3	100°F condition/50°F suction
20	259.9	43.0	105.0	40.0	3	120°F condition/20°F suction
21	259.9	61.5	105.0	55.0	3	120°F condition/35°F suction
22	259.9	84.0	105.0	70.0	3	120°F condition/50°F suction
23	296.8	43.0	115.0	40.0	3	130°F condition/20°F suction
24	296.8	61.5	115.0	55.0	3	130°F condition/35°F suction
25	296.8	84.0	115.0	70.0	3	130°F condition/50°F suction

Notes

1. Each test condition should be at steady state, in which none of the performance parameters differ from scan to scan by more than 3%. There should be at least three scans per test condition at 10-min intervals.
2. The engine coolant loop (water chiller rig) should be maintained at 2.5 gpm for all test conditions.
3. The engine coolant inlet temperature shall be 34°F for verification testing and all other test conditions. All qualification and parametric testing should be repeated for 70°F inlet temperature. Qualification test conditions (3) and (9) shall be performed at an additional cooling water inlet temperature of 104°F.
4. No oil should be returned to the suction line and provisions to capture and measure oil circulation (as percent of refrigerant flow) shall be performed at qualification test conditions (3) and (9).
5. The compressor stroke (capacity) and the engine operating parameters shall be controlled by personnel at the MTI operator's console. The compressor stroke will vary from 50% to full stroke.
6. There is a total of 144 test points excluding verification testing that will be repeated from day to day depending on the repeatability of the data with data recorded at MTI.

conditions for the verification and qualification tests. The variable cooler temperature testing was designed to determine the effect of raising the cooler temperature from 5 to 45°C on the unit's COP in both the heating and cooling modes. The results of the above testing are summarized below.

Verification Testing

Figure 8 presents the variation in the thermal cooling COP and engine efficiency over the 60-day test period. As shown, the unit performed well over this period and no degradation in performance was detected.

Qualification Testing

Figure 9 presents the results of the qualification testing. These data show the maximum capacity achieved at each ambient condition, the corresponding thermal COP, and the modulated capacity of the unit. Capacity modulation with this unit is achieved by varying the displacer stroke through the control provided by the displacer linear motor drive. In Figure 9, the measured data are referenced to the heating and cooling requirements (thermal load line) for a typical home in the mid-Atlantic region requiring 3.0 RT of cooling at 95°F. The thermal COP (COP(Thermal)) is defined as the ratio of the heating or cooling capacity (corrected to 15°F subcooling) to the thermal input energy (firing rate) based on the higher heating value of the fuel:

$$\text{COP (Thermal)} = \frac{\text{(Heating/Cooling Capacity)}}{\text{Firing Rate (HHV)}}$$

For the heating capacity, this includes 85% of the heat rejected by the engine to the coolant and the compressor capacity. As shown in Figure 10, the recovered heat used in the calculation includes only 60% of the total heat rejected from the heat pump module, or only that heat that can easily be recovered from the engine coolant.

The milestones achieved during this testing were:

	Capacity	Performance
Heating (47°F)	60,000 Btu/hr	1.61
Cooling (95°F)	3.2 RT	0.91

Parametric Mapping

Parametric mapping was performed to provide the performance maps required to evaluate the seasonal performance of the FPSE/HP. Maps were generated for the following parameters:

- Refrigerant flow versus evaporator temperature (ET), condenser temperature (CT), and piston stroke (Xp)
- Condenser reject heat versus ET, CT, and Xp
- Natural gas firing rate versus ET, CT, and XP

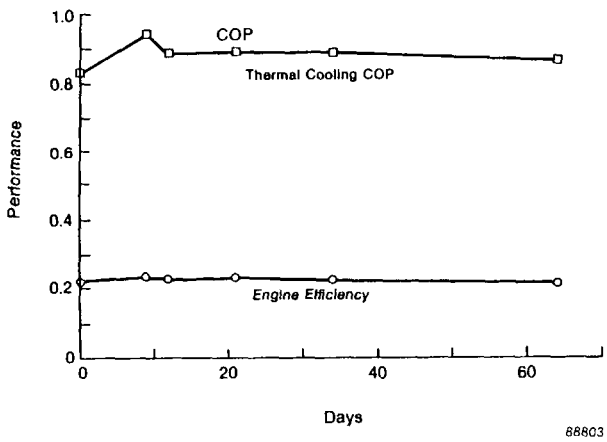

Fig. 8 Verification Test Data

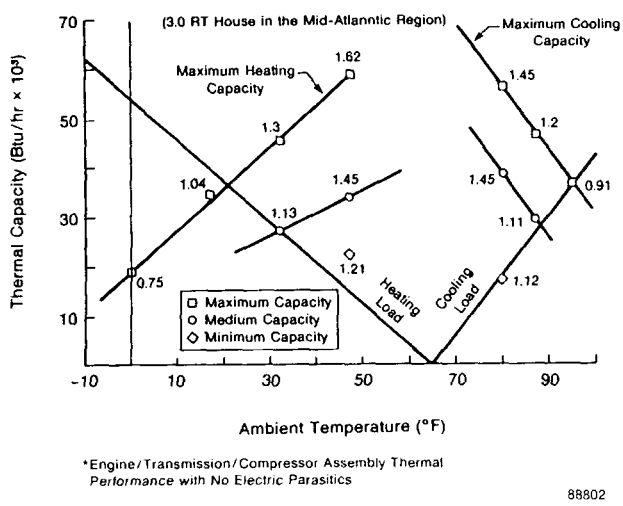

Fig. 9 Mark I FPSE/HP Performance*

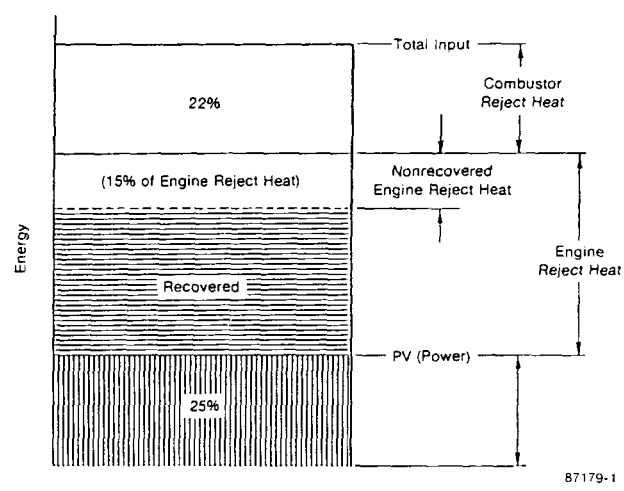

Fig. 10 Engine Heat Recovery

- Engine reject heat versus ET, CT, and Xp
- Displacer motor power versus ET, CT and Xp.

A typical plot obtained from these data is shown in Figure 11. As shown, these data were very consistent and the functional relationship between the dependent and independent variable well defined. The curves presented in Figure 11 enable one to quickly evaluate the performance of the unit at any specified evaporator and condenser saturated temperature.

Variable Cooler Temperature Testing

When the engineering model FPSE/HP was first run, it was necessary to maintain a 0°C coolant temperature in order to achieve the necessary PV power to drive the lower end. The Mark I engine represented a major improvement enabling the 3.0 RT capacity to be achieved at elevated cooler temperatures. The objective of this testing was to determine how the elevated cooler temperatures affected performance. Figure 12 shows the effect of cooler temperatures on engine efficiency and thermal cooling COP, and Figure 13 presents the effect on displacer motor power. As shown, the thermal efficiency and cooling COP are not affected by the elevated temperature. However, the displacer motor power must be increased to

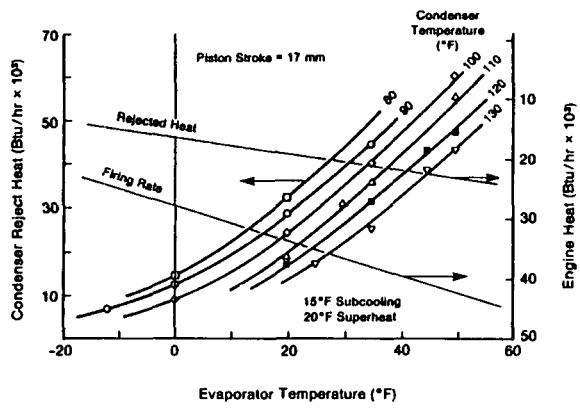

Fig. 11 Heat Pump Heating Performance*

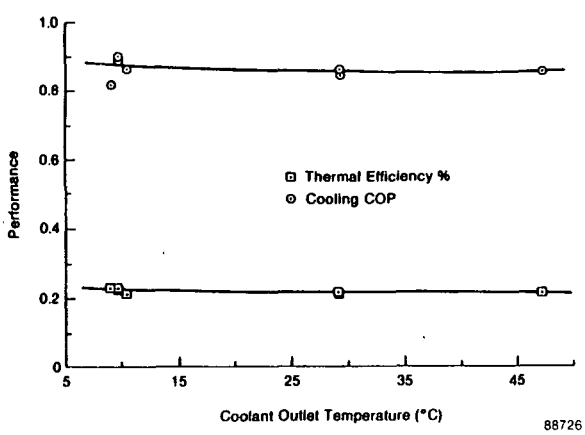

Fig. 12 Performance versus Coolant Temperature

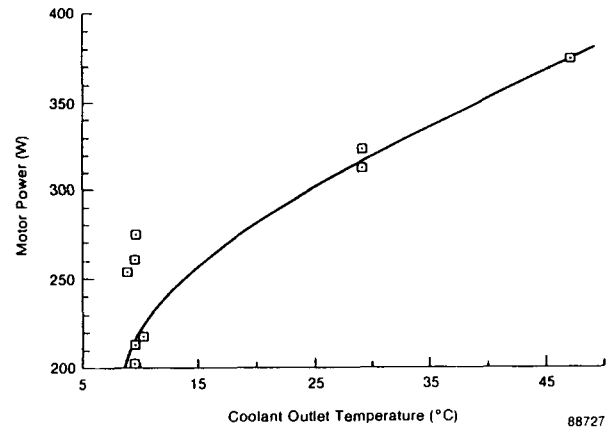

Fig. 13 Motor Power versus Coolant Temperature

maintain fixed capacity at the verification point. The cooling performance achieved at the 95°F ambient conditions for a coolant outlet temperature of 48°C (118°F) was:

- Capacity = 2.92 RT
- Thermal COP = 0.89.

Conclusions

Considerable progress has been made with the FPSE/HP through its six years of development at MTI. That development has involved the design and fabrication of a hydraulic transmission and compressor, the matching of that lower end to the engineering model FPSE, and the modifying of the FPSE through the design of an advanced displacer drive system. The Lennox testing of the Mark I FPSE/HP has demonstrated the unit's repeatability and reliability and was successful in achieving all of the proof-of-concept targets. Through the Lennox testing, the goals established in 1981 have all been achieved, and a watershed has been reached for future developments. The task at hand is to establish the goals for commercializing the FPSE/HP and evaluating the unit's potential for achieving those goals. A summary of the results achieved with the Mark I FPSE/HP and a comparison of the measured goals with the performance goals set in 1981 is given in Table 3.

Table 3

Comparison of Measured Results with Original Performance Targets

Parameter	FPSE/HP Targets	Mark I FPSE/HP Serial No. 2 Measured Data
Date	1981	Scan 32, 1/6/88
Ambient Temperature (°F)	95	95
Coolant Temperature (°F)	80	83
Cooling Capacity (RT*)	3.0	3.0
Displacer Motor Power (W)	<500	612
Engine Efficiency (%)	27.5	25.3
Hydraulic Trans. Efficiency (%)	82.7	83.7
Compressor Isentropic Eff. (%)	83.2	81.5
Lower End COP	3.63	3.78
HP Thermal COP	1.00	0.96

*Refrigeration tons.

Preliminary Assessment of a Magnetically Coupled Free-Piston Stirling Engine Heat Pump Compressor

W. T. Beale and *G. Chen*
Sunpower, Inc.
Athens, OH 45701

Summary

The potential advantages of direct magnetic coupling of a free-piston Stirling engine with a vapor compressor are being investigated experimentally. Results to date indicate no problems with dynamics, mechanical arrangement, efficiency or deterioration. The problems of size and cost remain, but these are determined by the properties of the magnetic material, which are improving rapidly. If the magnet material becomes available at a satisfactory price, the work undertaken here will facilitate a commercially attractive magnet drive system.

Introduction

The free-piston Stirling/vapor compressor combination has long been considered a desirable candidate for the heat-driven heat pump application. The hermetic sealing capability of the free-piston Stirling engine (FPSE), along with its very low noise and potential for long life make it attractive, and the high performance potential of the vapor cycle at low temperature difference, as is required of air-conditioning service, make it the preferred cycle. In the several attempts to use this combination, the problem which has proven to be most challenging is the coupling between the two machines. Previous attempts included the inertia compressor, the flexing diaphragm, and the direct shaft drive with sliding seal. Each of these methods has drawbacks in the form of complex dynamical interactions, mechanical complexity or life.

Another approach to achieve the goal of hermetically sealed heat-driven heat pumping is to use the already advanced free-piston Stirling/linear alternator to drive a conventional electrically operated heat pump. This has the advantage of versatility, since the electric power produced could be diverted to other needs as well as to the heat pump, but the cost relative to the direct drive is an impediment.

In comparison to these, the magnetic coupling gives promise of direct coupling, hermetic sealing, and mechanical simplicity. Its major and obvious drawbacks are size and cost. Until extremely powerful and inexpensive magnets became available, the magnetic coupling was of little interest to commercial producers of heat pumps. With the advent of such magnets in commercial quantities and relatively attractive prices, it became reasonable to investigate the characteristics of magnetic couplings and the systems which might use them. This report outlines the progress made in that direction during the preceding eight months of a DOE-sponsored effort to investigate the characteristics of magnetically coupled free-piston Stirling/vapor compressors.

Basic System Considerations

The concept of the free-piston Stirling/vapor compressor system is shown in Figure 1. The magnetic coupling is in effect a very stiff spring between the power piston of the Stirling engine and the vapor compressor piston, effected by a magnetic field linkage between the inner and outer magnet rings arranged to attract each other. The pressure vessel of the Stirling engine between the magnets serves to separate the two working fluids, helium for the Stirling engine, and a refrigerant for the vapor cycle system. In operation, the Stirling engine sees a load from the compressor and other system components, which is the equivalent of a damper, mass and spring, the same load which is seen by the FPSE when it is driving conventional loads, such as a linear alternator. The imposition of the stiff spring coupling does not increase the complexity of the system dynamics except to allow a small phase shift between the piston and compressor. In an ideally designed system, the maximum force which must be transmitted by the magnetic coupling need only be the damping force, since system inertia and spring forces may be designed to cancel one another. The allowed deflection of the magnetic coupling should be as close as possible to the point of instability (one-half the magnet ring width) in order to permit a minimum mass of magnet (Figure 2).

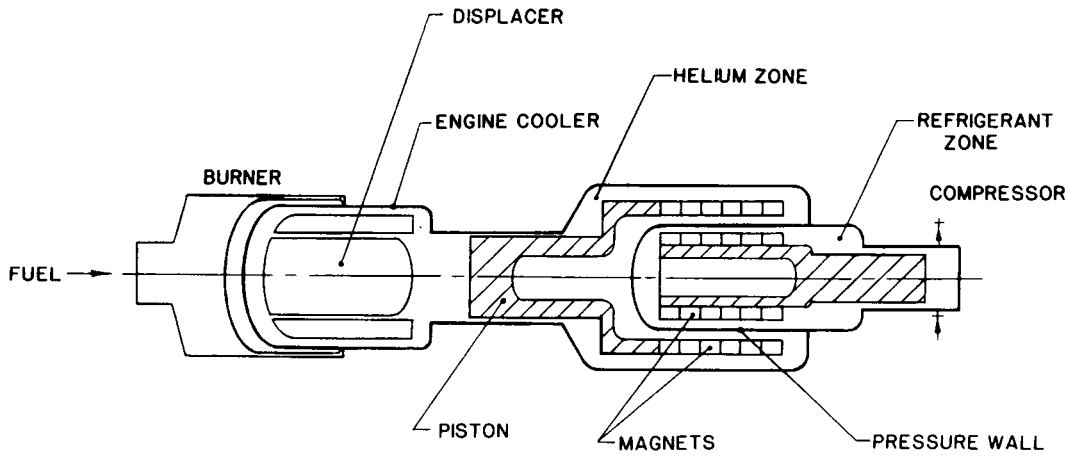

Figure 1: Schematic of FPSE/Magnetic Coupling/Compressor

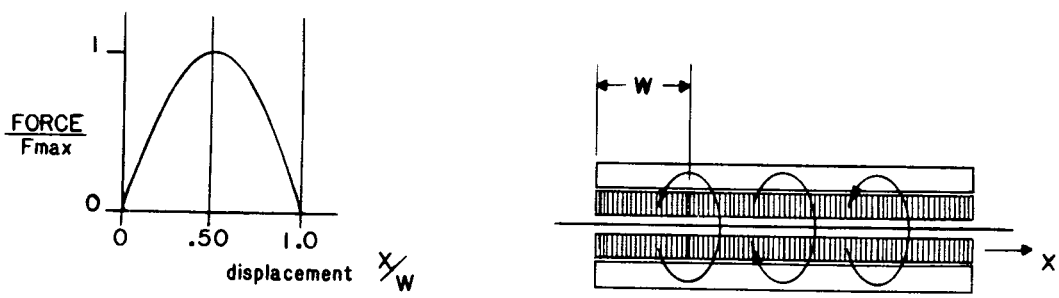

Figure 2: Force-Deflection Characteristic of Magnetic Coupling

In practice with the vapor compressor subjected to varying pressures and temperatures over the operating range of the heat pump, the situation becomes more complex. If the system is balanced in inertia and spring effects at one operating pressure, it may not be so at higher or lower pressures. This deviation from balance depends on the magnitude of the damping and spring effects from the compressor pressure, in comparison with those from the mass and other spring effects within the system. But in a typical 3 kilowatt engine/compressor design, it turns out that the variation in compressor damping and vapor spring contributions to the system dynamics is only about 5 percent of the total spring rate required to balance the oscillating mass of the piston and coupling; the effect on dynamics of the vapor cycle pressure variation is small over the operating range of the compressor. This means that a single point design may be expected to work well over the entire compressor pressure range.

There remains, however, the problem of matching the power output of the engine to the required power of the compressor. If the engine is designed to match compressor power at one pressure (and temperature) and at a set piston stroke, then it will tend to overstroke at lower compressor pressures, and understroke at higher pressures unless some power control method is exercised. Power from an FPSE

can be varied by changing displacer-piston phase angle or amplitude, by changing engine operating pressure, or by other methods, some purely mechanical and some electrical in their function. In operation, it would be necessary to have one of these power modulation systems in order to match engine output with compressor power demand. It is, incidentally, inappropriate to consider heater head temperature as a power control method, since not only is the thermal mass of the heater head very high in most instances, but also the thermodynamic performance is determined by heater temperature, which should, therefore, be kept at the maximum allowed by the structure.

It is always desirable, of course, to sweep the full available stroke of the compressor to avoid thermodynamic losses associated with partial delivery of the compressed vapor. This is facilitated with free-piston machines since an interference of piston with cylinder head is not necessarily damaging. This is because the engine piston is not driven by a stiff mechanical linkage, but instead only by the working gas forces. Also, for the same reason, liquid slugging in the compressor does not threaten the structural integrity of the system as it might in a linkage-driven device. Also, start up of the system occurs at low amplitude, further reducing such problems. These are unique advantages of free-piston machines not shared by linkage-driven machines.

Since the size and cost of the magnetic coupling are so critical to the commercial attractiveness of the system, it is desirable to minimize the magnetic force requirement. This can be done by operating the system at a maximum frequency and maximum stroke, since the power transmitted per unit of magnetic force is inversely proportional to both of these values. The maximum frequency is limited by the flow losses in both the engine and compressor, and the stroke is limited by other design considerations, such as the area available for compressor inlet and outlet valves.

Experimental Program

In order to investigate the details of the magnetic coupling, the present program was established with the following initial goals:

Determine the force-mass-geometrical relations for a magnetic coupling.

Investigate the effect of common refrigerants on available powerful magnetics (iron-boron-neodymium).

Design, fabricate and operate a test rig comprised of a mechanical driver, a magnetic coupling, and a vapor compressor and measure the dynamic characteristics and power transmission capability.

Design a complete Stirling/coupling/compressor system for evaluation before proceeding to a possible second phase system construction.

At the time of the writing of this report, all of these tasks have been completed. The optimum geometry of a magnetic coupling has been determined analytically and experimentally. From this, volume,

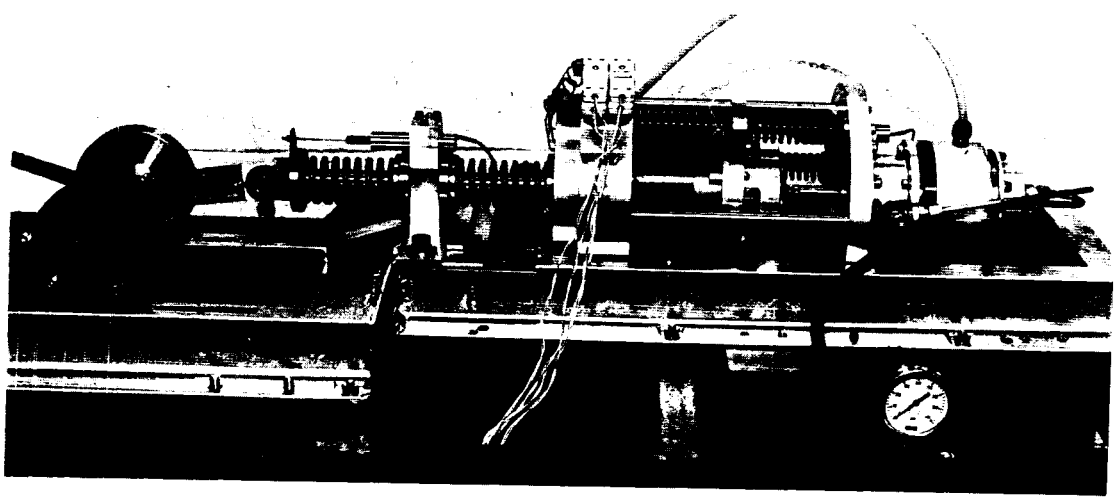

Figure 3: Magnetic Coupling/Compressor Test Rig

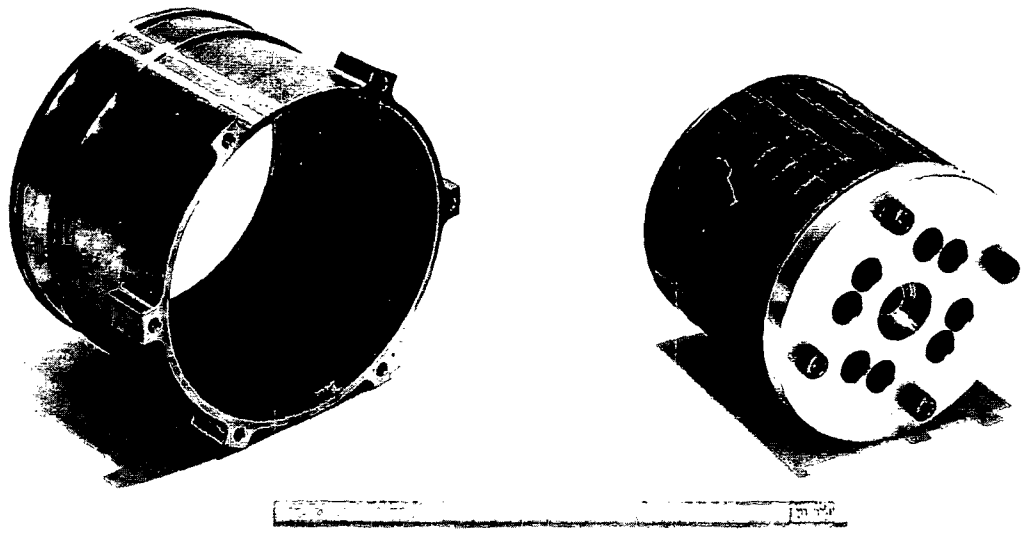

Figure 4: Magnetic Coupling Components

mass, and cost values for magnetic couplings are readily available as a function of the properties of the magnetic material.

The test rig is shown in Figure 3 and the magnetic coupling in Figure 4. An electric motor is used to drive the magnetic coupling, and a simple, nonoptimized compressor absorbs the power. Tests done on this rig have demonstrated power transmittal, and have also verified the expected magnetic coupling interactions.

Results to Date

At this writing (April, 1988) the tests for the effect of refrigerant show, after a month of exposure at varying temperatures and pressures, no discernable effects on magnetic or mechanical properties of the magnets. The rig tests show the measured stiffness of the magnetic coupling to be essentially exactly as was predicted by the analysis and early tests in the range of utilization. From this, the required mass of magnetic material may be accurately predicted for any design.

Eddy current losses in this rig associated with the presence of a conductor in the gap between the two magnet rings have been found to be about 10 percent of the transmitted power, but this loss is proportional to the volume of the conductor, the stroke, frequency and magnetic field strength, and, most important, to the conductivity of the material in the gap. Since there are many ways to select the structure to reduce these losses, it can be expected that a commercial design would have far lower losses than that of the experimental rig, which used a relatively conservative stainless steel pressure vessel in the gap. Other losses associated with the coupling, such as iron hysteresis loss, have been found to be trivial.

The operating temperature of the coupling was well below that which could cause permanent degradation of the magnetic strength. This, along with the absence of other known degradation effects, leads to the conclusion that the coupling life is essentially infinite.

Costs of magnetic material are highly variable with time, depending as they do on market demand, as well as on innovation on the part of the fabricators. The costs quoted at this time are approximately $260 per kilogram for the magnet formed to the correct shape, which reflects to a coupling cost of about $260 for a 3 kilowatt engine running at 60 hertz with a stroke of 30 millimeters. This is not a completely optimized design, so the cost may be expected to be lower in a final configuration.

Other Uses for the Magnetic Coupling

A successful development of the hermetic magnetic coupling allows its use to be considered in configurations other than the FPSE/compressor. These reciprocating couplings could also be used

with conventional rotary motor-compressor drives, allowing the motor and its linkage to be outside of the refrigerant portion of the system. The same motor-coupling could be used to drive hermetically sealed devices, such as a Stirling cycle heat pumps, gas compressors, and other devices which could profit from hermetic sealing. The extension of this design concept to rotating hermetic coupling applications is obvious.

Future Work

If the work in progress uncovers no insuperable problems, it is expected that the entire system will be designed to an approximation to a commercial configuration, built, and tested. If this is successful, then multiple copies should be made and used in field trials as heat-driven heat pumps.

Acknowledgments

This work was performed under Subcontract No. 86X-SA578V from Oak Ridge National Laboratories, Martin-Marietta Energy Systems for the U.S. Department of Energy under contract DE-8C05-840-R21400.

Integration of Analysis and Experiment for Stirling Cycle Processes. Part 1: Gas Spring Hysteresis Loss

A. A. Kornhauser and *J. L. Smith, Jr.*
Massachusetts Institute of Technology
Cambridge, MA 02139

Abstract

Heat transfer-related hysteresis loss can be an important factor in the performance of Stirling and other reciprocating machines. Analytical predictions of hysteresis loss have been available to designers, but until now they were not experimentally verified.

Hysteresis loss was measured in a piston-cylinder gas spring over a range of speeds, pressures, gases, bore/stroke ratios, volume ratios, and internal extended surface geometries. An analysis of a simplified one-dimensional energy equation produced non-dimensional parameters that were used to correlate the experimental data. The loss expression from the analysis was adjusted to fit the correlated data.

Nomenclature

D	Cylinder diameter
D_h	Hydraulic diameter, 4(volume)/(area) at mid-stroke
L_s	Stroke
Loss	Lost work per cycle, the integral of pdV
Loss_{nd}	Non-dimensional loss defined as in (1), (3), or (9)
p	Pressure
p_a	Pressure wave amplitude
p_{max}	Maximum cycle pressure
p_{min}	Minimum cycle pressure
p_0	Cyclic average pressure
Pe_D	Cyclic average Peclet number based on cylinder diameter
Pe_h	Cyclic average Peclet number based on hydraulic diameter
Pr	Prandtl Number
r_v	Volume ratio
Re	Cyclic average Reynolds number
V	Volume
V_0	Cyclic mean volume
V_{max}	Maximum volume
V_{min}	Minimum volume
v_p	Mean piston speed
W_{adiab}	Work of adiabatic compression
y	Variable in Lee expression, defined in (6)
y'	Variable in modified Lee expression, defined in (13)
α	Cyclic average thermal diffusivity
γ	Gas specific heat ratio
ν	Cyclic average kinematic viscosity

Introduction

Heat transfer-related hysteresis loss is an important factor in the design of many reciprocating machines. To date the significance of this effect has been recognized only for gas springs and the working spaces of Stirling machines and other advanced reciprocating engine and heat pump systems. It is possible that this effect may also be important in more traditional reciprocating machines such as internal combustion engines and refrigeration compressors.

In recent years many engine and refrigerator performance codes have been developed, some of which attempt to describe the processes occuring within a machine in great detail. These sophisticated codes, however, can be no more accurate than the many separate analyses of which they are composed. The expressions used for hysteresis loss have been based on analytic predictions which were not well verified experimentally. Lately, studies by Faulkner and Smith[1] and the authors[2] have provided experimental data on hysteresis loss. The range of conditions for those tests was, however, limited. The work presented here extends the range of operating conditions for which experimental data are available.

A full understanding of gas spring hysteresis loss requires an understanding of heat transfer processes during compression and expansion, and the study of these losses can therefore add to the understanding of those processes. The work which is presented here forms a part of a larger study devoted to an improved understanding of heat transfer during compression and expansion. Other aspects of the study are being reported elsewhere[3].

Faulkner and Smith[1] measured hysteresis loss by pressure and volume measurements on a piston-cylinder gas spring. They found that losses over a range of speeds and pressures could be correlated by plotting a non-dimensional loss defined as

$$\text{Loss}_{nd} = \frac{\oint_{cycle} pdV}{\int_{compression} pdV} \tag{1}$$

against a cyclic average Reynolds number defined as

$$\text{Re} = \frac{v_p D}{\nu}. \tag{2}$$

The mean pressure in compression and ambient temperature were used to define ν. Velocity was the mean piston speed over a cycle. The diameter was gas spring cylinder diameter.

Hysteresis loss was found to be maximum at intermediate Re (approximately 100), decreasing monotonically with Re on either side of the maximum. Near the point of maximum loss, the Loss_{nd}-Re correlation broke down, with low-speed, high-pressure runs showing greater loss than high-speed, low-pressure runs at the same Re. Results were reported for three gases and two volume ratios, but the loss was not correlated over these variations. Tests were run with cylinder wall materials of various heat storage capacities, but no significant change in loss was found.

The authors[2] performed further experiments using the same gas spring but with improved instrumentation. In order to make non-dimensionalizing factors a function of independent variables only, non-dimensional loss was defined as

$$\mathrm{Loss}_{nd} = \frac{\oint_{cycle} pdV}{W_{adiab}}, \tag{3}$$

where W_{adiab} was the work of adiabatic compression for the same gas, mean pressure, and geometry. It was found that for a given gas and geometry, (mean pressure)(mean volume) would in fact be an adequate non-dimensionalizing factor. Instead of Reynolds number, a cyclic average Peclet number

$$\mathrm{Pe}_D = \frac{v_p D}{\alpha} \tag{4}$$

was used (Pe=RePr). The time-mean cycle pressure and ambient temperature were used to define α. Velocity and diameter were defined as for the Reynolds number above.

The authors' results were similar to those of Faulkner and Smith, but data scatter was considerably smaller. Loss_{nd} was found to be proportional to Pe at Pe below the maximum loss point and proportional to $\mathrm{Pe}^{-1/2}$ at Pe above that point. The experiments were done only with helium at volume ratio 2.0. Results were compared to losses predicted by various loss and heat transfer expressions. The expression first presented by Lee[4] but also developed independently by Cooke-Yarborough and Ryden[5] was found to predict hysteresis loss better than any of the others.

Lee's expression was based on an exact solution of the one-dimensional energy equation for a sinusoidal pressure variation. Convection and density variations were neglected, so the solution was the same as for a one-dimensional solid with a sinusoidal heat source/heat sink. The temperature distribution was integrated to get mixed mean temperature as a function of time, and this temperature was used to calculate the integral of pdV around the cycle. The result was

$$\mathrm{Loss} = \oint pdV$$

$$= p_0 V_0 \frac{\pi}{2}\left(\frac{p_a}{p_0}\right)^2 \frac{\gamma-1}{\gamma}\frac{1}{y}\left(\frac{\cosh y \sinh y - \sin y \cos y}{\cosh^2 y - \sin^2 y}\right), \tag{5}$$

where

$$y = \left(\frac{\pi}{32}\mathrm{Pe}_h \frac{D_h}{L_s}\right)^{1/2}. \tag{6}$$

The success of this expression in predicting gas spring hysteresis loss suggested that losses over a range of operating conditions might be correlated in the form

$$\frac{\mathrm{Loss}}{p_0 V_0 \left(\frac{p_a}{p_0}\right)^2 \frac{\gamma-1}{\gamma}} = f\left(\mathrm{Pe}_h \frac{D_h}{L_s}\right). \tag{7}$$

The intent of the work described here was to collect gas spring loss data over a range of speeds, pressures, gases, compression ratios, bore/stroke ratios, and spring internal geometries. The collected data was used to test the correlation suggested by Lee's analysis.

Description of Experiments

The apparatus used in this experiment was a modification and extension of that used by the authors previously. It is shown schematically in Figure 1. The apparatus was constructed by building a test section on top of an existing compressor base, the cylinder of the compressor acting as a crosshead. The test section consisted of a piston and cylinder with an adjustable flat head. The adjustable head made possible various compression ratios. Two compressor bases were used: one with a 76.2 mm (3.00 in) stroke and one with a 41.2 mm (1.62 in) stroke. Two test sections were used: one 50.8 mm (2 in) diameter and one 31.5 mm (1.25 in) diameter. By combining these bases and test sections in different ways various bore/stroke ratios could be obtained. Each piston was sealed to the cylinder with a buna-n O-ring. The seal was located more than a stroke length from the piston face so that the frictional heating of the wall would effect results minimally. The piston top surface was brass, while the cylinder wall and head were steel. The apparatus was belt-driven by a D.C. motor to allow speed adjustment.

For some experiments the working space was provided with extended heat transfer surface in the form of interlocking concentric fins, as shown in Figure 2. These fins were made from brass tubing of 0.64 mm (0.025 in) wall thickness, soldered into grooved brass piston and head extensions. The soldered construction allowed the configuration of fins to be varied. Fin length was such that the fins were almost fully engaged at top center position and slightly disengaged at bottom center position.

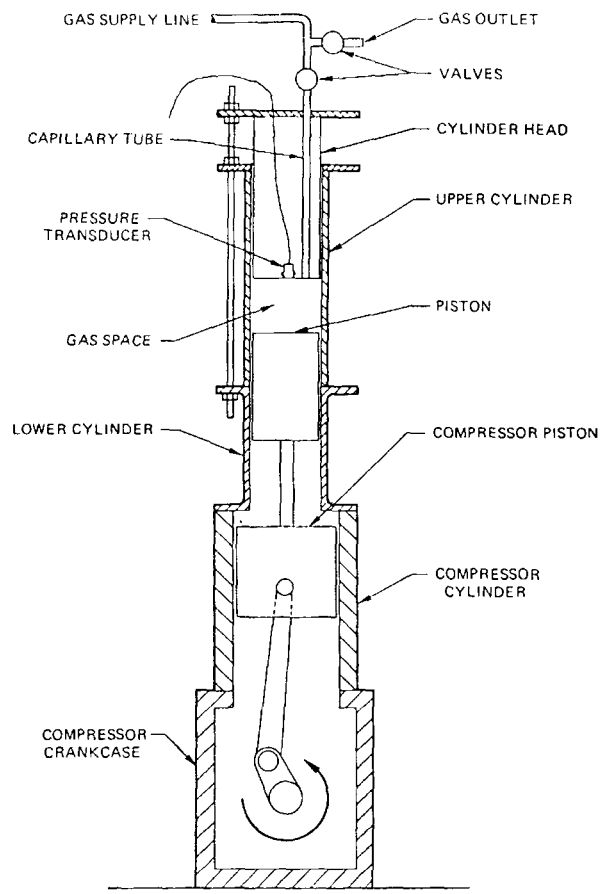

Figure 1. Equipment Schematic (from Faulkner and Smith[1])

Pressure was measured with semiconductor strain gage pressure transducers mounted essentially flush with the cylinder head. Two transducers were used: one with a 0-670 kPa (0-100 psia) range and one with a 0-3300 kPa (0-500 psia) range. Volume was calculated from the crank-connecting rod relationship and the crank angle signal provided by a 1200 count-per-turn optical encoder. Both these signals were recorded with a digital data acquisition system. During each cycle 150 pressure-volume data points were collected. Ambient temperature was measured with a mercury-in-glass thermometer.

Measurements were recorded as soon after apparatus startup as both speed and mean pressure became steady. In general, a variation of 0.1% per cycle was used as a criterion for steady-state operation, but at very low speeds random speed fluctuations made it necessary to relax the criterion to 1.0% variation per cycle. The constant value of cyclic mean pressure indicated that the thermodynamic processes within the gas had reached cyclic equilibrium. The cylinder walls, however, had a much larger thermal time constant than the gas and were therefore still essentially uniformly at ambient temperature. (This was demonstrated by Faulkner[6] in a similar apparatus equipped with wall thermocouples.) The number of cycles to reach steady state varied approximately from 5 to 75. In the cases where a large number of cycles were required, the

delay was a result of the time required for the motor to accelerate the apparatus, rather than a result of the time for the processes within the cylinder to reach cyclic equilibrium.

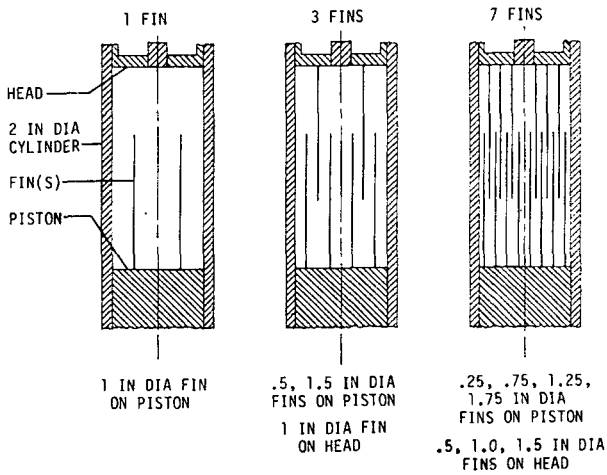

Figure 2. Schematic Cross Section Showing 1, 3, and 7 Fin Arrangements (Piston Shown at Mid-Stroke)

The cyclic lost work was calculated by trapezoidal rule integration of pdV around a cycle. The calculation was made for a single cycle rather than for data averaged over several cycles. Comparison of the loss calculated for two successive cycles of each run showed a variation that never exceeded 0.18% and was generally less than 0.01%. The pressure and volume data were also used to calculate mixed-mean gas temperature and instantaneous space-averaged heat transfer, but these results are reported elsewhere[3].

The baseline operating condition was with helium at 50.8 mm bore, 76.2 mm stroke (bore/stroke=.67), no fins, and volume ratio 2.0. At this baseline condition runs were made at speeds ranging from 0.034 Hz (2.0 rpm) to 16.8 Hz (1010 rpm) and mean cycle pressures ranging from 100 kPa (15 psia) to 1800 kPa (270 psia). From the baseline case, the adjustable parameters were varied one at a time as follows:

Gas: Helium (baseline), Hydrogen, Argon, and Nitrogen
Fins: 0 (baseline), 1, 3, and 7
Bore/Stroke: 0.67 (baseline), 0.42, and 1.23
Volume Ratio: 2.0 (baseline), 4.0, and 8.0.

In each of these cases speed and pressure were varied over the widest range possible within the capabilities of the apparatus and instrumentation, though for some cases this range was somewhat less than for the baseline case. Altogether, some 500 runs were made, comprised of 75,000 pressure-volume data points. The overall range of Pe_D was 1.2 to 110,000.

Potential sources of error were examined. The most important of these was phase lag between the pressure and volume measurements, since the hysteresis loss was, in a sense, a result of the pressure change leading the volume change. The lags in pressure transducers, shaft position transducer, amplifiers, and D/A conversion were small enough that they did not effect results appreciably. Another potential problem was transient thermal stress in the diaphragm of the pressure transducer. This was prevented by coating the transducer with a 1 mm (.04 in) layer of silicone grease. There was some deviation from a sinusoidal volume variation due to the crank-connecting rod geometry and due to motor loading at low speed and high pressure, but it was small.

In early phases of the experimentation error sources were discovered which had affected the results of work done with previous versions of this apparatus[1,2,6]. One was an oscillating volume error caused by load reversal on a keyway during high pressure runs. The error varied from + to - 0.07% of V_0 during a cycle. This problem was corrected by tightening hub clamps so that the keyway did not bear load. A second error was caused by gas contamination with trace amounts of water vapor. Some condensation apparently took place under certain conditions, affecting results. Sections of the piston were made of Micarta™ phenolic, which absorbs water, and though the apparatus was originally purged to an impurity level of less than 50 ppm, over time water vapor diffused into the gas. This problem was corrected by purging the apparatus immediately before testing.

The loss measured here may not have been entirely ordinary gas spring hysteresis loss: some of it may have been hysteresis loss related to flow into and out of the piston appendix gap. Because of the need to avoid frictional heating of the working space, the gap was long; while its volume was only 1.2% of mean volume and 1.7% of minimum volume for the baseline case, it was 2.7% of mean volume and 12.2% of minimum volume for r_v=8. Because of the temperature difference between the nearly isothermal gap gas and the more adiabatic cylinder gas, the gap could contain 25% of the mass at minimum volume and r_v=8. The appendix gap loss may therefore be a significant component of the loss measured for higher volume ratios.

Non-Dimensional Variables

In order to test the correlation (7) suggested by Lee's analysis, the independent variable used was

$$Pe_h \frac{D_h}{L_s}. \tag{8}$$

Here hydraulic diameter D_h was defined as 4(volume)/(surface area) at mid-stroke and Pe_h was Peclet number defined as in (4) but with D_h substituted for D. In calculating D_h, only piston, cylinder, head, and fin areas were considered: appendix gap area was neglected. Since D_h appeared both in the bore/stroke ratio and in the Peclet number, the change from D to D_h had a quadratic rather than linear effect.

The dependent variable used was

$$\mathrm{Loss}_{nd} = \frac{\mathrm{Loss}}{p_0 V_0 \left(\frac{p_a}{p_0}\right)^2 \frac{\gamma-1}{\gamma}}. \tag{9}$$

Here p_0 and V_0 were time-mean cycle pressure and volume. For the ratio of pressure amplitude to mean pressure, p_a/p_0,

$$\frac{p_a}{p_0} = \frac{p_{max} - p_{min}}{p_{max} + p_{min}} \tag{10}$$

was used.

This selection of dependent and independent variables presents some difficulties for design predictions, since for kinematic machines (devices with fixed volume cycles), p_0 and p_a are dependent rather than independent variables. It was observed, however, that for all operating conditions described here p_0 is very near the pressure at geometric mean volume, $(V_{max}V_{min})^{1/2}$, and wall temperature. As described in previous work[2], the pressure ratio could be approximated by

$$\frac{p_a}{p_0} = \frac{r_v - 1}{r_v + 1} \tag{11}$$

for near-isothermal cases ($Pe_h D_h/L_s < 10$), and by

$$\frac{p_a}{p_0} = \frac{r_v^\gamma - 1}{r_v^\gamma + 1} \tag{12}$$

for near-adiabatic cases ($Pe_h D_h/L_s > 10$). These approximations should allow application of the results to kinematic designs where pressure and volume variations are approximately sinusoidal.

Another difficulty with the dependent variable used was that it did not have a simple interpretation in terms of lost work vs. work stored in a gas spring for a reversible cycle as did the variable used previously. However, since it correlated data over a wider range of conditions, it was undoubtedly a better choice.

Results

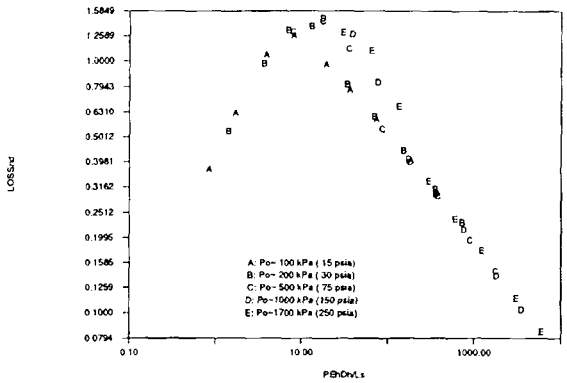

Figure 3. $Loss_{nd}$ vs. Pe_hD_h/L_s, Baseline Case

Helium, r_v=2.0, D/L_s=0.67, No Fins
Approximate Mean Pressure Indicated
Frequency 0.8-17 Hz at Each Pressure

The results of the baseline case are shown in Figure 3. As in previous work[1,2,6], the correlation broke down at the region of maximum loss. High pressure, low speed runs showed greater loss than low pressure, high speed runs at the same Pe_hD_h/L_s. When these results were compared with those obtained previously they showed slightly higher loss. The change was believed to be due to the effects of the gas contamination error and oscillating volume error described above, both of which were present in the previous work. The maximum loss for this case was approximately 14% of the adiabatic compression work.

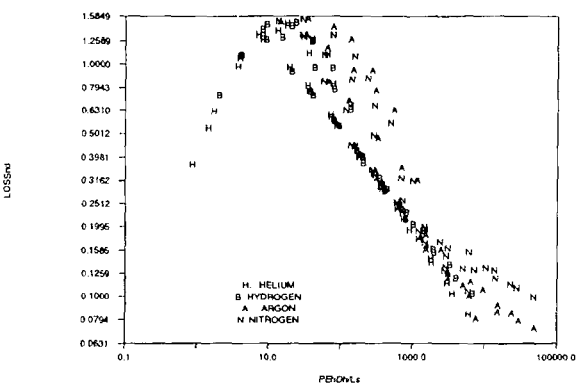

Figure 4. $Loss_{nd}$ vs. Pe_hD_h/L_s, Gas Comparison

Helium, Hydrogen, Argon, and Nitrogen; r_v=2.0, D/L_s=0.67,
No Fins, Mean Pressure and Frequency Varied

The runs made with various gases are compared in Figure 4. The correlation brought the data for helium and hydrogen together very well. The data for argon and nitrogen showed much more extensive correlation breakdown regions than the data for the lighter gases. The region near maximum loss was more extensive, and there was another breakdown region at high Pe_hD_h/L_s. In the regions where these breakdowns did not occur the correlation brought together the data for all four gases. The correlation here was due to the use of $Loss_{nd}$ as the dependent variable; Pe_D would have been adequate as independent variable. The maximum losses for helium and argon were approximately 14% of the adiabatic compression work, while for hydrogen and nitrogen they were approximately 9%.

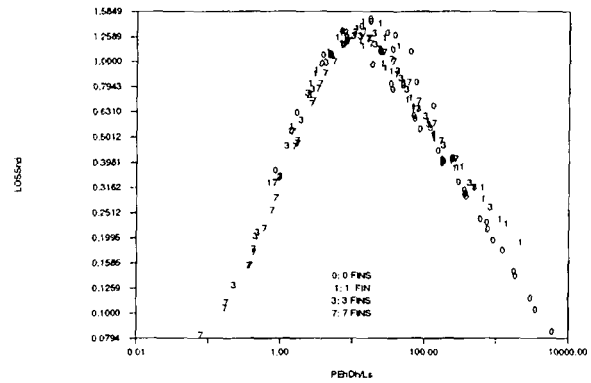

Figure 5. $Loss_{nd}$ vs. Pe_hD_h/L_s, Fin Comparison

0, 1, 3, and 7 Fins; Helium, r_v=2.0, D/L_s=0.67,
Mean Pressure and Frequency Varied

The runs made with various fin arrangements are compared in Figure 5. The correlation brought together the data for all four fin geometries. The data for one fin showed a smaller correlation breakdown region than that for no fins, and the data for three and seven fins showed no breakdown at all. The correlation here was due to the use of Pe_hD_h/L_s as the independent variable; $Loss/p_oV_o$ would have been adequate as a dependent variable. The maximum losses here were approximately 14% of the adiabatic compression work.

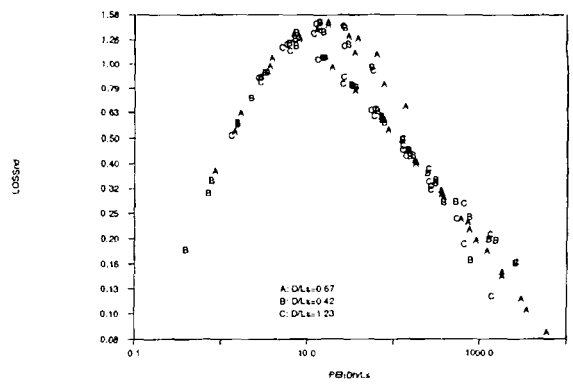

Figure 6. $Loss_{nd}$ vs. Pe_hD_h/L_s, Bore/Stroke Comparison

D/L_s=0.42, 0.67, and 1.23; Helium, r_v=2.0,
No Fins, Mean Pressure and Frequency Varied

The runs made with various bore/stroke ratios are compared in Figure 6. The correlation brought together the data for all three bore/stroke ratios. As in the fin comparison, the correlation here was due to the choice of independent variable. The maximum losses here were approximately 14% of the adiabatic compression work.

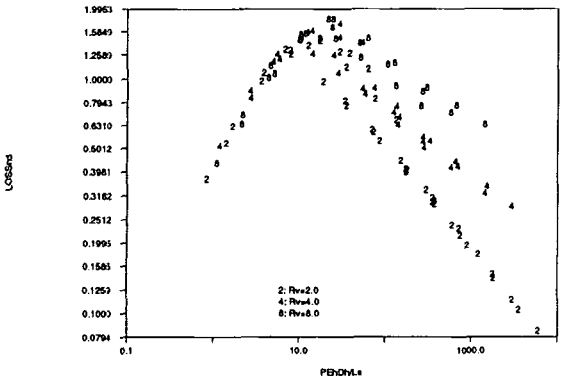

Figure 7. $Loss_{nd}$ vs. Pe_hD_h/L_s, Volume Ratio Comparison

r_v=2.0, 4.0, and 8.0; Helium, L_s/D=.67,
No Fins, Mean Pressure and Frequency Varied

The runs made with various volume ratios are compared in Figure 7. The correlation brought together the data for the three compression ratios at low Pe_hD_h/L_s but failed at higher values. It is believed that the measured loss at high volume ratios and high Pe_hD_h/L_s was a combination of gas spring hysteresis loss and appendix gap loss. As discussed previously, a significant portion of the gas flowed in and out of the appendix gap at high volume ratios. It appears likely that if experiments were performed on an apparatus with an appendix gap which was negligibly small even at high r_v, the correlation would bring data from different r_v together.

In comparing the results for different volume ratios, it should be noted that the limitations of the apparatus resulted in a decrease in mean pressure for the highest pressure run as volume ratio increased. The maximum mean pressure at r_v=4 was only 60%, and at r_v=8 only 30%, of that at r_v=2. The maximum measured losses were approximately 14% of the adiabatic compression work at r_v=2, approximately 19% at r_v=4, and approximately 17% at r_v=8.

Discussion

Overall, the correlation tested here gives good results. The range of conditions examined is broad enough that these test results may be used to predict losses in gas spring equipment with some degree of confidence. In addition, the similarity parameters tested can be used to predict hysteresis loss in a new design from measured loss in an older design.

The success of the independent variable Pe_hD_h/L_s over a range of geometries provides a useful tool for predicting losses in gas springs of various shapes. The fact that the hydraulic diameter appears as a quadratic term indicates that increasing surface area for a given volume has a large effect. This may have important implications for attempts to design isothermal gas springs and Stirling engine cylinders.

The correlation breakdown regions continue to be a puzzling problem. Dimensional analysis of the gas spring yields as non-dimensional variables volume ratio, ratios of various lengths, a Reynolds or Peclet number, and a Mach or Eckert number. The Mach and Eckert number are normally considered to be of importance only in flows of much higher velocity; the highest cyclic average Mach number in any of these runs was 0.008. However, the fact that both these compressible-flow numbers are functions of gas molecular weight, combined with the molecular weight effects observed here, seems to indicate that they have some significance. The suppression of the breakdowns by the presence of fins may be a sign that they are a result of some sort of large-scale eddy pattern which the fins prevent.

The failure of the correlation at high volume ratios was probably due to the increased flow into the appendix gap at high r_v. It appears probable that if the ordinary hysteresis loss were isolated from the appendix gap loss the correlation would be satisfactory. However, the analysis on which the correlation was based assumed sinusoidal pressure variation, no variation in surface area, and constant density over the cycle. All these assumptions are violated severely as the volume ratio becomes large. Before the correlation can be used with confidence at high r_v, experiments must be performed in an apparatus with a smaller appendix gap.

Figure 8 compares the results for the baseline case with loss predicted by Lee's expression. The match is fairly good at medium and high Pe_hD_h/L_s, but the expression underpredicts loss at low Pe_hD_h/L_s. In his paper, Lee suggested that the effects of turbulence might be accounted for by use of a turbulent thermal diffusivity, but the effect of this would simply be to shift the theoretical curve to the right.

In an effort provide better prediction of hysteresis loss, it is proposed that Lee's expression be modified by replacing y of (6) with

$$y' = 1.20y^{0.86} = 0.44\left(\mathrm{Pe}_h\frac{D_h}{L_s}\right)^{0.43}. \qquad (13)$$

This modified expression is also plotted in Figure 8. It matches experimental results well except where the correlation breaks down. In that region it matches the lower loss results. It should be noted that this correction is totally empirical; no theoretical basis for it is proposed.

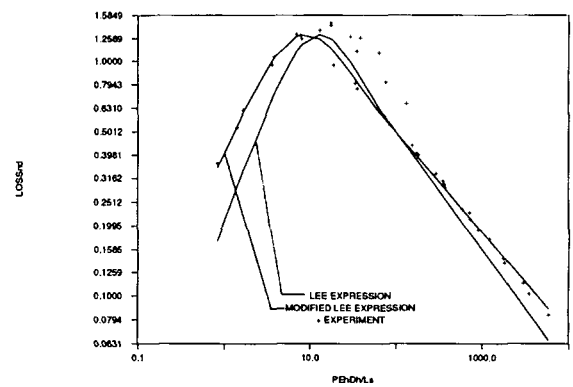

Figure 8. $Loss_{nd}$ vs. Pe_hD_h/L_s, Theory and Baseline Case

Helium, r_v=2.0, L_s/D=.67, No Fins, Mean Pressure and Frequency Varied

There are intrinsic limitations in attempting to predict gas spring hysteresis loss in a closed form expression. This is especially true when predicting hysteresis losses in systems with inflow and outflow. More accurate predictions should be possible by computer simulation of system performance with accurate prediction of heat transfer. The authors[2] showed that conventional engine and gas spring heat transfer correlations did not correctly predict loss in such a simulation. A new heat transfer correlation being developed as another part of this study[3] may prove more effective.

In terms of Stirling engine design, the results presented here are applicable to what Martini [7] called "second-order" design methods: methods in which relatively a simple initial design calculation is corrected with various loss factors. This study increases the accuracy of the correction for hysteresis loss. In free piston engines, not only hysteresis loss but also phase shift information is important. This study has generated phase shift data for the entire range of operating conditions, to be reported elsewhere.

For "third-order" methods, where all effects are included in a single detailed design calculation, the accurate heat transfer correlations now under development will be required. These correlations should be applicable not only to gas springs and Stirling engines but to other reciprocating engines and compressors.

The expressions presented here may be used with some confidence for predicting hysteresis loss in gas springs. They may also be used to estimate hysteresis losses in Stirling engine cylinders, heat exchangers, and regenerators, but only with caution. The combined effects of oscillating flow and compression/expansion may have loss effects very different from compression/expansion alone. Further work is needed in order to predict hysteresis loss for an entire Stirling engine.

Conclusions

This study shows that:

1. A correlation in the form of (7) works for gas spring hysteresis loss over a wide range of conditions. The correlation breaks down near the point of maximum loss, and its usefulness at high volume ratios is uncertain.

2. Correlation breakdown regions become larger as gas molecular weight increases and are suppressed by interlocking fins.

3. Hysteresis loss measured in these experiments is predicted by Lee's expression (5), modified as in (13).

Future work must:

1. Experimentally investigate the breakdown regions in the correlation developed here and test the correlation more thoroughly at high volume ratios.

2. Attempt to predict loss based on cyclic simulation of the effects of heat transfer.

3. Measure and correlate gas spring pressure wave magnitude and phase shift.

4. Study the combined effects of compression-expansion and oscillating flow on heat transfer and hysteresis loss.

The experimental program at M.I.T. is now addressing items two, three, and four.

Acknowledgements

This work was performed under Subcontract No. 19X-55915C from Martin Marietta Energy Systems (Oak Ridge National Laboratory). Prime contract was No. DE-AC05-840R21400 from the U.S. Department of Energy. We are grateful to ORNL and DOE for their support.

References

1. Faulkner, H.B. and Smith, J.L. Jr., "Heat Transfer During Compression and Expansion in Reciprocating Gas Handling Machinery," *Proceedings of the 18th Intersociety Energy Conversion Engineering Conference*, American Institute of Chemical Engineers, 1983, pp 724-730.

2. Kornhauser, A.A. and Smith, J.L. Jr., "A Comparison of Cylinder Heat Transfer Expressions Based on Prediction of Gas Spring Hysteresis Loss", *Fluid Flow and Heat Transfer in Reciprocating Machinery*, American Society of Mechanical Engineers, 1987, pp 89-96.

3. Kornhauser, A.A. and Smith, J.L. Jr., "Application of a Complex Nusselt Number to Heat Transfer During Compression and Expansion", submitted for the International Symposium on Flows in Reciprocating I.C. Engines, American Society of Mechanical Engineers, November, 1988.

4. Lee, K.P., "A Simplistic Model of Cyclic Heat Transfer Phenomena in Closed Spaces," *Proceedings of the 18th Intersociety Energy Conversion Engineering Conference*, American Institute of Chemical Engineers, 1983, pp 720-723.

5. Cooke-Yarborough, E.H. and Ryden, D.J., "Mechanical Power Losses Caused By Imperfect Heat Transfer in a Nearly-Isothermal Stirling Engine," *Proceedings of the 20th Intersociety Energy Conversion Engineering Conference*, Society of Automotive Engineers, 1985, pp 3.307-3.312.

6. Faulkner, H.B., "An Investigation of Instantaneous Heat Transfer During Compression and Expansion in Reciprocating Gas Handling Equipment," Ph.D. Thesis, Dept. of Mech. Eng., Massachusetts Institute of Technology, 1983.

7. Martini, W.R., *Stirling Engine Design Manual*, U.S. Department of Energy, DOE/NASA/3194-1 (NASA CR-168088), 1983.

Comparative Assessment of Free-Piston and Kinematic Stirling Engine Technologies

W. P. Teagan
Arthur D. Little, Inc.
Cambridge, MA 02140

(Paper not supplied in time for publication)

Author Index

A

Ackermann, R. A 189

B

Baxter, V. D. 75
Beale, W. T. 197
Bostick, D. T. 133
Braun, A. T. 155,161

C

Chen, F. C. 177
Chen, G. 197
Creswick, F. A. 93

D

DeVault, R. C. 105
Didion, D. A. 55

F

Fischer, S. K. 93

H

Hayes, F. C. 117
Ho, C-M. 169

J

Jou, W-H. 169

K

Kauffeld, M. 55
Klatt, L. N. 133
Knoke, G. S. 169
Kornhauser, A. A. 203

L

Lannus, A. 65

M

Macriss, R. A. 145
Maret, A. R. 153
McLinden, M. 55
Mei, V. C. 75
Melikian, Gorken 127
Merriam, R. L. 35
Miller, W. A. 7
Modahl, R. J. 117
Mulroy, W. 55
Murphy, R. W. 163

P

Patterson, M. R. 133
Perez-Blanco, H. 133
Phillips, B. A. 111
Prekker, R. J. 161
Privon, G. T. 155

R

Reimann, R. C. 127
Rice, C. K. 23
Ryan, J. D. 101

S

Sand, J. R. 47
Schneeberger, A. P. 161
Smith, J. L., Jr. 203
Statt, T. G. 3

T

Teagan, W. P. 209

U

Ushimaru, Kenji 85

V

Vineyard, E. A. 47

Z

Zawacki, T. S. 145

Conference Attendees

Abramson, Douglas
U.S. Department of Energy
CE-132, GF-217/FORS
1000 Independence Avenue, S.W.
Washington, DC 20585

Ackermann, Robert
Mechanical Technology, Inc.
968 Albany-Shaker Road
Latham, NY 12110

Anderson, Kent
5602 Vernon Place
Bethesda, MD 20817

Applequist, Charles D.
Minnegasco, Inc.
201 South 7 Street
Minneapolis, MN 55402

Aspelin, Erik
Briggs & Stratton Corp.
P.O. Box 702
Milwaukee, WI 53210

Ball, David
Battelle Columbus Laboratories
505 King Avenue
Columbus, OH 43201-2693

Barrows, Kenneth C.
Carrier Corp.
Carlyle Compressor Co.
P.O. 4800
Syracuse, NY 13221

Baxter, Van D.
Oak Ridge National Laboratory
P.O. Box 2009, Bldg. 9102-1
Oak Ridge, TN 37831

Beale, William T.
Sunpower, Inc.
6 Byard Street
Athens, OH 45701

Bernstein, Samuel
Energy International, Inc.
127 Bellevue Way, S.E.
Bellevue, WA 98004-6229

Biermann, Wendell J.
45 Foxcroft Drive
Fayetteville, NY 13066

Bryant, Ralph S.
Heil-Quaker Corp.
1136 Heil-Quaker Boulevard
LaVergne, TN 37086-1985

Budzyko, Edward J.
Tectonics Engineering Corp.
9556 West Bloomington Freeway
Minneapolis, MN 55431

Chen, Fang C.
Oak Ridge National Laboratory
P.O. Box 2009, Bldg. 9102-2
Oak Ridge, TN 37831

Clinch, J. Michael
Gas Research Institute
8600 West Bryn Mawr Avenue
Chicago, IL 60631

Colosimo, Donald D.
Mechanical Technology, Inc.
968 Albany-Shaker Road
Latham, NY 12110

Creswick, Fred
Oak Ridge National Laboratory
P.O. Box 2009, Bldg. 9102-2
Oak Ridge, TN 37831

Davis, Thomas L.
Carolina Power & Light Co.
25 Turner Street
Raleigh, NC 27607

DeVault, Robert C.
Oak Ridge National Laboratory
P.O. Box 2009, Bldg. 9102-2
Oak Ridge, TN 37831

Erickson, Donald C.
Energy Concepts Co.
627 Ridgely Avenue
Annapolis, MD 21401

Erickson, Ellen L.
Energy Concepts Co.
627 Ridgely Avenue
Annapolis, MD 21401

Fairchild, Phillip D.
Oak Ridge National Laboratory
P.O. Box 2009, Bldg. 9102-1
Oak Ridge, TN 37831

Feder, Laurence M.
Institute of Gas Technology
1825 K Street, N.W.
Washington, DC 20006

Fischer, Steven K.
Oak Ridge National Laboratory
P.O. Box 2009, Bldg. 9102-2
Oak Ridge, TN 37831

Freedman, Steven
Gas Research Institute
8600 West Bryn Mawr Avenue
Chicago, IL 60631

French, Charles E.
Gas Research Institute
8600 West Bryn Mawr Avenue
Chicago, IL 60631

Gilles, Ted C.
Lennox Industries, Inc.
Promenade Towers
P.O. Box 809000
Dallas, TX 75380

Goldschmidt, Victor W.
Ray W. Herrick Laboratories
Purdue University
West Lafayette, IN 47907

Groff, Gerald C.
Solar Energy Research Institute
1298 Northridge Court
Golden, CO 80403

Hale, Harry T.
Carrier Corp.
Research Division
P.O. 4808
Syracuse, NY 13221

Hammarstedt, Gloria D.
Pacific Gas & Electric Co.
3400 Crow Canyon Road
San Ramon, CA 94583

Hanks, Nicholas F.
Washington Gas Light Co.
6801 Industrial Road
Springfield, VA 22151

Harnish, James R.
York International Corp.
Unitary Products Engineering
P.O. Box 1592
York, PA 17405-1592

Heard, Steve
Lennox Industries
P.O. Box 877
Carrollton, TX 75011-0877

Helmick, Richard L.
David Taylor Research Center
Code 2722
Annapolis, MD 21402

Henderson, Hugh I.
Florida Solar Energy Center
University of Florida
300 State Road 401
Cape Canaveral, FL 32930

Holzapfel, Karl
Joseph Haydn Str. 29
D 7524 Oestringen
Federal Republic of Germany

Izawa, Howard S.
Washington Gas Light Co.
6801 Industrial Road
Springfield, VA 22151

Jakob, Frank E.
Battelle Columbus Laboratories
505 King Avenue
Columbus, OH 43201-2693

Jou, Wen-Huei
Flow Research Co.
21414 68th Street South
Kent, WA 98032

Joyner, Powell A.
Electric Power Research Institute
P.O. Box 10412
Palo Alto, CA 94303

Kapus, Ted
U.S. Department of Energy
CE-132, GF-217/FORS
Washington, DC 20585

Kauffeld, Michael
Institut für Kaltetechnik
Universitat Hannover
Welfengarten 1A, 3000 Hannover 1
Federal Republic of Germany

Kornhauser, Alan A.
Massachusetts Institute of
Technology
77 Massachusetts Avenue
Cambridge, MA 02139

Kountz, Kenneth J.
Institute of Gas Technology
4201 West 36th Street
Chicago, IL 60632

Kuliasha, Michael A.
Oak Ridge National Laboratory
P.O. Box 2009, Bldg. 9102-2
Oak Ridge, TN 37831

Lannus, Arvo
Electric Power Research Institute
P.O. Box 10412
Palo Alto, CA 94303

Lewis, Pamela J.
Oak Ridge National Laboratory
P.O. Box 2009, Bldg. 9102-2
Oak Ridge, TN 37831

Lewis, Paul
Battelle Pacific
P.O. Box 999
Richland, WA 99352

Loomis, Lee M.
Rochester Gas & Electric Corp.
89 East Avenue
Rochester, NY 14649

Lowe, Ian R. G.
National Research Council Canada
Division of Mechanical Engineering
Ottawa, Canada, K1A OR6

Macriss, Robert A.
Institute of Gas Technology
4201 West 36th Street
Chicago, IL 60632

Maret, Arthur R.
Gas Research Institute
8600 West Bryn Mawr Avenue
Chicago, IL 60631

Marsala, Joseph
Tecogen, Inc.
45 1st Avenue
Waltham, MA 02254-9046

McLinden, Mark O.
National Bureau of Standards
Bldg. 226, Room B114
Gaithersburg, MD 20899

McNamara, Jr., Thomas R.
Washington Gas Light Co.
6801 Industrial Road
Springfield, VA 22151

Melikian, Gorken
United Technologies Research
Energy Conservation Technologies
East Hartford, CT 06108

Metrish, Donald C.
A. O. Smith Corp.
12100 West Park Place
Milwaukee, WI 53223

Miller, William A.
Oak Ridge National Laboratory
P.O. Box 2009, Bldg. 9102-1
Oak Ridge, TN 37831

Modahl, Robert
Trane Co.
3600 Pammel Creek Road
La Crosse, WI 54601-7599

Mulroy, William J.
National Bureau of Standards
Bldg. 226, Room B126
Gaithersburg, MD 20899

Murphy, Richard W.
Oak Ridge National Laboratory
P.O. Box 2009, Bldg. 9102-2
Oak Ridge, TN 37831

Nowakowski, Gary A.
Gas Research Institute
8600 West Bryn Mawr Avenue
Chicago, IL 60631

Oppenheim, Paul
NAHB National Research Center
400 Prince Georges Boulevard
Upper Marlboro, MD 20772-8731

Parent, Denis
C.R.I.Q.
333, rue Franquet
Case postale 9038
Sainte-Foy, Quebec, Canada
G1V 4C7

Perez-Blanco, Horacio
Oak Ridge National Laboratory
P.O. Box 2009, 9102-2
Oak Ridge, TN 37831

Pham, Hung M.
Copeland Corp.
1675 West Campbell Road
Sydney, OH 45365

Phillips, Benjamin
Phillips Engineering Co.
721 Pleasant Street
St. Joseph, MI 49085

Privon, George T.
Oak Ridge National Laboratory
P.O. Box 2009, Bldg. 9102-2
Oak Ridge, TN 37831

Radtke, Gerald W.
Aisin Seiki Co., Ltd.
14109 Farmington Road
Livonia, MI 48154

Rasson, Joseph
Lawrence Berkeley Laboratory
1 Cyclotron Road, Bldg. 90
Berkeley, CA 94720

Recchi, Vincenzo
Technars
Via Pionieri Comm. Barese
I-70123 Bari, Italy

Reimann, Robert C.
United Technologies-Carrier
Research Division
P.O. Box 4808
Syracuse, NY 13221

Rice, C. Keith
Oak Ridge National Laboratory
P.O. Box 2009, Bldg. 9102-1
Oak Ridge, TN 37831

Ryan, John D.
U.S. Department of Energy
CE-132, GF-217/FORS
1000 Independence Avenue, S.W.
Washington, DC 20585

Ryan, William A.
Gas Research Institute
8600 West Bryn Mawr Avenue
Chicago, IL 60631

Sand, James R.
Oak Ridge National Laboratory
P.O. Box 2009, Bldg. 9102-2
Oak Ridge, TN 37831

Sgamboti, Carl
United Technologies Research
Silver Lane
East Hartford, CT 06108

Shirilau, Mark S.
Southern California Edison
2244 Walnut Grove Avenue
Rosemead, CA 91770

Smith, Jr., Joseph L.
Massachusetts Institute of
Technology
77 Massachusetts Avenue
Cambridge, MA 02139

Snelson, W. Keith
National Research Council of Canada
Montreal Road, Building M-17
Ottawa, Ontario K1J 8K8, Canada

Spauschus, Hans. O.
Georgia Tech. Research Institute
Georgia Institute of Technology
Atlanta, GA 30332

Springer, Walter V.
Rochester Gas & Electric Corp.
89 East Avenue
Rochester, NY 14649-0001

Statt, Terry
U.S. Department of Energy
CE-132, GF-217/FORS
1000 Independence Avenue, S.W.
Washington, DC 20585

Syniuta, Walter D.
Advanced Mechanical Technology
151 California Street
Newton, MA 02158

Teagan, W. Peter
Arthur D. Little, Inc.
32 Acorn Park
Cambridge, MA 02140

Tremayne, Michael
Consumers Gas Co., Ltd.
P.O. Box 650
Scarborough, Ontario, Canada M1K 5E3

Ushimaru, Kenji
Energy International, Inc.
127 Bellevue Way, S.E.
Bellevue, WA 98004

Vincenzo, Bruno
Technars
Via Pionieri Comm. Barese
I-70123 Bari, Italy

Vineyard, Edward A.
Oak Ridge National Laboratory
P.O. Box 2009, Bldg. 9102-1
Oak Ridge, TN 37831

Wahlig, Michael A.
Lawrence Berkeley Laboratory
Bldg. 90, Room 2024
Berkeley, CA 94720

Walukas, Donald
Gas Research Institute
8600 West Bryn Mawr Avenue
Chicago, IL 60631

Wells, Raymond D.
Aloha Systems
14751 Sweetan Street
Irvine, CA 92714

Young, David J.
Ontario Hydro
800 Kipling Avenue
Toronto, Ontario, Canada M8Z 5S4

APPENDIX A

International Cooperation in Heat Pump and Refrigeration Research Through the International Energy Agency

J. D. Ryan
U.S. Department of Energy
Washington, DC 20585

1. Background on The International Energy Agency

Introduction

The growing need for international cooperation in energy led to the establishment of the International Energy Agency (IEA) in 1974 as a forum for the 21 participating countries to coordinate their energy planning. The IEA provides a framework by which the cooperative efforts of its participating countries will reinforce one another to improve the overall energy situation. The Agency carries out the International Energy Program and a Long-Term Cooperation Agreement and works:

- to mold a better world energy supply and demand structure, now and for the future;
- to prepare participating countries against risk of oil supply disruptions and to share remaining oil supplies in a period of severe supply disruption;
- to develop alternative energy sources and to increase the efficiency of energy use through a cooperative research and development program;
- to promote cooperative relations with oil-producing nations and other oil consuming countries.

The countries cooperating in the IEA are: Australia, Austria, Belgium, Canada, Denmark, Germany, Greece, Ireland, Italy, Japan, Luxembourg, the Netherlands, New Zealand, Norway, Portugal, Spain, Sweden, Switzerland, Turkey, United Kingdom and the United States. The Commission of the European Communities also participates in work of the IEA.

Organization

The IEA is an autonomous agency within the Organization for Economic Cooperation and development (OECD). Its principal decision-making body is the Governing Board, composed of senior level representatives from each participating country. The Governing Board also meets at the Ministerial Level from time to time. A Secretariat headquartered in Paris with a permanent staff of energy experts drawn from member countries, supports the work of the Governing Board and subordinate bodies.

The IEA Secretariat is headed by the Executive Director who is appointed by the Governing Board.

The Governing Board directs the activities and makes the major policy decisions of the IEA. In most cases, issues are decided by consensus; where a vote is required, a system of weighted voting would apply.

The Governing Board regularly reviews the world energy situations as well as domestic energy policies in order to assess future energy supply and demand patterns, and to formulate appropriate policies to meet changing conditions.

Standing Groups

The Governing Board is supported in its work by four Standing Groups and a High-Level Committee. These groups, comprised of senior-level energy specialists from the national capitals of participating countries convene in Paris on a regular basis. Their responsibilities relate to a particular area of the IEA program:

- Long-Term Cooperation (SLT) -promotes conservation and efficient use of energy,

increased production and use of alternative sources of energy and other measures designed to reduce long-term dependance on oil;

- Oil Market Information (SOM) -receives, collects, and analyzes information on the international oil market and oil company activities;

- Emergency Questions (SEQ) -refines, tests and maintains on a stand-by basis the IEA Emergency Oil Sharing System and the IEA Dispute Settlement Centre for supply emergencies;

- Relations with Producer and other Consumer Countries (SPC) -encourages cooperative relations with other nations, both oil producers and non-Member oil consumers;

- Committee on Energy Research and Development (CRD) -encourages accelerated research on new technologies to increase efficient energy use and develop alternative sources through cooperative multinational projects.

Committee for Research and Development

The principal orientation and direction of the IEA RD&D program thrusts under the aegis of the CRD are towards:

(a) supporting technologies designed to maximize the role of alternative conventional fuels to oil, especially coal and nuclear, in the near to mid-term;

(b) assisting the development of technologies which make the use of energy more efficient;

(c) continuing to pursue technologies which promise large contributions in the future, but are high risk and whose introduction would coincide with the inevitable depletion of fossil resources;

(d) pressing the exploitation of renewable energy sources; and

(e) the continued nurturing of the technology base which forms the foundation for creating future technologies options.

The IEA has four principal programmatic thrusts which support the foregoing objectives. They are:

Collaborative Projects: designed to foster international collaboration as a means of sharing the costs and benefits of technological advance among IEA Member countries, large or small. There are presently some 57 such projects.

Technology Reviews: which examine the technological progress made to date by a particular technology, an examination of the factors which appear to influence its future development and market penetration, and its potential role in addressing the energy supply/demand balance.

National Program Reviews: performed on an annual basis to assess national RD&D policies and thereby to evaluate the progress of IEA nations as a whole towards energy security through the contribution of technology.

An Energy Technology Policy Study: which examines the role of technologies as a whole in terms of their contribution to energy security of IEA Member countries as a group. This study carries the Group Strategy, published in 1980, still closer to issues of current political relevance to the Member countries.

The CRD created Working Parties responsible for sectoral technologies, on the premise that it required advice from more technologically-oriented groups on a standing basis. The working Parties, subsequently reduced from ten to four, are the:

(a) Fossil Fuels Working Party
(b) End-Use Efficiency Working Party
(c) Renewable Energies Working Party
(d) Fusion Energy Working Party

The responsibilities of the Working Parties are to:

- monitor the progress of ongoing collaborative projects with a view to ensuring high technical quality and termination as appropriate,

- initiate, and carry through to an Implementing Agreement, new collaborative ventures,

- advise the CRD on embarking upon new Technology Reviews, and also upon follow-up actions on completion of the Review,

- pursue specific studies, within their area of competence, on the request of the CRD.

Working Party for End-Use Efficiency

At the first meeting of the reconstituted Working Party on End-Use Efficiency held on 15-16 March 1982, it was agreed that the mandate of the group was:

- To assess the role, future prospects and significance of energy technologies within the cognizance of the Working Party;

- To assess national progress towards commercialization;

- To continue the process of developing a high-quality R&D project portfolio; evaluate the project portfolio; monitor the progress of the collaborative projects; make judgements on the scientific, technical and management quality of on-going work and make recommendations to the CRD on the future of these projects.

The Working Party on End-Use Technologies is presently sponsoring work under implementing agreements in eleven areas:

- Buildings and Community Systems;
- Heat Pumps;
- District Heating;
- Combustion;
- Heat Transfer and Heat Exchangers;
- Energy Storage;
- High Temperature Materials for Automotive Engines;
- Cement Manufacture;
- Pulp and Paper;
- Iron and Steel;
- Energy Cascading.

Work in each area is administered by an executive committee composed of representatives of interested countries. Where appropriate, funding for projects is contributed by Member countries, in other areas the work involves task-sharing. The IEA has no budget of its own to sponsor R&D.

2. The Implementing Agreement on Advanced Heat Pumps- R&D Activities

Background and Objectives

The implementing agreement on advanced heat pumps was initiated in 1978 with thirteen countries participating. The objectives are to provide a framework for cooperative research, development, demonstrations and exchanges of information. Such activities are implemented by means of projects (annexes) which can be carried out by two or more participating countries.

Annex I Common Study

The initial project (created concurrent with the establishment of the implementing agreement) was designed to provide a common basis for all participants for planning and implementing future R&D cooperation under the agreement.

The objectives of this project were to collect and evaluate data from international experience, to develop proposals for needed developments and to recommend future R&D program direction. The project was carried out by means of a technology survey and a market survey which covered all participating countries and a wide range of technologies, both thermally activated heat pumps and electrically-driven heat pumps for residential and commercial buildings.

The results of this project are contained in the report "Common Study on Advanced Heat Pump Systems" available to the public from: Verlag TUEV Rheinland GmbH, Am Grauen Stein, D-5000 Koeln 91, West Germany.

Completed Annexes

Following the general directions set by Common Study, and governed by national R&D program directions, areas were identified for cooperative R&D focussing on specific technologies or issues. To date, five annexes have been completed on a wide range of topics as listed below by annex number:

1. Common Study
2. Vertical Earth Heat Sources
3. Industrial Heat Pumps
5. Heat Pumps for District Heating
6. Working Fluids for Compression Systems

The results of these annexes are usually only available to those countries which participated.

Current Annexes

A further ten projects are currently in force, in various stages of completion. Several of these are follow-on projects to the completed projects listed above. Again, a wide variety of topics is included, as is clear from the following list, by annex number:

4. Heat Pump Center
7. New Evaporator Developments
8. Advanced Ground Heat Exchangers
9. High Temperature Industrial H.P.
10. Technical and Market Analysis
11. Stirling Engine Technology
12. Modelling Techniques
13. Properties of Novel Fluids
14. Working Fluids-Absorption
15. Direct Expansion Ground Coils

A typical project would last for 3 years with four to six countries participating. However project durations have ranged from two to six years and participation has varied from two to eleven countries. A typical project would consist of a domestic R&D project conducted in each participating country, the results of which would be assembled and analyzed by a lead country for the annex. The lead country analysis could include literature surveys, reporting formats, analysis and comparisons of national projects, state of the art assessments, conclusions and further R&D needs. The work of the lead country would typically be funded by contributions from each of the participating countries.

There are thirteen countries currently participating in one or more annexes. These countries are: Austria, Belgium, Canada, Denmark, Finland, Germany, Italy, Japan, The Netherlands, Norway, Sweden, Switzerland, and the U.S.A.

Future Annexes

As part of a continuous process, the executive committee explores potential new areas for cooperative R&D. Currently, active discussions on at least five topics are taking place:

(a) chlorofluorocarbon replacement
(b) industrial process integration
(c) compression-absorption systems
(d) properties of mixtures
(e) compressors

Several new annexes could result from these topic area discussions. However there is no certainty at this time that annexes will result from any or all of the topic areas.

In an effort to sharpen discussions on the CFC issue and the potential cooperative role of IEA, a workshop will be held in Rome on May 30-31. Participation is expected by technical experts from most countries participating in the Advanced Heat Pumps activity. Specific CFC annex concepts are expected to emerge and will be discussed at the executive committee meeting on June 3, 1988. Fully elaborated annexes could be proposed in the Fall of 1988 for executive committee endorsement.

3. Conference Activities

The Executive Committee on Advanced Heat Pumps has also sponsored two international conferences on advanced heat pumps and a third is being planned. While not specifically constituted as formal annexes, the committee views these conferences as an intergral part of its function to provide a framework for exchange of information.

These conferences have been carefully tailored through the use of invited papers to provide a broad, policy-oriented viewpoint on the present state and future potential of heat pumps. The conferences are designed to achieve balanced coverage of the various national/regional situations, and the many applications and technologies of heat pumps.

The conferences are as follows:

(a) 1984 - Graz, Austria
(b) 1987 - Orlando, Florida
(c) 1990 - Tokyo, Japan

Published proceedings from the previous conferences are available and provide a unique and comprehensive international overview of heat pump technology.

4. Benefits and Needs

Benefits of Participation

It is difficult to quantify the benefits from participation in the IEA Advanced Heat Pumps activity. Nevertheless experience has demonstrated several very clear ways in which the U.S. gains from this effort.

Technology Transfer: There are specific areas in which technology is further developed in foreign countries, or where the development has proceeded in a different direction. In these areas, the U.S. can materially gain from learning what our international colleagues already know. The IEA specifically provides the legal and institutional framework for easily undertaking jointly-funded research in such areas of benefit, thus overcoming many of the start-up barriers associated with international collaboration in research and development.

Broaden Viewpoints: Despite the normalizing effect of developments such as the European Commom Market, there is a very wide diversity of domestic environments worldwide under which heat pump technology must develop. This diversity stems from substantial differences in energy supply and prices, climates, building stock, industrial/technical infrastracture, political context and ecological concerns, These environments, often differing substantially from the U.S., produce a host of different ideas and approaches to common technical problems. These ideas may be directly applicable in the U.S. or may point to infrastructural limitations to technology development in the U.S.

Communications: The advanced heat pump activities, consisting of two executive committee meetings per year, ten or more active annexes, triennial conferences and the IEA Heat Pump Center, provide a great opportunity to establish and maintain lines of communication with organizations and individual researchers, managers and policy makers. Many of these key people do not frequently travel to the U.S. or are otherwise not well known internationally. Often, some of the most interesting research does not result in formal publications which are entered into retrievable data bases. Therefore identification of appropriate contacts can be a formidable task.

Improved assessments: The triennial conferences, several of the annexes and the specific tasks of the Heat Pump Center are intended to provide a broader, more complete view of the worldwide heat pump situation. These activities enable U.S. industry to

better assess general research and development trends and to better understand the foreign market situation. This in turn provides a basis for improved understanding of specific research directions and policies and to better anticipate future market and technical developments. In this way the IEA activities provide an information service which is not normally provided by professional societies or technical journals.

Future needs

Ten years of experience with international collaboration on advanced heat pumps through IEA has pointed out several areas where improvements are needed to further increase the benefits to the U.S. In general there is a need to increase participation by U.S. industry in the planning, execution and information transfer of the IEA activities. Specifically, the following actions are needed:

(a) identify and implement new projects (annexes) to meet specific industry needs

(b) obtain more direct industry involvement in the execution of the IEA activities

(c) enhance information flow to U.S. industry on project results

Due to the flexibility of the IEA framework, a wide range of possibilities exist for industry direct involvement. These possibilities can be part of the formal structure of an annex or can be carried out informally. Some of the possible approaches to industry involvement are as follows:

(a) carry out technical tasks assigned to the U.S. in a cooperative annex

(b) monitor R&D activities being carried by other participants in an annex

(c) provide a guest scientist to work at foreign research centers which are carrying out tasks related to an IEA annex

(d) initiation and/or funding of IEA annex activities.

An example of U.S. industry involvement is the participation of the Electric Power Research Institute (EPRI) in IEA Annex XV. This annex is focussed on direct expansion vertical ground coils for use as a heat source/sink for a heat pump. The lead country is Canada and four other countries are participating. Each participant is carrying out a domestic R&D project in this area and will contribute the full results therefrom to the annex participants. Canada will coordinate and compile the results from the projects, drawing conclusions where possible.

For the U.S. contribution to this project, EPRI is funding a laboratory investigation of ground coil performance at the Oak Ridge National Laboratory. The Department of Energy provides no direct funding of this effort, except for facilities support.

5. Summary

The IEA's implementing agreement on advanced heat pumps is effectively fostering a wide range of collaborative R&D and information exchange activities. The IEA's flexible R&D structure provides an opportunity to tailor international collaborative activities to meet U.S. industry needs. Effort is needed to fully realize this potential by obtaining greater industry involvement in the IEA program.